

WCAP-16045-NP-A
Revision 0

August 2004

Qualification of the Two-Dimensional Transport Code PARAGON



Page Intentionally Left Blank

WCAP-16045-NP-A
Revision 0

Qualification of the Two-Dimensional Transport Code PARAGON

Original Version: March 2003
Approved Version: August 2004

Prepared by:

W. H. Slagle

Authors:

M. Ouisloumen
H. Huria
L. T. Mayhue
R. M. Smith
S. W. Park
M. J. Kichy

Westinghouse Electric Company LLC
4350 Northern Pike
Monroeville, PA 15146-2886

Page Intentionally Left Blank

Table of Contents

<u>Section</u>	<u>Description</u>
A	Letter from H. N. Berkow (NRC) to J. A. Gresham (Westinghouse), "Final Safety Evaluation for Westinghouse Topical Report, WCAP-16045-P, Revision 0, 'Qualification of the Two-Dimensional Transport Code PARAGON', (TAC No. MB8040)," March 18, 2004.
B	Letter from H. A. Sepp (Westinghouse) to J. S. Wermiel (NRC), "WCAP-16045-P, Revision 0, 'Qualification of the Two-Dimensional Transport Code PARAGON', (Proprietary)," LTR-NRC-03-6, March 7, 2003.
C	Letter from B. F. Maurer (Westinghouse) to J. S. Wermiel (NRC), "Response to Request for Additional Information Regarding WCAP-16045-P, 'Qualification of the Two-Dimensional Transport Code PARAGON', (Proprietary)," LTR-NRC-03-55, September 9, 2003.

Page Intentionally Left Blank

Section A

Page Intentionally Left Blank

MAR-22-2004 11:09

P.02/10



UNITED STATES
NUCLEAR REGULATORY COMMISSION
WASHINGTON, D.C. 20555-0001

March 18, 2004

Mr. James A. Gresham, Manager
Regulatory and Licensing Engineering
Westinghouse Electric Company
P.O. Box 355
Pittsburgh, PA 15230-0355

SUBJECT: FINAL SAFETY EVALUATION FOR WESTINGHOUSE TOPICAL REPORT
WCAP-16045-P, REVISION 0, "QUALIFICATION OF THE TWO-DIMENSIONAL
TRANSPORT CODE PARAGON" (TAG NO. MB8040)

Dear Mr. Gresham:

By letter dated March 7, 2003, and supplement dated September 9, 2003, the Westinghouse Electric Company (Westinghouse) submitted Topical Report (TR) WCAP-16045-P, Revision 0, "Qualification of the Two-Dimensional Transport Code PARAGON" to the staff for review. On February 8, 2004, an NRC draft safety evaluation (SE) regarding our approval of the TR was provided for your review and comments. By fax dated February 19, 2004, Westinghouse commented on the draft SE. The staff's disposition of Westinghouse's comments on the draft SE is discussed in the attachment to the final SE enclosed with this letter.

The staff has found that the TR is acceptable for referencing as an approved methodology in plant licensing applications. The enclosed SE documents the staff's evaluation of Westinghouse's justification for the improved methodology.

Our acceptance applies only to the material provided in the subject TR. We do not intend to repeat our review of the acceptable material described in the TR. When the TR appears as a reference in license applications, our review will ensure that the material presented applies to the specific plant involved. License amendment requests that deviate from this TR will be subject to a plant-specific review in accordance with applicable review standards.

In accordance with the guidance provided on the NRC's TR website, we request that Westinghouse publish an accepted version of this TR within three months of receipt of this letter. The accepted version shall incorporate this letter and the enclosed SE between the title page and the abstract. It must be well indexed such that information is readily located. Also, it must contain in appendices historical review information, such as questions and accepted responses, draft SE comments, and original report pages that were replaced. The accepted version shall include a "-A" (designating "accepted") following the report identification symbol.

MAR-22-2004 11:09

P.03/10

J. Gresham

- 2 -

If the NRC's criteria or regulations change so that its conclusions in this letter, that the TR is acceptable, is invalidated, Westinghouse and/or the licensees referencing the TR will be expected to revise and resubmit its respective documentation, or submit justification for the continued applicability of the TR without revision of the respective documentation.

Sincerely,



Herbert N. Berkow, Director
Project Directorate IV
Division of Licensing Project Management
Office of Nuclear Reactor Regulation

Project No. 700

Enclosure: Safety Evaluation

cc w/enc:
Mr. Gordon Bischoff, Manager
Owners Group Program Management Office
Westinghouse Electric Company
P.O. Box 355
Pittsburgh, PA 15230-0355

MAR-22-2004 11:09

P. 84/10



UNITED STATES
NUCLEAR REGULATORY COMMISSION
WASHINGTON, D.C. 20555-0001

SAFETY EVALUATION BY THE OFFICE OF NUCLEAR REACTOR REGULATION
WESTINGHOUSE TOPICAL REPORT WCAP-16045-P, REV.0, "QUALIFICATION OF THE
TWO-DIMENSIONAL TRANSPORT CODE PARAGON"
WESTINGHOUSE ELECTRIC COMPANY
PROJECT NO. 700

1.0 INTRODUCTION

By letter dated March 7, 2003, as supplemented by letter dated September 9, 2003, the Westinghouse Electric Company (Westinghouse) submitted Topical Report (TR) WCAP-16045-P, "Qualification of the Two-Dimensional Transport Code PARAGON," to the NRC for review and approval. The objective of this TR was to provide the information and data necessary to license PARAGON both as a stand-alone transport code and as a nuclear data source for a core simulator in a complete nuclear design code system for core design, safety and operational calculations. PARAGON is a new transport code developed by Westinghouse. PARAGON is based on collision probability methods and is written entirely in FORTRAN 90/95. PARAGON can provide nuclear data, both cross sections and pin power information, to a core simulator code such as ANC.

2.0 REGULATORY EVALUATION

Section 50.34, "Contents of Applications; Technical Information," of Title 10 of the Code of Federal Regulations requires that safety analysis reports be submitted that analyze the design and performance of structures, systems, and components provided for the prevention of accidents and the mitigation of the consequences of accidents. As part of the core reload design process, licensees (or vendors) perform reload safety evaluations to ensure that their safety analyses remain bounding for the design cycle. To confirm that the analyses remain bounding, licensees confirm that key inputs to the safety analyses (such as the critical power ratio) are conservative with respect to the current design cycle. If key safety analysis parameters are not bounded, a reanalysis or reevaluation of the affected transients or accidents is performed to ensure that the applicable acceptance criteria are satisfied.

There are no specific regulatory requirements or guidance available for the review of TR revisions. As such, the staff review will be based on the evaluation of technical merit and compliance with any applicable regulations associated with reviews of TRs.

3.0 TECHNICAL EVALUATION

The qualification presented in this TR followed a systematic qualification process which has been used previously by Westinghouse to qualify nuclear design codes. This process starts with the qualification of the basic methodology used in the code and proceeds in logical steps to

- 2 -

qualification of the code as applied to a complete nuclear design code system. The qualification process consists of benchmarking the code against raw data and industry accepted Monte-Carlo codes such as MCNP.

3.1 Benchmarking and Monte-Carlo Code Calculations

Consistent with the qualification process described above, Westinghouse presented the results of PARAGON runs for a series of critical experiments. These experiments included the Strawbridge-Barry 101 criticals, the KRITZ high temperature criticals, and a large number of spatial criticals from the Babcock and Wilcox (B&W) physics verification program. The B&W critical calculations provided both reactivity and power distribution measurements data to benchmark PARAGON output predictability.

The Strawbridge-Barry 101 critical calculations (criticals) cover a wide range of lattice parameters, providing an important test for the PARAGON lattice code. Since these experiments are uniform lattices, the criticals were run as single pin cells in PARAGON. There are 40 UO₂ experiments among the 101 criticals. The results produced by PARAGON showed no particular bias or trends as a function of uranium enrichment, experimental buckling, pellet diameter or soluble boron.

The KRITZ high-temperature calculations provide critical benchmark data for uranium-fueled, water-moderated lattices at high temperatures. The calculations were performed at temperatures as high as 245°C. PARAGON modeled 12 KRITZ experiments. No significant trends across the large temperature range of these critical calculations were observed. The small standard deviation obtained is indicative of PARAGON predictive capabilities across the large temperature range.

The B&W spatial criticals provided data on both reactivity and power distribution for a variety of uranium-oxide fueled lattices. A total of 29 configurations were analyzed by the vendor, at different enrichments and burnable poisons. K-infinity comparisons were carried out between PARAGON and the Monte Carlo code MCNP for all 29 experiments. In addition, the measured axial bucklings were used with the PARAGON results to calculate K_{eff} . The reactivity results for all configurations resulted in a very comparable K_{eff} for the 29 experiments, with a standard deviation of less than 0.05 percent. Westinghouse also submitted rod power distribution comparisons of PARAGON results against measurements for six experiments, two with no burnable absorbers, two with gadolinia burnable absorbers, and two with Pyrex burnable absorbers. The average difference between the measured and PARAGON power distribution for the six experiments was slightly greater than 1.0 percent with an average standard deviation of 1.5 percent.

Westinghouse also benchmarked PARAGON against well known Monte-Carlo codes. Specifically, Westinghouse performed 13 different assembly configuration calculations using both PARAGON and the Monte Carlo code MCNP. These assembly configurations were chosen to cover a variety of lattice types and burnable absorbers over a large enrichment range. These calculations included 11 Westinghouse and 2 Combustion Engineering (CE) assemblies. The PARAGON and MCNP calculations were compared for both reactivity and power distribution. The mean difference in reactivity between the MCNP and PARAGON calculations over the 13 assemblies was about 100 percent mill (pcm), with a standard deviation

MAR-22-2004 11:10

P. 05/10

- 3 -

of less than 100 pcm. The results of comparison between the MCNP and PARAGON power distributions showed very good agreement. The average difference in rod powers for each assembly ranged from less than 0.4 percent to less than 0.8 percent.

Westinghouse also performed calculations using PARAGON to compare with spectrograph-measured isotopics data from the Saxton reactor Cores 2 and 3 containing mixed oxide fuel. Additional comparisons were performed using PARAGON to other plants such as Yankee Cores 1, 2, and 4 with stainless steel clad fuel, and Yankee Core 5 with zircaloy clad fuel. In these calculations isotopic concentrations from PARAGON were used to simulate the power history corresponding to these cores. The results of these isotopic comparisons show no significant trend for any isotope with burnup, again demonstrating the capability of PARAGON for predicting the depletion characteristics of UO₂ light-water reactor fuel over a wide range of burnup conditions. Although Westinghouse included mixed oxide fuel (MOX) data in the TR, the data base is insufficient to enable the staff to reach a conclusion regarding PARAGON's ability to predict depletion characteristics for a MOX fueled core at this time.

3.2 Plant Cycles Operation Comparisons

Westinghouse stated in the submittal that the primary use of PARAGON will be to generate nuclear data for use in Westinghouse core simulator codes. Thus, the most important qualification for PARAGON is the comparison of results of core calculations using PARAGON supplied nuclear data against plant measured data. In the submittal, Westinghouse presented ANC results for pressurized water reactor (PWR) core calculations with nuclear data supplied by PARAGON (PARAGON/ANC) which were compared to corresponding plant measurements, where available, and to PHOENIX-P/ANC results for the same calculations. The results of the calculations demonstrated the accuracy of the PARAGON nuclear data when applied to a complete nuclear design system.

Cycles from 11 plants including both Westinghouse and CE type plants, were used for measured-to-PARAGON/ANC-predicted comparisons of startup data and at-power critical boron versus cycle burnup data. In addition, measured radial power data was compared to PARAGON/ANC predicted values from 28 radial power maps from 6 different plants. Beginning-of-cycle (BOC) and end-of-cycle (EOC) radial power and EOC burnup predictions from PHOENIX-P/ANC were compared to those calculated by PARAGON/ANC for nine cycles in five plants.

PARAGON/ANC axial power predictions were compared to PHOENIX-P/ANC at BOC, middle-of-cycle (MOC), and EOC for four plants. Finally, PARAGON/ANC results were compared to PHOENIX-P/ANC results for events for which measurements are generally not made or cannot be made. These are ARI-WSR (worst stuck rod) rodworth (four plants), dropped rod events (four plants) and rod ejection events (BOC and EOC for four plants).

The PARAGON code qualification included 24 cycles from 11 different plants. These plants included both Westinghouse (15 cycles) and Combustion Engineering (9 cycles) type cores. The vendor chose the plants to cover a wide variety of lattices, burnable absorbers, blanket types, core sizes, as well as the availability of plant measured data.

- 4 -

Some of the tests considered were startup physics tests. Comparisons were made for PARAGON/ANC predictions against measurements for BOC hot zero power (HZP) all rods out (ARO) critical boron, BOC HZP ARO isothermal temperature coefficient (ITC), and BOC HZP rodworths. Results from 22 cycles from 11 different plants were compared for the BOC HZP critical boron concentration.

The mean difference between measured and predicted boron was found to be about 15 ppm for both PARAGON/ANC and PHOENIX-P/ANC, with standard deviations for both code systems of about 15 ppm.

For the same 22 cycles, results from BOC HZP ARO ITC were also compared. The statistics from the isothermal temperature coefficient (ITC) comparison were quite similar between the two code systems. The mean predicted to measured difference in ITC was less than 0.2 pcm/°F for PARAGON/ANC and less than 0.3 pcm/°F for PHOENIX-P/ANC. The standard deviations were the same for both code systems at less than 1.0 pcm/°F.

Predicted versus measured rodworths were compared for nine cycles in seven plants. The cycles used three different methods for rodworth measurement: dynamic rod worth measurement, rod swap, and boron dilution. All rodworth predictions met the measurement review criteria.

Westinghouse also performed at-power critical boron calculations. At-power critical boron measurements were compared to results from PARAGON/ANC and PHOENIX-P/ANC core depletion calculations for 22 plant cycles. The results showed very good performance by PARAGON/ANC for EOC predictions. All plant cycles showed the effects of B10 depletion since the uncorrected measured and predicted critical boron values difference grew through the MOC. Accounting for B10 depletion reduces the difference between measured and predicted values through the middle of the cycle as was demonstrated in the report for one of the cycles.

Measured to PARAGON-predicted radial assembly power comparisons were made for 5 plants (28 total flux maps). These plants included both even (16x16 and 14x14) and odd (15x15 and 17x17) lattices. The average value of the measured to predicted differences over the 28 maps was less than 1.0 percent with an average standard deviation of 1.0 percent. These results show that the radial assembly powers are indeed well predicted by PARAGON/ANC.

3.3 PARAGON/ANC to PHOENIX-P/ANC Comparison Results

PARAGON/ANC and PHOENIX-P/ANC calculational results were compared for radial assembly power distribution, axial power distribution, all rods in minus worst rod stuck (ARI-WSR) rodworth, rod drop, and rod ejection calculations. Radial assembly power (BOC and EOC) distributions were compared for nine cycles in five plants. EOC assembly bumup distributions were compared for the same cycles. Axial power distributions are shown at BOC, MOC, and EOC for eight cycles in four plants. The plant cycles for both radial and axial comparisons include Westinghouse and CE type cores. The results of both radial and axial power comparisons show very little difference between PARAGON/ANC and PHOENIX-P/ANC. The small difference between the PARAGON/ANC results and those from PHOENIX-P/ANC confirms that PARAGON/ANC also predicts these power distributions very well.

MAR-22-2004 11:11

P. 08/10

- 5 -

ARI-WSR shutdown rodworths were calculated in PARAGON/ANC at BOC for four plants. The results were compared to PHOENIX-P/ANC for the same calculations. The largest difference for the worst stuck rodworth was less than 7 pcm. The largest peaking factor difference was about three percent in local peaking factor (F_p). Both differences are well within the uncertainties used with the ARI-WSR calculations.

Dropped rod calculations were also performed with PARAGON/ANC at BOC for four plants and the results were compared to corresponding PHOENIX-P/ANC results. The largest difference in the dropped rod worth was less than 6 pcm. The largest difference in peaking factor was less than 1.7 percent in F_p . The last set of comparisons between PARAGON/ANC and PHOENIX-P/ANC was for BOC and EOC rod ejection calculations for four plants. The rod ejection calculations were performed for both HZP and hot full power conditions. Rod ejection calculations are similar to stuck rod calculations except the feedback is frozen from pre-ejection conditions leading to much larger peaking factors and rodworths. The largest difference in rodworth was less than 16 pcm. The peaking factor differences were very small and well within the uncertainties used with this event.

4.0 CONDITIONS AND LIMITATIONS

1. The PARAGON code can be used as a replacement for the PHOENIX-P lattice code, wherever the PHOENIX-P code is used in NRC-approved methodologies.
2. The data base is insufficient to enable the staff to reach a conclusion regarding PARAGON's ability to predict depletion characteristics for a MOX fueled core at this time.

5.0 CONCLUSION

The staff has reviewed the analyses and results presented in the TR and determined that the analyses and results are in accordance with the guidance and limitations, and the applicable sections of NUREG-0800, "Standard Review Plan." The staff concludes that PARAGON is acceptable for use as a stand-alone lattice code and as a nuclear data source for core simulators for PWR analyses for uranium-fuel cores. In addition, the staff considers the new PARAGON code to be well qualified as a stand-alone code replacement for the PHOENIX-P lattice code, wherever the PHOENIX-P code is used in NRC-approved methodologies. The staff concludes that it is acceptable for licensing applications.

Attachment: Resolution of Comments

Principle Contributor: A. Attard

Date: March 18, 2004

RESOLUTION OF COMMENTS**ON DRAFT SAFETY EVALUATION FOR WCAP-16045-P, REVISION 0, "QUALIFICATION OF
THE TWO-DIMENSIONAL TRANSPORT CODE PARAGON"**

By fax dated February 19, 2004, Westinghouse provided comments on the draft safety evaluation (SE) for WCAP-16045-P, Revision 0, "Qualification of the Two-Dimensional Transport Code PARAGON". The following is the staff's resolution of those comments.

1. **Westinghouse Comment:** Section 3.1, third paragraph, fifth sentence stated, "The reactivity results for all configurations resulted in a very comparable K_{eff} for the 29 experiments, with a standard deviation of less than 0.4 percent."
Westinghouse Proposed Resolution: The reactivity results for all configurations resulted in a very comparable K_{eff} for the 29 experiments, with a standard deviation of less than 0.05 percent.
NRC Action: The comment was fully adopted into the final SE.
2. **Westinghouse Comment:** Section 3.1, fifth paragraph, fourth sentence contained numbers that Westinghouse considered proprietary.
Westinghouse Proposed Resolution: The mean difference in reactivity between the MCNP and PARAGON calculations over the 13 assemblies was about 100 percent mill (pcm), with a standard deviation of less than 100 pcm.
NRC Action: The comment was fully adopted into the final SE.
3. **Westinghouse Comment:** Section 3.2, sixth paragraph contained numbers that Westinghouse considered proprietary.
Westinghouse Proposed Resolution: The mean difference between measured and predicted boron was found to be about 15 ppm for both PARAGON/ANC and PHOENIX-P/ANC, with standard deviations for both code systems of about 15 ppm.
NRC Action: The comment was fully adopted into the final SE.
4. **Westinghouse Comment:** Section 3.2, seventh paragraph, last sentence contained a number that Westinghouse considered proprietary.
Westinghouse Proposed Resolution: The standard deviations were the same for both code systems at less than 1.0 pcm/F.
NRC Action: The comment was fully adopted into the final SE.

- 2 -

5. Westinghouse Comment: Section 3.2, last paragraph, third sentence contained numbers that Westinghouse considered proprietary.
- Westinghouse Proposed Resolution: The average value of the measured to predicted differences over the 28 maps was less than 1.0 percent with an average standard deviation of 1.0 percent.
- NRC Action: The comment was fully adopted into the final SE.
6. Westinghouse Comment: Section 3.3, first paragraph, next to last sentence contained a number that Westinghouse considered proprietary.
- Westinghouse Proposed Resolution: The largest peaking factor difference was about three percent in local peaking factor (F_p).
- NRC Action: The comment was fully adopted into the final SE.
7. Westinghouse Comment: Section 5.0, second paragraph could be more clearly stated as a new second sentence in the conclusion.
- Westinghouse Proposed Resolution: Add, "The staff concludes that PARAGON is acceptable for use as a stand-alone lattice code and as a nuclear data source for core simulators for PWR analyses for uranium-fuel cores." and eliminate, "Therefore, on the basis of the above review and justification, the staff concludes that the proposed change to the Westinghouse control rod ejection methodology is acceptable for use as a replacement code for the PHOENIX-P lattice code."
- NRC Action: The comment was fully adopted into the final SE.

Page Intentionally Left Blank

Section B

Page Intentionally Left Blank



Westinghouse Electric Company
Nuclear Services
P.O. Box 355
Pittsburgh, Pennsylvania 15230-0355
USA

U.S. Nuclear Regulatory Commission
Document Control Desk
Washington, DC 20555-0001

Direct tel: (412) 374-5282
Direct fax: (412) 374-4011
e-mail: sepp1ha@westinghouse.com

Our ref: LTR-NRC-03-6

Attn: J. S. Wermiel, Chief
Reactor Systems Branch
Division of Systems Safety and Analysis

March 7, 2003

Enclosed are:

1. Five (5) copies of WCAP-16045-P, "Qualification of the Two-Dimensional Transport Code PARAGON" (Proprietary)
2. Five (5) copies of WCAP-16045-NP, "Qualification of the Two-Dimensional Transport Code PARAGON" (Non-Proprietary)

Also enclosed is:

1. One (1) copy of the Application for Withholding, AW-03-1605 (Non-Proprietary) with Proprietary Information Notice.
2. One (1) copy of Affidavit (Non-Proprietary).

This information is being submitted by Westinghouse Electric Company LLC to obtain Nuclear Regulatory Commission ("NRC") generic approval of PARAGON, a new Westinghouse neutron transport code. Generic NRC approval is also requested for the use of PARAGON with Westinghouse's nuclear design code system or as a stand-alone code.

This submittal contains proprietary information of Westinghouse Electric Company LLC. In conformance with the requirements of 10 CFR Section 2.790, as amended, of the Commission's regulations, we are enclosing with this submittal an Application for Withholding from Public Disclosure and an affidavit. The affidavit sets forth the basis on which the information identified as proprietary may be withheld from public disclosure by the Commission.

Page 2 of 2
LTR-NRC-03-6
March 7, 2003

Correspondence with respect to the affidavit or Application for Withholding should reference AW-03-1605 and should be addressed to the undersigned.

Very truly yours,



H. A. Sepp, Manager
Regulatory and Licensing Engineering

Enclosures

cc: G. Shukla/NRR
R Caruso/NRR
U. Shoop/NRR
S. L. Wu/NRR



Westinghouse Electric Company
Nuclear Services
P.O. Box 355
Pittsburgh, Pennsylvania 15230-0355
USA

U.S. Nuclear Regulatory Commission
Document Control Desk
Washington, DC 20555-0001

Direct tel: (412) 374-5282
Direct fax: (412) 374-4011
e-mail: sepp1ha@westinghouse.com

Our ref: AW-03-1605

March 7, 2003

**APPLICATION FOR WITHHOLDING PROPRIETARY
INFORMATION FROM PUBLIC DISCLOSURE**

Subject: WCAP-16045-P, "Qualification of the Two-Dimensional Transport Code PARAGON"
(Proprietary);

Reference: Letter from H. A. Sepp to J. S. Wermiel, LTR-NRC-03-6, dated March 7, 2003

The Application for Withholding is submitted by Westinghouse Electric Company LLC ("Westinghouse"), pursuant to the provisions of Paragraph (b) (1) of Section 2.790 of the Commission's regulations. It contains commercial strategic information proprietary to Westinghouse and customarily held in confidence.

The proprietary material for which withholding is being requested is identified in the proprietary version of the subject report. In conformance with 10 CFR Section 2.790, Affidavit AW-03-1605 accompanies this Application for Withholding, setting forth the basis on which the identified proprietary information may be withheld from public disclosure.

Accordingly, it is respectfully requested that the subject information which is proprietary to Westinghouse be withheld from public disclosure in accordance with 10 CFR Section 2.790 of the Commission's regulations.

Correspondence with respect to this Application for Withholding or the accompanying affidavit should reference AW-03-1605 and should be addressed to the undersigned.

Very truly yours,


H. A. Sepp, Manager
Regulatory and Licensing Engineering

Enclosures

cc: J. S. Wermiel/NRR

AFFIDAVIT

COMMONWEALTH OF PENNSYLVANIA:

ss

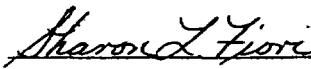
COUNTY OF ALLEGHENY:

Before me, the undersigned authority, personally appeared H. A. Sepp, who, being by me duly sworn according to law, deposes and says that he is authorized to execute this Affidavit on behalf of Westinghouse Electric Company LLC ("Westinghouse"), and that the averments of fact set forth in this Affidavit are true and correct to the best of his knowledge, information, and belief:

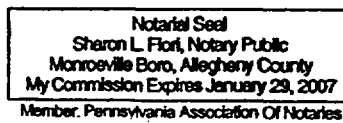


H. A. Sepp, Manager
Regulatory and Licensing Engineering

Sworn to and subscribed
before me this 7th day
of March, 2003



Notary Public



- (1) I am Manager, Regulatory and Licensing Engineering, in Nuclear Services, Westinghouse Electric Company LLC ("Westinghouse"), and as such, I have been specifically delegated the function of reviewing the proprietary information sought to be withheld from public disclosure in connection with nuclear power plant licensing and rule making proceedings, and am authorized to apply for its withholding on behalf of the Westinghouse Electric Company LLC.
- (2) I am making this Affidavit in conformance with the provisions of 10 CFR Section 2.790 of the Commission's regulations and in conjunction with the Westinghouse application for withholding accompanying this Affidavit.
- (3) I have personal knowledge of the criteria and procedures utilized by the Westinghouse Electric Company LLC in designating information as a trade secret, privileged or as confidential commercial or financial information.
- (4) Pursuant to the provisions of paragraph (b)(4) of Section 2.790 of the Commission's regulations, the following is furnished for consideration by the Commission in determining whether the information sought to be withheld from public disclosure should be withheld.
 - (i) The information sought to be withheld from public disclosure is owned and has been held in confidence by Westinghouse.
 - (ii) The information is of a type customarily held in confidence by Westinghouse and not customarily disclosed to the public. Westinghouse has a rational basis for determining the types of information customarily held in confidence by it and, in that connection, utilizes a system to determine when and whether to hold certain types of information in confidence. The application of that system and the substance of that system constitutes Westinghouse policy and provides the rational basis required.

Under that system, information is held in confidence if it falls in one or more of several types, the release of which might result in the loss of an existing or potential competitive advantage, as follows:

 - (a) The information reveals the distinguishing aspects of a process (or component, structure, tool, method, etc.) where prevention of its use by any of

Westinghouse's competitors without license from Westinghouse constitutes a competitive economic advantage over other companies.

- (b) It consists of supporting data, including test data, relative to a process (or component, structure, tool, method, etc.), the application of which data secures a competitive economic advantage, e.g., by optimization or improved marketability.
- (c) Its use by a competitor would reduce his expenditure of resources or improve his competitive position in the design, manufacture, shipment, installation, assurance of quality, or licensing a similar product.
- (d) It reveals cost or price information, production capacities, budget levels, or commercial strategies of Westinghouse, its customers or suppliers.
- (e) It reveals aspects of past, present, or future Westinghouse or customer funded development plans and programs of potential commercial value to Westinghouse.
- (f) It contains patentable ideas, for which patent protection may be desirable.

There are sound policy reasons behind the Westinghouse system which include the following:

- (a) The use of such information by Westinghouse gives Westinghouse a competitive advantage over its competitors. It is, therefore, withheld from disclosure to protect the Westinghouse competitive position.
- (b) It is information that is marketable in many ways. The extent to which such information is available to competitors diminishes the Westinghouse ability to sell products and services involving the use of the information.
- (c) Use by our competitor would put Westinghouse at a competitive disadvantage by reducing his expenditure of resources at our expense.

- (d) Each component of proprietary information pertinent to a particular competitive advantage is potentially as valuable as the total competitive advantage. If competitors acquire components of proprietary information, any one component may be the key to the entire puzzle, thereby depriving Westinghouse of a competitive advantage.
 - (e) Unrestricted disclosure would jeopardize the position of prominence of Westinghouse in the world market, and thereby give a market advantage to the competition of those countries.
 - (f) The Westinghouse capacity to invest corporate assets in research and development depends upon the success in obtaining and maintaining a competitive advantage.
- (iii) The information is being transmitted to the Commission in confidence and, under the provisions of 10 CFR Section 2.790, it is to be received in confidence by the Commission.
 - (iv) The information sought to be protected is not available in public sources or available information has not been previously employed in the same original manner or method to the best of our knowledge and belief.
 - (v) The proprietary information sought to be withheld in this submittal is that which is appropriately marked, WCAP-16045-P – “Qualification of the Two-Dimensional Transport Code PARAGON”, dated March 7, 2003, for submittal to the Commission, being transmitted by Westinghouse Electric Company (LTR-NRC-03-6) letter and Application for Withholding Proprietary Information from Public Disclosure, to the Document Control Desk, Attention Mr. J. S. Wermiel. The proprietary information as submitted by Westinghouse Electric Company LLC is that associated with Westinghouse’s request for NRC approval of PARAGON.

This information is part of that which will enable Westinghouse to:

- (a) Obtain NRC approval of the Two-Dimensional Transport Code PARAGON.

- (b) Promote convergence between Westinghouse organizations.
- (c) Assist our customer in obtaining enhanced nuclear design input data for fuel reload analysis

Further this information has substantial commercial value as follows:

- (a) Westinghouse plans to sell the use of this information to its customers for purposes of developing nuclear design input data into the Westinghouse' nuclear design code system or as a stand-alone code.
- (b) Westinghouse can sell support for PARAGON.
- (c) The information requested to be withheld reveals the distinguishing aspects of a methodology which was developed by Westinghouse.

Public disclosure of this proprietary information is likely to cause substantial harm to the competitive position of Westinghouse because it would enhance the ability of competitors to provide similar calculations and licensing defense services for commercial power reactors without commensurate expenses. Also, public disclosure of the information would enable others to use the information to meet NRC requirements for licensing documentation without purchasing the right to use the information.

The development of the technology described in part by the information is the result of applying the results of many years of experience in an intensive Westinghouse effort and the expenditure of a considerable sum of money.

In order for competitors of Westinghouse to duplicate this information, similar technical programs would have to be performed and a significant manpower effort, having the requisite talent and experience, would have to be expended.

Further the deponent sayeth not.

PROPRIETARY INFORMATION NOTICE

Transmitted herewith are proprietary and/or non-proprietary versions of documents furnished to the NRC in connection with requests for generic and/or plant-specific review and approval.

In order to conform to the requirements of 10 CFR 2.790 of the Commission's regulations concerning the protection of proprietary information so submitted to the NRC, the information which is proprietary in the proprietary versions is contained within brackets, and where the proprietary information has been deleted in the non-proprietary versions, only the brackets remain (the information that was contained within the brackets in the proprietary versions having been deleted). The justification for claiming the information so designated as proprietary is indicated in both versions by means of lower case letters (a) through (f) located as a superscript immediately following the brackets enclosing each item of information being identified as proprietary or in the margin opposite such information. These lower case letters refer to the types of information Westinghouse customarily holds in confidence identified in Sections (4)(ii)(a) through (4)(ii)(f) of the affidavit accompanying this transmittal pursuant to 10 CFR 2.790(b)(1).

COPYRIGHT NOTICE

The reports transmitted herewith each bear a Westinghouse copyright notice. The NRC is permitted to make the number of copies of the information contained in these reports which are necessary for its internal use in connection with generic and plant-specific reviews and approvals as well as the issuance, denial, amendment, transfer, renewal, modification, suspension, revocation, or violation of a license, permit, order, or regulation subject to the requirements of 10 CFR 2.790 regarding restrictions on public disclosure to the extent such information has been identified as proprietary by Westinghouse, copyright protection notwithstanding. With respect to the non-proprietary versions of these reports, the NRC is permitted to make the number of copies beyond those necessary for its internal use which are necessary in order to have one copy available for public viewing in the appropriate docket files in the public document room in Washington, DC and in local public document rooms as may be required by NRC regulations if the number of copies submitted is insufficient for this purpose. Copies made by the NRC must include the copyright notice in all instances and the proprietary notice if the original was identified as proprietary.

Acknowledgement

The authors wish to acknowledge the contributions made by J. D. St. John, A. N. Piplica, R. D. Erwin, R. T. Smith, and T. J. Congedo. The authors also want to acknowledge the reviews of this document by R. A. Loretz, Waldemar Lipek, Y. A. Chao, R. B. Sisk, and W. H. Slagle. The authors also wish to thank C. Bolton and J. Pavlecic for help in preparation of this document.

Page Intentionally Left Blank

Table of Contents

Section 1.0: Introduction	1-1
Section 2.0: PARAGON Methodology	2-1
2.1 Introduction	2-1
2.2 PARAGON Cross-sections Library	2-1
2.3 Theory of PARAGON modules	2-1
2.3.1 Cross-section resonance self-shielding module	2-1
2.3.2 Flux calculation module	2-2
2.3.3 Homogenization module	2-3
2.3.4 Depletion module	2-4
2.4 Other Modeling Capabilities	2-5
2.4.1 Temperature Model	2-5
2.4.2 Doppler Branch Calculation	2-5
2.4.3 Thermal Expansion	2-5
2.4.4 Interface Module	2-5
2.4.5 Reflector Modeling	2-6
Section 3.0: Critical Experiments and Isotopics	3-1
3.1 Critical Experiments	3-1
3.1.1 Strawbridge-Barry 101 Criticals	3-1
3.1.2 KRITZ High-Temperature Criticals	3-2
3.1.3 Babcock & Wilcox Spatial Criticals	3-2
3.2 Monte Carlo Assembly Benchmarks	3-3
3.3 Saxton and Yankee Isotopics Data	3-3
Section 4.0: Plant Qualification	4-1
4.1 Plant Cycles used for Comparisons	4-1
4.2 Startup Test Results Comparisons	4-2
4.3 Critical Boron versus Burnup Comparisons	4-3
4.4 Radial Power Distributions	4-4
4.5 PARAGON/ANC versus PHOENIX-P/ANC Comparisons	4-4
Section 5.0: Conclusion	5-1
5.1 PARAGON Benchmarking	5-1
5.1.1 Strawbridge-Barry Critical Experiments	5-1
5.1.2 KRITZ high temperature critical experiments	5-1
5.1.3 B&W spatial critical experiments	5-1
5.1.4 Monte Carlo Assembly Benchmarks	5-2

5.1.5	Saxton and Yankee Isotopics Data	5-2
5.2	Plant comparisons	5-2
5.2.1	Plants Cycles used for Comparison	5-3
5.2.2	Startup Test Results Comparisons	5-3
5.2.3	Critical boron comparisons	5-3
5.2.4	Radial Power Distributions	5-3
5.2.5	PARAGON/ANC to PHOENIX-P/ANC results	5-4
5.3	Conclusion	5-4
Section 6.0: References		6-1

List of Tables

Table 3-1: Strawbridge –Barry Critical Experiment Data versus PARAGON predictions3-5

Table 3-2: PARAGON Keff for KRITZ Experiments3-5

Table 3-3: Results for B&W Core XI with PYREX rods.....3-6

Table 3-4: Results for B&W Cores with 2.46 w/o U²³⁵ and Gadolinia Rods.....3-6

Table 3-5: Results from B&W Cores with 2.46 w/o U235, Gadolinia Rods and Control Rods3-7

Table 3-6: Results from B&W Cores with 4.02 w/o U235, Gadolinia Rods and Control Rods3-7

Table 3-7: Results from B&W Cores with 4.02 w/o U235, CE 16x16 Lattice with 2x2 Water Rods3-7

Table 3-8: Results of Assembly Benchmarks3-8

Table 4-1: Plant and Cycle Descriptions4-7

Table 4-2: Hot Zero Power All Rods Out Critical Boron4-10

Table 4-3: Hot Zero Power All Rods Out Isothermal Temperature Coefficients4-11

Table 4-4: Hot Zero Power Control Bank Worth: Plant A, Cycle 114-12

Table 4-5: Hot Zero Power Control Bank Worth: Plant B, Cycle 174-12

Table 4-6: Hot Zero Power Control Bank Worth: Plant C, Cycle 24.....4-13

Table 4-7: Hot Zero Power Control Bank Worth: Plant D, Cycle 10.....4-13

Table 4-8: Hot Zero Power Control Bank Worth : Plant E, Cycle 24.....4-14

Table 4-9: Hot Zero Power Control Bank Worth: Plant I, Cycle 134-14

Table 4-10: Hot Zero Power Control Bank Worth: Plant I, Cycle 144-14

Table 4-11: Hot Zero Power Control Bank Worth: Plant J, Cycle 104-15

Table 4-12: Hot Zero Power Control Bank Worth: Plant J, Cycle 114-15

Table 4-13: ARI-WSR Control Rod Worth Comparison:4-16

Table 4-14: Dropped Rod Worth Comparison.....4-17

Table 4-15: Rod Ejection Comparison4-18

Table 4-16: End of Life HFP Moderator Temperature Coefficient4-19

Page Intentionally Left Blank

List of Figures

Figure 3-1:	Strawbridge-Barry Critical Experiments: PARAGON Prediction versus Lattice Water to Uranium Ratio	3-9
Figure 3-2:	Strawbridge-Barry Critical Experiments: PARAGON Prediction versus Fuel Enrichment	3-9
Figure 3-3:	Strawbridge-Barry Critical Experiments: PARAGON Prediction versus Pellet Diameter	3-10
Figure 3-4:	Strawbridge-Barry Critical Experiments: PARAGON Prediction versus Experimental Buckling	3-10
Figure 3-5:	Strawbridge-Barry Critical Experiments: PARAGON Prediction versus Soluble Boron Concentration	3-11
Figure 3-6:	Babcock & Wilcox Critical Experiments: Core XI, Loading 2 Center Assembly Rod Power Distribution.....	3-12
Figure 3-7:	Babcock & Wilcox Critical Experiments: Core XI, Loading 6 Center Assembly Rod Power Distribution.....	3-13
Figure 3-8:	Babcock & Wilcox Critical Experiments: Core XI, Loading 9	3-14
Figure 3-9:	Babcock & Wilcox Critical Experiments: Core 5, 28 Gadolinia Rods.....	3-15
Figure 3-10:	Babcock & Wilcox Critical Experiments: Core 12, No Gadolinia Rods	3-16
Figure 3-11:	Babcock & Wilcox Critical Experiments: Core 14, 28 Gadolinia Rods.....	3-17
Figure 3-12:	MCNP vs PARAGON: 14x14 Westinghouse Assembly (4.00 w/o No BA) Assembly Rod Power Distribution	3-18
Figure 3-13:	MCNP vs PARAGON: 15x15 Westinghouse Assembly (3.90 w/o No BA) Assembly Rod Power Distribution	3-19
Figure 3-14:	MCNP vs PARAGON: 15x15 Westinghouse Assembly (5.0 w/o 60 IFBA) Assembly Rod Power Distribution	3-20
Figure 3-15:	MCNP vs PARAGON: 16x16 Westinghouse Assembly (4.00 w/o No BA) Assembly Rod Power Distribution	3-21
Figure 3-16:	MCNP vs PARAGON: 17x17 Standard Westinghouse Assembly (2.10 w/o No BA) Assembly Rod Power Distribution	3-22
Figure 3-17:	MCNP vs PARAGON: 17x17 Standard Westinghouse Assembly (4.10 w/o No BA) Assembly Rod Power Distribution	3-23
Figure 3-18:	MCNP vs PARAGON: 17x17 OFA Westinghouse Assembly (4.70 w/o 156 IFBA) Assembly Rod Power Distribution	3-24
Figure 3-19:	MCNP vs PARAGON: 17x17 Standard Westinghouse Assembly (5.0 w/o 128 IFBA) Assembly Rod Power Distribution	3-25
Figure 3-20:	MCNP vs PARAGON: 17x17 Standard Westinghouse Assembly (4.00 w/o 12 Gd ₂ O ₃ Rods) Assembly Rod Power Distribution	3-26
Figure 3-21:	MCNP vs PARAGON: 17x17 Standard Westinghouse Assembly (6.1 w/o MOX, No BA) Assembly Rod Power Distribution	3-27
Figure 3-22:	MCNP vs PARAGON: 17x17 OFA Westinghouse Assembly (4.00 w/o 72 Er ₂ O ₃ Rods) Assembly Rod Power Distribution	3-28
Figure 3-23:	MCNP vs PARAGON: 14x14 CE Assembly (4.30,3.40 w/o 44 Er ₂ O ₃ Rods) Assembly Rod Power Distribution	3-29
Figure 3-24:	MCNP vs PARAGON: 16x16 CE Assembly (4.05,3.65 w/o 52 Er ₂ O ₃ Rods) Assembly Rod Power Distribution.....	3-30
Figure 3-25:	Saxton Fuel Performance Evaluation Program: PARAGON U ²³⁵ /U Prediction Versus Burnup.....	3-31
Figure 3-26:	Saxton Fuel Performance Evaluation Program: PARAGON U ²³⁶ /U Prediction Versus Burnup.....	3-31
Figure 3-27:	Saxton Fuel Performance Evaluation Program: PARAGON U ²³⁸ /U Prediction Versus Burnup.....	3-32
Figure 3-28:	Saxton Fuel Performance Evaluation Program: PARAGON Pu ²³⁹ /Pu Prediction Versus Burnup.....	3-32

Figure 3-29: Saxton Fuel Performance Evaluation Program: PARAGON Pu²⁴⁰/Pu Prediction Versus Burnup.....3-33

Figure 3-30: Saxton Fuel Performance Evaluation Program: PARAGON Pu²⁴¹/Pu Prediction Versus Burnup.....3-33

Figure 3-31: Saxton Fuel Performance Evaluation Program: PARAGON Pu²⁴²/Pu Prediction Versus Burnup.....3-34

Figure 3-32: Saxton Fuel Performance Evaluation Program: PARAGON Pu²³⁹/U²³⁸ Prediction Versus Burnup.....3-34

Figure 3-33: Saxton Fuel Performance Evaluation Program: PARAGON Pu²³⁹/Pu²⁴⁰ Prediction Versus Burnup.....3-35

Figure 3-34: Saxton Fuel Performance Evaluation Program: PARAGON Pu²⁴⁰/Pu²⁴¹ Prediction Versus Burnup.....3-35

Figure 3-35: Saxton Fuel Performance Evaluation Program: PARAGON Pu²⁴¹/Pu²⁴² Prediction Versus Burnup.....3-36

Figure 3-36: Saxton Fuel Performance Evaluation Program: PARAGON U²³⁶/U²³⁵ Prediction Versus Burnup.....3-36

Figure 3-37: Saxton Fuel Performance Evaluation Program: PARAGON U²³⁵/U²³⁸ Prediction Versus Burnup.....3-37

Figure 3-38: Yankee Core Evaluation Program (Stainless Steel Clad): PARAGON U²³⁵/U Prediction Versus Burnup.....3-37

Figure 3-39: Yankee Core Evaluation Program (Stainless Steel Clad): PARAGON U²³⁶/U Prediction Versus Burnup.....3-38

Figure 3-40: Yankee Core Evaluation Program (Stainless Steel Clad): PARAGON U²³⁸/U Prediction Versus Burnup.....3-38

Figure 3-41: Yankee Core Evaluation Program (Stainless Steel Clad): PARAGON Pu²³⁹/Pu Prediction Versus Burnup.....3-39

Figure 3-42: Yankee Core Evaluation Program (Stainless Steel Clad): PARAGON Pu²⁴⁰/Pu Prediction Versus Burnup.....3-39

Figure 3-43: Yankee Core Evaluation Program (Stainless Steel Clad): PARAGON Pu²⁴¹/Pu Prediction Versus Burnup.....3-40

Figure 3-44: Yankee Core Evaluation Program (Stainless Steel Clad): PARAGON Pu²⁴²/Pu Prediction Versus Burnup.....3-40

Figure 3-45: Yankee Core Evaluation Program (Stainless Steel Clad): PARAGON Pu²³⁹/U²³⁸ Prediction Versus Burnup.....3-41

Figure 3-46: Yankee Core Evaluation Program (Stainless Steel Clad): PARAGON Pu²³⁹/Pu²⁴⁰ Prediction Versus Burnup.....3-41

Figure 3-47: Yankee Core Evaluation Program (Stainless Steel Clad): PARAGON Pu²⁴⁰/Pu²⁴¹ Prediction Versus Burnup.....3-42

Figure 3-48: Yankee Core Evaluation Program (Stainless Steel Clad): PARAGON Pu²⁴¹/Pu²⁴² Prediction Versus Burnup.....3-42

Figure 3-49: Yankee Core Evaluation Program (Stainless Steel Clad): PARAGON U²³⁶/U²³⁵ Prediction Versus Burnup.....3-43

Figure 3-50: Yankee Core Evaluation Program (Stainless Steel Clad): PARAGON U²³⁵/U²³⁸ Prediction Versus Burnup.....3-43

Figure 3-51: Yankee Core Evaluation Program (Zircaloy Clad): PARAGON U²³⁵/U Prediction Versus Burnup.....3-44

Figure 3-52: Yankee Core Evaluation Program (Zircaloy Clad): PARAGON U²³⁶/U Prediction Versus Burnup.....3-44

Figure 3-53: Yankee Core Evaluation Program (Zircaloy Clad): PARAGON U²³⁸/U Prediction Versus Burnup.....3-45

Figure 3-54: Yankee Core Evaluation Program (Zircaloy Clad): PARAGON Pu²³⁹/Pu Prediction Versus Burnup.....3-45

Figure 3-55: Yankee Core Evaluation Program (Zircaloy Clad): PARAGON Pu²⁴⁰/Pu Prediction Versus Burnup.....3-46

Figure 3-56: Yankee Core Evaluation Program (Zircaloy Clad): PARAGON Pu²⁴¹/Pu Prediction Versus Burnup.....3-46

Figure 3-57: Yankee Core Evaluation Program (Zircaloy Clad): PARAGON Pu²⁴²/Pu Prediction Versus Burnup.....3-47

Figure 3-58: Yankee Core Evaluation Program (Zircaloy Clad): PARAGON Pu²³⁹/U²³⁸ Prediction Versus Burnup.....3-47

Figure 3-59: Yankee Core Evaluation Program (Zircaloy Clad): PARAGON Pu²³⁹/Pu²⁴⁰ Prediction Versus Burnup.....3-48

Figure 3-60: Yankee Core Evaluation Program (Zircaloy Clad): PARAGON Pu²⁴⁰/Pu²⁴¹ Prediction Versus Burnup.....3-48

Figure 3-61: Yankee Core Evaluation Program (Zircaloy Clad): PARAGON Pu²⁴¹/Pu²⁴² Prediction Versus Burnup.....3-49

Figure 3-62: Yankee Core Evaluation Program (Zircaloy Clad): PARAGON U²³⁶/U²³⁵ Prediction Versus Burnup.....3-49

Figure 3-63: Yankee Core Evaluation Program (Zircaloy Clad): PARAGON U²³⁵/U²³⁸ Prediction Versus Burnup.....3-50

Figure 4-1: Critical Boron Concentration Versus Cycle Burnup Comparisons: Plant A Cycle 104-20

Figure 4-2: Critical Boron Concentration Versus Cycle Burnup Comparisons: Plant A Cycle 11 ...4-21

Figure 4-3: Critical Boron Concentration Versus Cycle Burnup Comparisons: Plant B Cycle 174-22

Figure 4-4: Critical Boron Concentration Versus Cycle Burnup Comparisons: Plant B Cycle 184-23

Figure 4-5: Critical Boron Concentration Versus Cycle Burnup Comparisons: Plant C Cycle 25 ...4-24

Figure 4-6: Critical Boron Concentration Versus Cycle Burnup Comparisons: Plant C Cycle 26 ...4-25

Figure 4-7: Critical Boron Concentration Versus Cycle Burnup Comparisons: Plant D Cycle 94-26

Figure 4-8: Critical Boron Concentration Versus Cycle Burnup Comparisons: Plant D Cycle 10 ...4-27

Figure 4-9: Critical Boron Concentration Versus Cycle Burnup Comparisons: Plant D Cycle 11 ...4-28

Figure 4-10: Critical Boron Concentration Versus Cycle Burnup Comparisons: Plant E Cycle 25 ...4-29

Figure 4-11: Critical Boron Concentration Versus Cycle Burnup Comparisons: Plant F Cycle 10 ...4-30

Figure 4-12: Critical Boron Concentration Versus Cycle Burnup Comparisons: Plant F Cycle 11 ...4-31

Figure 4-13: Critical Boron Concentration Versus Cycle Burnup Comparisons: Plant F Cycle 12 ...4-32

Figure 4-14: Critical Boron Concentration Versus Cycle Burnup Comparisons: Plant G Cycle 13...4-33

Figure 4-15: Critical Boron Concentration Versus Cycle Burnup Comparisons: Plant H Cycle 14-34

Figure 4-16: Critical Boron Concentration Versus Cycle Burnup Comparisons: Plant I Cycle 13.....4-35

Figure 4-17: Critical Boron Concentration Versus Cycle Burnup Comparisons: Plant I Cycle 14.....4-36

Figure 4-18: Critical Boron Concentration Versus Cycle Burnup Comparisons: Plant J Cycle 10...4-37

Figure 4-19: Critical Boron Concentration Versus Cycle Burnup Comparisons: Plant J Cycle 11....4-38

Figure 4-20: Critical Boron Concentration Versus Cycle Burnup Comparisons: Plant K Cycle 14-39

Figure 4-21: Critical Boron Concentration Versus Cycle Burnup Comparisons: Plant K Cycle 24-40

Figure 4-22: Critical Boron Concentration Versus Cycle Burnup Comparisons: Plant K Cycle 34-41

Figure 4-23: Critical Boron Concentration Versus Cycle Burnup Comparisons: Plant F Cycle 11
 –Calculated values with and without B10 correction.....4-42

Figure 4-24: Assembly Average Power Distribution: Plant A, Cycle 10, 3355 MWD/MTU Burnup...4-43

Figure 4-25: Assembly Average Power Distribution: Plant A, Cycle 10, 11958 MWD/MTU Burnup.4-44

Figure 4-26: Assembly Average Power Distribution: Plant A, Cycle 11, 1460 MWD/MTU Burnup...4-45

Figure 4-27: Assembly Average Power Distribution: Plant A, Cycle 11, 13052 MWD/MTU Burnup.4-46

Figure 4-28: Assembly Average Power Distribution: Plant A, Cycle 11, 19738 MWD/MTU Burnup.4-47

Figure 4-29: Assembly Average Power Distribution: Plant B, Cycle 17, 386 MWD/MTU Burnup.....4-48

Figure 4-30: Assembly Average Power Distribution: Plant B, Cycle 17, 7878 MWD/MTU Burnup...4-49

Figure 4-31: Assembly Average Power Distribution: Plant B, Cycle 17, 10930 MWD/MTU Burnup.4-50

Figure 4-32: Assembly Average Power Distribution: Plant B, Cycle 18, 1375 MWD/MTU Burnup...4-51

Figure 4-33: Assembly Average Power Distribution: Plant B, Cycle 18, 6926 MWD/MTU Burnup...4-52

Figure 4-34: Assembly Average Power Distribution: Plant C, Cycle 25, 252 MWD/MTU Burnup4-53

Figure 4-35: Assembly Average Power Distribution: Plant C, Cycle 25, 7080 MWD/MTU Burnup ..4-54

Figure 4-36: Assembly Average Power Distribution: Plant C, Cycle 25, 13400 MWD/MTU Burnup 4-55

Figure 4-37: Assembly Average Power Distribution: Plant C, Cycle 26, 788 MWD/MTU Burnup4-56

Figure 4-38: Assembly Average Power Distribution: Plant C, Cycle 26, 8073 MWD/MTU Burnup ..4-57

Figure 4-39: Assembly Average Power Distribution: Plant C, Cycle 26, 14838 MWD/MTU Burnup 4-58

Figure 4-40: Assembly Average Power Distribution: Plant D, Cycle 10, 1980 MWD/MTU Burnup ..4-59

Figure 4-41: Assembly Average Power Distribution: Plant D, Cycle 10, 9700 MWD/MTU Burnup ..4-60

Figure 4-42: Assembly Average Power Distribution: Plant D, Cycle 10, 20829 MWD/MTU Burnup 4-61

Figure 4-43: Assembly Average Power Distribution: Plant D, Cycle 11, 1010 MWD/MTU Burnup ..4-62

Figure 4-44: Assembly Average Power Distribution: Plant D, Cycle 11, 7309 MWD/MTU Burnup ..4-63

Figure 4-45: Assembly Average Power Distribution: Plant D, Cycle 11, 14998 MWD/MTU Burnup 4-64

Figure 4-46: Assembly Average Power Distribution: Plant J, Cycle 10, 4282 MWD/MTU Burnup ...4-65

Figure 4-47: Assembly Average Power Distribution: Plant J, Cycle 10, 11864 MWD/MTU Burnup .4-66

Figure 4-48: Assembly Average Power Distribution: Plant J, Cycle 10, 20700 MWD/MTU Burnup .4-67

Figure 4-49: Assembly Average Power Distribution: Plant J, Cycle 11, 638 MWD/MTU Burnup4-68

Figure 4-50: Assembly Average Power Distribution: Plant J, Cycle 11, 12294 MWD/MTU Burnup .4-69

Figure 4-51: Assembly Average Power Distribution: Plant J, Cycle 11, 20539 MWD/MTU Burnup .4-70

Figure 4-52: Assembly Average Power Distribution (PARAGON versus PHOENIX-P): Plant A, Cycle 10 BOC.....4-71

Figure 4-53: Assembly Average Power Distribution (PARAGON versus PHOENIX-P) : Plant A, Cycle 10 EOC.....4-72

Figure 4-54: Assembly Average Burnup Distribution (PARAGON versus PHOENIX-P) : Plant A, Cycle 10 EOC.....4-73

Figure 4-55: Assembly Average Power Distribution (PARAGON versus PHOENIX-P): Plant A, Cycle 11 BOC.....4-74

Figure 4-56: Assembly Average Power Distribution (PARAGON versus PHOENIX-P): Plant A, Cycle 11 EOC.....4-75

Figure 4-57: Assembly Average Burnup Distribution (PARAGON versus PHOENIX-P): Plant A, Cycle 11 EOC.....4-76

Figure 4-58: Assembly Average Power Distribution (PARAGON versus PHOENIX-P): Plant C, Cycle 25 BOC.....4-77

Figure 4-59: Assembly Average Power Distribution (PARAGON versus PHOENIX-P): Plant C, Cycle 25 EOC.....4-77

Figure 4-60: Assembly Average Burnup Distribution (PARAGON versus PHOENIX-P): Plant C, Cycle 25 EOC.....4-78

Figure 4-61: Assembly Average Power Distribution (PARAGON versus PHOENIX-P): Plant C, Cycle 26 BOC.....4-78

Figure 4-62: Assembly Average Power Distribution (PARAGON versus PHOENIX-P): Plant C, Cycle 26 EOC.....4-79

Figure 4-63: Assembly Average Burnup Distribution (PARAGON versus PHOENIX-P): Plant C, Cycle 26 EOC.....4-79

Figure 4-64: Assembly Average Power Distribution (PARAGON versus PHOENIX-P): Plant D, Cycle 10 BOC.....4-80

Figure 4-65: Assembly Average Power Distribution (PARAGON versus PHOENIX-P): Plant D, Cycle 10 EOC.....4-81

Figure 4-66: Assembly Average Burnup Distribution (PARAGON versus PHOENIX-P): Plant D, Cycle 10 EOC.....4-82

Figure 4-67: Assembly Average Power Distribution (PARAGON versus PHOENIX-P): Plant D, Cycle 11 BOC.....4-83

Figure 4-68: Assembly Average Power Distribution (PARAGON versus PHOENIX-P): Plant D, Cycle 11 EOC.....4-84

Figure 4-69: Assembly Average Burnup Distribution (PARAGON versus PHOENIX-P): Plant D, Cycle 11 EOC.....4-85

Figure 4-70: Assembly Average Power Distribution (PARAGON versus PHOENIX-P): Plant E, Cycle 25 BOC.....4-86

Figure 4-71: Assembly Average Power Distribution (PARAGON versus PHOENIX-P): Plant E, Cycle 25 EOC.....4-86

Figure 4-72: Assembly Average Burnup Distribution (PARAGON versus PHOENIX-P): Plant E, Cycle 25 EOC.....4-87

Figure 4-73: Assembly Average Power Distribution (PARAGON versus PHOENIX-P): Plant F, Cycle 11 BOC.....4-88

Figure 4-74: Assembly Average Power Distribution (PARAGON versus PHOENIX-P): Plant F, Cycle 11 EOC.....4-89

Figure 4-75: Assembly Average Burnup Distribution (PARAGON versus PHOENIX-P): Plant F, Cycle 11 EOC.....4-90

Figure 4-76: Assembly Average Power Distribution (PARAGON versus PHOENIX-P): Plant F, Cycle 12 BOC.....4-91

Figure 4-77: Assembly Average Power Distribution (PARAGON versus PHOENIX-P): Plant F, Cycle 12 EOC.....4-92

Figure 4-78: Assembly Average Burnup Distribution (PARAGON versus PHOENIX-P): Plant F, Cycle 12 EOC.....4-93

Figure 4-79: Core Average Axial Power Distribution (PARAGON versus PHOENIX-P): Plant A, Cycle 10, BOC.....4-94

Figure 4-80: Core Average Axial Power Distribution (PARAGON versus PHOENIX-P): Plant A, Cycle 10, MOC4-95

Figure 4-81: Core Average Axial Power Distribution (PARAGON versus PHOENIX-P): Plant A, Cycle 10, EOC..... 4-96

Figure 4-82: Core Average Axial Power Distribution (PARAGON versus PHOENIX-P): Plant A, Cycle 11, BOC..... 4-97

Figure 4-83: Core Average Axial Power Distribution (PARAGON versus PHOENIX-P): Plant A, Cycle 11, MOC4-98

Figure 4-84: Core Average Axial Power Distribution (PARAGON versus PHOENIX-P): Plant A, Cycle 11, EOC.....4-99

Figure 4-85: Core Average Axial Power Distribution (PARAGON versus PHOENIX-P): Plant C, Cycle 25, BOC.....4-100

Figure 4-86: Core Average Axial Power Distribution (PARAGON versus PHOENIX-P): Plant C, Cycle 25, MOC4-101

Figure 4-87: Core Average Axial Power Distribution (PARAGON versus PHOENIX-P): Plant C, Cycle 25, EOC.....4-102

Figure 4-88: Core Average Axial Power Distribution (PARAGON versus PHOENIX-P): Plant C, Cycle 26, BOC.....4-103

Figure 4-89: Core Average Axial Power Distribution (PARAGON versus PHOENIX-P): Plant C, Cycle 26, MOC4-104

Figure 4-90: Core Average Axial Power Distribution (PARAGON versus PHOENIX-P): Plant C, Cycle 26, EOC.....4-105

Figure 4-91: Core Average Axial Power Distribution (PARAGON versus PHOENIX-P): Plant F, Cycle 11, BOC.....4-106

Figure 4-92: Core Average Axial Power Distribution (PARAGON versus PHOENIX-P): Plant F, Cycle 11, MOC4-107

Figure 4-93: Core Average Axial Power Distribution (PARAGON versus PHOENIX-P): Plant F, Cycle 11, EOC.....4-108

Figure 4-94: Core Average Axial Power Distribution (PARAGON versus PHOENIX-P): Plant F, Cycle 12, BOC.....4-109

Figure 4-95: Core Average Axial Power Distribution (PARAGON versus PHOENIX-P): Plant F, Cycle 12, MOC4-110

Figure 4-96: Core Average Axial Power Distribution (PARAGON versus PHOENIX-P): Plant F, Cycle 12, EOC.....4-111

Figure 4-97: Core Average Axial Power Distribution (PARAGON versus PHOENIX-P): Plant G, Cycle 13, BOC.....4-112

Figure 4-98: Core Average Axial Power Distribution (PARAGON versus PHOENIX-P): Plant G, Cycle 13, MOC4-113

Figure 4-99: Core Average Axial Power Distribution (PARAGON versus PHOENIX-P): Plant G, Cycle 13, EOC.....4-114

Figure 4-100: Core Average Axial Power Distribution (PARAGON versus PHOENIX-P): Plant G, Cycle 14, BOC.....4-115

Figure 4-101: Core Average Axial Power Distribution (PARAGON versus PHOENIX-P): Plant G, Cycle 14, MOC4-116

Figure 4-102: Core Average Axial Power Distribution (PARAGON versus PHOENIX-P): Plant G, Cycle 14, EOC.....4-117

Section 1.0: Introduction

The purpose of this report is to provide documentation of the qualification of PARAGON, a new Westinghouse neutron transport code. It is also requested that the NRC provide generic approval of PARAGON for use with Westinghouse's nuclear design code system or as a standalone code. The code will be used primarily to calculate nuclear input data for three-dimensional core simulators. Based on the qualification of PARAGON as documented herein, PARAGON can be used as a standalone or as a direct replacement for all the previously licensed Westinghouse Pressurized Water Reactor ("PWR") lattice codes, such as PHOENIX-P. Thus, other topicals that reference the Westinghouse nuclear design code system will remain applicable with PARAGON.

A major nuclear design code system in use at Westinghouse since 1988 consists of two primary codes, PHOENIX-P and ANC. PHOENIX-P is the neutron transport code currently used to provide nuclear input data for ANC. The qualification and license approval of the use of PHOENIX-P for PWR core design calculations is provided in Reference 1-2.

PARAGON is a new code written entirely in FORTRAN 90/95. PARAGON is a replacement for PHOENIX-P and its primary use will be to provide the same types of input data that PHOENIX-P generates for use in three dimensional core simulator codes. This includes macroscopic cross sections, microscopic cross sections for feedback adjustments to the macroscopic cross sections, pin factors for pin power reconstruction calculations, and discontinuity factors for a nodal method solution.

PARAGON is based on collision probability – interface cell coupling methods. PARAGON provides flexibility in modeling that was not available in PHOENIX-P including exact cell geometry representation instead of cylinderization, multiple rings and regions within the fuel pin and the moderator cell geometry, and variable cell pitch. The solution method permits flexibility in choosing the quality of the calculation through both increasing the number of regions modeled within the cell and the number of angular current directions tracked at the cell interfaces. Section 2 will provide further details on PARAGON theory and features.

The qualification of a nuclear design code is a large undertaking since it must address the qualification of the methodology used in the code, the implementation of that methodology, and its application within a nuclear design system. For this reason, Westinghouse has historically used a systematic qualification process, which starts with the qualification of the basic methodology used in the code and proceeds through logical steps to the qualification of the code as used with the entire system. This process was used when qualifying PHOENIX-P/ANC system in Reference 1-2. This same process is followed for the qualification of PARAGON in this report.

Consistent with the qualification process described above, the qualification of PARAGON will consist of three parts: 1) comparisons to critical experiments and isotopic measurements, 2) comparisons of assembly calculations with Monte Carlo method calculations (MCNP), and 3) comparisons against measured plant data. The first two parts will qualify the methodology used in PARAGON and its implementation. The third part will qualify the use of PARAGON data for core design applications. Where appropriate, comparisons will also be made to PHOENIX-P results.

The current PARAGON cross section library is a 70-group library with the same group structure as the library currently used with PHOENIX-P. The PARAGON qualification library has been improved []^{a,c}.

This report is organized in the Sections as described below.

Section 2 presents an overview of the PARAGON theory and its implementation. The nuclear data library used for this qualification is also described in this section.

Section 3 presents the results of PARAGON calculations for many standard critical experiments. These include the Strawbridge-Barry 101 criticals, the Kritz high temperature experiments, and the Babcock and Wilcox critical experiments with Urania-Gadolinia fuel. Section 3 also presents reactivity and power distribution comparisons between PARAGON and Monte Carlo (MCNP) calculations for single assembly problems. Various assembly designs similar to those currently in use in PWR cores are included in these MCNP/PARAGON comparisons. Finally, isotopic comparisons are made between PARAGON and the Yankee and Saxton isotopic measurements.

Section 4 presents the results of using PARAGON input data with a three-dimensional core simulator model (in this case ANC) and compares the calculations to actual plant measurements. The parameters compared are boron letdown curves, beginning of cycle (BOC) HZP critical boron, BOC isothermal temperature coefficients (ITC), and BOC rodworths. Comparisons of the results of using PARAGON input data with a three-dimensional core simulator model (ANC) against measured core power distributions are also shown for several cycles. Section 4 also presents comparisons of PARAGON/ANC model results against those of PHOENIX-P/ANC for core calculations for which there are no plant measurements (e.g. shutdown margin, ejected rod, etc).

Section 2.0: PARAGON Methodology

2.1 Introduction

PARAGON is a two-dimensional multi-group neutron (and gamma) transport code. It is an improvement over the Westinghouse licensed code PHOENIX-P (Reference 2-1). The main difference between PARAGON (Reference 2-2) and PHOENIX-P resides in the flux solution calculation. PHOENIX-P uses a nodal cell solution coupled to an S4 transport solution as described in Reference 2-1. PARAGON uses the Collision Probability theory within the interface current method to solve the integral transport equation. Throughout the whole calculation, PARAGON uses the exact heterogeneous geometry of the assembly and the same energy groups as in the cross-section library to compute the multi-group fluxes for each micro-region location of the assembly.

In order to generate the multi-group data that will be used by a core simulator code PARAGON goes through four steps of calculations: resonance self-shielding, flux solution, homogenization and burnup calculation. This section will describe the theoretical models that each of the PARAGON components is using.

2.2 PARAGON Cross-sections Library

The current PARAGON cross section library uses ENDF/B as the basic evaluated nuclear data files. Currently the library has 70 neutron energy groups []^{a,c}. But PARAGON is designed to work with any number of energy groups that is specified in the library, and Westinghouse intends to continuously improve the library as better data become available and recommended by the data evaluation community. This library has been generated using the NJOY processing code (Reference 2-3). To account for the resonance self-shielding effect, the group cross-sections are tabulated as a function of both temperature and background scattering cross-section (dilution). The resonance self-shielding module of the code uses these resonance self-shielding tables to compute the isotopic self-shielded cross-section in the real heterogeneous situation. The library contains energy group cross-sections and transport-corrected P0 scattering matrices as a function of temperature. The P0 scattering matrices contain diagonal corrections for anisotropic scattering. []^{a,c}.

2.3 Theory of PARAGON modules

This section will describe in detail the physics models and different mathematical approximations that each of the PARAGON components is using.

2.3.1 Cross-section resonance self-shielding module

PARAGON uses the same resonance self-shielding theory as in PHOENIX-P (Reference 2-1) but generalized to handle the multi-regions in cells which is needed mainly to support the fuel rod design codes. PHOENIX-P method is based on an average-rod resonance self-shielding algorithm (Reference 2-4). The non-regularity of the lattice is taken into account using space dependent Dancoff factor corrections. In the resonance energy range, the neutron slowing-down is the most dominant process. This remark supports the assumption of the factorization of the flux into a product of a macroscopic term ψ varying slowly with the lethargy and a term ϕ describing the local variations due to the resonances of the isotopes:

$$\phi = \psi\varphi \quad (2-1)$$

As in the PHOENIX-P code, PARAGON uses the collision probabilities to solve the slowing-down equation in pin cells with the real heterogeneous geometry. The rational approximation is used to evaluate the fuel to fuel collision probabilities and the flux ϕ is approximated using the intermediate resonance approximation (Reference 2-4).

2.3.2 Flux calculation module

The neutron (or gamma) flux, obtained from the solution of the transport equation, is a function of three variables: energy, space and angle. For the energy variable, PARAGON (Reference 2-2) uses the multi-group method where the flux is integrated over the energy groups. For the spatial variable, the assembly is subdivided into a number of sub-domains or cells and the integral transport equation is solved in the cells using the collision probability method. The cells of the assembly are then coupled together using the interface current technique (Reference 2-2). At the interface, the solid angle is discretized into a set of cones (Reference 2-2, 2-5) where the surface fluxes are assumed to be constant over each angular cone. PARAGON has been written in a general way so that the cell coupling order is limited only by the computer memory. The collision probability method is based on the flat-flux assumption, which will require subdividing the cells into smaller zones. Thus, for each cell in the assembly, the system of equations to be solved is given by the discretized one energy group transport equation:

$$\begin{aligned}\phi_i &= \sum_{\alpha, \rho\nu} P_{is_\alpha}^{\rho\nu} J_{-\alpha}^{\rho\nu} + \sum_j V_j P_{ij} F_j, \\ J_{+\alpha}^{\rho\nu} &= \sum_{\beta, \eta\mu} P_{s_\alpha s_\beta}^{\rho\nu \eta\mu} J_{-\beta}^{\eta\mu} + \sum_i P_{s_\alpha i}^{\rho} F_i, \\ J_{-\alpha}^{\rho\nu} &= \sum_{\beta, \eta\mu} B_{\alpha\beta}^{\rho\nu \eta\mu} J_{+\beta}^{\eta\mu}\end{aligned}\quad (2-2)$$

The following notations are used: ϕ_i for the average flux in zone i (flat-flux assumption), $J_{\pm\alpha}^{\rho\nu}$ for the current entering (-) or leaving (+) the cell through the surface oriented by the exterior or interior normal $\vec{n}_{\pm\alpha}$, $B_{\alpha\beta}^{\rho\nu \eta\mu}$ for the albedo coefficients and F_j for the neutron (fission and scattering) emission density or gamma production density (prompt fission, neutron capture, scattering, decay of fission products, etc). In those equations, the set of cones are indicated by (ρ, ν) and (η, μ) defining the azimuthal φ (not to be confused with the flux ϕ in the previous section) and polar ϑ coupling orders:

$$[\varphi, \vartheta] \in [0, 2\pi] \times [0, \pi] = \bigcup_{\rho} [\varphi_{\rho}, \varphi_{\rho+1}] \times \bigcup_{\nu} [\vartheta_{\nu}, \vartheta_{\nu+1}] \quad (2-3)$$

The first flight collision probabilities (P_{ij}), transmission probabilities (P_{ss}) and leakage (P_{si}) (or surface to volume (P_{is})) collision probabilities are given by:

$$\begin{aligned}P_{ij} &= \frac{1}{V_j} \int_{D_i} d\vec{r} \int_{D_j} d\vec{r}' \frac{e^{-\tau(u)}}{4\pi u^2}, \\ P_{is_\alpha}^{\rho\nu} &= \frac{1}{\pi S_\alpha \sqrt{A_\alpha^{\rho\nu}}} \int_{D_i} d\vec{r} \int_{\partial D_\alpha} d^2 r_s \psi_{-\alpha}^{\rho\nu}(\vec{\Omega})(\vec{\Omega} \cdot \vec{n}_{-\alpha}) \frac{e^{-\tau(r)}}{t^2}, \\ P_{s_\alpha s_\beta}^{\rho\nu \eta\mu} &= \frac{\sqrt{A_\alpha^{\rho\nu}}}{\pi S_\beta \sqrt{A_\beta^{\eta\mu}}} \int_{\partial D_\alpha} d^2 r_s' \int_{\partial D_\beta} d^2 r_s \psi_{+\alpha}^{\rho\nu}(\vec{\Omega}) \psi_{-\beta}^{\eta\mu}(\vec{\Omega})(\vec{\Omega} \cdot \vec{n}_{+\alpha})(\vec{\Omega} \cdot \vec{n}_{-\beta}) \frac{e^{-\tau(r')}}{t'^2}\end{aligned}\quad (2-4)$$

where the following definitions are used:

- $t' = \|\vec{r}'_s - \vec{r}_s\|$, $t = \|\vec{r}'_s - \vec{r}\|$ and $u = \|\vec{r} - \vec{r}'\|$ are the path of neutrons from surface to surface, volume to surface and volume to volume respectively, and $\tau(x)$ is the optical path.
- S_α is the surface area of the cell's surface element α and V_i is the volume of zone i .
- The domains of integration cover the zone's volume D_i and the cell's surface element ∂D_α .

The transmission (P_{ss}) and leakage (P_{si}) collision probabilities in the equations above have been derived by expanding the angular fluxes, at cell surfaces ∂D_α , in a finite set of discrete angular fluxes with the representative functions $\psi_{\pm,\alpha}^{\rho\nu}(\vec{\Omega})$. Two distinct components are used for entering and outgoing fluxes:

$$\psi_{\pm,\alpha}^{\rho\nu}(\vec{\Omega}) = \frac{1}{\sqrt{A_\alpha^{\rho\nu}}} H(\vec{\Omega} \in \Omega_{\rho\nu}) \quad (2-5)$$

where

$$A_\alpha^{\rho\nu} = \frac{1}{\pi} \int_{(4\pi)} (\vec{\Omega} \cdot \vec{n}_{\pm,\alpha}) H(\vec{\Omega} \in \Omega_{\rho\nu}) d\vec{\Omega}, \quad (2-6)$$

and $H(\vec{\Omega} \in \Omega_{\rho\nu})$ is the Heaviside distribution defined by:

$$H(\vec{\Omega} \in \Omega_{\rho\nu}) = \begin{cases} 1 \Rightarrow \vec{\Omega} \in \Omega_{\rho\nu} \Leftrightarrow [\varphi, \vartheta] \in [\varphi_\rho, \varphi_{\rho+1}] \times [\vartheta_\nu, \vartheta_{\nu+1}] \\ 0 \Rightarrow \vec{\Omega} \notin \Omega_{\rho\nu} \end{cases} \quad (2-7)$$

The solution of the above algebraic system of equation (2-2) over the entire assembly is obtained by the response heterogeneous matrix method, which uses current-flux iterations (Reference 2-2, 2-6). The flux solver module has been extensively tested and proved to perform very accurately (Reference 2-2, 2-7, 2-8).

2.3.3 Homogenization module

The next step in PARAGON calculation after the flux solution is the leakage correction. The purpose of this module is to compute the multi-group diffusion coefficients and the multi-group critical flux (spectrum) for the entire homogenized assembly (or parts of the assembly, like baffle/reflector regions). This is usually achieved by solving the fundamental mode of the transport equation (Reference 2-4). The flux solution to the transport equation is assumed to be separable in a space part and an energy and angle part: $\phi(\vec{r}, E, \vec{\Omega}) = \varphi(\vec{r})\psi(E, \vec{\Omega})$. This assumption leads to the following B_1 system of equations (flux-current) to be solved (Reference 2-4):

$$\begin{aligned} \Sigma_g \psi_g \pm iB J_g &= \sum_{g'} \Sigma_{0,g' \rightarrow g} \psi_{g'} + \chi_g, \\ \pm iB \psi_g + 3\alpha_g \Sigma_g J_g &= 3 \sum_{g'} \Sigma_{1,g' \rightarrow g} J_{g'}. \end{aligned} \quad (2-8)$$

where: (ψ_g, J_g) are the fundamental mode flux and current for group g , Σ_g is the homogenized total cross-section, $\Sigma_{0,g \rightarrow g}$ and $\Sigma_{1,g \rightarrow g}$ are the isotropic and the anisotropic scattering matrices, χ_g is the fission spectrum (normalized to one), $i^2 = -1$, B is the fundamental material buckling and

$$\alpha_g = \begin{cases} \frac{1}{3}x^2 \left(\frac{\arctan(x)}{x - \arctan(x)} \right) & \text{if } x^2 = \left(\frac{B}{\Sigma_g}\right)^2 > 0 \\ \frac{1}{3}x^2 \left(\frac{\ln\left(\frac{1+x}{1-x}\right)}{\ln\left(\frac{1+x}{1-x}\right) - 2x} \right) & \text{if } x^2 = -\left(\frac{B}{\Sigma_g}\right)^2 > 0 \end{cases} \quad (2-9)$$

Note that the above equations are usually solved for the critical material buckling B^2 which makes the neutron multiplication factor equal to one.

For each energy group, the micro-region fluxes are corrected by the ratio of the fundamental mode fluxes and the assembly averaged fluxes to get the final micro-region critical fluxes.

Another model (Reference 2-9) to compute the critical flux has been implemented in PARAGON. In this model, the neutron source has been modified by adding an artificial absorption cross-section $D_g B^2$ in each micro-region of the assembly. In this case, the diffusion coefficients are first computed by using the previous model. In case of fuel assemblies, the two models are comparable. The second model is mainly used in the case of critical experiments for which a measured buckling is usually available.

2.3.4 Depletion module

The assembly composition changes following neutron irradiation are obtained by calculating the isotopic depletion and buildup in the heterogeneous geometry, using an effective one-group collapsed flux and cross-sections. The differential equations solved by PARAGON depletion module are given by:

$$\frac{d}{dt} N_i(t) = \sum_j \gamma_{j \rightarrow i} \sigma_{f,j} \phi(t) N_j(t) - N_i(t) [\sigma_{a,i} \phi(t) + \lambda_i] + N_j(t) \lambda_j + N_k(t) \sigma_{ki} \phi(t) \quad (2-10)$$

Where:

N_i is the concentration (number density) for the isotope i

$\gamma_{j \rightarrow i}$ is the yield of isotope i per fission of isotope j

$\sigma_{f,j}$ is the energy-integrated microscopic fission cross-section of isotope j

$\sigma_{a,i}$ is the energy-integrated microscopic absorption cross-section of isotope i

λ_i is the decay constant of isotope i

λ_j is the decay constant of the parent isotope j

σ_{ki} is the energy-integrated microscopic capture cross-section of isotope k leading to the formation of isotope i

$\phi(t)$ is the energy-integrated flux for the zone where the isotope is present.

PARAGON uses the predictor-corrector technique to better account for the flux level variation (Reference 2-4). The module is, however general enough to the extent that any new chain can be added easily with very minor changes in the code.

The code detects automatically the regions to be depleted, but the user has the option to hold any region in the assembly as non-depletable. For the boron depletion, the user has a choice of depleting it according to a letdown curve that is provided through the input or exponentially (i.e depletion chain). Note that gamma heating is taken into account in the evaluation of the flux level during the burnup depletion.

2.4 Other Modeling Capabilities

This section will describe the other capabilities implemented in PARAGON such as the fuel temperatures, branch calculations etc.

2.4.1 Temperature Model

Through the input, PARAGON is provided with []^{a,c} temperature tables [

]^{a,c}.

PARAGON has a module that interpolates in these tables to compute the temperatures for each isotope present in the model before calling the self-shielding module for cross-sections calculations.

2.4.2 Doppler Branch Calculation

A Doppler branch calculation capability is built into PARAGON. This capability permits fuel temperature variations to be modeled while keeping all other parameters constant. Results of these calculations are used to generate changes in []^{a,c} which are passed to the core models to capture Doppler effects. [

]^{a,c}.

2.4.3 Thermal Expansion

A model to expand the radii of the cylindrical region has been implemented in PARAGON. [

]^{a,c}. The code uses this capability mainly in the case of the Doppler branch calculation. It also has a flag to turn it on in any calculation step.

2.4.4 Interface Module

PARAGON has the flexibility of printing many types of micro and macro physics parameters. Hence the user can request to edit the fluxes, partial currents, surface fluxes, different reaction rates, isotopic distribution etc. The editing could be done for micro-regions, or as an average over a cell or as an average over a group of cells, and for any number of energy groups (i.e. the code can collapse to any number of groups for editing).

PARAGON uses files to store the data needed for core calculations. Those files are processed by other codes used for core modeling and analysis.

2.4.5 Reflector Modeling

PARAGON generates the reflector constants [

] ^{a, c}.

Section 3.0: Critical Experiments and Isotopics

The primary use of PARAGON will be to generate nuclear data for three dimensional core simulator models. Thus, the best qualification of PARAGON is through comparison of core simulator plant models developed using PARAGON-calculated nuclear input data against measured plant data. These comparisons will be made in section 4 of this report.

As described in Section 1.0, Westinghouse has historically used a systematic qualification process which starts with the qualification of the basic methodology used in the code and proceeds through logical steps to the qualification of the code as used with a complete nuclear code system (Reference 3-1). Following this process for the PARAGON code, PARAGON has been used in stand-alone mode to model standard critical experiments. The results of these calculations are presented in this section. In addition, comparisons of the results of PARAGON single assembly calculations with the same assembly run in the Monte Carlo code MCNP (Reference 3-12) are shown for both reactivity and power distribution. The MCNP calculations used a continuous energy ENDF/B-VI based library.

At the end of this section, a comparison of PARAGON calculated isotopics against those measured at Saxton and Yankee is presented.

3.1 Critical Experiments

PARAGON results from modeling the following experiments are provided in this section: 1) the Strawbridge-Barry 101 Criticals (Section 3.1.1), 2) the KRITZ high-temperature criticals (Section 3.1.2), and 3) the Babcock & Wilcox Spatial Criticals (Section 3.1.3).

3.1.1 Strawbridge-Barry 101 Criticals

The Strawbridge and Barry criticals contains 101 uniform, light water lattices. These criticals contain 40 uranium oxide and 61 uranium metal cold clean experiments (Reference 3-2). These critical experiments have historically been included in Westinghouse code qualifications since they cover a wide range of lattice parameters and therefore provide a severe test for the lattice code to predict reactivities accurately over a broad range of conditions.

Since the Strawbridge-Barry criticals are uniform lattices for which experimental bucklings have been reported, these criticals have been treated as single pin cells in PARAGON. The range of lattice parameters covered by these criticals are:

Enrichment (a/o U ²³⁵) :	1.04 to 4.069
Boron concentration (ppm):	0 to 3392
Water to uranium ratio:	1.0 to 11.96
Pellet diameter (cm):	0.44 to 2.35
Lattice pitch (cm):	0.95 to 4.95
Clad material:	none, aluminum, stainless steel
Lattice type:	square, hexagonal
Fuel density (g/cm ³):	7.5 to 18.9

Since the current version of PARAGON does not model hexagonal fuel, the hexagonal pin cells were replaced by equivalent square pin cells which preserve moderator area.

A summary of the results is shown in Table 3-1. This table shows reactivity predictions for various groupings of the criticals. Of particular interest is the result for all UO₂ experiments. The mean K_{eff} for these forty experiments is []^{a,c} with a standard deviation of []^{a,c}. The mean K_{eff} for all experiments was []^{a,c} with a standard deviation of []^{a,c}. Figures 3-1 through 3-5 show the PARAGON results as a function of water to uranium ratio, enrichment, pellet diameter, experimental buckling, and soluble boron concentration (seven criticals had soluble boron). The results in these figures

show excellent performance for PARAGON over the entire range of each parameter with no significant bias or trends for any lattice parameter.

3.1.2 KRITZ High-Temperature Criticals

The KRITZ high-temperature critical experiments series (Reference 3-3) provide critical benchmark data for uranium-fueled, water moderated lattices at high temperatures. These experiments were run at temperatures up to 245 °C (473 °F) covering temperatures close to the range used in light water reactor cores. The details of the experiments are provided in Reference 3-3. Twelve KRITZ experiments were modeled in PARAGON. The modeled experiments included two lattice configurations (39x39 and 46x46) over a temperature range from 41.2 to 245.8 °C with boron concentrations from essentially zero to 175 ppm. The axial bucklings provided in the reference were used to calculate K_{eff} . Table 3-2 summarizes the results of the PARAGON calculations for these criticals. For each experiment, the table shows the lattice configuration, the soluble boron concentration, the water temperature, the axial buckling used to determine K_{eff} , and the PARAGON calculated K_{eff} . The mean K_{eff} for all twelve experiments was []^{a,c} with a standard deviation of []^{a,c}. The very small standard deviation shows that PARAGON predicts very consistently across the large temperature range of these experiments with no significant trend.

3.1.3 Babcock & Wilcox Spatial Criticals

A large physics verification program sponsored by USAEC and Babcock & Wilcox (B&W) was conducted at B&W's Lynchburg Research Center during the 1970's. These experiments, which are documented in References 3-4 and 3-5, provided reactivity and power distribution measurements for typical PWR lattices at cold conditions for various configurations of fuel rods, guide thimbles, and several different burnable absorbers.

Since PARAGON can handle large problems, these experiments were modeled directly in PARAGON. For each experiment, the PARAGON k-infinity was compared to the k-infinity calculated by the Monte Carlo code MCNP for the same configuration. A cross section library developed by Westinghouse based on ENDF/B-VI was used with MCNP for the Monte Carlo calculations in this report. In addition, the axial buckling provided in the references was used with the PARAGON reactivity result to calculate K_{eff} . Details for each configuration are provided in the references.

Table 3-3 presents the PARAGON and MCNP results for B&W Core XI for loadings 1 through 9. Core XI contained low enriched uranium clad in aluminum in a 15x15 lattice. For each of the nine loadings, Table 3-3 shows the number of fuel rods, water rods and Pyrex burnable absorbers, the MCNP calculated k-infinity and standard deviation, the PARAGON calculated k-infinity, and the PARAGON K_{eff} calculated using the axial buckling. The mean PARAGON k-infinity for the nine configurations was []^{a,c} with a standard deviation of []^{a,c} which is within []^{a,c} pcm of the mean MCNP k-infinity of []^{a,c} which has a standard deviation of []^{a,c}. The mean PARAGON K_{eff} was []^{a,c} with a standard deviation of []^{a,c}. Power distributions for three of these experiments are shown in Figures 3-6 (loading 2), 3-7 (loading 6), and 3-8 (loading 9). The results shown in these figures demonstrate that the predicted PARAGON power distribution agrees very well with measurement with the average difference being about []^{a,c}.

Tables 3-4, 3-5, 3-6 and 3-7 present PARAGON results for B&W cores with gadolinia rods, with and without control rods. Table 3-4 shows results for cores with the number of gadolinia rods varying from 0 to 36 in 15x15 lattices of 2.46 w/o enriched fuel. Table 3-5 shows results from the same cores in the presence of B_4C control rods. Table 3-6 shows results from cores with varying number of gadolinia rods (0 to 36) with and without control rods in 15x15 lattices of 4.02 w/o enriched fuel. Table 3-7 simulates a CE 16x16 lattice with 2x2 water rods with 4.02 w/o enriched fuel and from 0 to 32 gadolinia rods. As in the B&W pyrex experiments shown in Table 3-3, MCNP was run for all configurations for k-infinity comparisons to PARAGON. The maximum difference between the mean MCNP and PARAGON k-infinities for these tables is []^{a,c}. The mean PARAGON K_{eff} varies from critical by []^{a,c}. The standard deviations are all below []^{a,c}.

Comparisons of measured and PARAGON predicted power distributions for three of these experiments are provided in Figures 3-9 (Core 5, 28 gadolinia rods), 3-10 (Core 12, no gadolinia rods), and 3-11 (Core 14, 28 gadolinia rods). As with the pyrex cores, the power distributions of these cores were very well predicted by PARAGON with the mean measured to predicted rod power difference being less than []^{a,c} for all three core configurations.

The reactivity results for all twenty-nine B&W critical experiments were very good with a mean keff of []^{a,c} and a standard deviation of []^{a,c}. The average difference between the measured and PARAGON power distribution for the six experiments shown in Figures 3-6 through 3-11 was []^{a,c} per cent with an average standard deviation of []^{a,c} per cent.

3.2 Monte Carlo Assembly Benchmarks

Thirteen different assembly configurations were calculated in both PARAGON and the Monte Carlo code MCNP. These assembly configurations were chosen to cover a variety of lattice types, burnable absorbers, a large enrichment range and both UO₂ and MOX. Specifically, the following describes the parameter range covered by these configurations:

Lattice types:	Westinghouse Combustion Engineering	14x14, 15x15, 16x16, 17x17 14x14, 16x16
Burnable absorbers:		Integral Fuel Burnable Absorber (IFBA), gadolinia (Gd ₂ O ₃), erbia (Er ₂ O ₃)
Enrichment:		2.10 to 5.00 w/o
Fuel:		UO ₂ and MOX

Table 3-8 presents the reactivity results of these assembly calculations. For each assembly configuration, the table presents the lattice type, the enrichment, the number and type of burnable absorber present, the MCNP calculated k-infinity, the PARAGON calculated k-infinity and the difference in pcm between the PARAGON and MCNP k-infinities. As can be seen from the table, the mean difference between the PARAGON and MCNP k-infinities was very good at []^{a,c} with a standard deviation of []^{a,c}. The largest difference is for the MOX assembly at []^{a,c}. The agreement for the gadolinia assembly is very good at []^{a,c}.

Figures 3-12 through 3-24 present comparisons between MCNP and PARAGON rod power distributions for the thirteen assemblies listed in Table 3-8. For each power distribution figure, three statistical quantities are listed: 1) the maximum difference between the MCNP and PARAGON rod powers, 2) the average deviation from the mean of the rod power differences, and 3) the standard deviation of the rod power differences. These figures demonstrate that PARAGON rod power predictions are well predicted. The average rod power differences ranged from []^{a,c}. Sufficient histories were run so that the MCNP standard deviation for each rod power was less than []^{a,c} in all cases.

3.3 Saxton and Yankee Isotopics Data

The spectrograph-measured isotopics data for Saxton Cores 2 and 3 with mixed oxide fuel, Yankee cores 1, 2, and 4 with stainless steel clad fuel, and Yankee Core 5 with zircaloy clad fuel have been compared to PARAGON isotopic concentrations. The measured data for these isotopics are documented in References 3-6, 3-7, 3-8, and 3-9 (Saxton) and 3-10 and 3-11 (Yankee). Since the measured fuel rods for both the Saxton and Yankee cases were far enough away from lattice heterogeneities that they were exposed to the asymptotic flux spectrum, PARAGON pin cell calculations were used for these comparisons. The pin cell cases were set up to approximate the core operating history for each isotopic data set.

The Saxton Cores 2 and 3 isotopic comparisons for the major isotopes are shown in Figures 3-25 through 3-37. Comparisons for the Yankee Cores 1,2, and 4 stainless steel clad UO_2 fuel isotopics are shown in Figures 3-38 through 3-50. Comparisons for Yankee Core 5 zircaloy clad UO_2 fuel isotopics are shown in Figures 3-51 through 3-63.

As noted in Reference 3-1, the Saxton isotopic case was particularly challenging since it is for a mixture of PuO_2 in a natural uranium matrix. In addition, the wet fraction was changed at an intermediate burnup due to the removal of fuel rods for isotopics measurements. As seen in the figures, PARAGON matches the measured values both in shape and magnitude.

The Yankee core data represent a typical UO_2 light water lattice with two clad materials. The figures comparing measured to PARAGON isotopics for these data also show very good agreement throughout the isotopic burnup range.

The isotopic comparisons for both the Saxton and Yankee isotopics show no significant trend for any isotope with burnup. These excellent results demonstrate the capability of PARAGON for predicting the depletion characteristics of both UO_2 and PuO_2 LWR fuel over a wide range of burnup conditions.

Table 3-1: Strawbridge –Barry Critical Experiment Data versus PARAGON predictions

	Data Points	Keff	Deviation	
Hexagonal lattice	[]	[]	[]	a, b, c
Square lattice				
Aluminum clad				
Stainless Steel clad				
No Clad				
Dissolved boron				
No Boron				
UO2 experiments				
Uranium metal experiments				
All				

Table 3-2: PARAGON Keff for KRITZ Experiments

[]	[]	[]	a, b, c

Table 3-3: Results for B&W Core XI with PYREX rods



a, b, c

Table 3-4: Results for B&W Cores with 2.46 w/o U²³⁵ and Gadolinia Rods



a, b, c

Table 3-5: Results from B&W Cores with 2.46 w/o U235, Gadolinia Rods and Control Rods

	a, b, c
--	---------

Table 3-6: Results from B&W Cores with 4.02 w/o U235, Gadolinia Rods and Control Rods

	a, b, c
--	---------

Table 3-7: Results from B&W Cores with 4.02 w/o U235, CE 16x16 Lattice with 2x2 Water Rods

	a, b, c
--	---------

Table 3-8: Results of Assembly Benchmarks



Figure 3-1: Strawbridge-Barry Critical Experiments: PARAGON Prediction versus Lattice Water to Uranium Ratio



Figure 3-2: Strawbridge-Barry Critical Experiments: PARAGON Prediction versus Fuel Enrichment



Figure 3-3: Strawbridge-Barry Critical Experiments: PARAGON Prediction versus Pellet Diameter



Figure 3-4: Strawbridge-Barry Critical Experiments: PARAGON Prediction versus Experimental Buckling

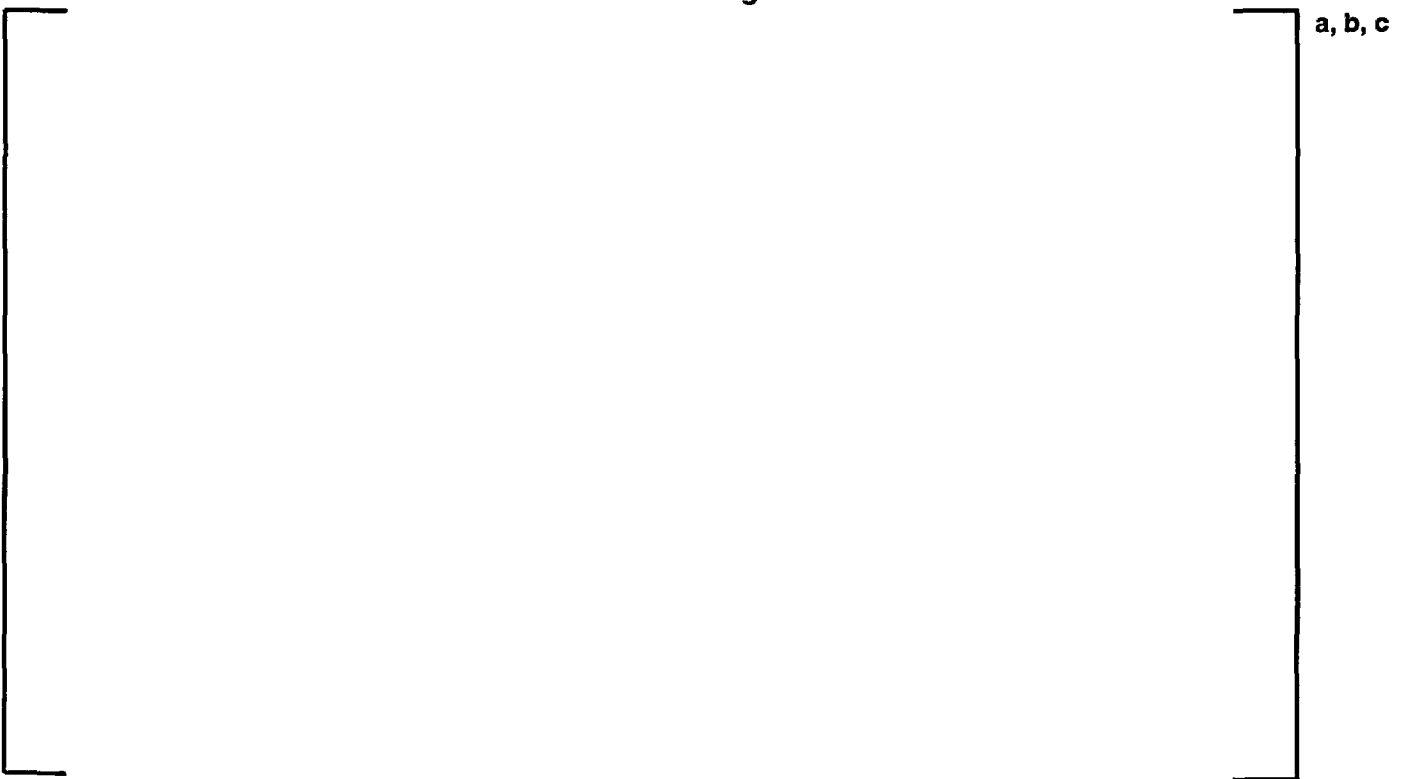


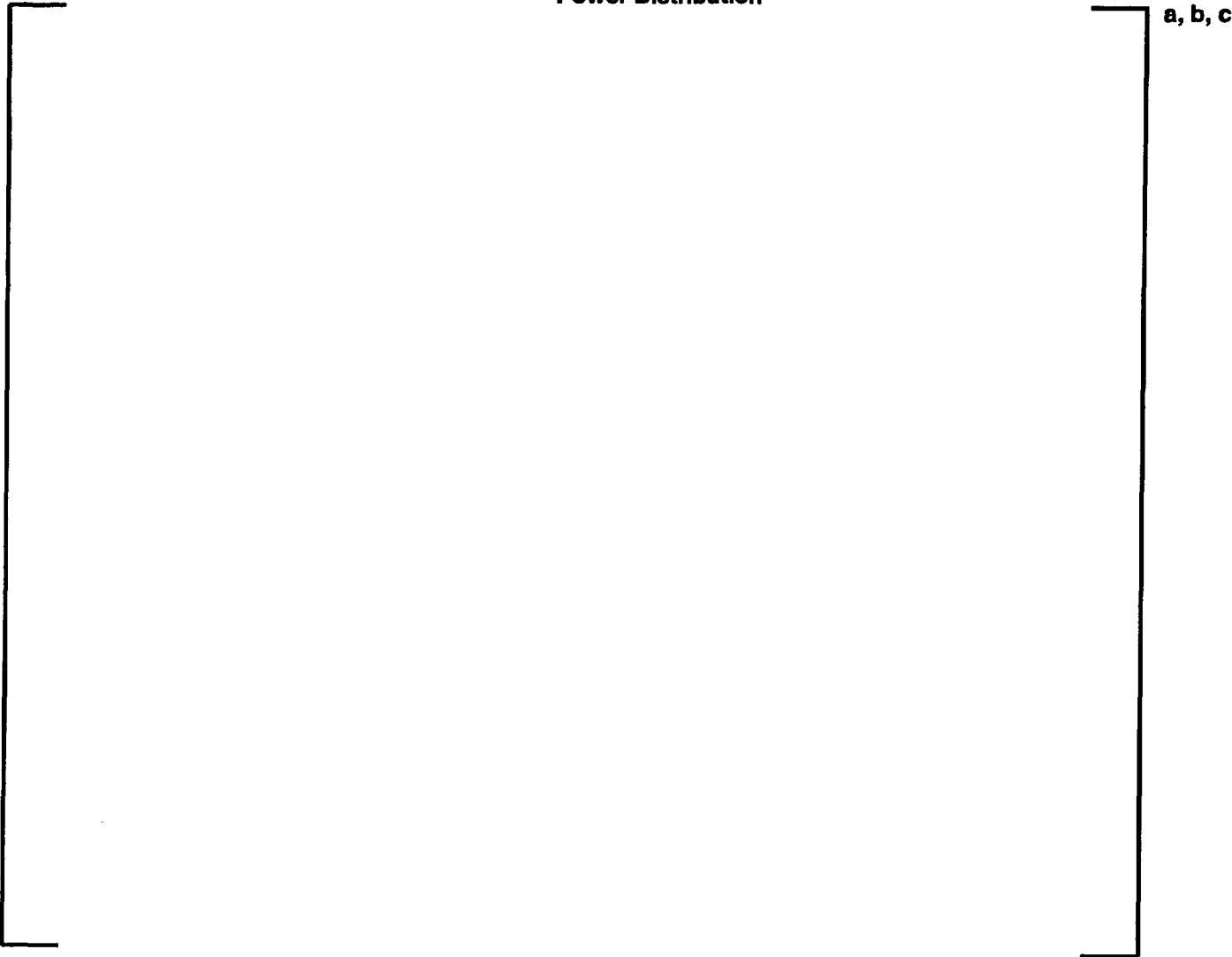
Figure 3-5: Strawbridge-Barry Critical Experiments: PARAGON Prediction versus Soluble Boron Concentration



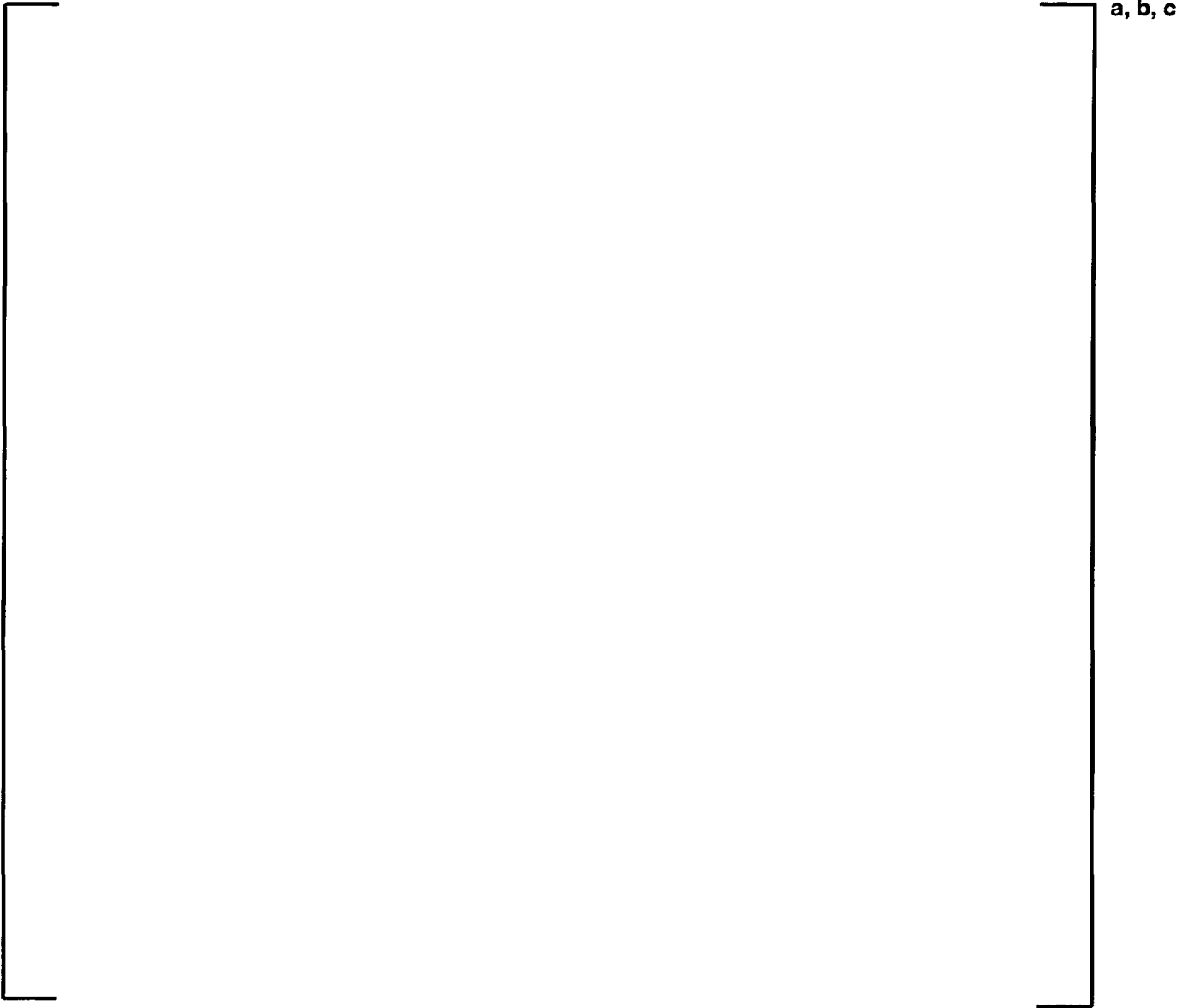
Figure 3-6: Babcock & Wilcox Critical Experiments: Core XI, Loading 2 Center Assembly Rod Power Distribution



Figure 3-7: Babcock & Wilcox Critical Experiments: Core XI, Loading 6 Center Assembly Rod Power Distribution



**Figure 3-8: Babcock & Wilcox Critical Experiments: Core XI, Loading 9
Center Assembly Rod Power Distribution**



**Figure 3-9: Babcock & Wilcox Critical Experiments: Core 5, 28 Gadolinia Rods
Center Assembly Rod Power Distribution**



**Figure 3-10: Babcock & Wilcox Critical Experiments: Core 12, No Gadolinia Rods
Center Assembly Rod Power Distribution**



**Figure 3-11: Babcock & Wilcox Critical Experiments: Core 14, 28 Gadolinia Rods
Center Assembly Rod Power Distribution**



Figure 3-12: MCNP vs PARAGON: 14x14 Westinghouse Assembly (4.00 w/o No BA) Assembly Rod Power Distribution



Figure 3-13: MCNP vs PARAGON: 15x15 Westinghouse Assembly (3.90 w/o No BA) Assembly Rod Power Distribution

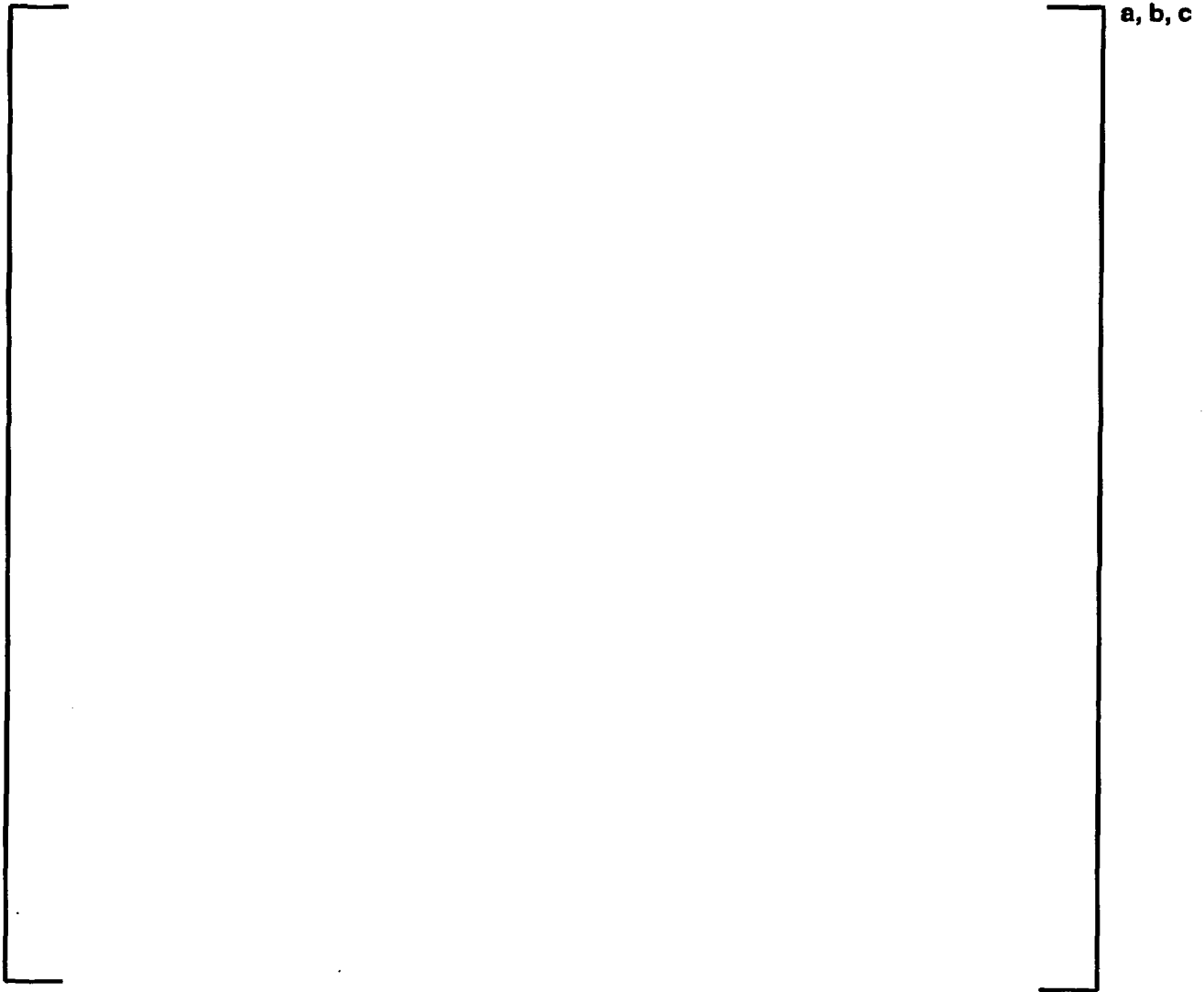


Figure 3-14: MCNP vs PARAGON: 15x15 Westinghouse Assembly (5.0 w/o 60 IFBA) Assembly Rod Power Distribution

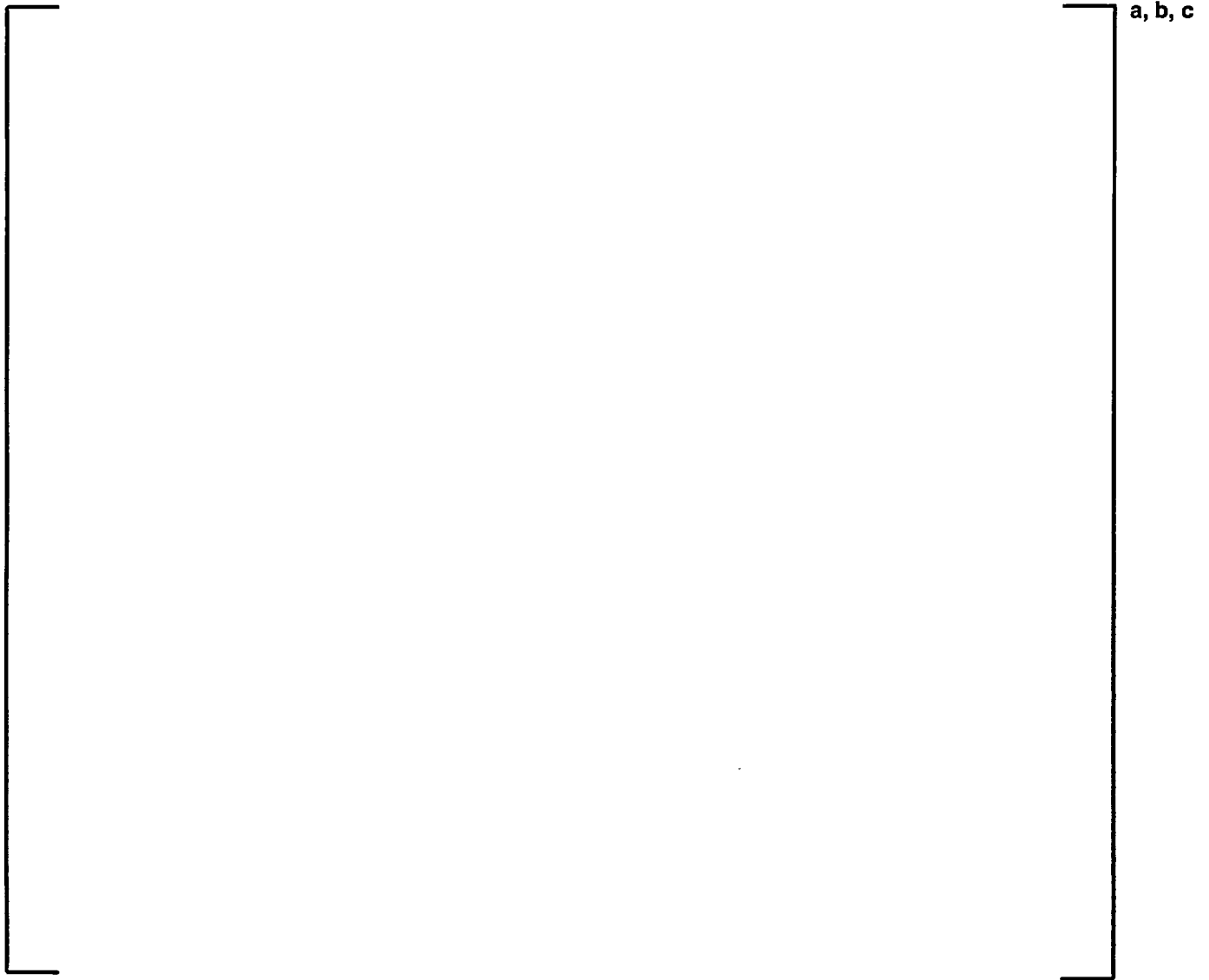
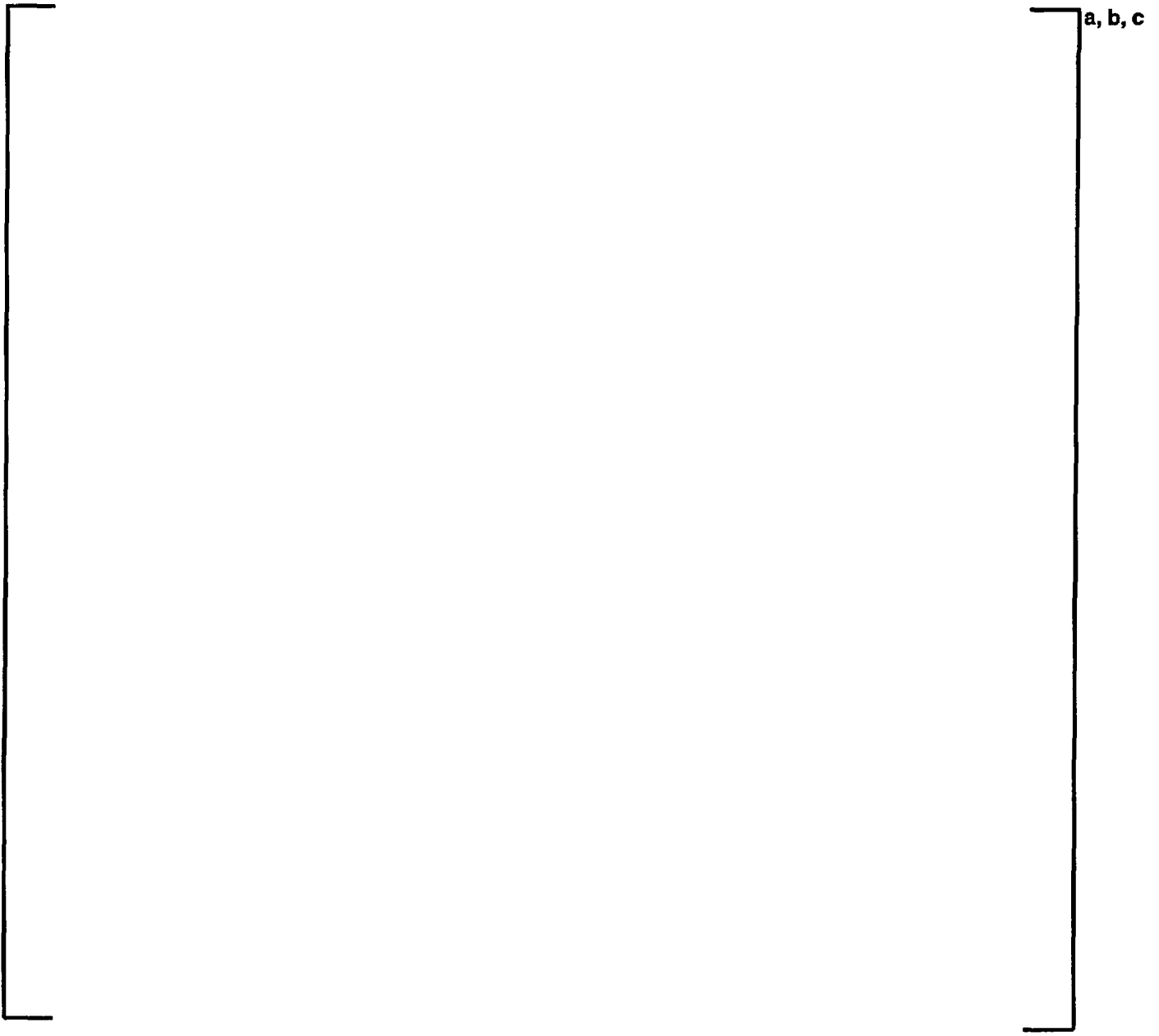


Figure 3-15: MCNP vs PARAGON: 16x16 Westinghouse Assembly (4.00 w/o No BA) Assembly Rod Power Distribution



**Figure 3-16: MCNP vs PARAGON: 17x17 Standard Westinghouse Assembly (2.10 w/o No BA)
Assembly Rod Power Distribution**



**Figure 3-17: MCNP vs PARAGON: 17x17 Standard Westinghouse Assembly (4.10 w/o No BA)
Assembly Rod Power Distribution**

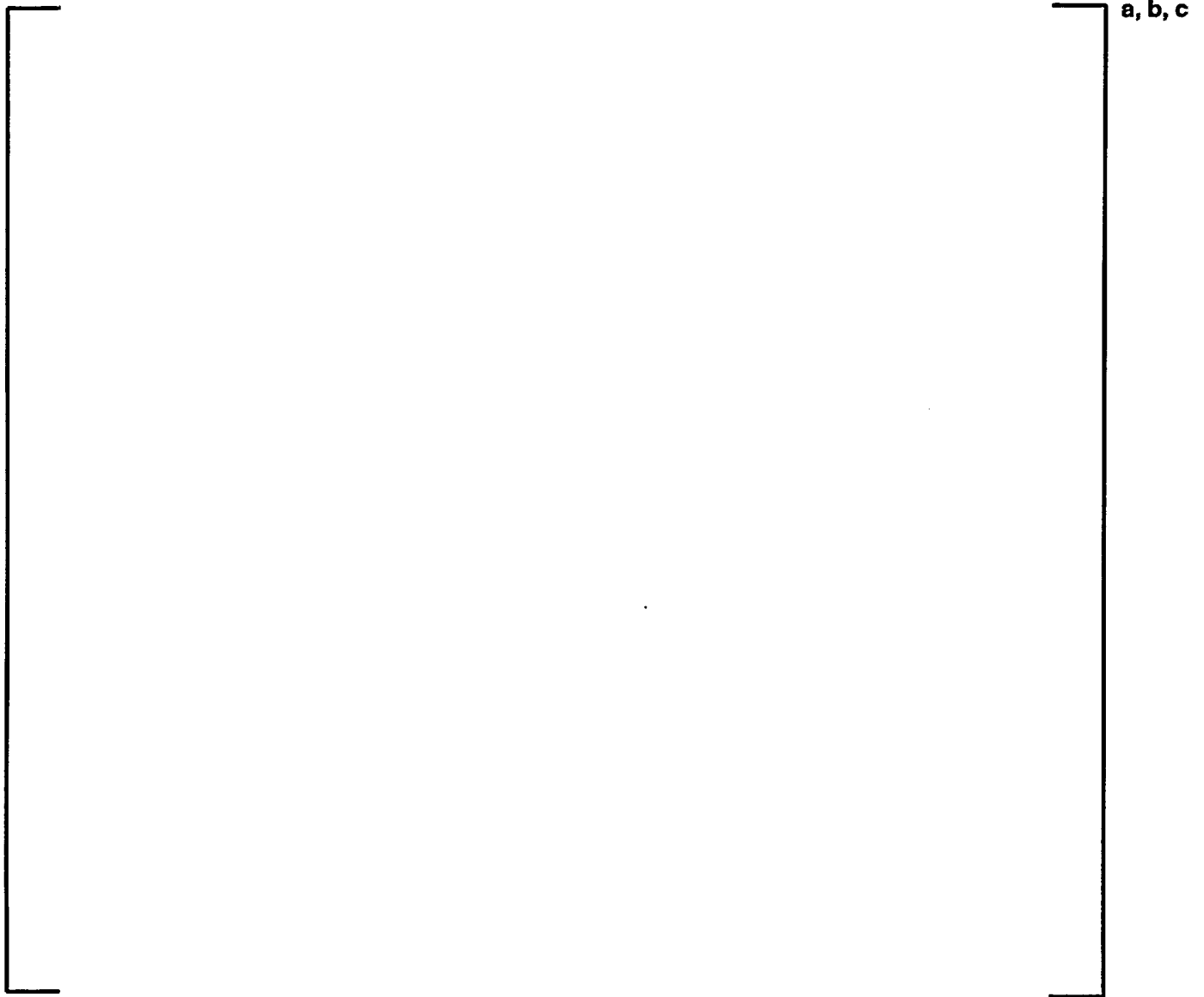


**Figure 3-18: MCNP vs PARAGON: 17x17 OFA Westinghouse Assembly (4.70 w/o 156 IFBA)
Assembly Rod Power Distribution**



a, b, c

**Figure 3-19: MCNP vs PARAGON: 17x17 Standard Westinghouse Assembly (5.0 w/o 128 IFBA)
Assembly Rod Power Distribution**

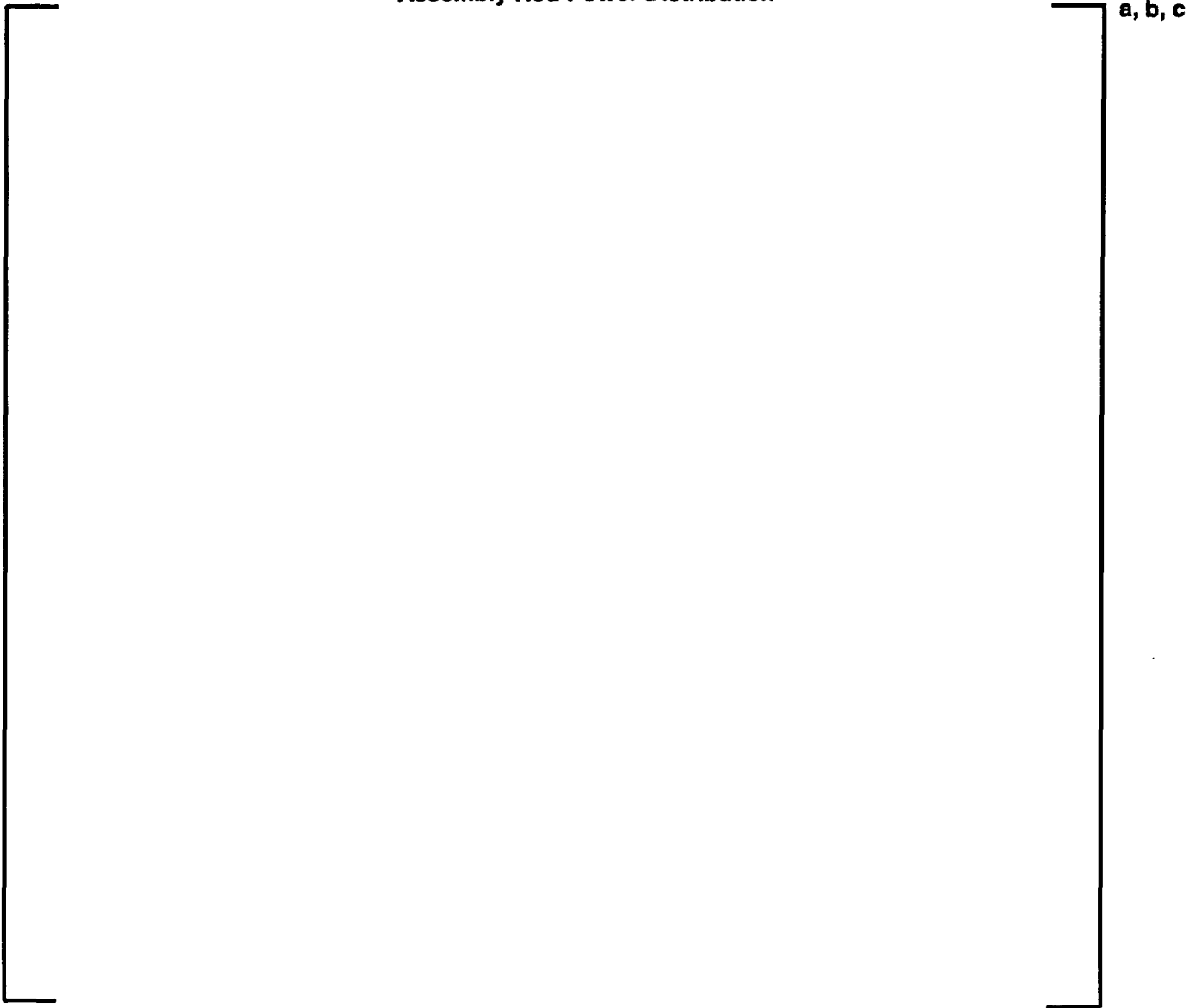
a, b, c



Figure 3-20: MCNP vs PARAGON: 17x17 Standard Westinghouse Assembly (4.00 w/o 24 Gd_2O_3 Rods) Assembly Rod Power Distribution



**Figure 3-21: MCNP vs PARAGON: 17x17 Standard Westinghouse Assembly (6.1 w/o MOX, No BA)
Assembly Rod Power Distribution**



**Figure 3-22: MCNP vs PARAGON: 17x17 OFA Westinghouse Assembly (4.00 w/o 72 Er₂O₃ Rods)
Assembly Rod Power Distribution**

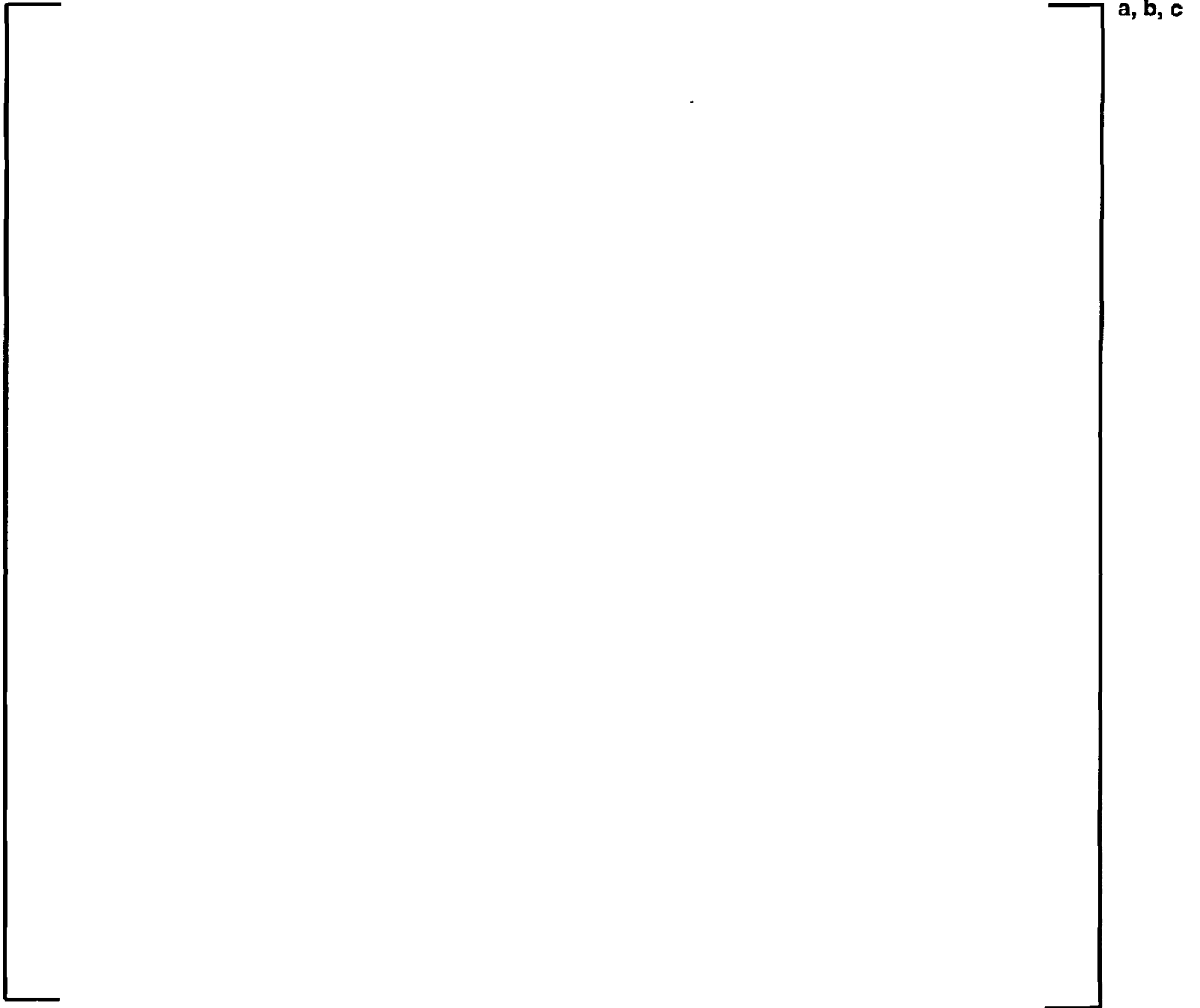


Figure 3-23: MCNP vs PARAGON: 14x14 CE Assembly (4.30,3.40 w/o 44 Er₂O₃ Rods) Assembly Rod Power Distribution



Figure 3-24: MCNP vs PARAGON: 16x16 CE Assembly (4.05,3.65 w/o 52 Er₂O₃ Rods) Assembly Rod Power Distribution



Figure 3-25: Saxton Fuel Performance Evaluation Program: PARAGON U²³⁵/U Prediction Versus Burnup



Figure 3-26: Saxton Fuel Performance Evaluation Program: PARAGON U²³⁶/U Prediction Versus Burnup



Figure 3-27: Saxton Fuel Performance Evaluation Program: PARAGON U²³⁸/U Prediction Versus Burnup



Figure 3-28: Saxton Fuel Performance Evaluation Program: PARAGON Pu²³⁹/Pu Prediction Versus Burnup



Figure 3-29: Saxton Fuel Performance Evaluation Program: PARAGON Pu²⁴⁰/Pu Prediction Versus Burnup



Figure 3-30: Saxton Fuel Performance Evaluation Program: PARAGON Pu²⁴¹/Pu Prediction Versus Burnup



Figure 3-31: Saxton Fuel Performance Evaluation Program: PARAGON Pu²⁴²/Pu Prediction Versus Burnup

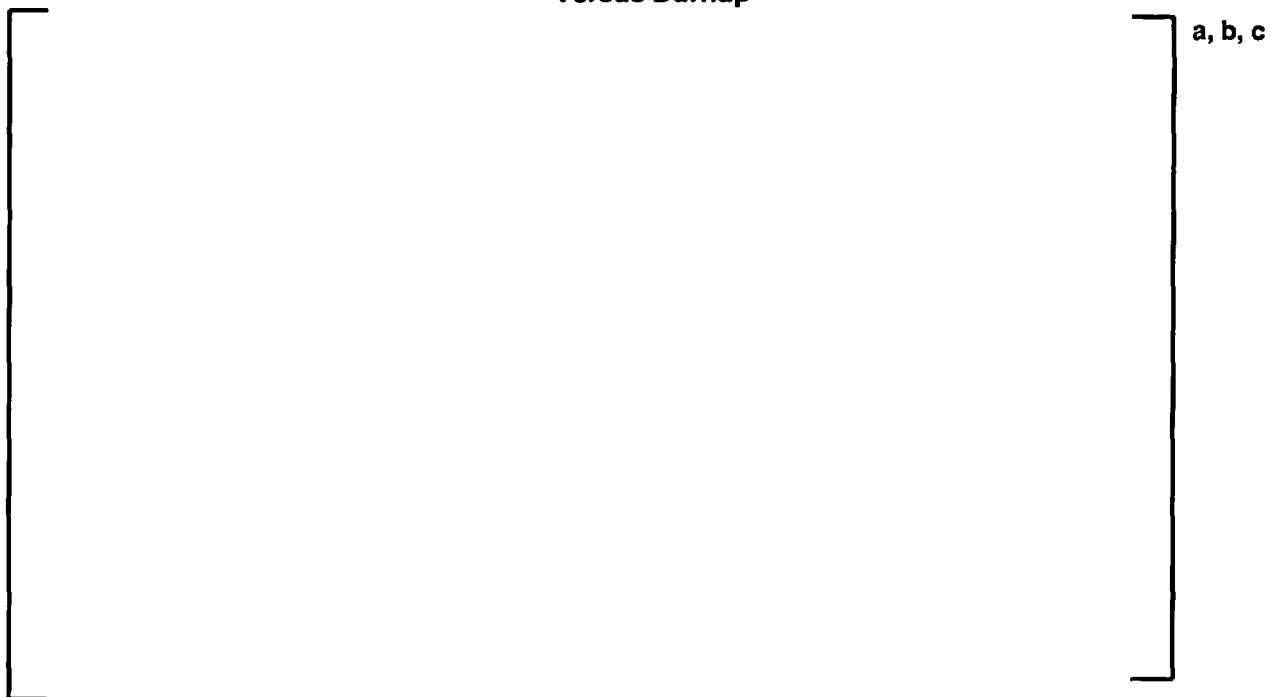


Figure 3-32: Saxton Fuel Performance Evaluation Program: PARAGON Pu²³⁹/U²³⁸ Prediction Versus Burnup



Figure 3-33: Saxton Fuel Performance Evaluation Program: PARAGON Pu²³⁹/Pu²⁴⁰ Prediction Versus Burnup



Figure 3-34: Saxton Fuel Performance Evaluation Program: PARAGON Pu²⁴⁰/Pu²⁴¹ Prediction Versus Burnup



Figure 3-35: Saxton Fuel Performance Evaluation Program: PARAGON Pu²⁴¹/Pu²⁴² Prediction Versus Burnup

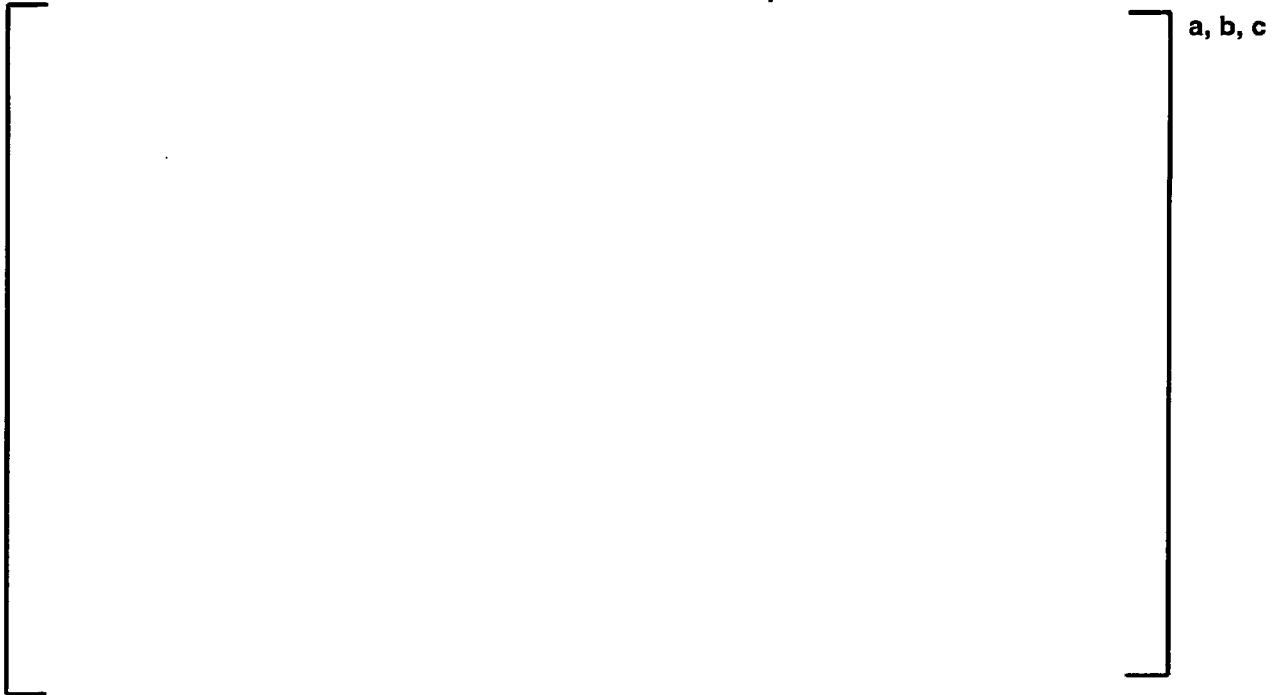


Figure 3-36: Saxton Fuel Performance Evaluation Program: PARAGON U²³⁶/U²³⁵ Prediction Versus Burnup



Figure 3-37: Saxton Fuel Performance Evaluation Program: PARAGON U^{235}/U^{238} Prediction Versus Burnup



Figure 3-38: Yankee Core Evaluation Program (Stainless Steel Clad): PARAGON U^{235}/U Prediction Versus Burnup



Figure 3-39: Yankee Core Evaluation Program (Stainless Steel Clad): PARAGON U²³⁶/U Prediction Versus Burnup



Figure 3-40: Yankee Core Evaluation Program (Stainless Steel Clad): PARAGON U²³⁸/U Prediction Versus Burnup



Figure 3-41: Yankee Core Evaluation Program (Stainless Steel Clad): PARAGON Pu²³⁹/Pu Prediction Versus Burnup

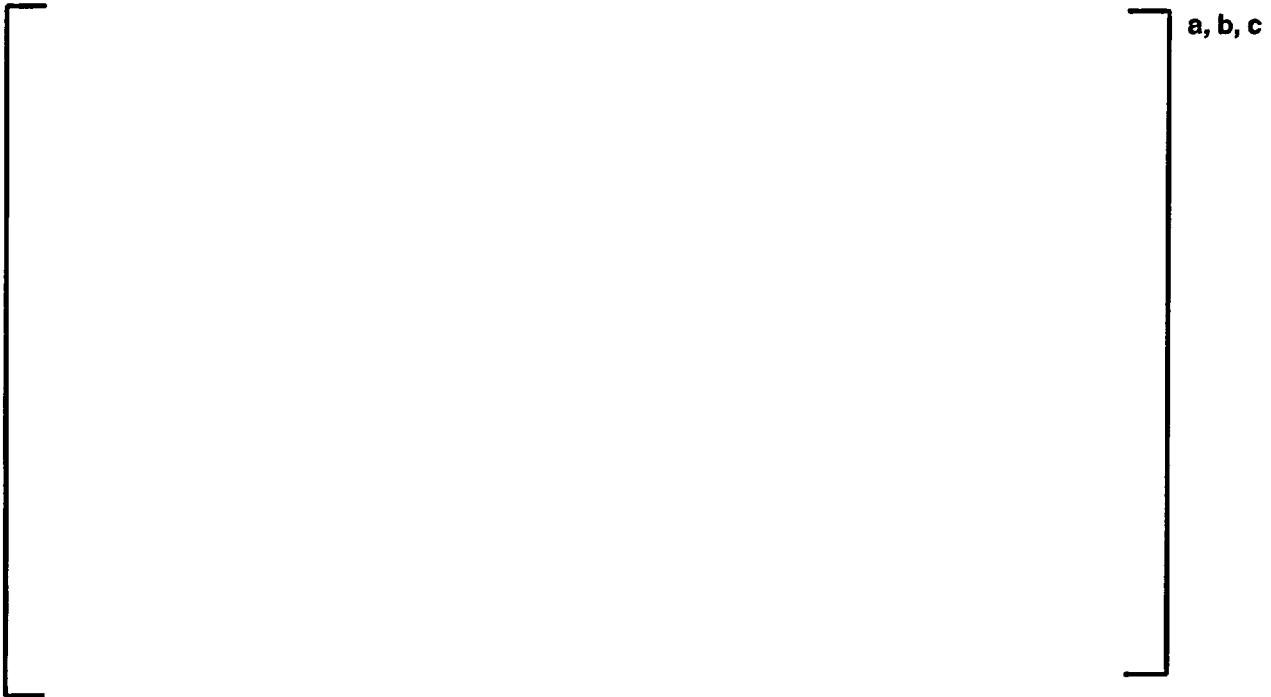


Figure 3-42: Yankee Core Evaluation Program (Stainless Steel Clad): PARAGON Pu²⁴⁰/Pu Prediction Versus Burnup



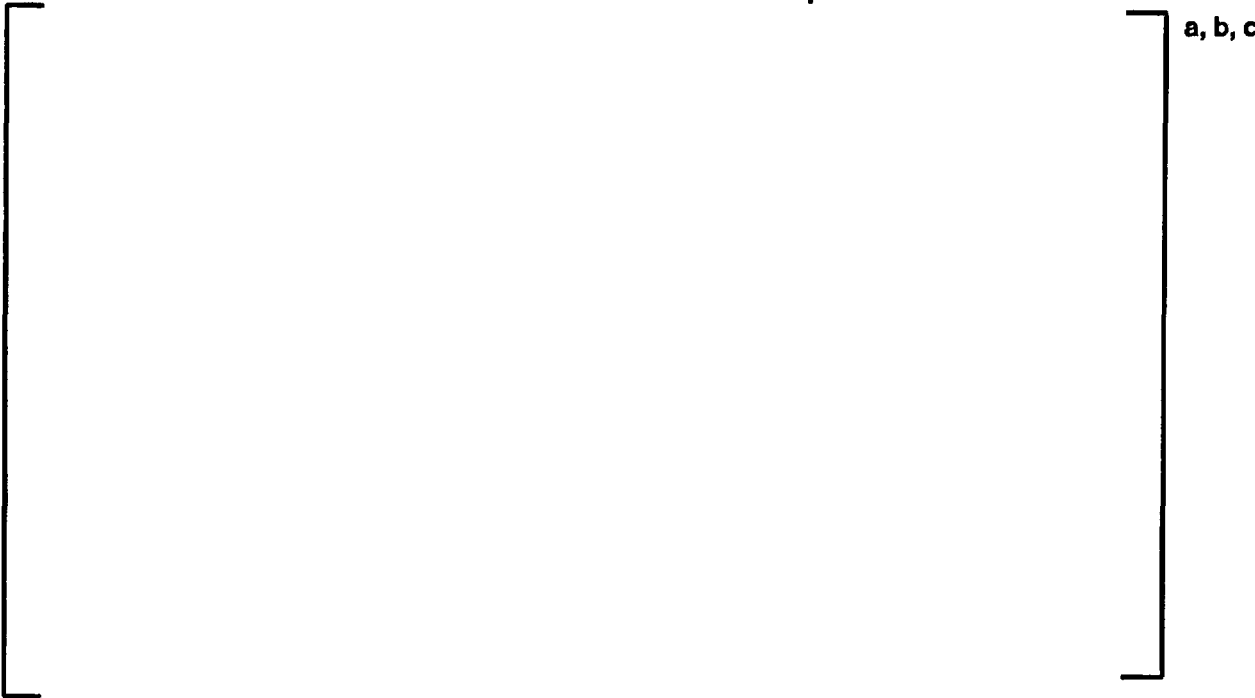
Figure 3-43: Yankee Core Evaluation Program (Stainless Steel Clad): PARAGON Pu²⁴¹/Pu Prediction Versus Burnup



Figure 3-44: Yankee Core Evaluation Program (Stainless Steel Clad): PARAGON Pu²⁴²/Pu Prediction Versus Burnup



**Figure 3-45: Yankee Core Evaluation Program (Stainless Steel Clad): PARAGON Pu²³⁹/U²³⁸
Prediction Versus Burnup**



**Figure 3-46: Yankee Core Evaluation Program (Stainless Steel Clad): PARAGON Pu²³⁹/Pu²⁴⁰
Prediction Versus Burnup**



Figure 3-47: Yankee Core Evaluation Program (Stainless Steel Clad): PARAGON Pu²⁴⁰/Pu²⁴¹ Prediction Versus Burnup



Figure 3-48: Yankee Core Evaluation Program (Stainless Steel Clad): PARAGON Pu²⁴¹/Pu²⁴² Prediction Versus Burnup



**Figure 3-49: Yankee Core Evaluation Program (Stainless Steel Clad): PARAGON U²³⁶/U²³⁵
Prediction Versus Burnup**



**Figure 3-50: Yankee Core Evaluation Program (Stainless Steel Clad): PARAGON U²³⁵/U²³⁸
Prediction Versus Burnup**



Figure 3-51: Yankee Core Evaluation Program (Zircaloy Clad): PARAGON U²³⁵/U Prediction Versus Burnup

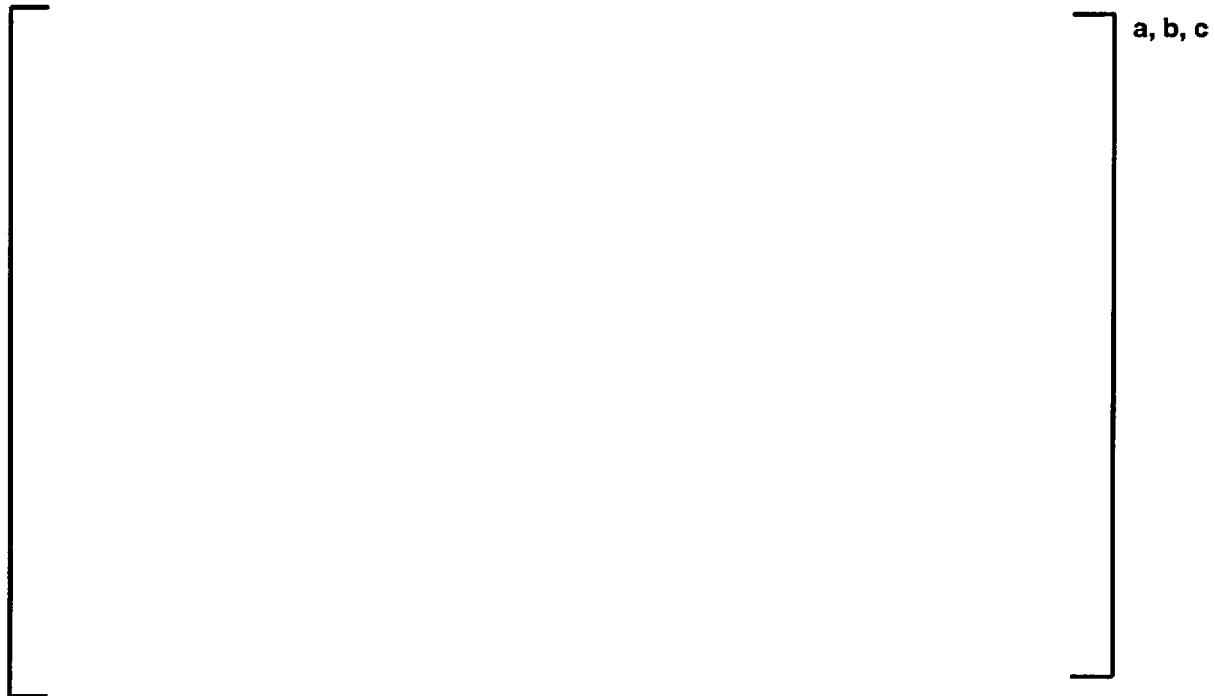


Figure 3-52: Yankee Core Evaluation Program (Zircaloy Clad): PARAGON U²³⁶/U Prediction Versus Burnup



Figure 3-53: Yankee Core Evaluation Program (Zircaloy Clad): PARAGON U^{238}/U Prediction Versus Burnup



Figure 3-54: Yankee Core Evaluation Program (Zircaloy Clad): PARAGON Pu^{239}/Pu Prediction Versus Burnup



Figure 3-55: Yankee Core Evaluation Program (Zircaloy Clad): PARAGON Pu²⁴⁰/Pu Prediction Versus Burnup



Figure 3-56: Yankee Core Evaluation Program (Zircaloy Clad): PARAGON Pu²⁴¹/Pu Prediction Versus Burnup



Figure 3-57: Yankee Core Evaluation Program (Zircaloy Clad): PARAGON Pu²⁴²/Pu Prediction Versus Burnup



Figure 3-58: Yankee Core Evaluation Program (Zircaloy Clad): PARAGON Pu²³⁹/U²³⁸ Prediction Versus Burnup



Figure 3-59: Yankee Core Evaluation Program (Zircaloy Clad): PARAGON Pu²³⁹/Pu²⁴⁰ Prediction Versus Burnup

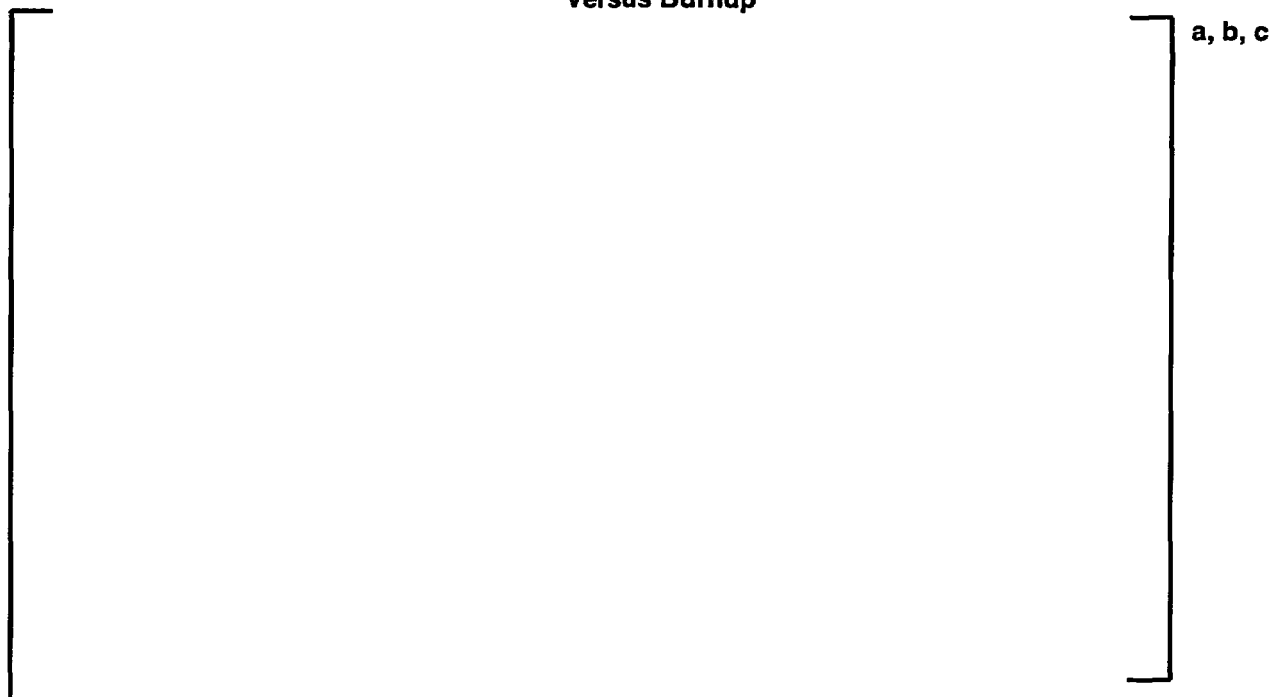


Figure 3-60: Yankee Core Evaluation Program (Zircaloy Clad): PARAGON Pu²⁴⁰/Pu²⁴¹ Prediction Versus Burnup



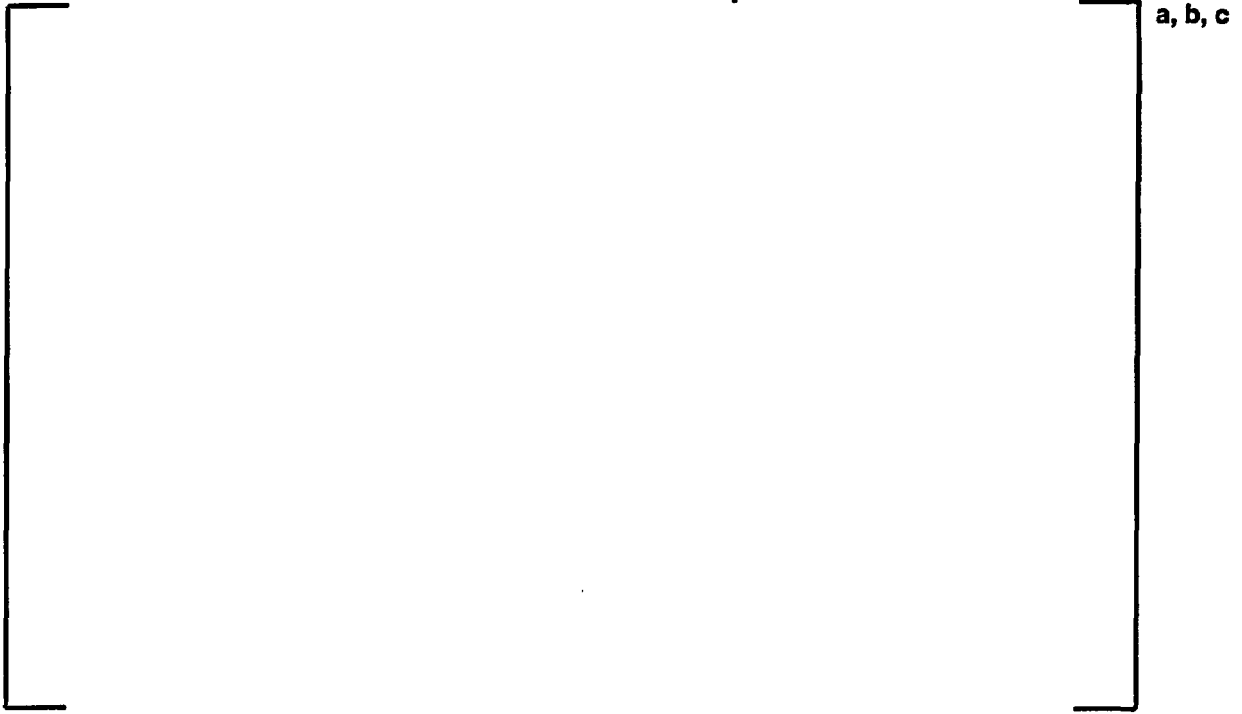
Figure 3-61: Yankee Core Evaluation Program (Zircaloy Clad): PARAGON Pu²⁴¹/Pu²⁴² Prediction Versus Burnup



Figure 3-62: Yankee Core Evaluation Program (Zircaloy Clad): PARAGON U²³⁶/U²³⁵ Prediction Versus Burnup



Figure 3-63: Yankee Core Evaluation Program (Zircaloy Clad): PARAGON U^{235}/U^{238} Prediction Versus Burnup



Section 4.0: Plant Qualification

The basic methodology of PARAGON was qualified in Section 3 by demonstrating the accuracy of the code in predicting the results of critical experiments and isotopic evaluations. However, the primary use of PARAGON will be to generate nuclear data for use in various core simulators. Thus, the most important qualification for PARAGON is comparisons of the results of core calculations using PARAGON supplied nuclear data against plant measured data. These comparisons are provided in this section.

For PWR cores, a Westinghouse core simulator currently being used for core design and safety calculations is the Advanced Nodal Code (ANC) which was licensed by the NRC for PWR core design in 1986 (Reference 4-1). Since 1988, ANC has been using nuclear data provided by the Westinghouse transport code PHOENIX-P (Reference 4-2). The PHOENIX-P/ANC code system has been a primary nuclear design system in use at Westinghouse for PWR core analysis and has been used in the design of over 400 PWR cores.

This section will present ANC results for PWR core calculations with nuclear data supplied by PARAGON. These results will be compared to corresponding plant measurements where available and to PHOENIX-P/ANC results for the same calculations. These calculations demonstrate the accuracy of the PARAGON nuclear data when applied to a complete nuclear design code system.

Section 4-1 describes the plant cycles which were used in these comparisons. Section 4-2 will present comparisons of PARAGON/ANC calculations to plant measurements and PHOENIX-P/ANC calculations for startup physics tests. These include all rods out (ARO) hot zero power (HZP) beginning of life (BOC) critical boron concentration, ARO HZP BOC isothermal temperature coefficient (ITC) and HZP BOC control rod worths. Section 4-3 will present critical boron versus burnup comparisons of PARAGON/ANC against both measurement and PHOENIX-P/ANC results for a large number of plant cycles. Section 4-4 will present radial power (assembly power) distribution comparisons of PARAGON/ANC against measurement. Section 4-5 will present comparisons of PARAGON/ANC results against PHOENIX-P/ANC results for radial and axial power distributions for a variety of cores. Section 4-5 will also present comparisons of PARAGON/ANC results against those of PHOENIX-P/ANC for worst stuck rod, dropped rod, and rod ejection calculations for several plants.

4.1 Plant Cycles used for Comparisons

The database of plant cycles used for the PARAGON/ANC comparisons to plant measurements is listed in Table 4-1. These particular cycles were chosen based on the need to cover a large variety of plant types, lattice types, burnable absorber types, and axial blanket types. The availability of reliable plant data was also a basic consideration. The PARAGON qualification included 24 cycles and 11 plants. The plants included both Westinghouse (15 cycles) and Combustion Engineering (9 cycles) type cores. All Westinghouse core configurations were included (2 loop: 121 assemblies, 3 loop: 157 assemblies, 4 loop: 193 assemblies). CE cores in the database included 177, 217, and 241 assembly cores. For Westinghouse plants, all lattice configurations were covered (14x14, 15x15, 16x16, and 17x17). Both the 14x14 and 16x16 CE lattices were included in the database of plants. Fuel rod sizes ranged from 0.360 to 0.440 inches diameter. The enrichment range covered was from 1.30 w/o to 4.95 w/o U^{235} . One core with mixed oxide fuel was also included. The burnable absorber types covered were: 1) the integral fuel burnable absorber (IFBA), 2) the wet annular burnable absorber (WABA), 3) pyrex burnable absorbers, 4) gadolinia burnable absorbers, 5) erbia burnable absorbers, and 6) fuel displacing B_4C burnable absorbers. One plant (Plant D) had multiple burnable absorbers (IFBA and WABA) in the same assembly. Axial blanket designs range from enriched annular to natural solid axial blankets (thus bounding all Westinghouse design configurations). Some of the included cores had no axial blankets. Cycle lengths for the cycles ranged from 310 to 654 EFPD. The cores included 2 first cores and 20 reload cycles. Not all cycles are used for every type of calculation in this report. A particular cycle may not be used for a certain calculation because of a lack of a complete set of data. For comparisons against PHOENIX-P/ANC calculations, a representative subset of the cores shown in Table 4-1 was used. In all calculations, the particular cores being used for that calculation are clearly identified.

The large variety in the cycles chosen for this qualification serves two purposes: 1) it demonstrates the robustness of PARAGON and its library to analyze over a large range of cycle designs, and 2) it serves to qualify PARAGON to analyze each feature by direct comparison of results.

4.2 Startup Test Results Comparisons

Three common tests performed at PWR startups are: ARO HZP critical boron, ARO isothermal temperature coefficient, and HZP rodworth measurements. Since these measurements are taken in the just-loaded core at zero power, the complexities which come into play in analyzing a core at power with depletion including power history, feedback effects and B¹⁰ depletion are not present. Thus, these tests provide a good measure of the accuracy of the code system since the core conditions are well-defined and can be simulated with high reliability in the ANC code.

A comparison of HZP ARO startup critical boron results for 22 cycles is presented in Table 4-2. The table includes the measured critical boron as well as the value calculated by both PARAGON/ANC and PHOENIX-P/ANC. All calculations are within the measured to predicted difference review criteria of 50 ppm with the largest difference for PARAGON/ANC at []^{a,c} and for PHOENIX-P/ANC at []^{a,c}. The mean measured minus predicted differences are negative for both codes meaning that both codes have a tendency to overpredict BOC HZP critical boron. The difference in the mean values is about []^{a,c} with PARAGON being slightly more negative but with both codes having acceptable means. Both codes have very small standard deviations: []^{a,c} for PARAGON/ANC and []^{a,c} for PHOENIX-P/ANC. Over the last several years, Westinghouse has noticed a reduction in the standard deviation for the measured minus predicted BOC HZP critical boron to about []^{a,c}. This is directly in line with the mean value seen in Table 4-2 for PHOENIX-P/ANC. The PARAGON/ANC standard deviation value shown in Table 4-2, []^{a,c}. This small standard deviation is especially good considering the wide variety of lattice types, enrichments, and burnable absorbers included in the 22 core cycles shown in the table and demonstrates the wide range of applicability for PARAGON/ANC. The performance of PARAGON/ANC for BOC HZP critical boron is thus very good.

Table 4-3 shows a comparison of startup HZP isothermal temperature coefficient results for both PARAGON/ANC and PHOENIX-P/ANC for the same 22 cycles reported in Table 4-2. The results in Table 4-3 show that there is no significant difference in the performance of the two code systems for predicting ITC. The mean for PARAGON/ANC is within []^{a,c} of the mean of PHOENIX-P/ANC. []^{a,c}.

Rodworth comparison results for PARAGON/ANC against measurement and PHOENIX-P/ANC are shown for nine cycles in Tables 4-4 through 4-12. In general the performance of PARAGON/ANC is the same as PHOENIX-P/ANC. The difference in total rodworth between PARAGON/ANC and PHOENIX-P/ANC was less than []^{a,c} for all nine cases. All cases met the individual rodworth criteria of 15% difference on an individual bank or 100 pcm for small worth banks. The average difference over all the rods in all nine cycles for the PARAGON/ANC code system was []^{a,c} with a standard deviation of []^{a,c}. For the PHOENIX-P/ANC code system the corresponding values are []^{a,c} and []^{a,c}. The average difference for total rodworth was []^{a,c} for the PARAGON/ANC code system with a standard deviation of []^{a,c}. The corresponding values for the PHOENIX-P/ANC code system are []^{a,c}.

4.3 Critical Boron versus Burnup Comparisons

PARAGON/ANC predictions for at-power critical boron versus burnup are presented for 22 plant cycles in Figures 4-1 through 4-23. Measured critical boron and the PHOENIX-P/ANC predictions are also presented in these figures. Examining the figures, the following conclusions can be made:

- 1-1. Both PARAGON/ANC and PHOENIX-P/ANC generally predict the shape of the boron letdown curve and the end of cycle well. PARAGON/ANC does slightly better in [

] ^{a,c}.

- 1-2. Most cycles present clear evidence of significant B¹⁰ depletion. B¹⁰ isotopic information was not available for most of the cycles used in this analysis. Therefore, depletion was not included in any of the predictions or measured values. B¹⁰ depletion is characterized by the measured to predicted critical boron difference becoming larger throughout the middle of the cycle, then becoming smaller at end of cycle when the boron concentration is low and the B¹⁰ depletion is no longer important. B¹⁰ depletion has become a significant effect in boron letdown curves since, over the last several years, plants are operating with very few shutdowns and B¹⁰ depletion effects can be larger than [^{a,c}. The effect of B¹⁰ depletion, unless accurately accounted for, makes statistical analysis of the measured to predicted critical boron differences yield an inaccurate measure of how well a code system predicts reactivity. In all cases except [^{a,c}, the measured critical boron values are larger than the predicted critical boron values, accounting for B¹⁰ depletion thus making the measured to predicted differences smaller. This is because, if B¹⁰ depletion is accounted for in the prediction, the predicted values will get larger since they are currently based on a larger B¹⁰ concentration than is actually in the core. If the measured values are adjusted, they will get smaller since they inherently include a smaller isotopic percentage of B¹⁰. Either way of accounting for B¹⁰ depletion will improve the mid-cycle measured to predicted critical boron differences. [

] ^{a,c}.

- 1-3. An interesting case is presented in Figure 4-7. This cycle had several very long shutdowns and took about 3 years to complete. [

] ^{a,c}.

- 1-4. Figure 4-10, which presents the results for a 121 assembly core with MOX fuel, shows the [

] ^{a,c}. The B¹⁰ depletion effect is small for this

cycle.

1-5. Figure 4-20 shows the results for a first core. [

] ^{a,c}.

4.4 Radial Power Distributions

In addition to reactivity, a nuclear code system must be able to calculate core power distributions accurately. To provide this evidence for the PARAGON/ANC system, assembly power comparisons were made for five plants. For these plants, measured assembly power values based on core flux maps were compared to predicted assembly powers from PARAGON/ANC at the same conditions. Maps from five plants were used in this analysis. These plants are:

Plant	Lattice	Fuel	Assemblies in core	Cycles
A	17x17	UO ₂	157	10, 11
B	16x16	UO ₂	121	17, 18
C	14x14	UO ₂	121	25, 26
D	15x15	UO ₂	193	10, 11
J	17x17	UO ₂	193	10, 11

The measured to predicted comparisons for these maps are presented in Figures 4-24 through 4-51. For each cycle, two or three maps are presented at different burnups during the cycle. The cycle burnups range for the maps is from [

] ^{a,c}. The average difference between the measured and predicted normalized powers is shown in each figure as well as the standard deviation of these differences. The measured to predicted average difference over all twenty-eight maps is [] ^{a,c} and the average standard deviation of the differences over all the maps is [] ^{a,c}. These very small values show that PARAGON/ANC predicts assembly power with high accuracy over a wide range of different lattice types and over the large burnup range seen in plant cycles.

4.5 PARAGON/ANC versus PHOENIX-P/ANC Comparisons

As described earlier in this report, the PHOENIX-P/ANC nuclear code system has been licensed by the NRC since 1988 and has had extensive use in PWR safety and design calculations. Therefore, as part of the qualification of PARAGON, comparisons have been made between the results of core calculations with the two systems to demonstrate that PARAGON/ANC predictions for operating PWR cores are essentially of the same quality, or better, as those of PHOENIX-P/ANC and therefore any [] ^{a,c} used for the PHOENIX-P/ANC system will be applicable to the PARAGON/ANC code system. Reactivity comparisons between the two code systems have been shown in the HZP ARO critical boron results presented in section 4-2 and in the at power critical boron versus burnup results presented in section 4-3. Comparisons for rodworths between the two code systems were also made in section 4-2. In this section, comparisons are made between radial and axial power distributions calculated by both code systems for several different plants with different lattices and core sizes. In addition, the results of calculations for core conditions which are [

] ^{a,c}.

Figures 4-52 through 4-78 show comparisons of radial power and burnup distributions calculated with both PARAGON/ANC and PHOENIX-P/ANC. The cycles shown are listed in the table below:

Plant	Lattice	Fuel	Assemblies in core	Cycles
A	17x17	UO ₂	157	10, 11
C	14x14	UO ₂	121	25, 26
D	15x15	UO ₂	193	10, 11
E	14x14	MOX	121	25
F	16x16 CE	UO ₂	217	11, 12

For each cycle, comparisons between the normalized assembly powers from both code systems are shown at BOC and EOC. In addition, the radial assembly burnups predicted at EOC from both code systems are compared. As can be seen by examining these figures, the differences between the PARAGON/ANC predictions and those of PHOENIX-P/ANC for both power and burnup are very small.

Figures 79-102 show comparisons of axial power predictions from PARAGON/ANC versus those from PHOENIX-P ANC for four plants listed in the table below:

Plant	Lattice	Fuel	Assemblies in core	Cycles
A	17x17	UO ₂	157	10, 11
C	14x14	UO ₂	121	25, 26
F	16x16 CE	UO ₂	217	11, 12
G	14x14 CE	UO ₂	217	13, 14

Plants A and C are Westinghouse type plants with axial blankets. Plants F and G are Combustion Engineering type plants with no axial blankets. Axial power comparisons are made for three times in life for each cycle: BOC, MOC (i.e., middle of cycle), and EOC. As can be seen by examining each of these figures, the axial power shapes predicted by the two code systems are virtually identical.

Table 4-13 presents the results from worst stuck rod calculations for the following four plants:

Plant	Lattice	Fuel	Assemblies in core	Cycles
A	17x17	UO ₂	157	11
B	16x16	UO ₂	121	17
C	14x14	UO ₂	121	24
D	15x15	UO ₂	193	10

These calculations were performed in full core geometry at BOC HZP conditions with all the rods completely inserted (ARI) except the highest worth rod (called the worst stuck rod or WSR) which was completely withdrawn from the core. The parameters of interest for this calculation are the worth of the worst stuck rod, and the total peaking factor F_q , the radial peaking factor $F_{\Delta h}$, and the axial peaking factor F_z . The worth of the worst stuck rod is determined by performing a calculation at the same conditions except all the rods are inserted. The difference between the ARI and ARI-WSR eigenvalues is the worth of the WSR. Table 4-13 summarizes the results of the ARI-WSR calculation for the four plants for both code systems. As can be seen from the table, the PARAGON/ANC results are within []^{a,c} for the worth of the WSR. The peaking factors are also similar with the largest difference being []^{a,c} in Plant C.

Table 4-14 presents the results from BOC dropped rod calculations for the same four plants performed with PARAGON/ANC and PHOENIX-P/ANC. The table presents the rodworth, the total peaking factor F_q , the radial peaking factor $F_{\Delta h}$, and the axial peaking factor F_z for the dropped rod calculation from each code system. As seen in the table, the dropped rod worths for the two code systems are within []^{a,c} and the peaking factors differences are also very small, the largest being []^{a,c} for F_q of Plant D.

Table 4-15 presents the results from rod ejection calculations performed with both code systems for the same four plants. Four rod ejection calculations were performed for each plant: BOC HFP, BOC HZP, EOC HFP, and EOC HZP. Rod ejection calculations are similar to stuck rod calculations except that feedback is frozen at the pre-ejection conditions because of the speed of the event. This leads to much larger rod worths and peaking factors. Comparing the rod ejection cases, the differences in rod worth between the calculations from the two code systems show that the largest difference in rod worth is []^{a,c}. The differences in peaking factors between the PARAGON/ANC cases and the PHOENIX-P/ANC cases are also within expected differences considering the large peaking factor values for ejected rod cases.

Table 4-16 presents results for hot full power, end of cycle moderator temperature coefficient calculations performed in both PHOENIX-P/ANC and PARAGON/ANC. These calculations were performed at []^{a,c} with all rods withdrawn. These calculations demonstrate that the PARAGON-based model calculates EOC HFP MTC values within []^{a,c} of the PHOENIX-P model.

The results presented in this section demonstrate that PARAGON-based models compare well to measurements and to PHOENIX-P model results. The good agreement between PHOENIX-P models and PARAGON models has been shown for startup measurement parameters such as HZP boron, HZP ITC, and HZP rodworths and for full power critical boron letdown predictions. This good agreement has also been demonstrated for off normal calculations such as ARI -WSR, dropped rod, and ejected rod calculations. EOC HFP MTC predictions are also very similar between PARAGON-based models and PHOENIX-P-based models. The calculations documented in this section demonstrate that PARAGON can be used as a replacement for PHOENIX-P without changing any licensing bases currently in place for PHOENIX-P based models.

Table 4-1: Plant and Cycle Descriptions

a, b, c

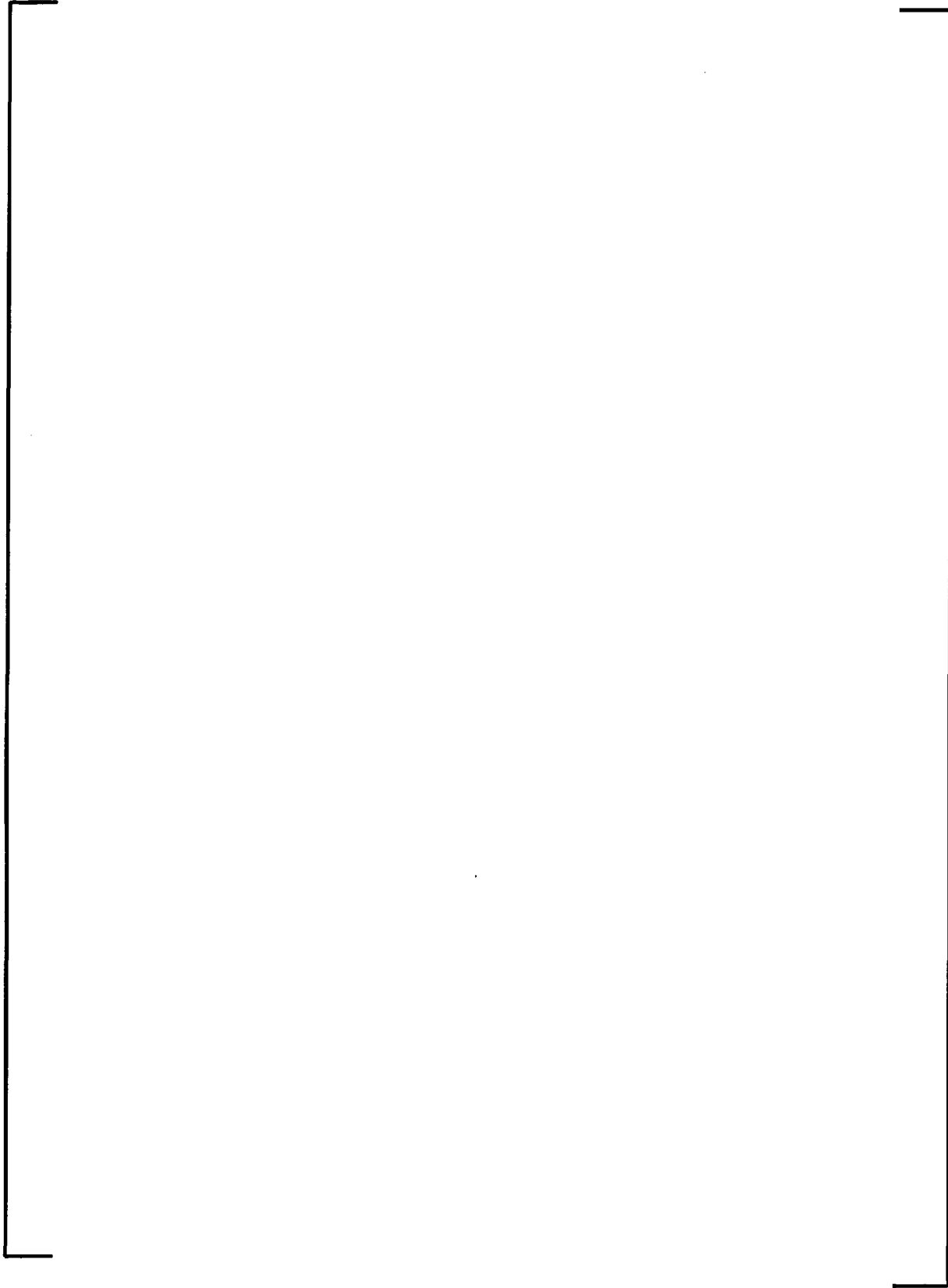


Table 4-1 (cont'd): Plant and Cycle Descriptions

a, b, c

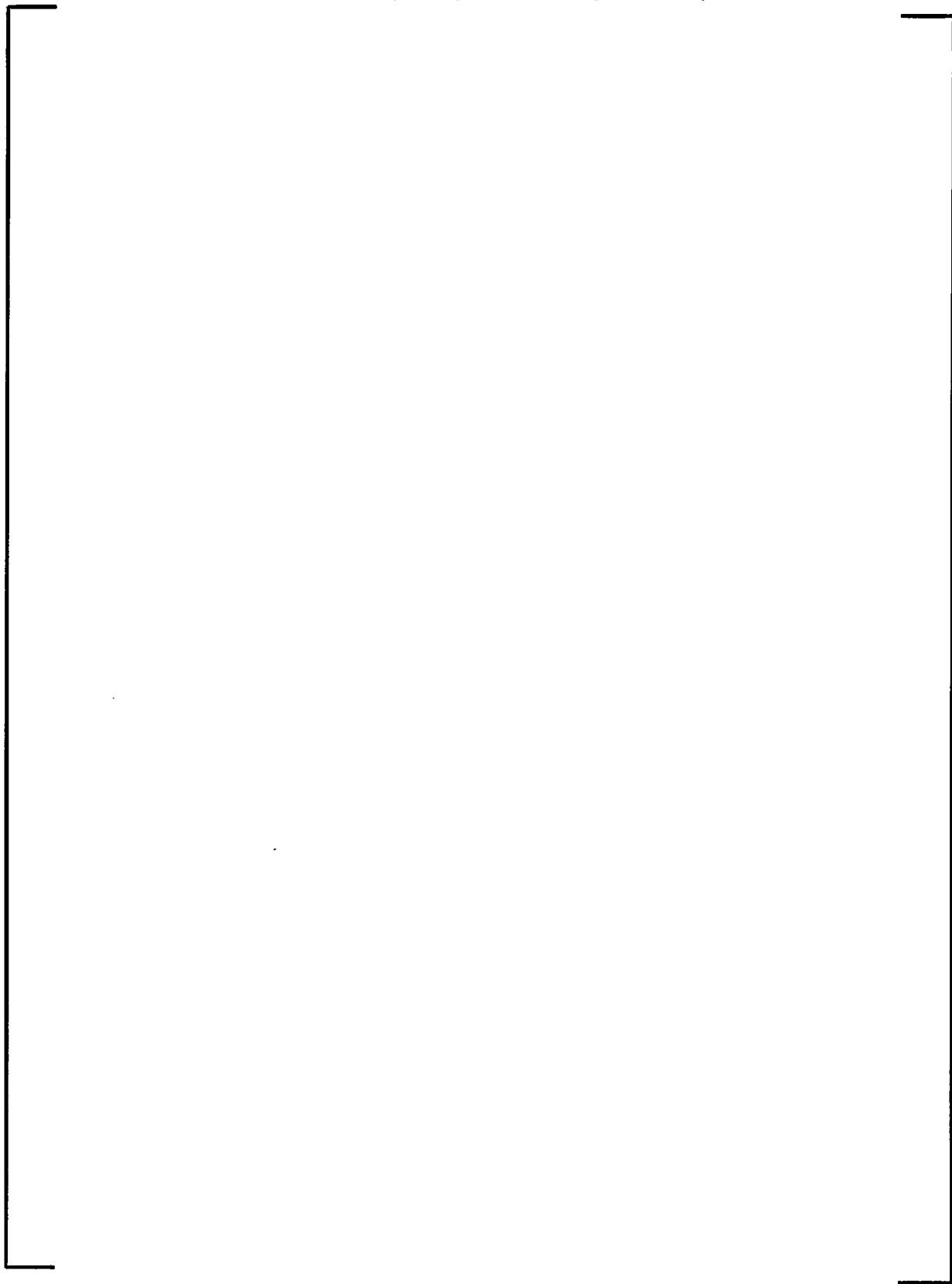
A large, empty rectangular frame with a thin black border, spanning most of the page width and height. It is positioned between the caption and the text 'a, b, c', suggesting it is the main content area of the table.

Table 4-1 (cont'd): Plant and Cycle Descriptions



a, b, c

Table 4-2: Hot Zero Power All Rods Out Critical Boron



a, b, c

Table 4-4: Hot Zero Power Control Bank Worth: Plant A, Cycle 11

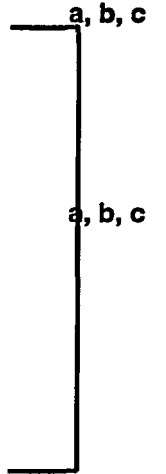


Table 4-5: Hot Zero Power Control Bank Worth: Plant B, Cycle 17



Table 4-6: Hot Zero Power Control Bank Worth: Plant C, Cycle 24

a, b, c



Table 4-7: Hot Zero Power Control Bank Worth: Plant D, Cycle 10

a, b, c



Table 4-8: Hot Zero Power Control Bank Worth: Plant E, Cycle 24

a, b, c



Table 4-9: Hot Zero Power Control Bank Worth: Plant I, Cycle 13

a, b, c



Table 4-10: Hot Zero Power Control Bank Worth: Plant I, Cycle 14

a, b, c



Table 4-11: Hot Zero Power Control Bank Worth: Plant J, Cycle 10

a, b, c



Table 4-12: Hot Zero Power Control Bank Worth: Plant J, Cycle 11

a, b, c



Table 4-13: ARI-WSR Control Rod Worth Comparison



a, b, c

Table 4-14: Dropped Rod Worth Comparison

a, b, c

Table 4-15: Rod Ejection Comparison

a, b, c

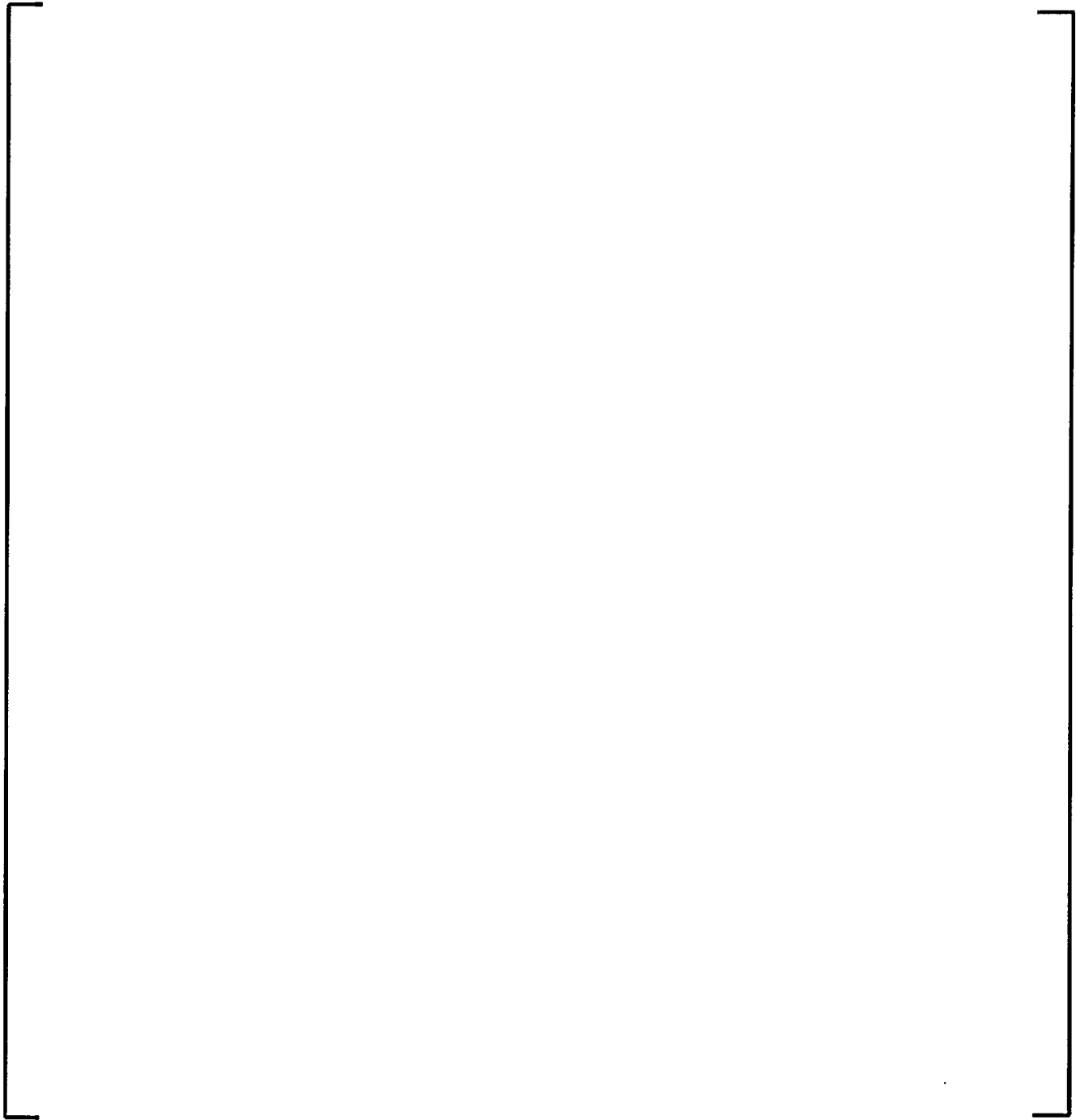
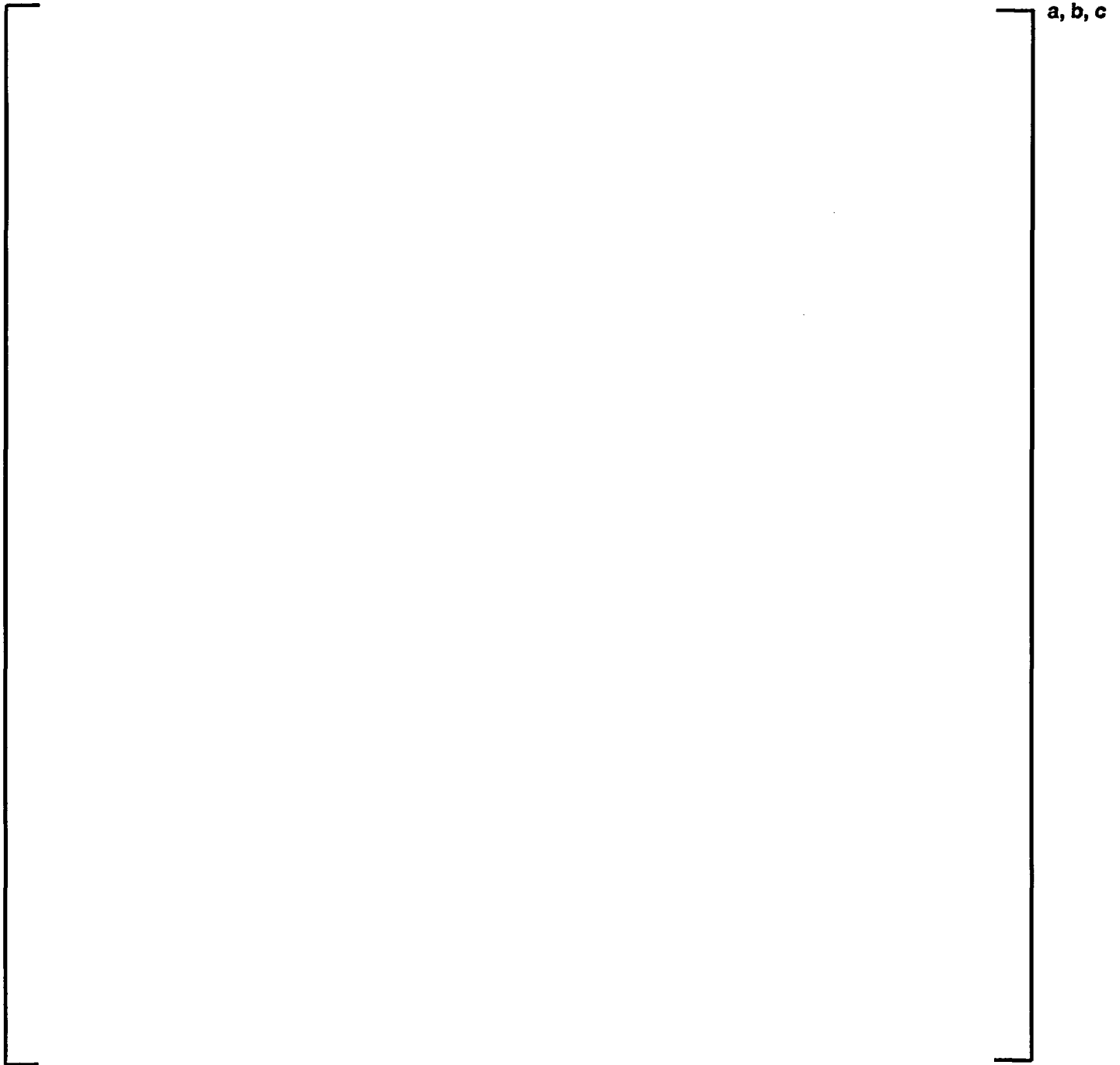


Table 4-16: End of Life HFP Moderator Temperature Coefficient

[

] a, b, c

**Figure 4-1: Critical Boron Concentration Versus Cycle Burnup Comparisons: Plant A
Cycle 10**



**Figure 4-2: Critical Boron Concentration Versus Cycle Burnup Comparisons: Plant A
Cycle 11**

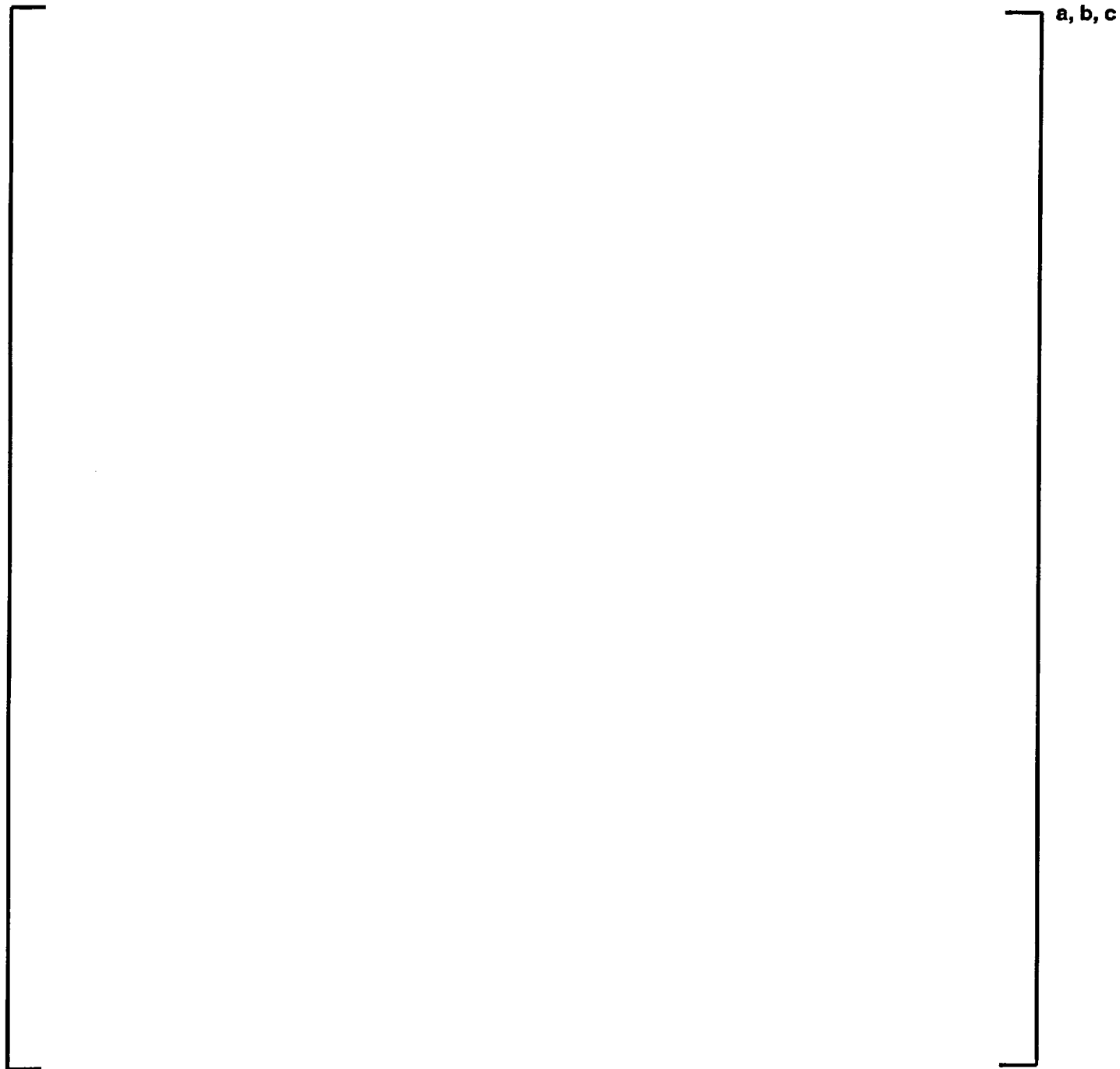


**Figure 4-3: Critical Boron Concentration Versus Cycle Burnup Comparisons: Plant B
Cycle 17**

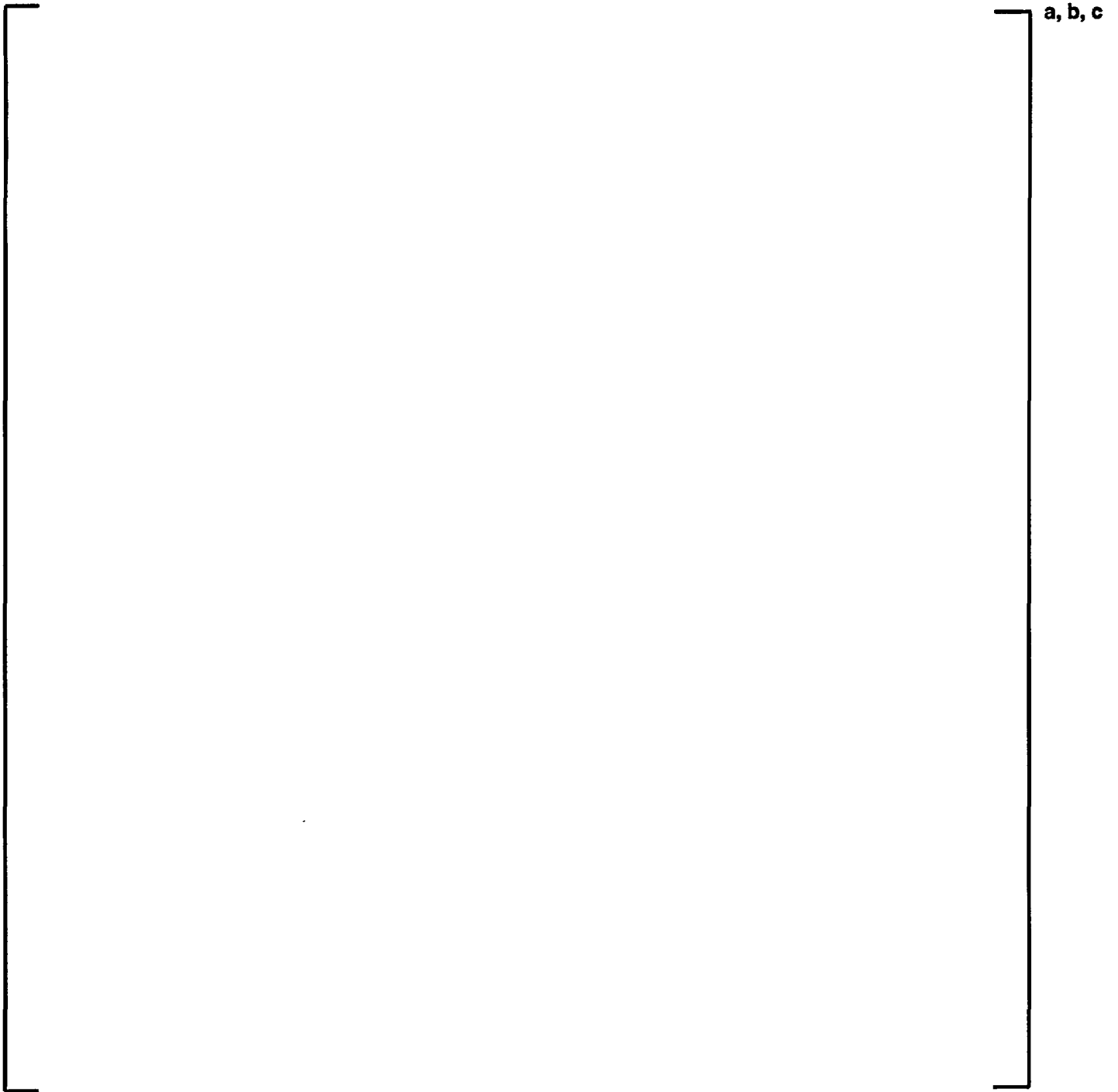


**Figure 4-4: Critical Boron Concentration Versus Cycle Burnup Comparisons: Plant B
Cycle 18**

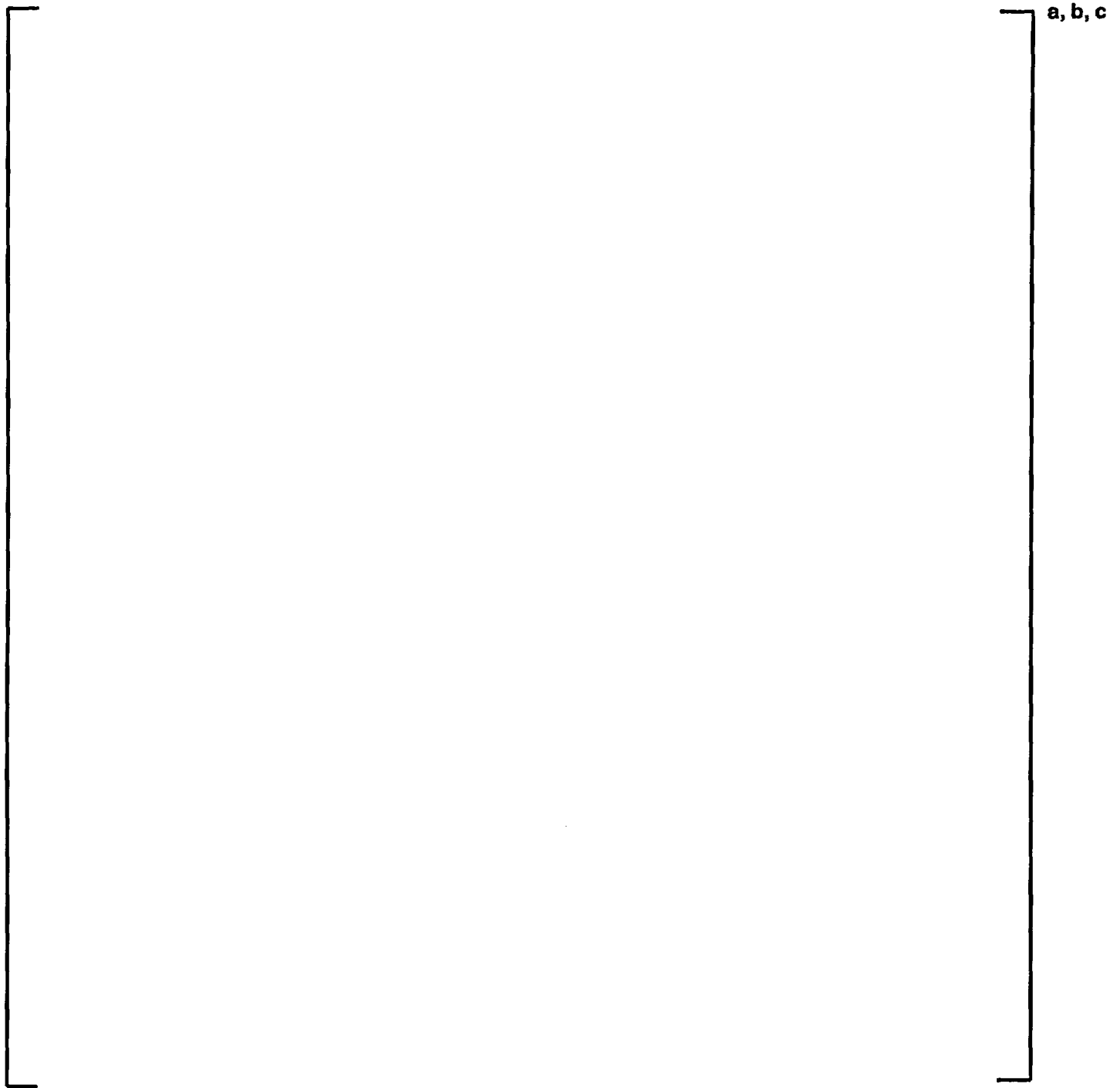


**Figure 4-5: Critical Boron Concentration Versus Cycle Burnup Comparisons: Plant C
Cycle 25**

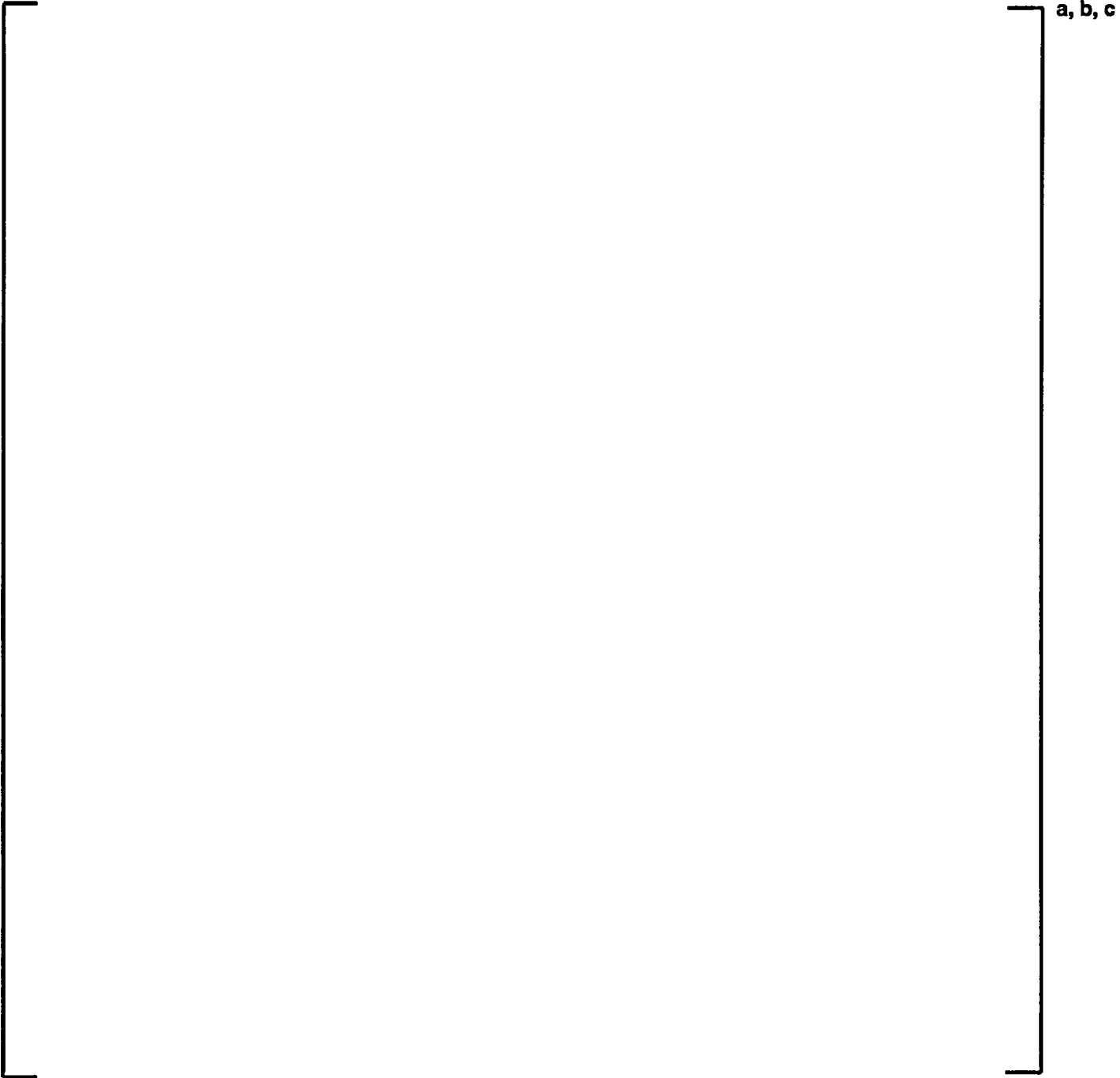


**Figure 4-6: Critical Boron Concentration Versus Cycle Burnup Comparisons: Plant C
Cycle 26**

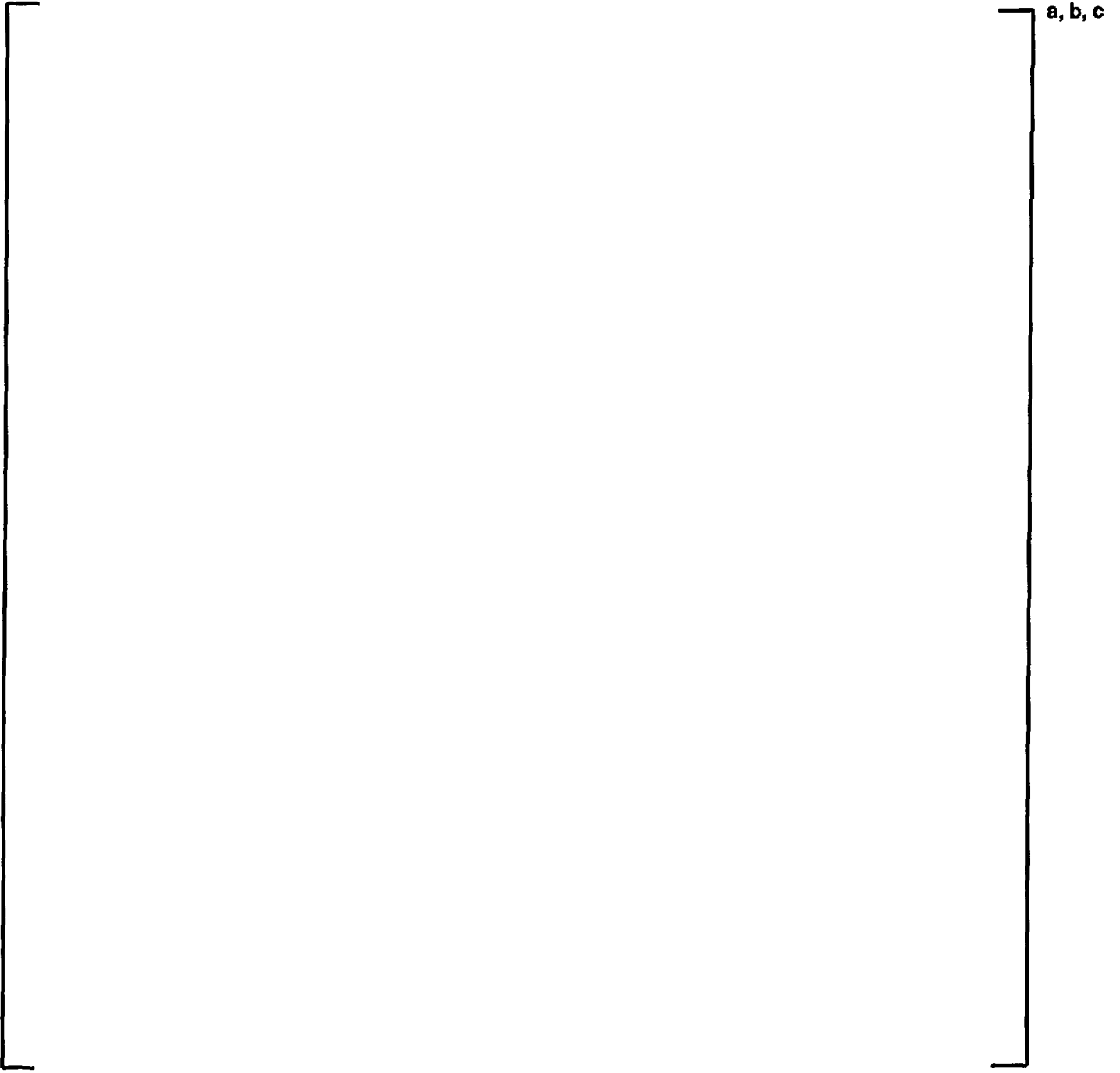


**Figure 4-7: Critical Boron Concentration Versus Cycle Burnup Comparisons: Plant D
Cycle 9**

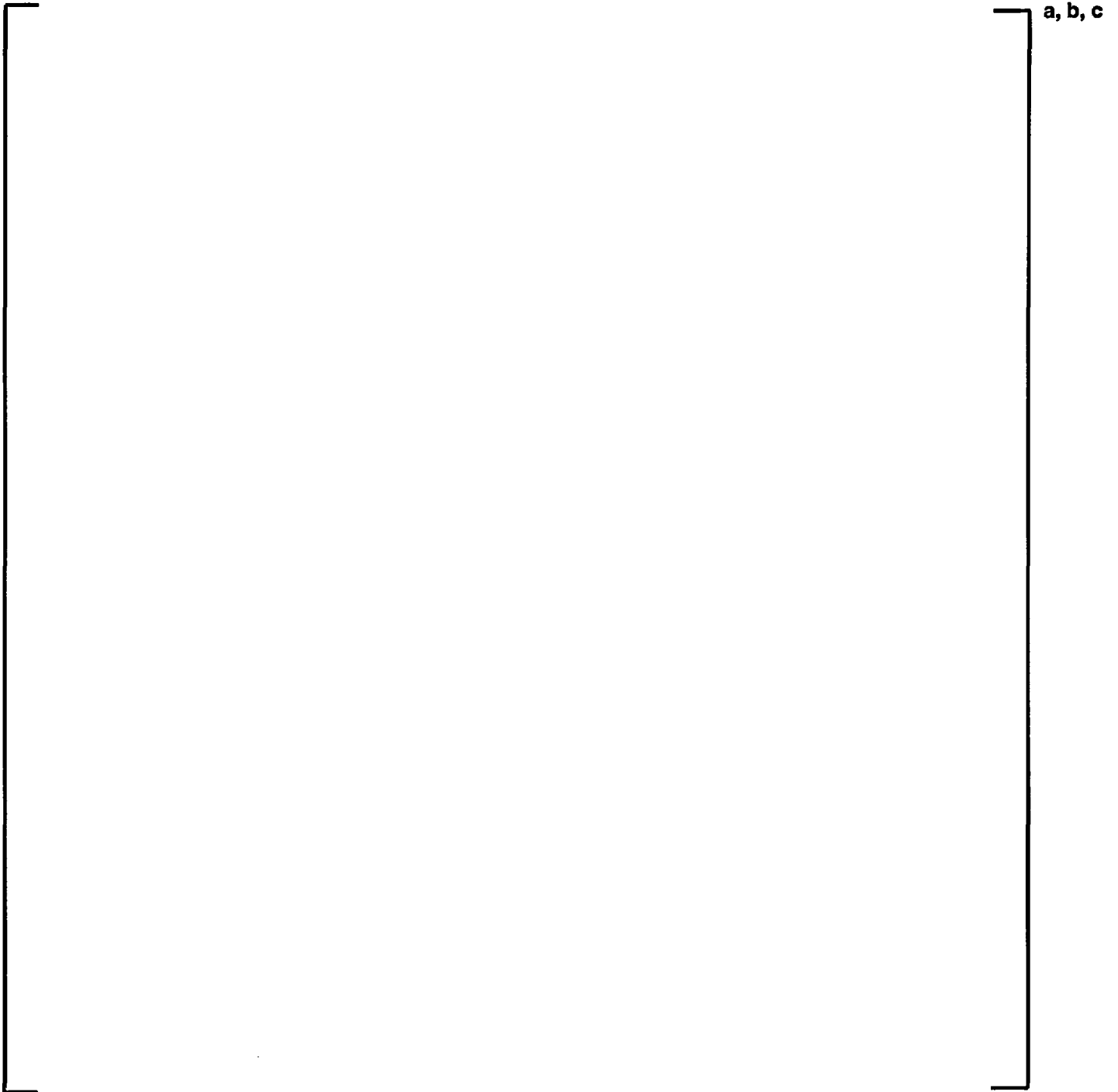


**Figure 4-8: Critical Boron Concentration Versus Cycle Burnup Comparisons: Plant D
Cycle 10**

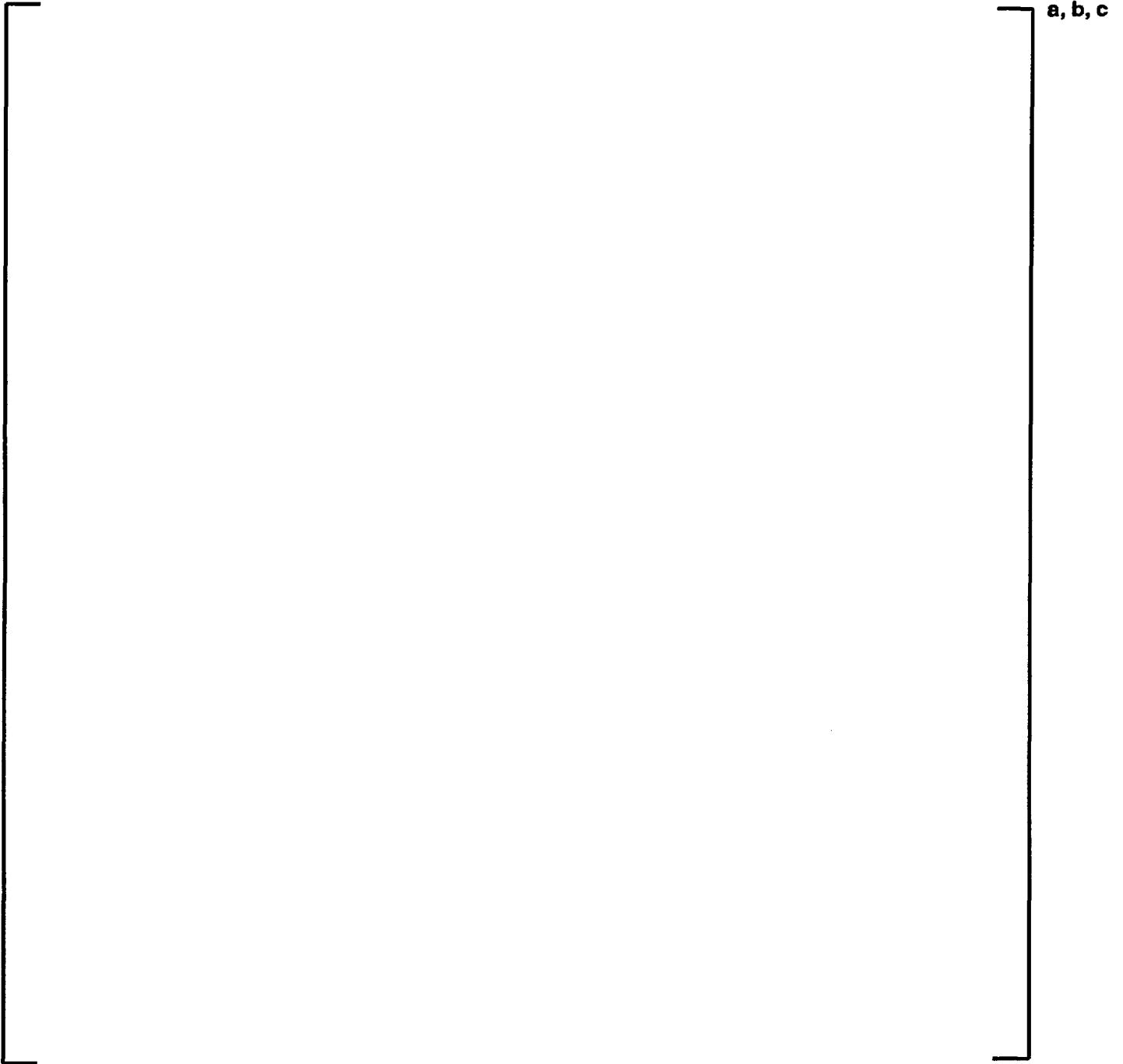
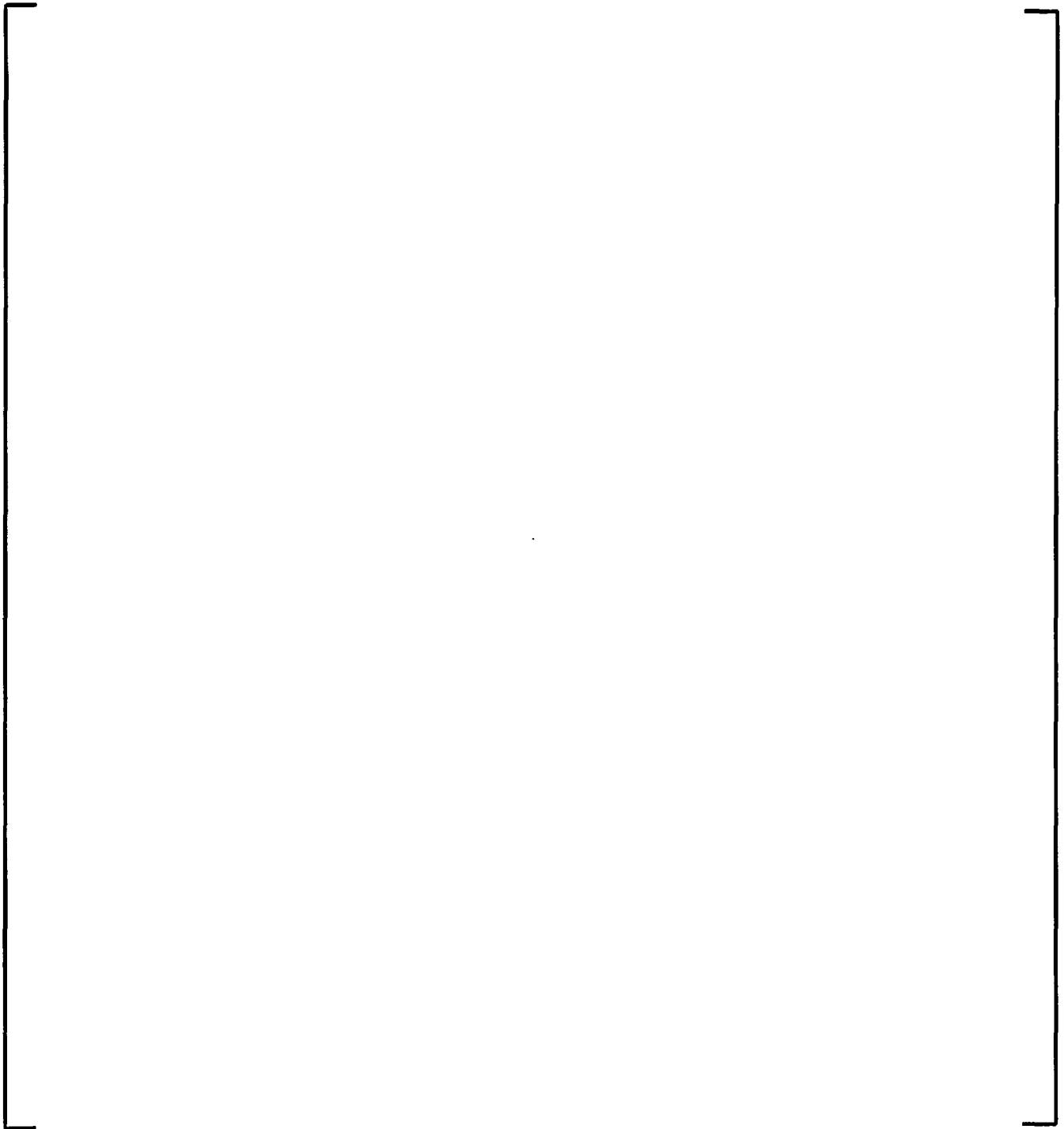


**Figure 4-9: Critical Boron Concentration Versus Cycle Burnup Comparisons: Plant D
Cycle 11**



a, b, c

**Figure 4-10: Critical Boron Concentration Versus Cycle Burnup Comparisons: Plant E
Cycle 25**

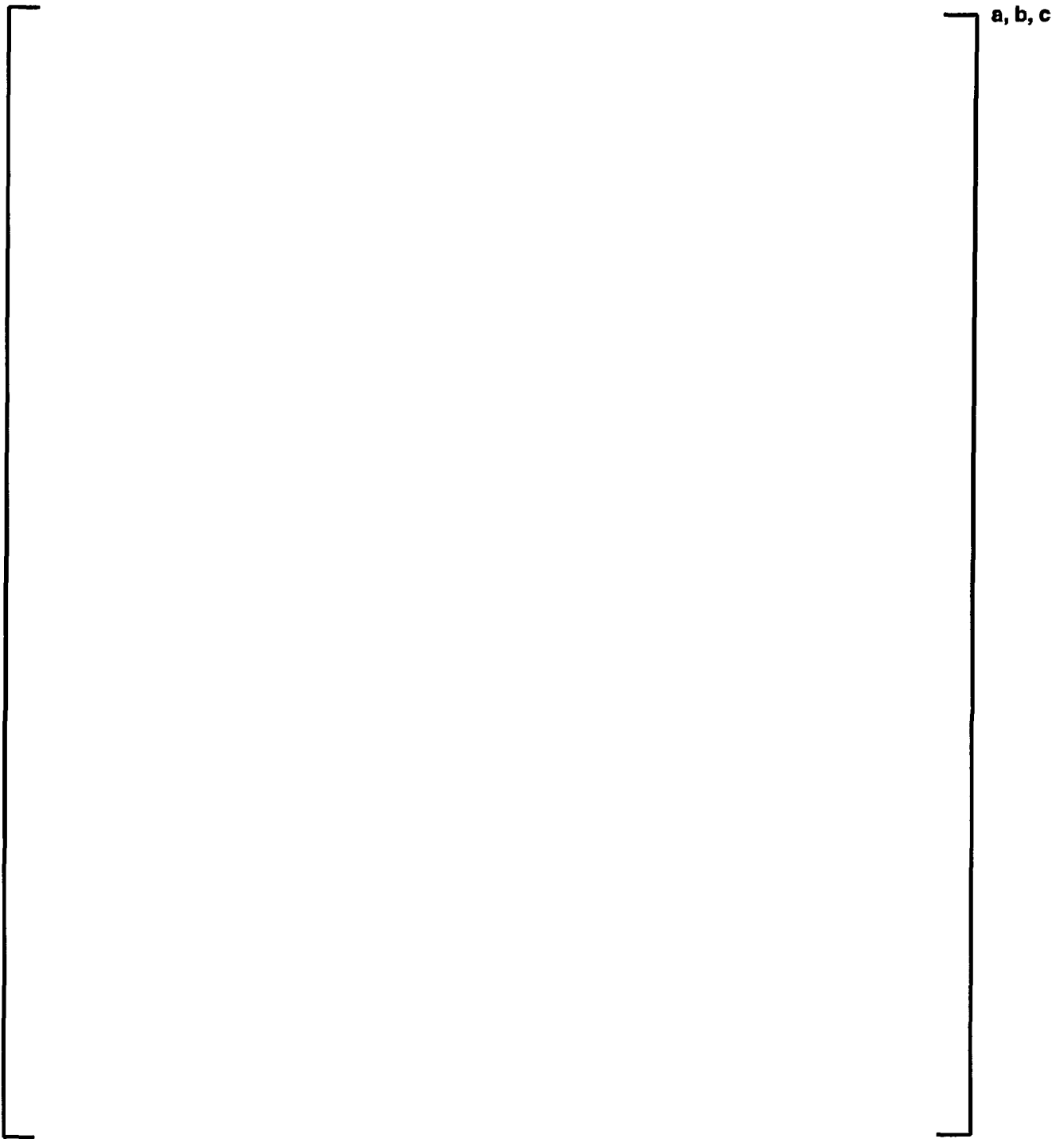


**Figure 4-11: Critical Boron Concentration Versus Cycle Burnup Comparisons: Plant F
Cycle 10**

a, b, c

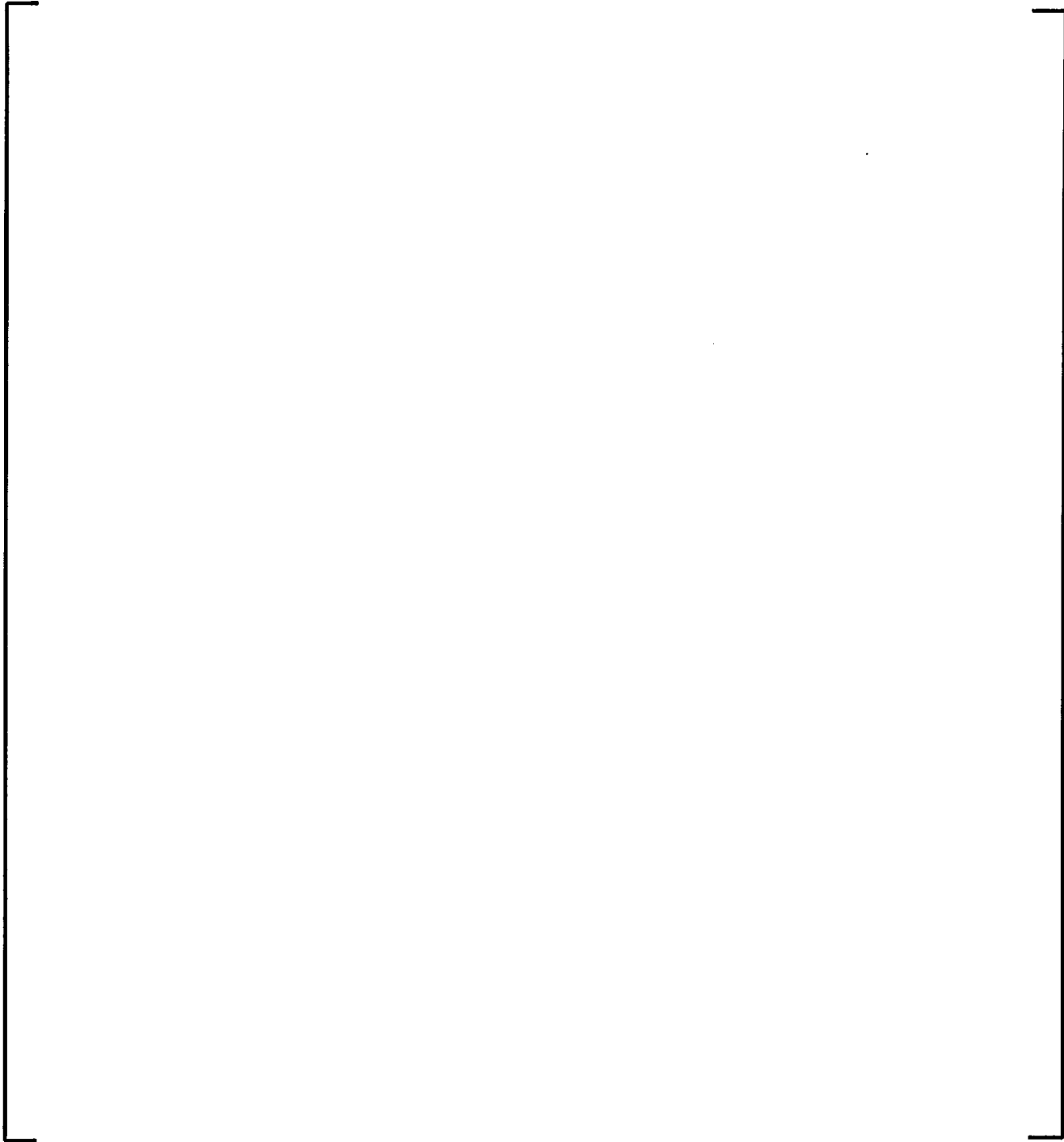


**Figure 4-12: Critical Boron Concentration Versus Cycle Burnup Comparisons: Plant F
Cycle 11**

a, b, c

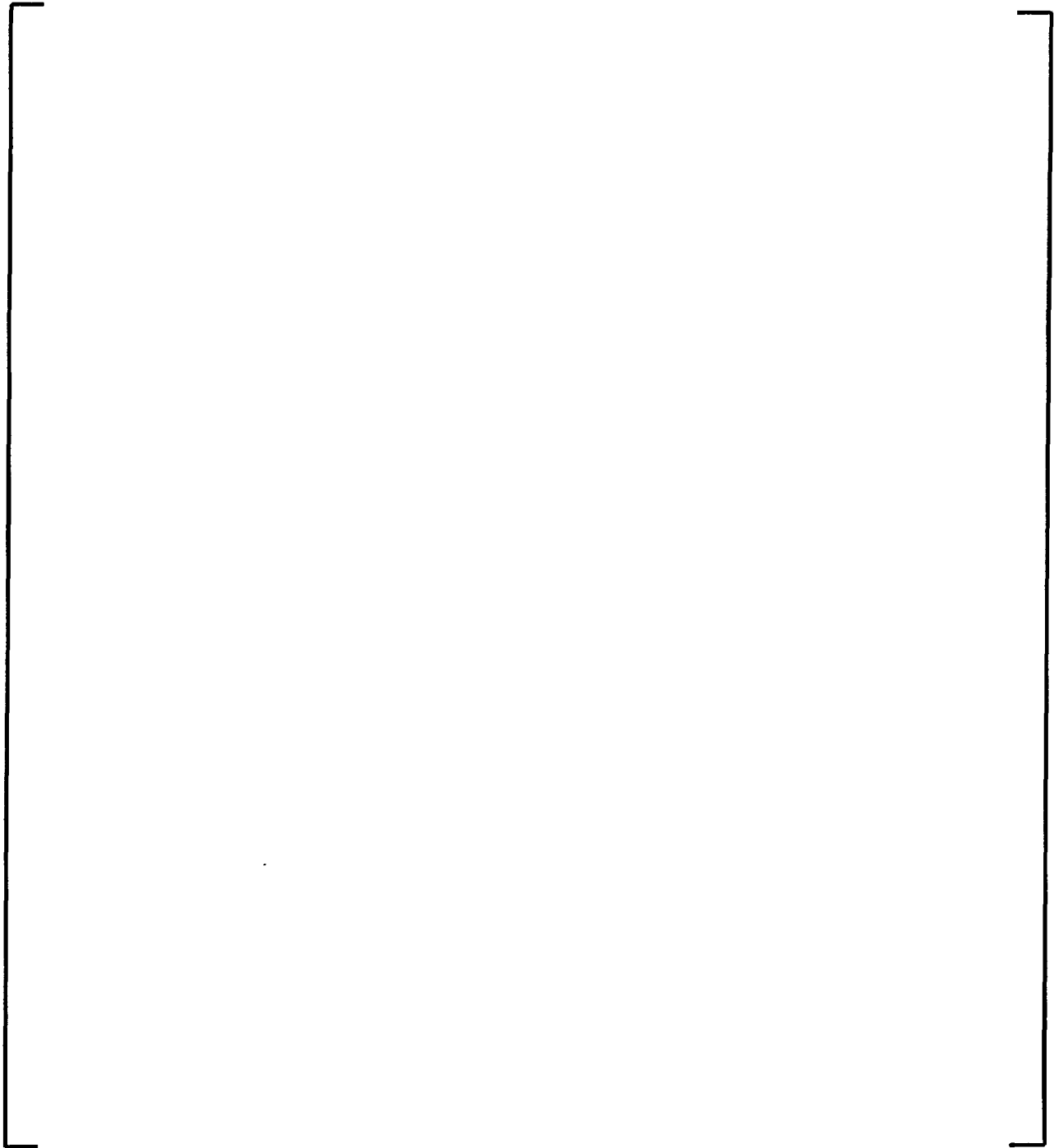


**Figure 4-13: Critical Boron Concentration Versus Cycle Burnup Comparisons: Plant F
Cycle 12**

a, b, c

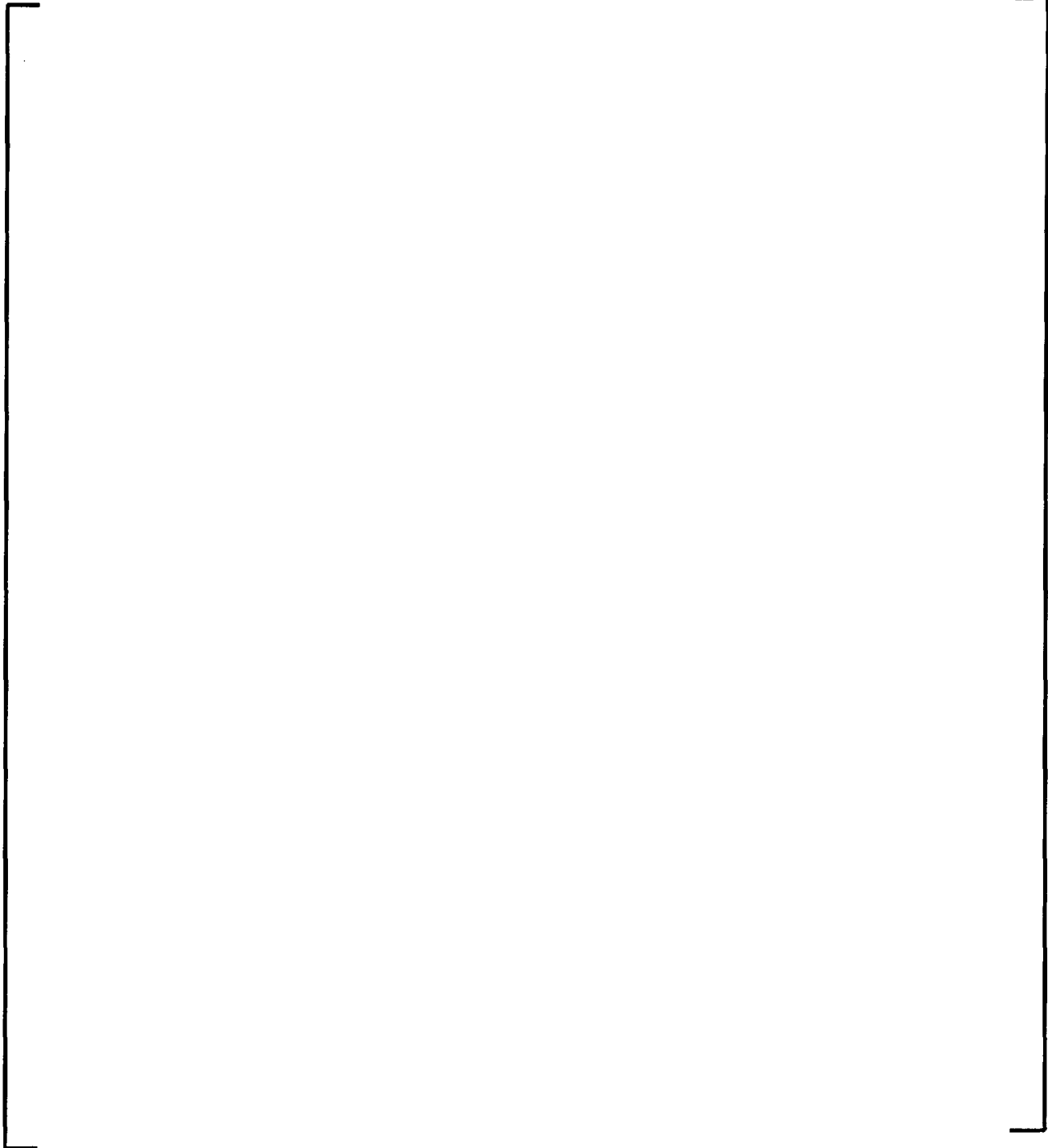


**Figure 4-14: Critical Boron Concentration Versus Cycle Burnup Comparisons: Plant G
Cycle 13**

a, b, c

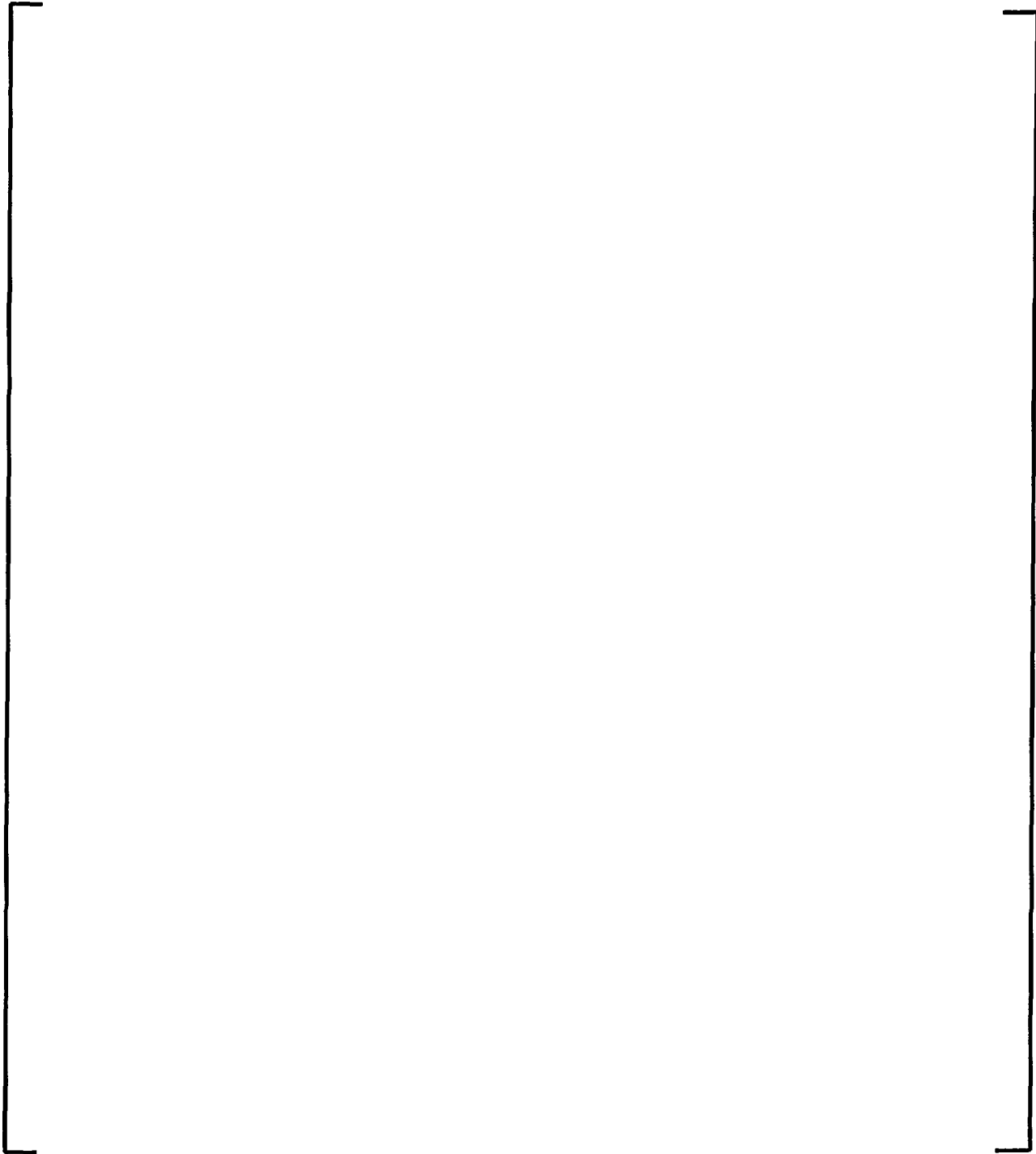


**Figure 4-15: Critical Boron Concentration Versus Cycle Burnup Comparisons: Plant H
Cycle 1**

a, b, c

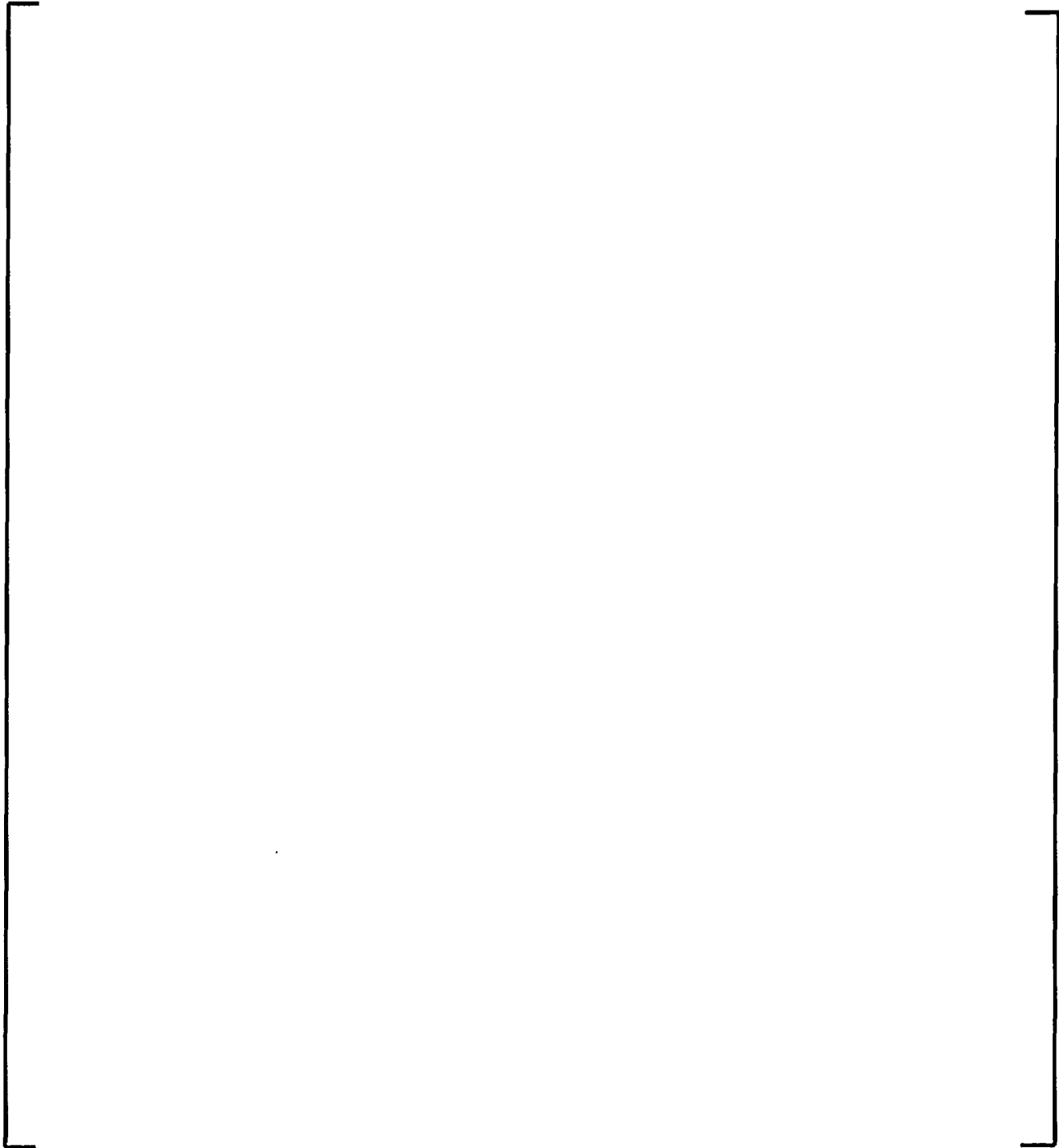


**Figure 4-16: Critical Boron Concentration Versus Cycle Burnup Comparisons: Plant I
Cycle 13**

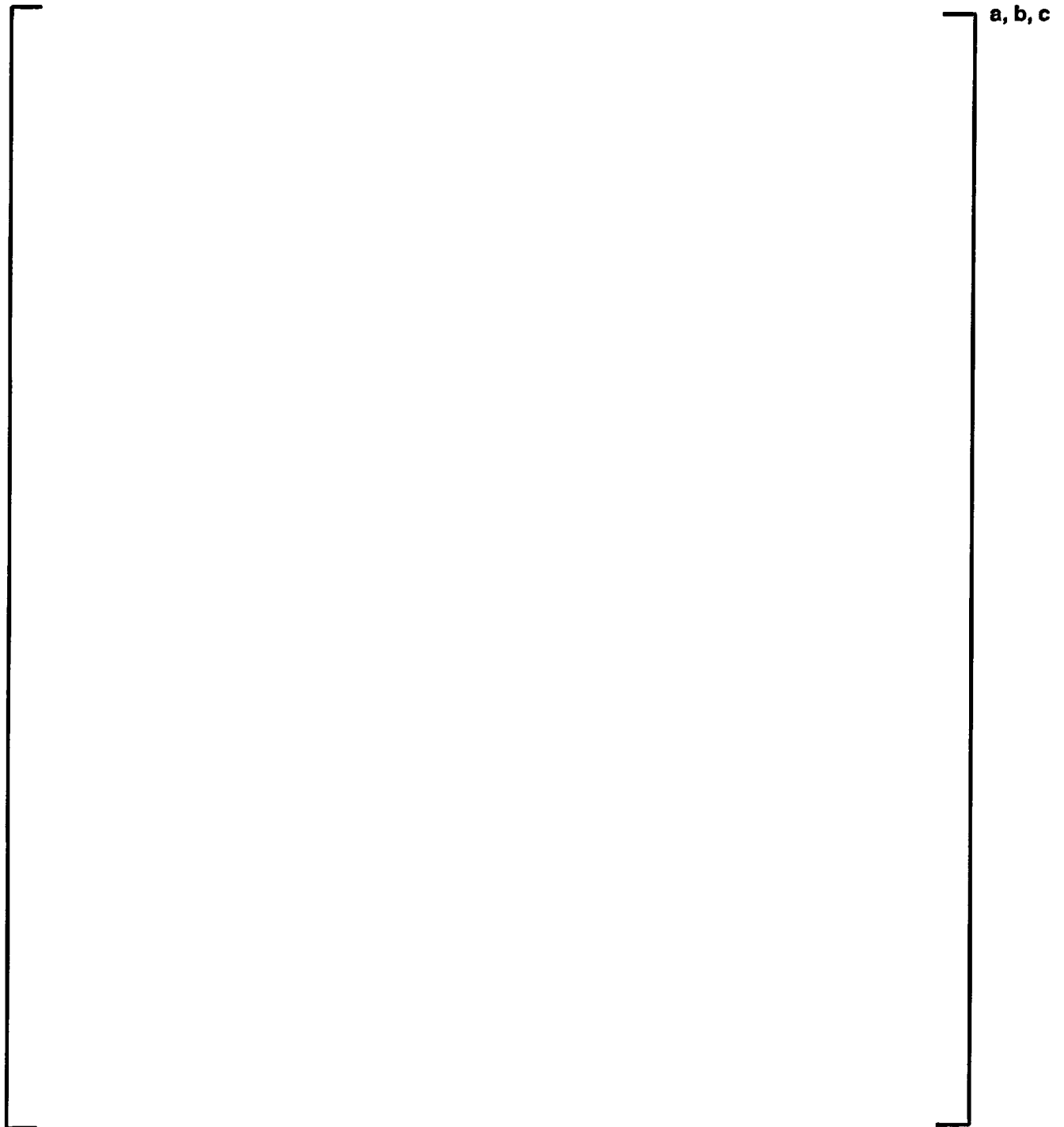


**Figure 4-17: Critical Boron Concentration Versus Cycle Burnup Comparisons: Plant I
Cycle 14**

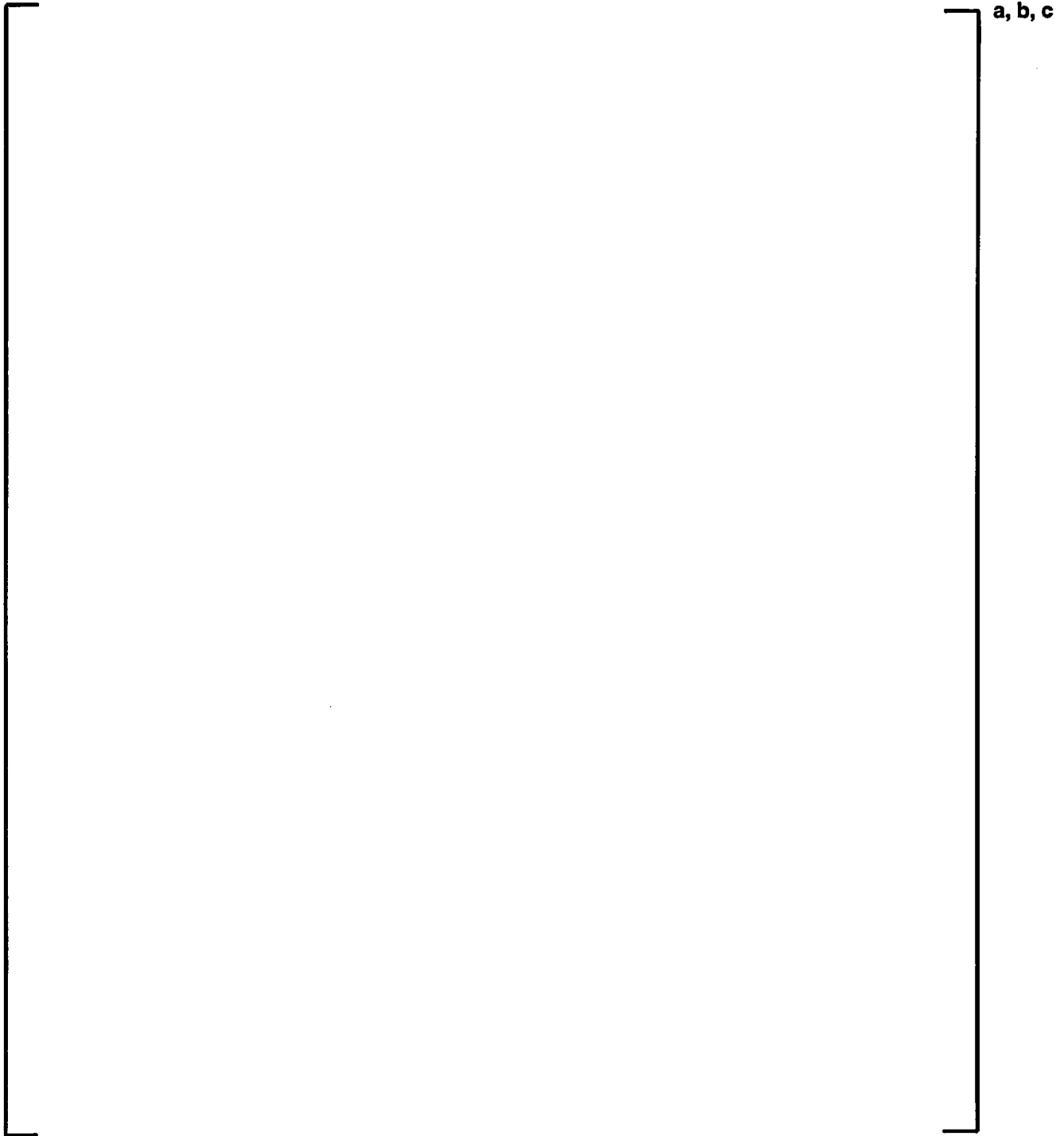


**Figure 4-18: Critical Boron Concentration Versus Cycle Burnup Comparisons: Plant J
Cycle 10**

a, b, c

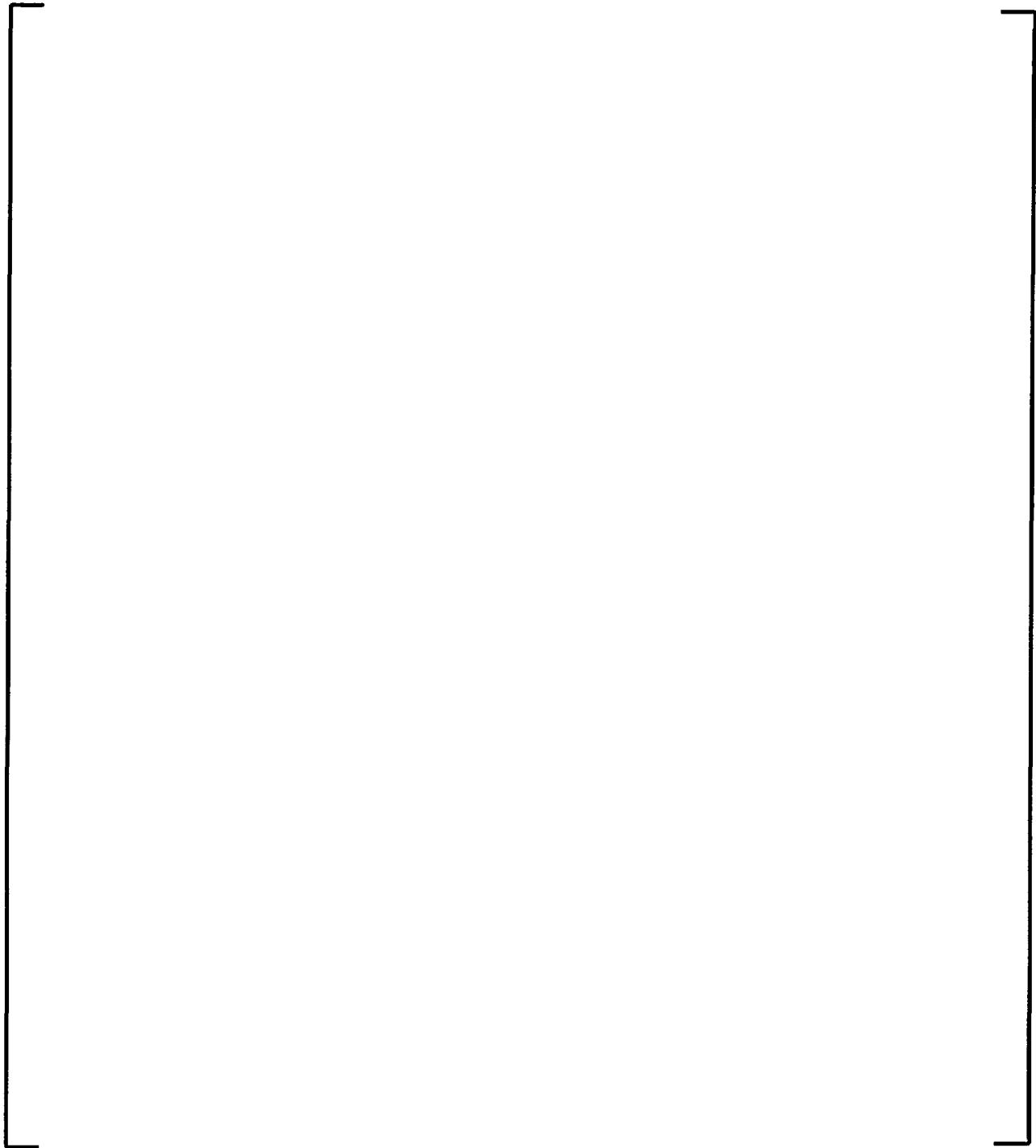


**Figure 4-19: Critical Boron Concentration Versus Cycle Burnup Comparisons: Plant J
Cycle 11**

a, b, c

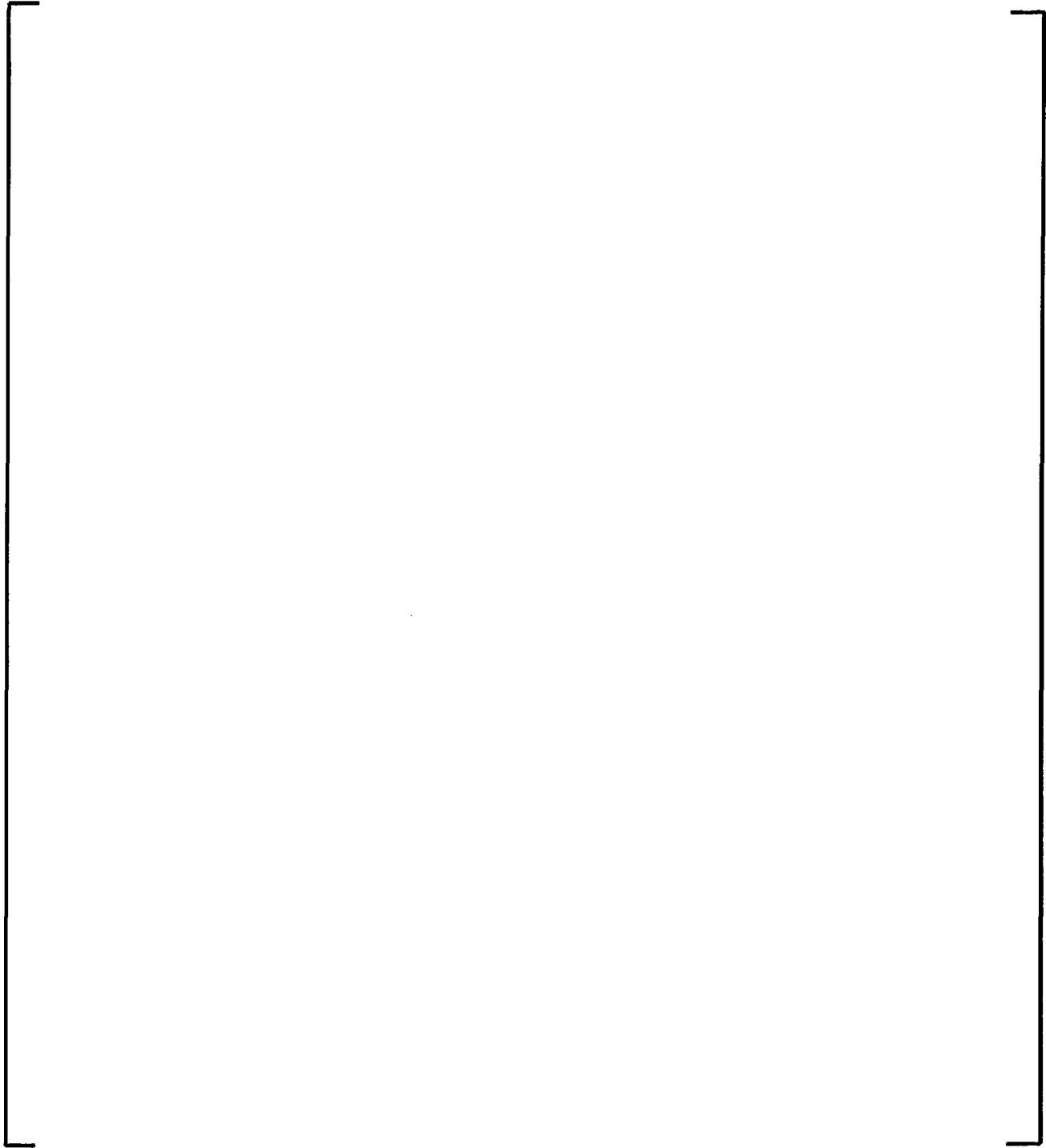


**Figure 4-20: Critical Boron Concentration Versus Cycle Burnup Comparisons: Plant K
Cycle 1**

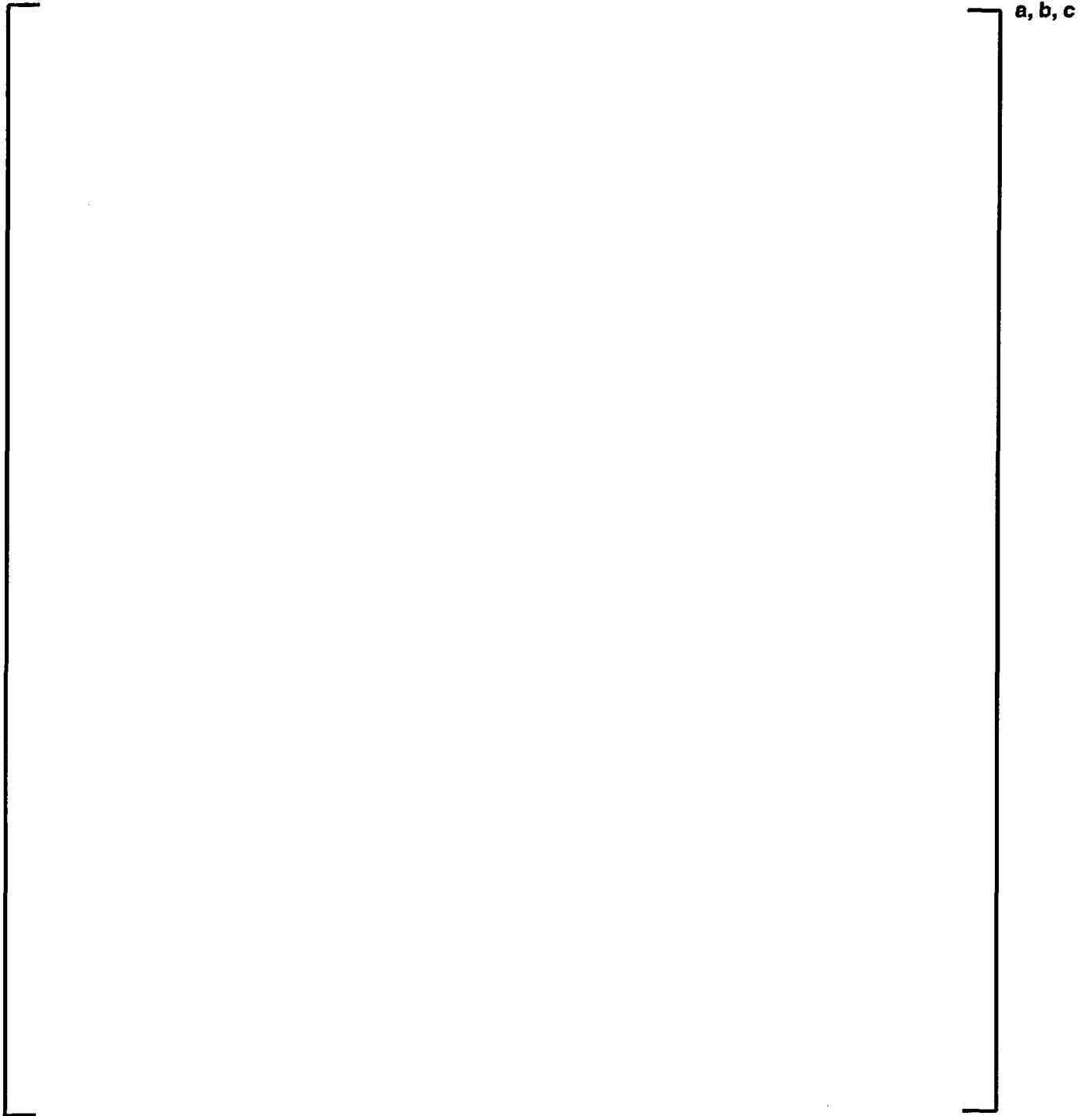


**Figure 4-21: Critical Boron Concentration Versus Cycle Burnup Comparisons: Plant K
Cycle 2**

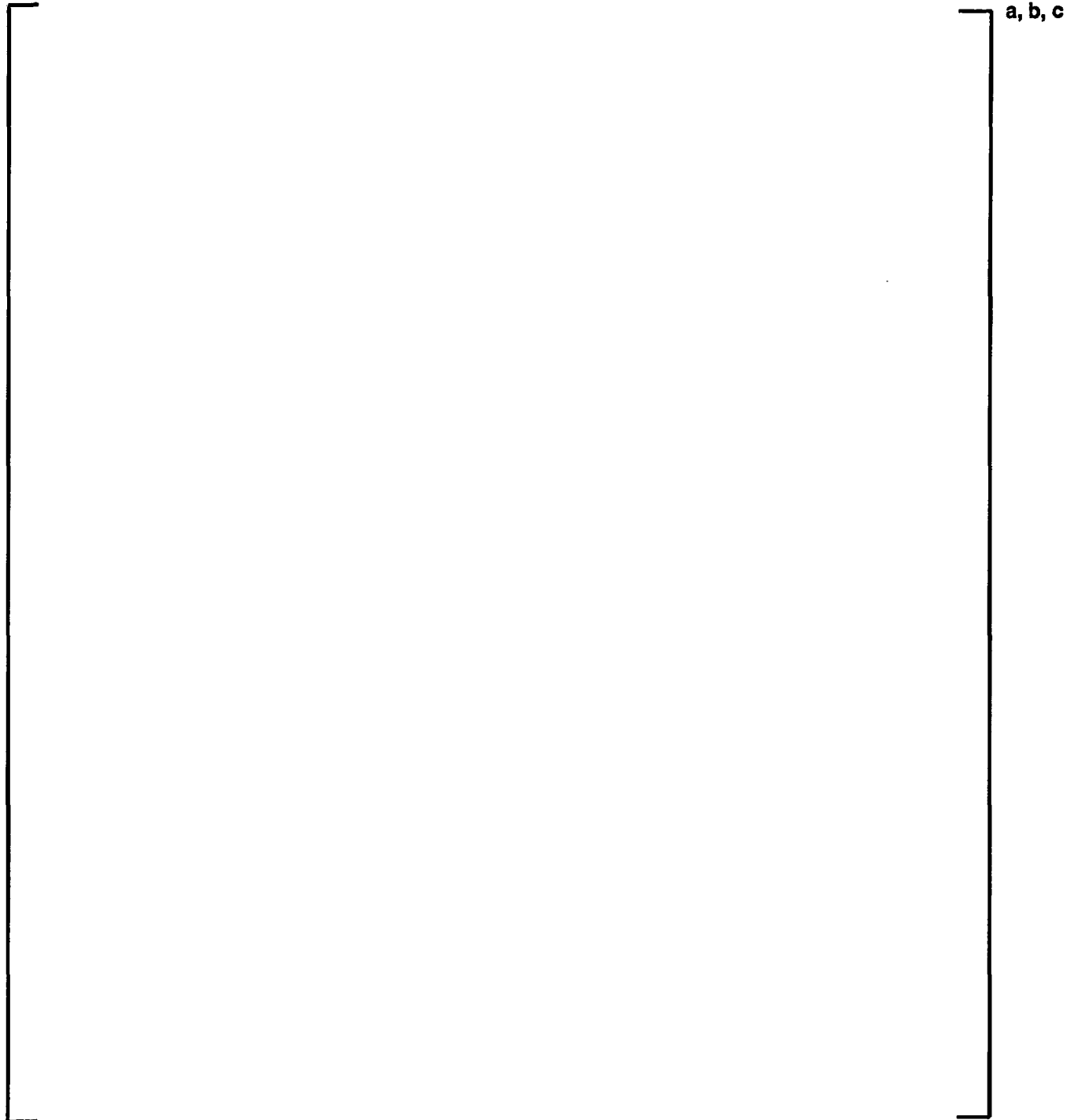


**Figure 4-22: Critical Boron Concentration Versus Cycle Burnup Comparisons: Plant K
Cycle 3**

a, b, c

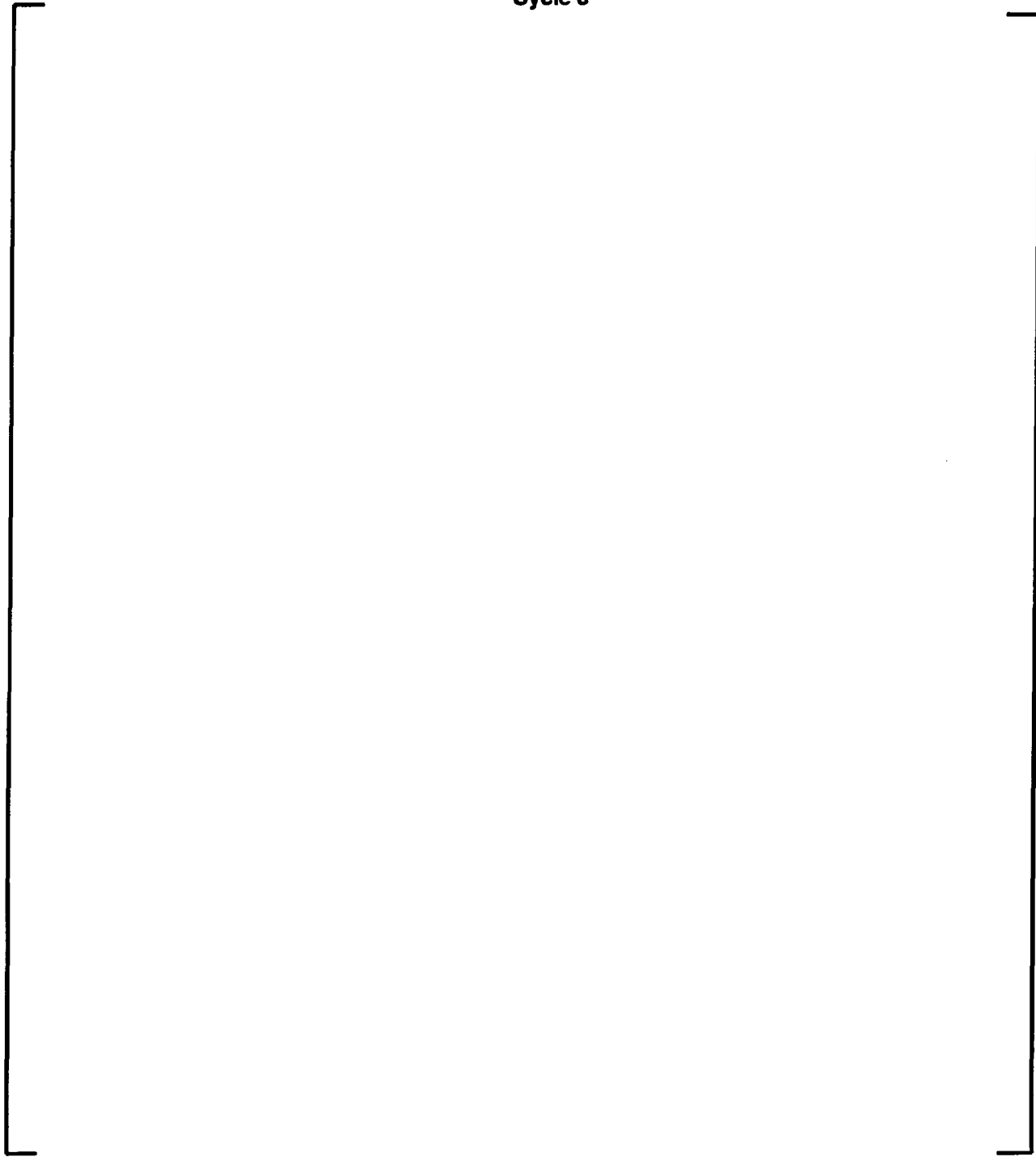
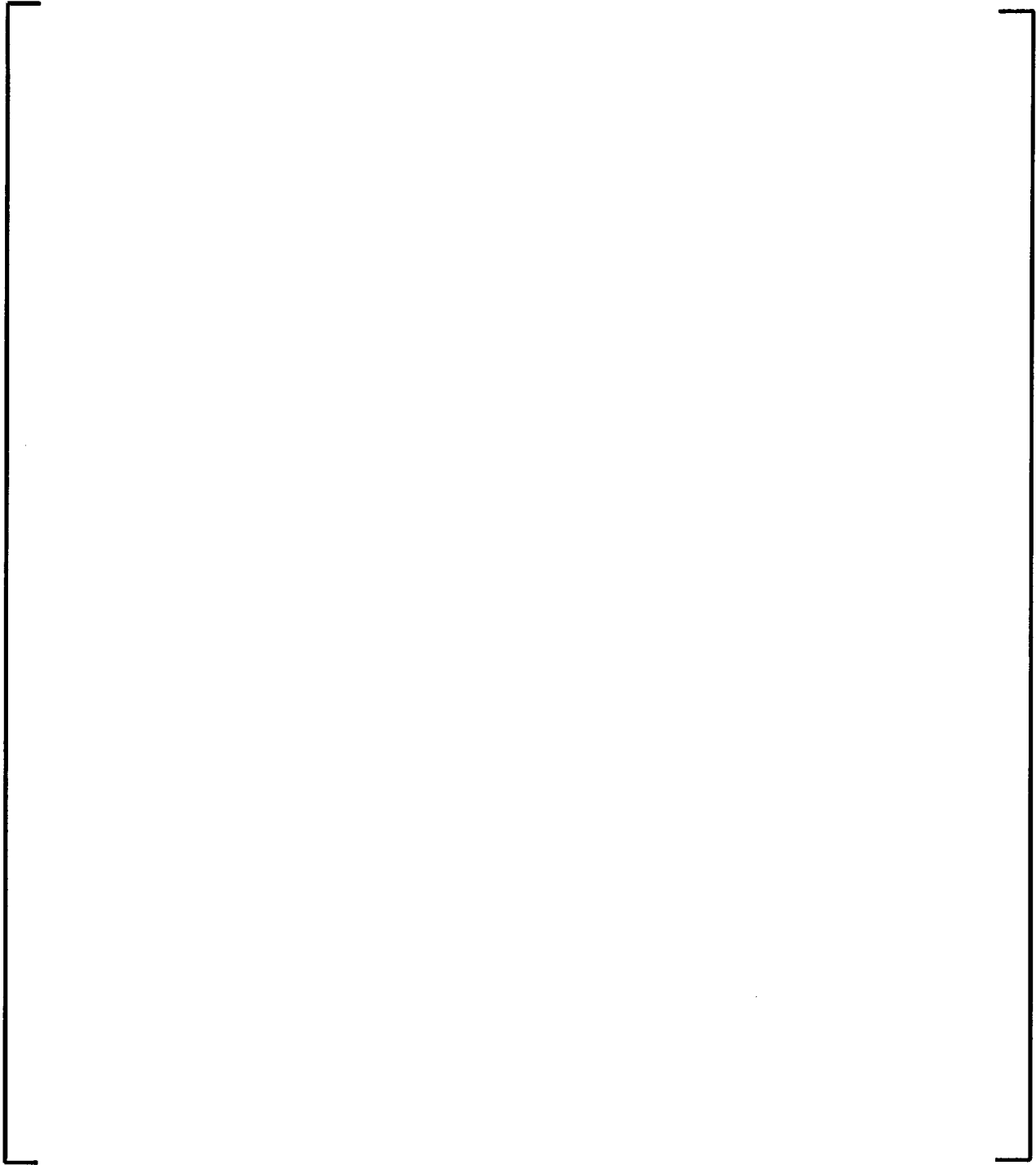


**Figure 4-23: Critical Boron Concentration Versus Cycle Burnup Comparisons: Plant F
Cycle 11 –Calculated values with and without B10 correction**



a, b, c

Figure 4-24: Assembly Average Power Distribution: Plant A, Cycle 10, 3355 MWD/MTU Burnup



Figure 4-25: Assembly Average Power Distribution: Plant A, Cycle 10, 11958 MWD/MTU Burnup



a, b, c

Figure 4-26: Assembly Average Power Distribution: Plant A, Cycle 11, 1460 MWD/MTU Burnup



**Figure 4-27: Assembly Average Power Distribution: Plant A, Cycle 11, 13052 MWD/MTU
Burnup**



**Figure 4-28: Assembly Average Power Distribution: Plant A, Cycle 11, 19738 MWD/MTU
Burnup**

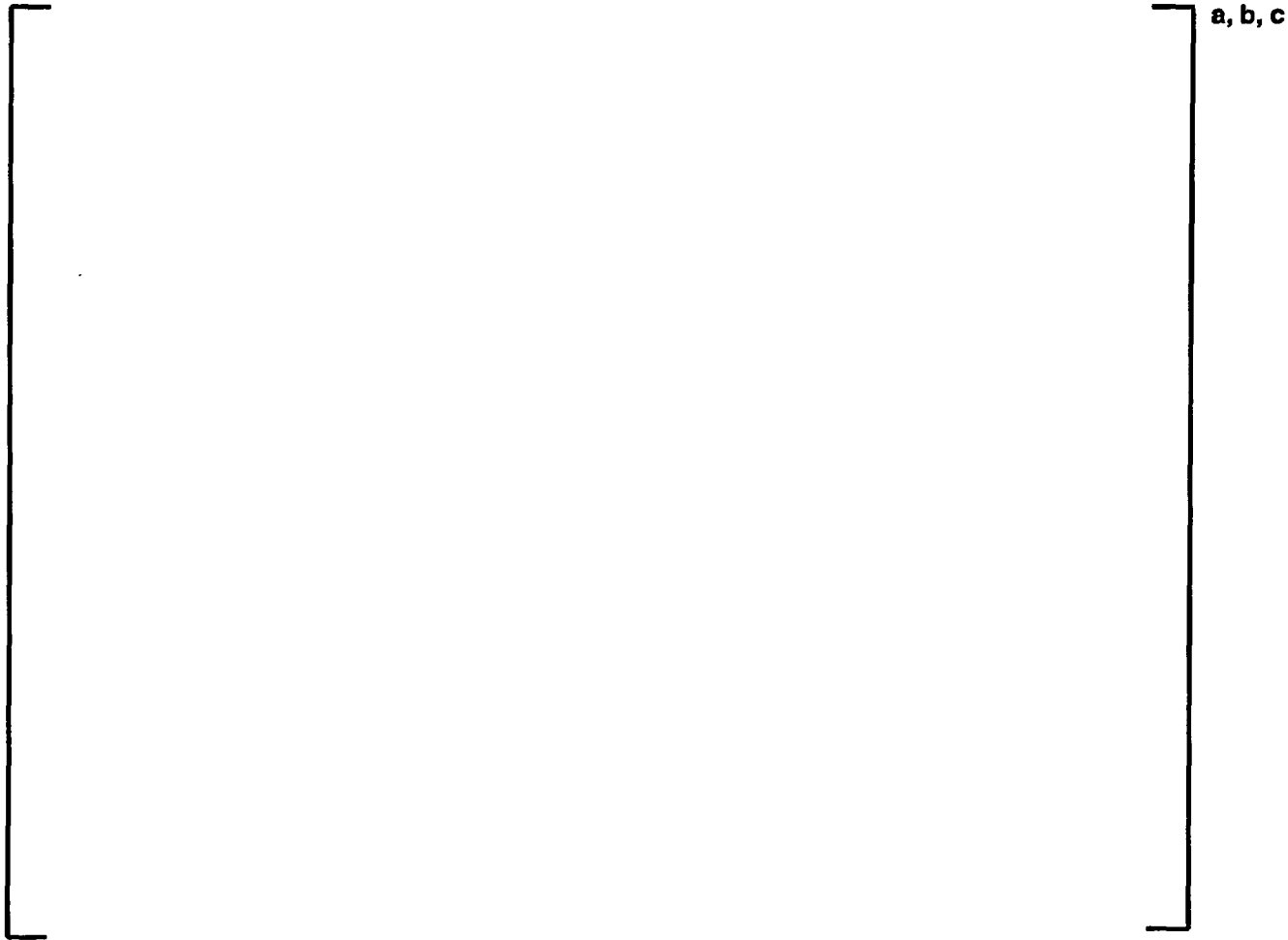


Figure 4-29: Assembly Average Power Distribution: Plant B, Cycle 17, 386 MWD/MTU Burnup



Figure 4-30: Assembly Average Power Distribution: Plant B, Cycle 17, 7878 MWD/MTU Burnup



Figure 4-31: Assembly Average Power Distribution: Plant B, Cycle 17, 10930 MWD/MTU Burnup



**Figure 4-32: Assembly Average Power Distribution: Plant B, Cycle 18, 1375 MWD/MTU
Burnup**



Figure 4-33: Assembly Average Power Distribution: Plant B, Cycle 18, 6926 MWD/MTU Burnup



Figure 4-34: Assembly Average Power Distribution: Plant C, Cycle 25, 262 MWD/MTU Burnup



Figure 4-35: Assembly Average Power Distribution: Plant C, Cycle 25, 7080 MWD/MTU Burnup



Figure 4-36: Assembly Average Power Distribution: Plant C, Cycle 25, 13400 MWD/MTU Burnup



**Figure 4-37: Assembly Average Power Distribution: Plant C, Cycle 26, 788 MWD/MTU
Burnup**



Figure 4-38: Assembly Average Power Distribution: Plant C, Cycle 26, 8073 MWD/MTU Burnup



a, b, c

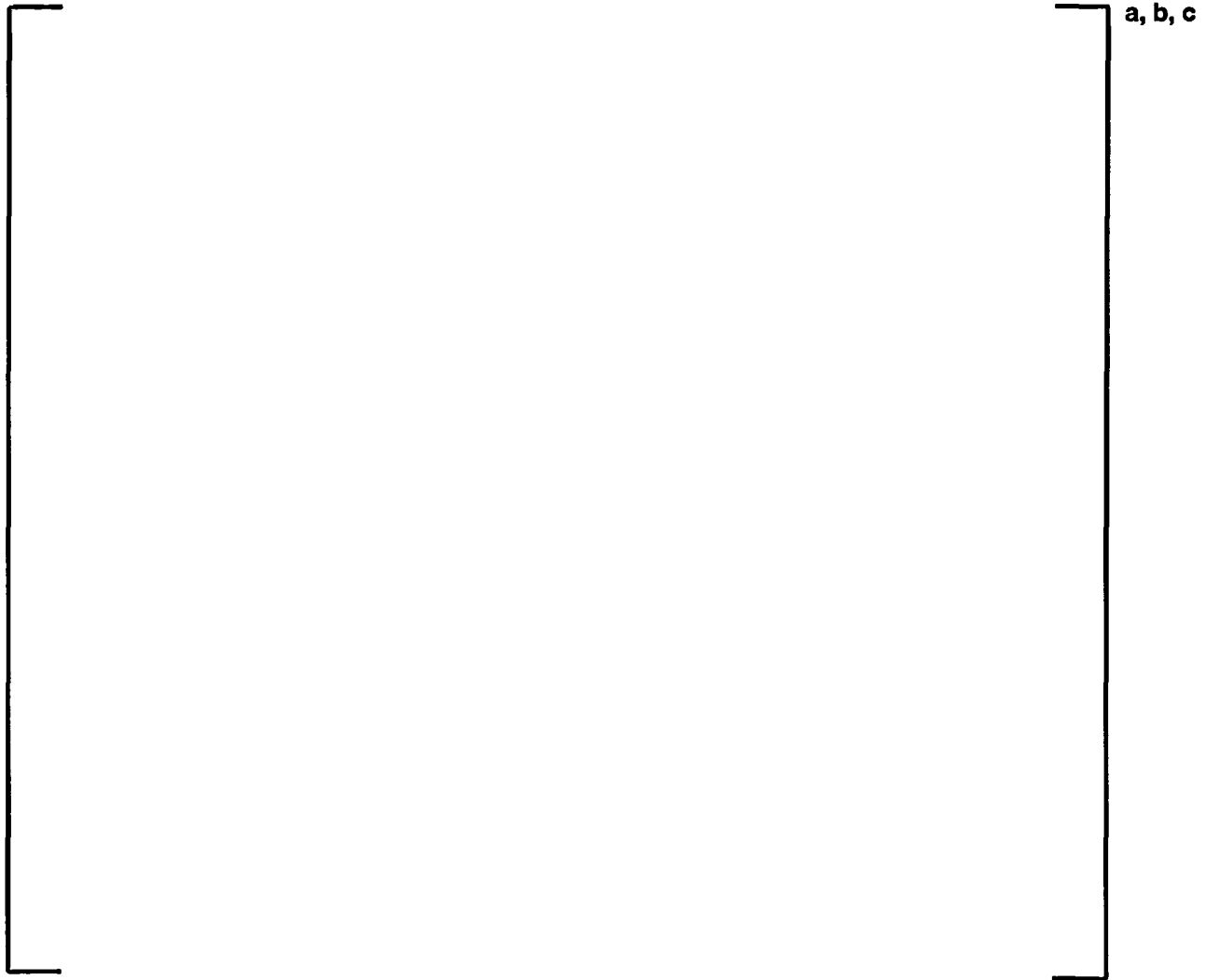
**Figure 4-39: Assembly Average Power Distribution: Plant C, Cycle 26, 14838 MWD/MTU
Burnup**



Figure 4-40: Assembly Average Power Distribution: Plant D, Cycle 10, 1980 MWD/MTU Burnup



Figure 4-41: Assembly Average Power Distribution: Plant D, Cycle 10, 9700 MWD/MTU Burnup



**Figure 4-42: Assembly Average Power Distribution: Plant D, Cycle 10, 20829 MWD/MTU
Burnup**

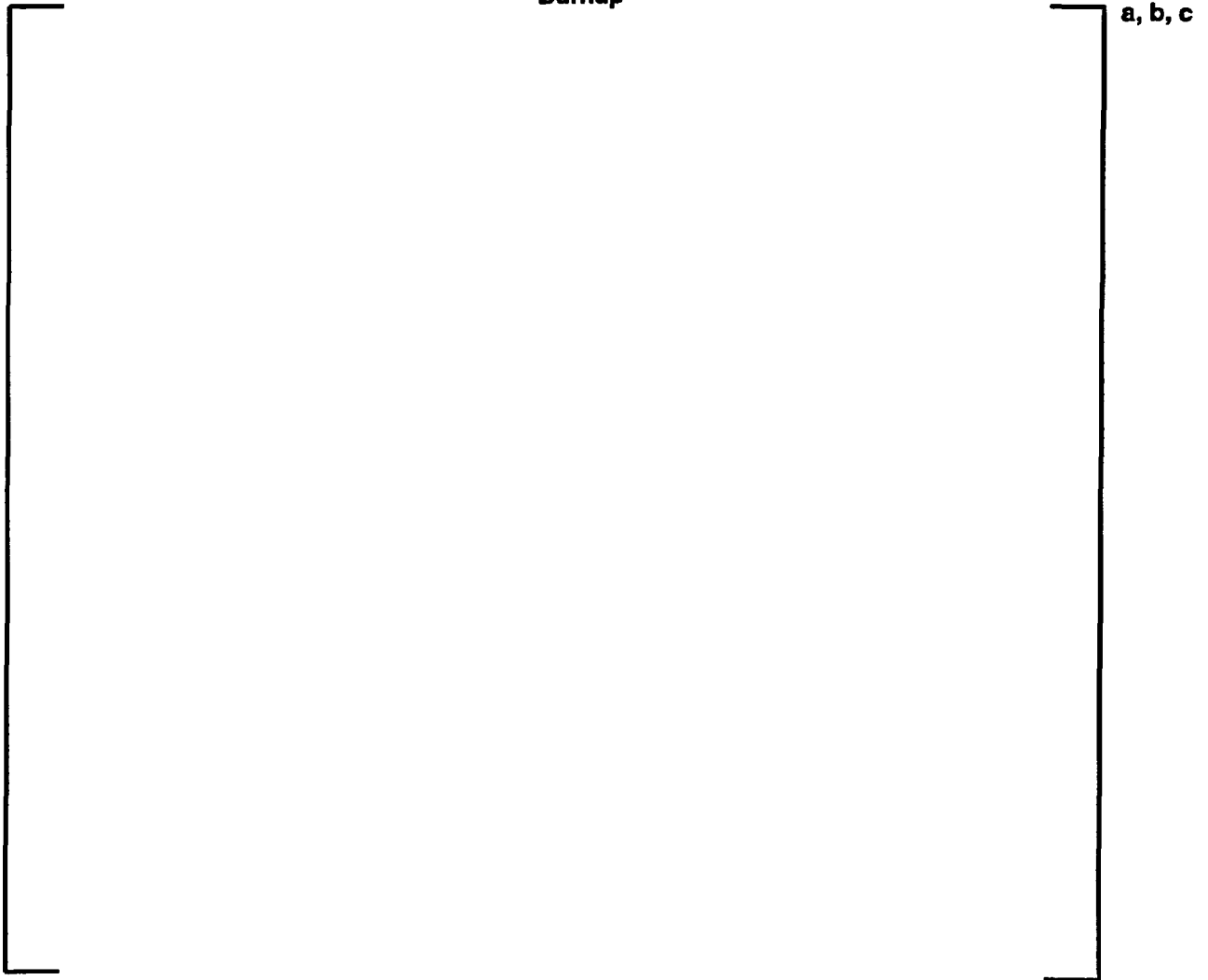


Figure 4-43: Assembly Average Power Distribution: Plant D, Cycle 11, 1010 MWD/MTU Burnup

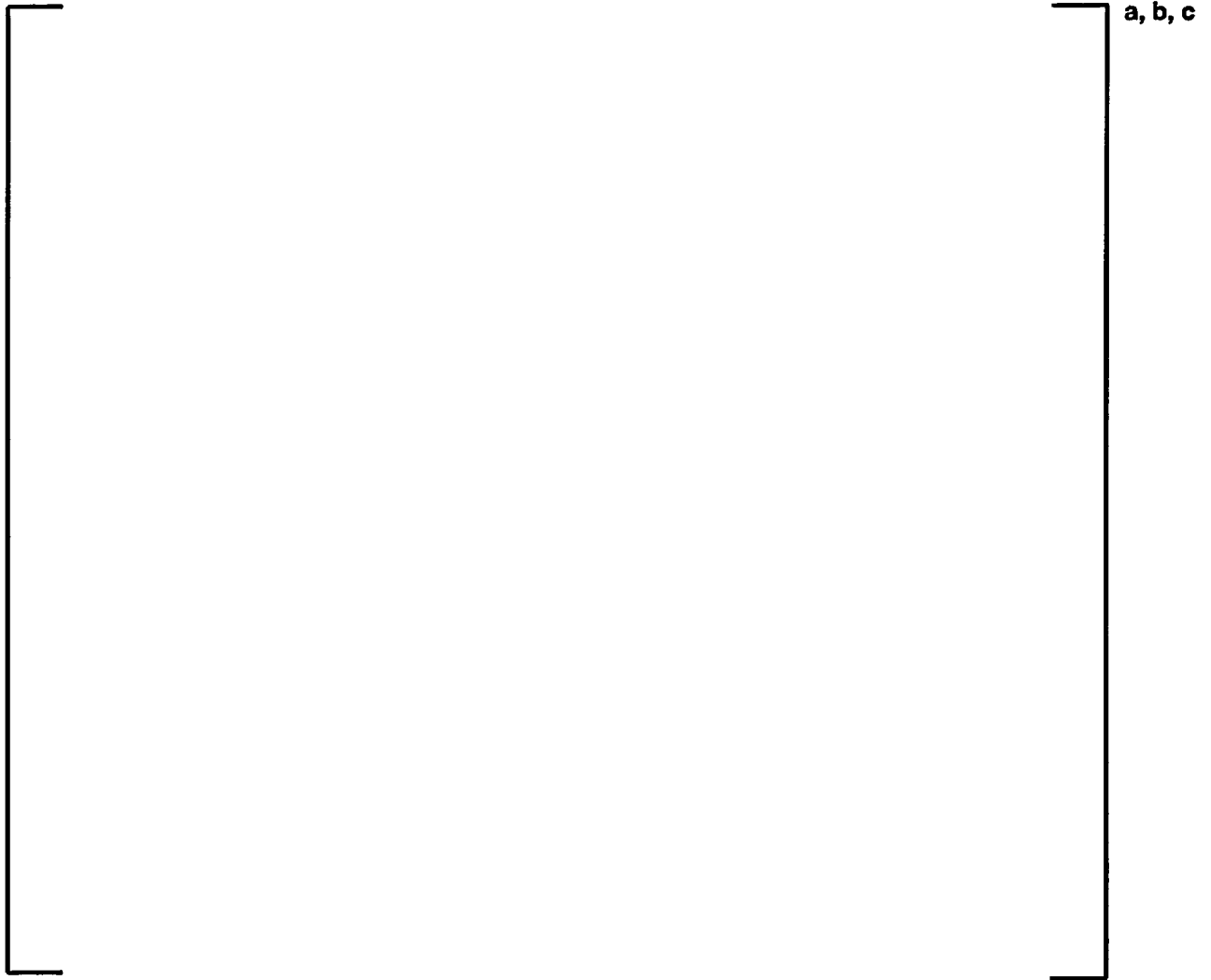
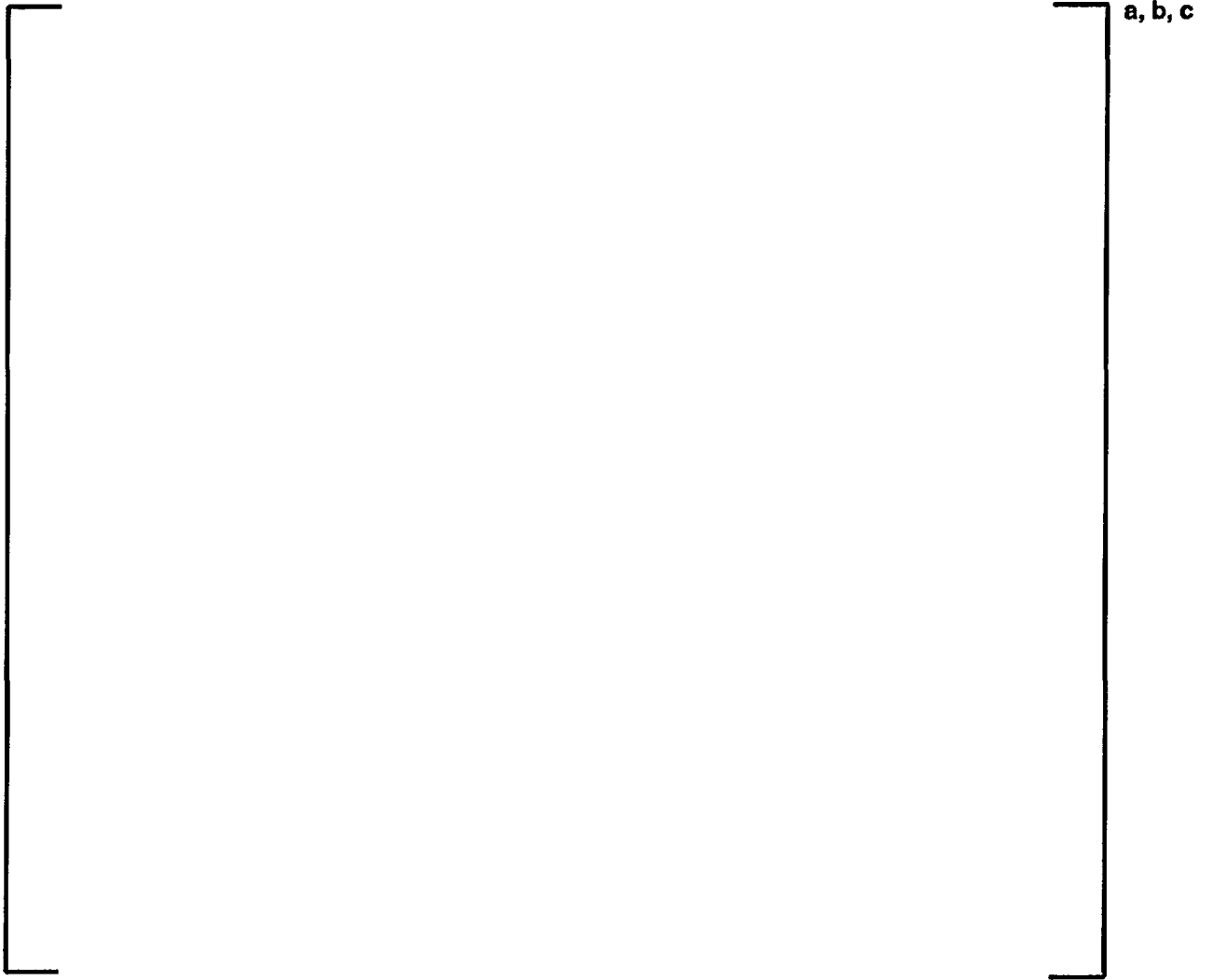


Figure 4-44: Assembly Average Power Distribution: Plant D, Cycle 11, 7309 MWD/MTU Burnup



**Figure 4-45: Assembly Average Power Distribution: Plant D, Cycle 11, 14998 MWD/MTU
Burnup**

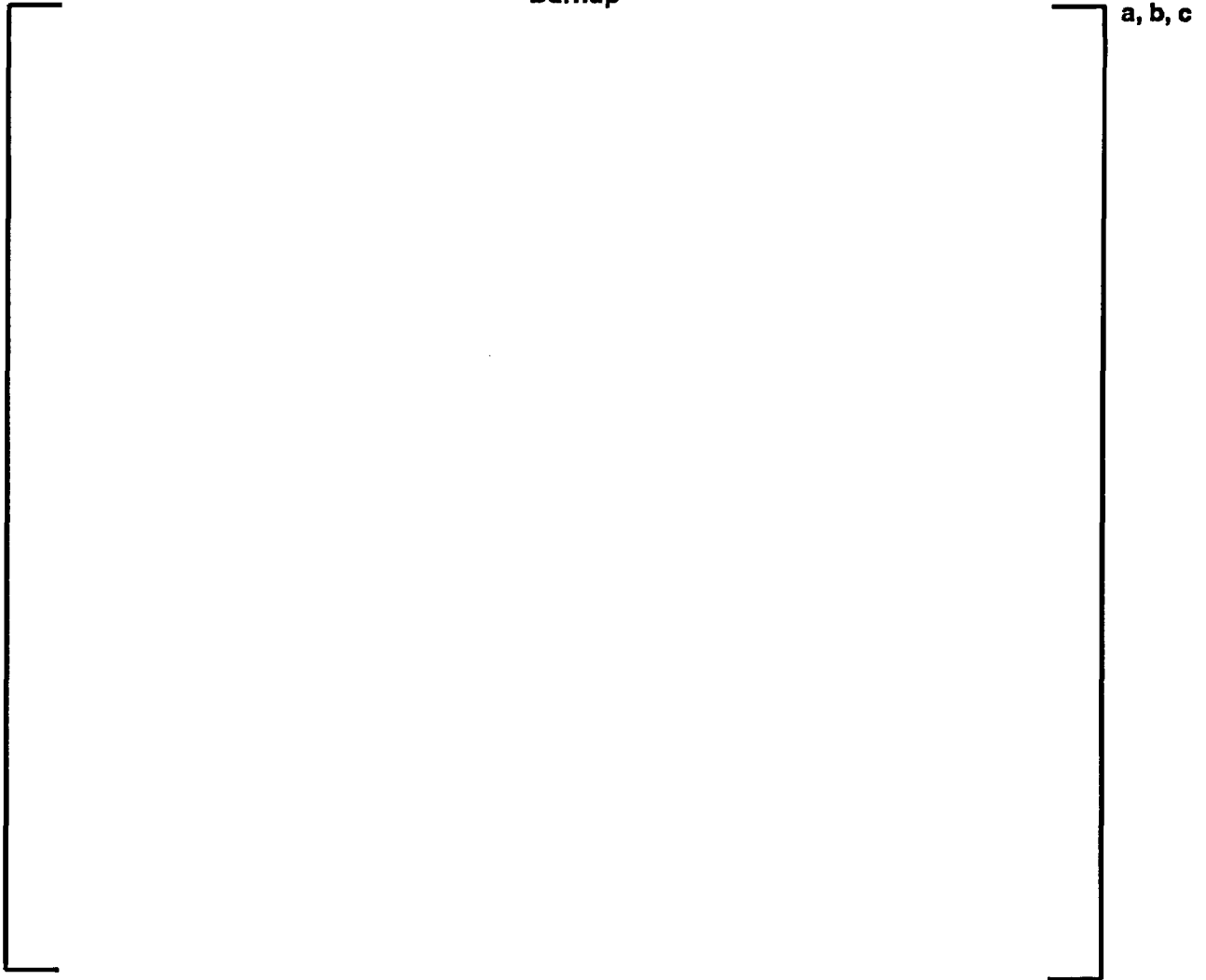
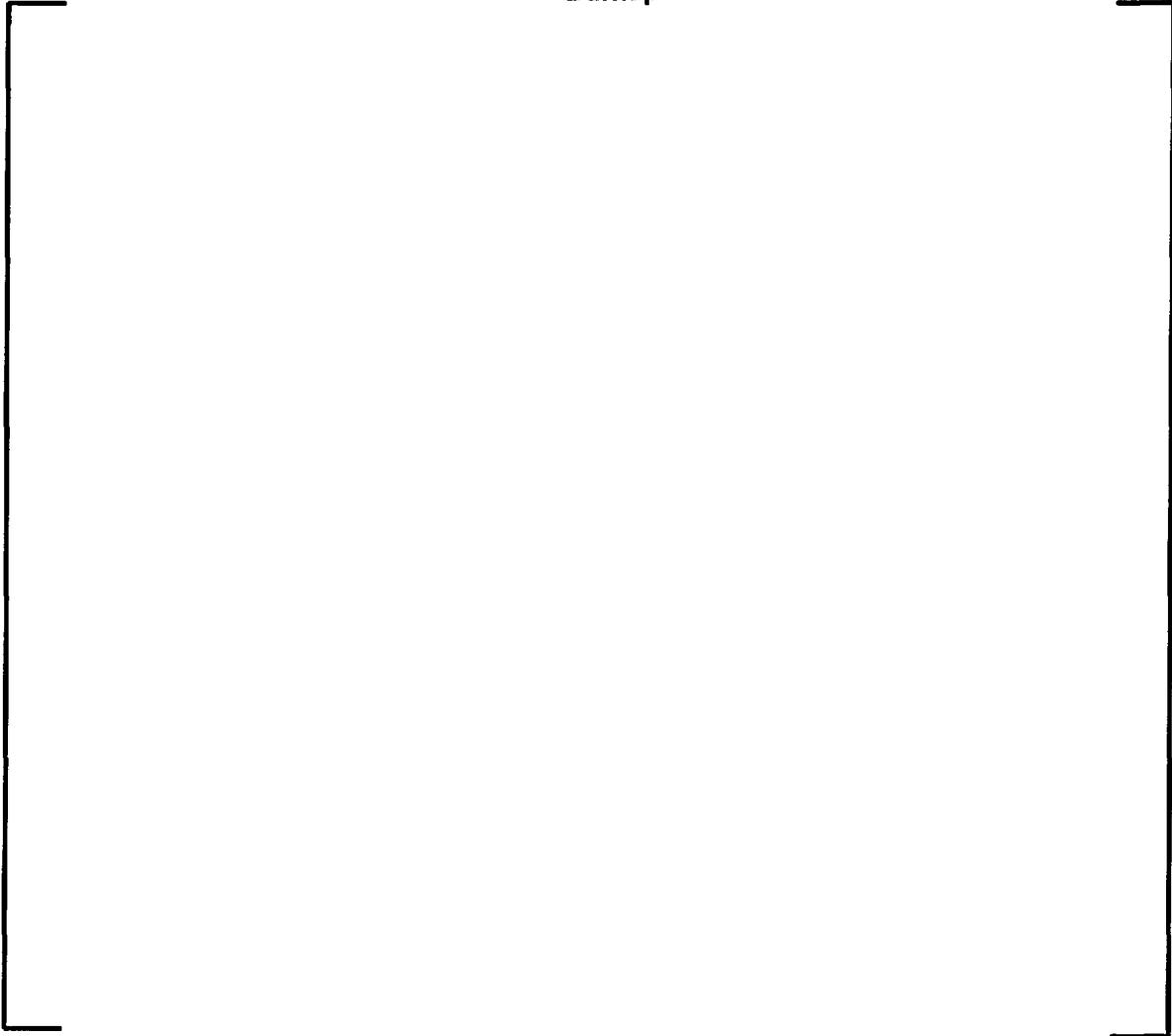


Figure 4-46: Assembly Average Power Distribution: Plant J, Cycle 10, 4282 MWD/MTU Burnup



a, b, c

**Figure 4-47: Assembly Average Power Distribution: Plant J, Cycle 10, 11864 MWD/MTU
Burnup**

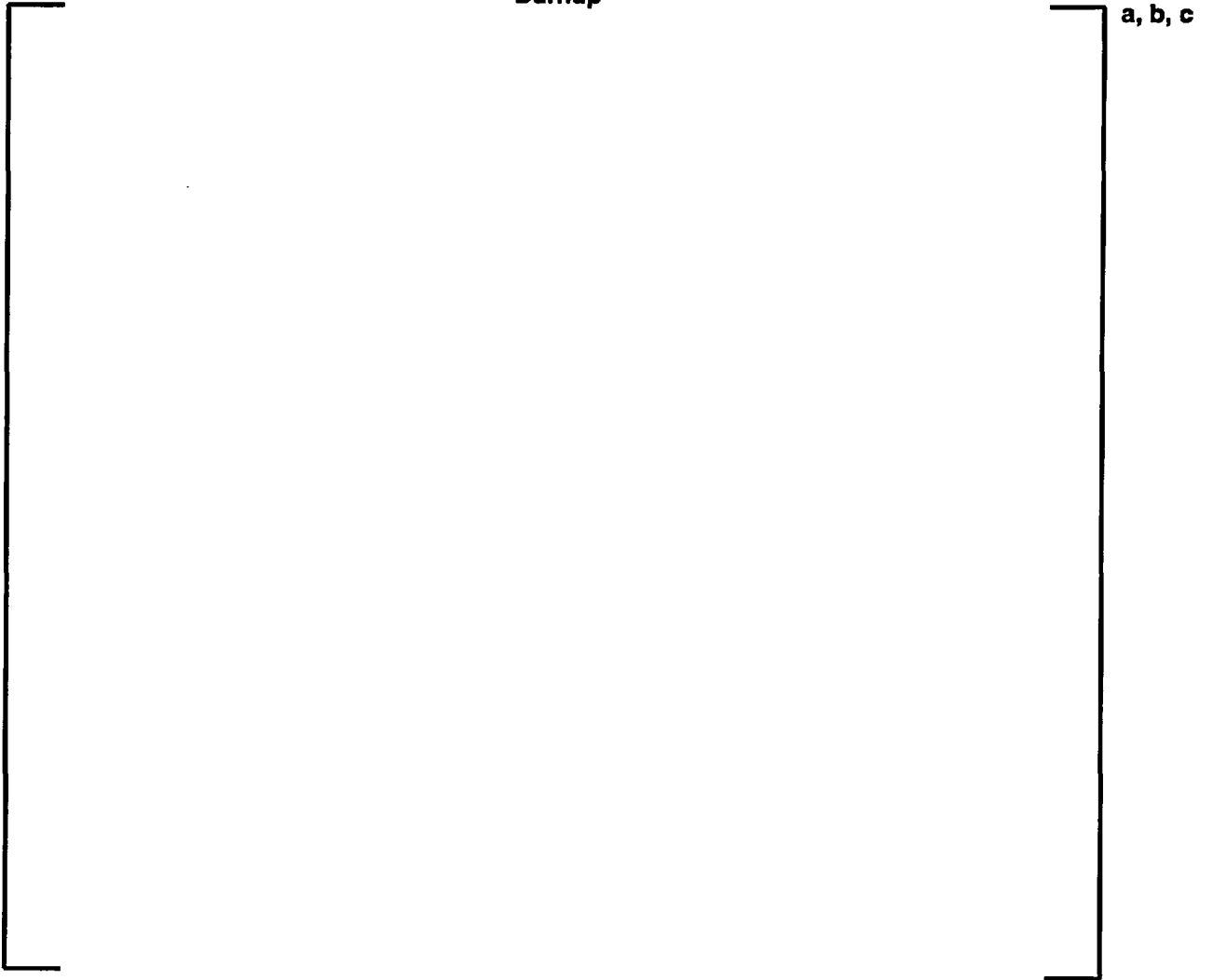
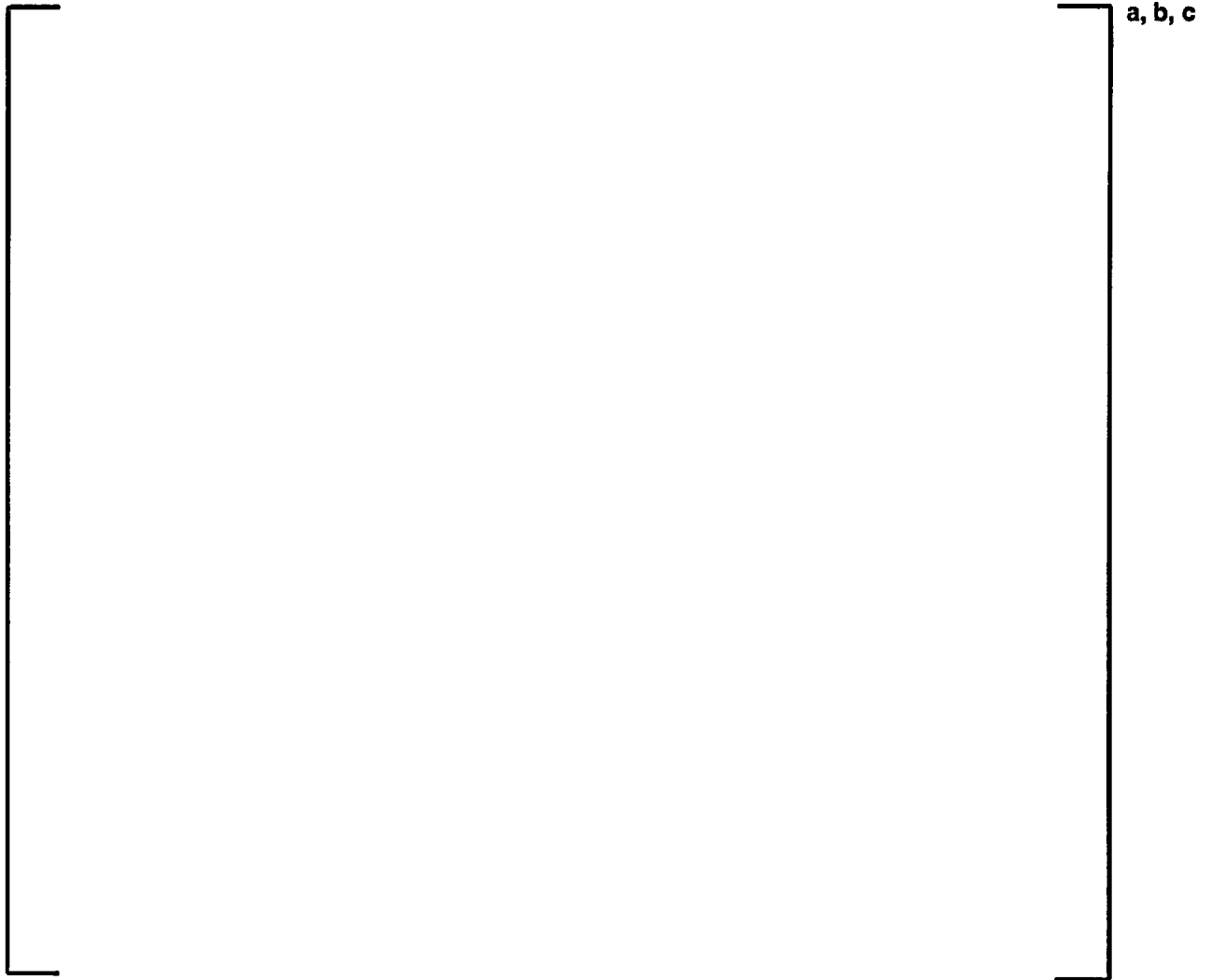


Figure 4-48: Assembly Average Power Distribution: Plant J, Cycle 10, 20700 MWD/MTU Burnup



Figure 4-49: Assembly Average Power Distribution: Plant J, Cycle 11, 638 MWD/MTU Burnup



**Figure 4-50: Assembly Average Power Distribution: Plant J, Cycle 11, 12294 MWD/MTU
Burnup**

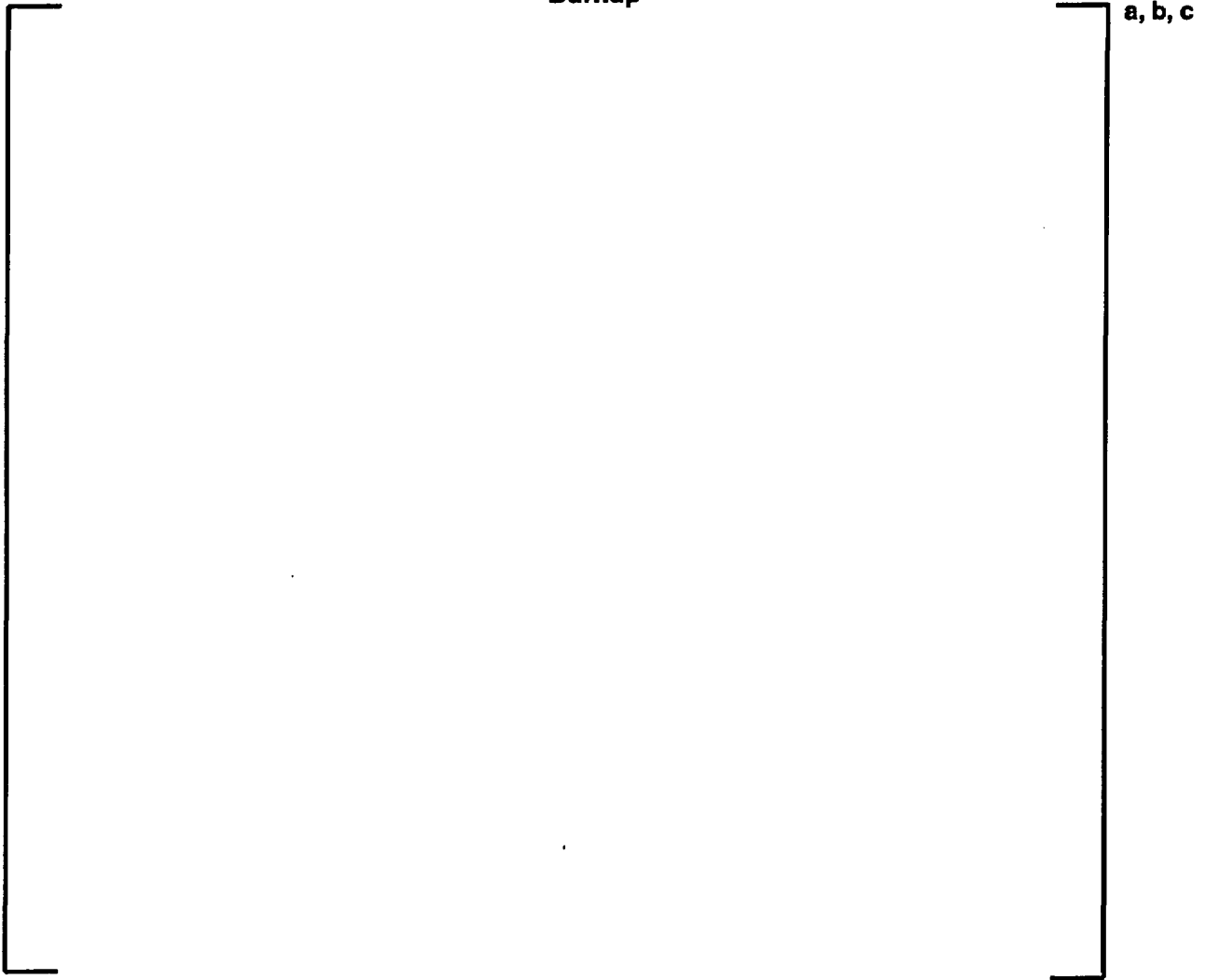


Figure 4-51: Assembly Average Power Distribution: Plant J, Cycle 11, 20539 MWD/MTU Burnup



a, b, c

Figure 4-52: Assembly Average Power Distribution (PARAGON versus PHOENIX-P): Plant A, Cycle 10 BOC

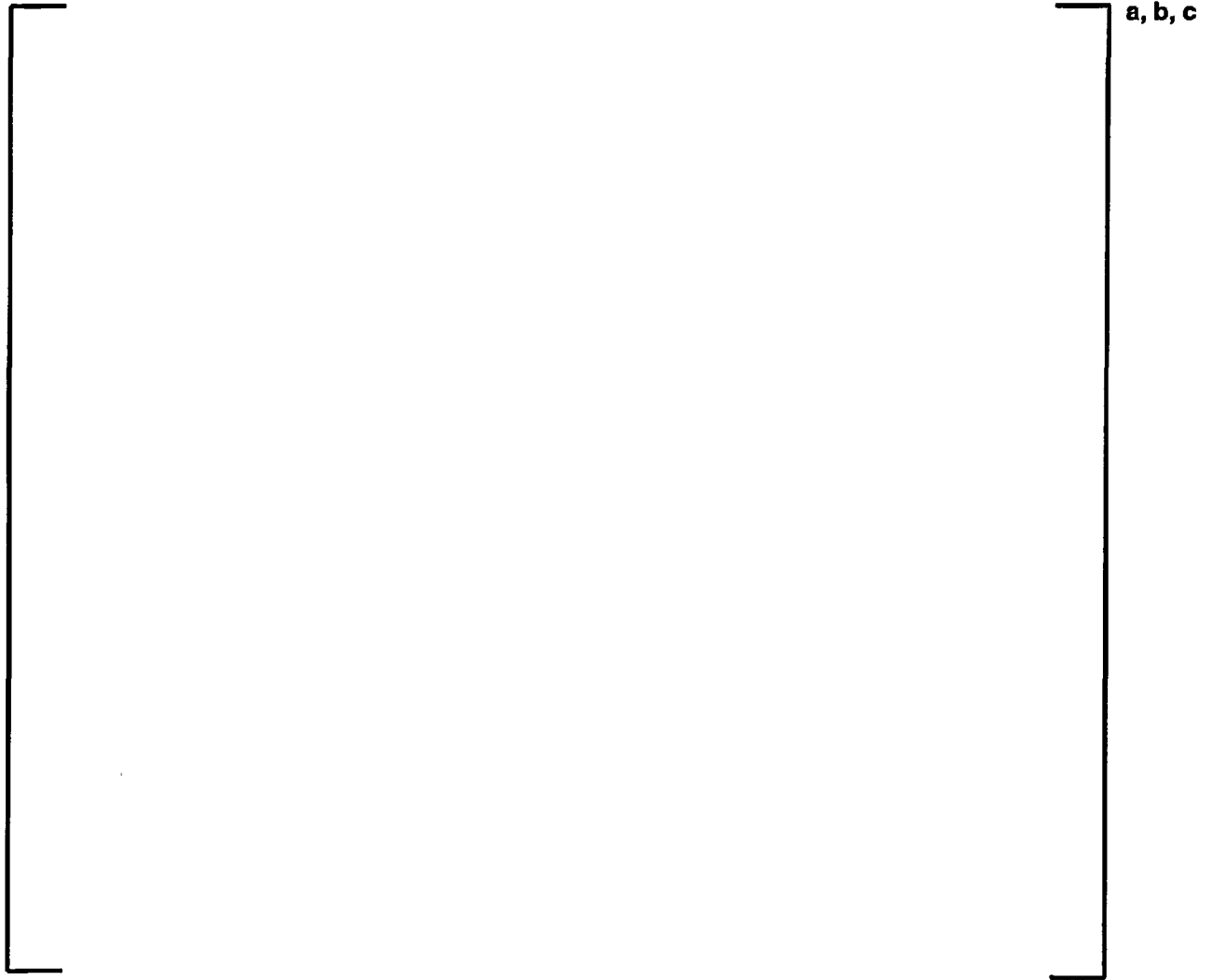


Figure 4-53: Assembly Average Power Distribution (PARAGON versus PHOENIX-P): Plant A, Cycle 10 EOC



Figure 4-54: Assembly Average Burnup Distribution (PARAGON versus PHOENIX-P): Plant A, Cycle 10 EOC

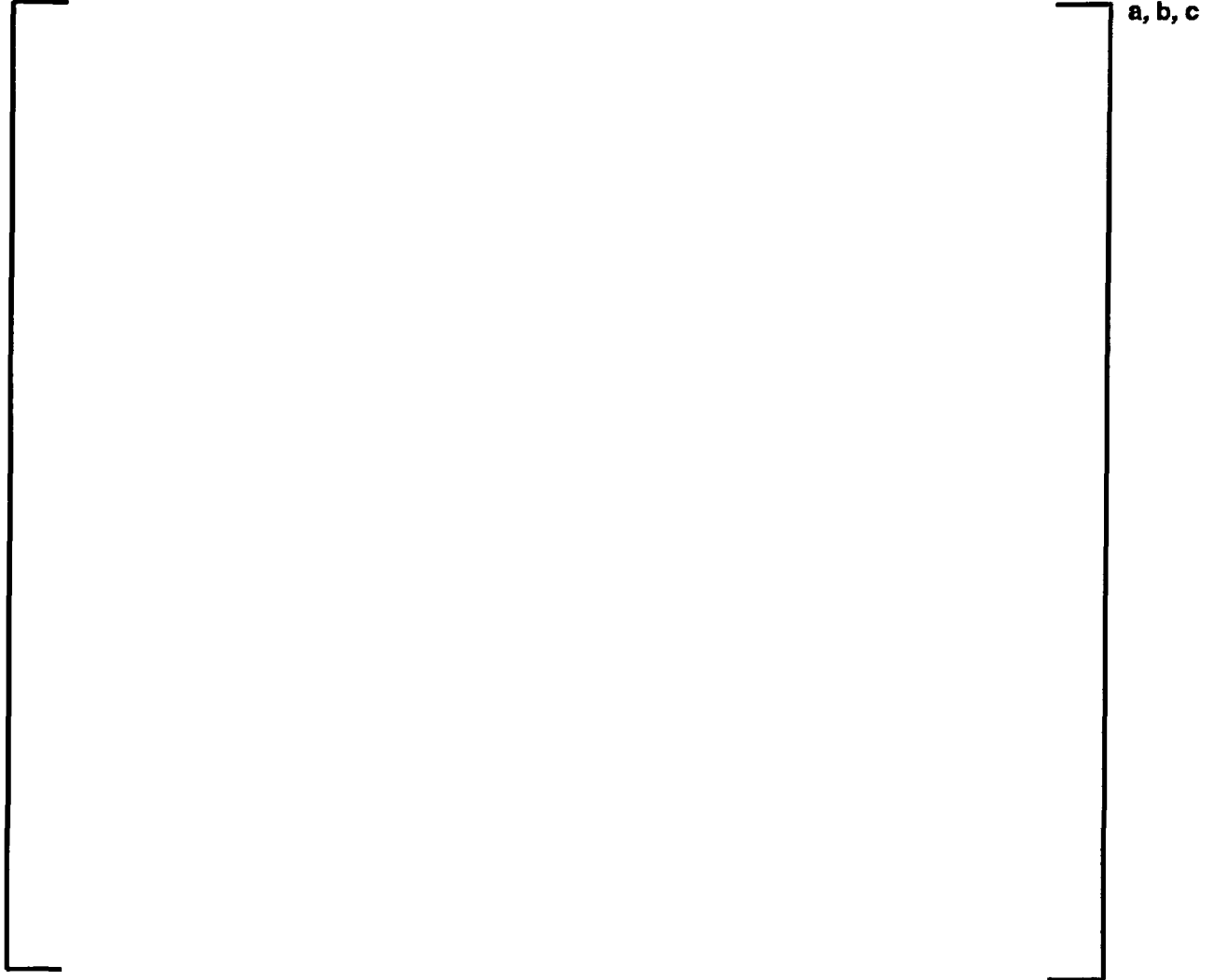


Figure 4-55: Assembly Average Power Distribution (PARAGON versus PHOENIX-P): Plant A, Cycle 11 BOC



Figure 4-56: Assembly Average Power Distribution (PARAGON versus PHOENIX-P): Plant A, Cycle 11 EOC



Figure 4-57: Assembly Average Burnup Distribution (PARAGON versus PHOENIX-P): Plant A, Cycle 11 EOC

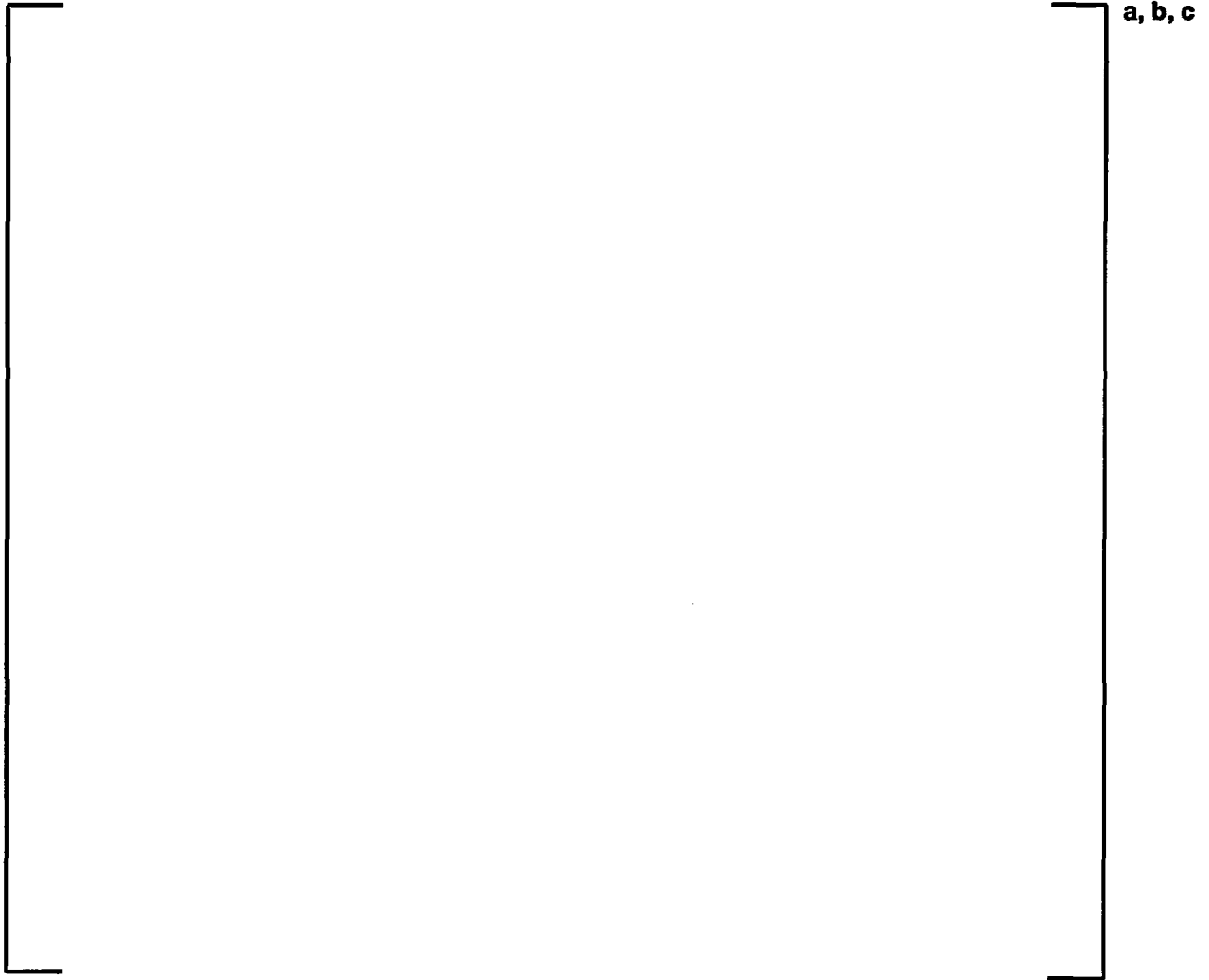


Figure 4-58: Assembly Average Power Distribution (PARAGON versus PHOENIX-P): Plant C, Cycle 25 BOC

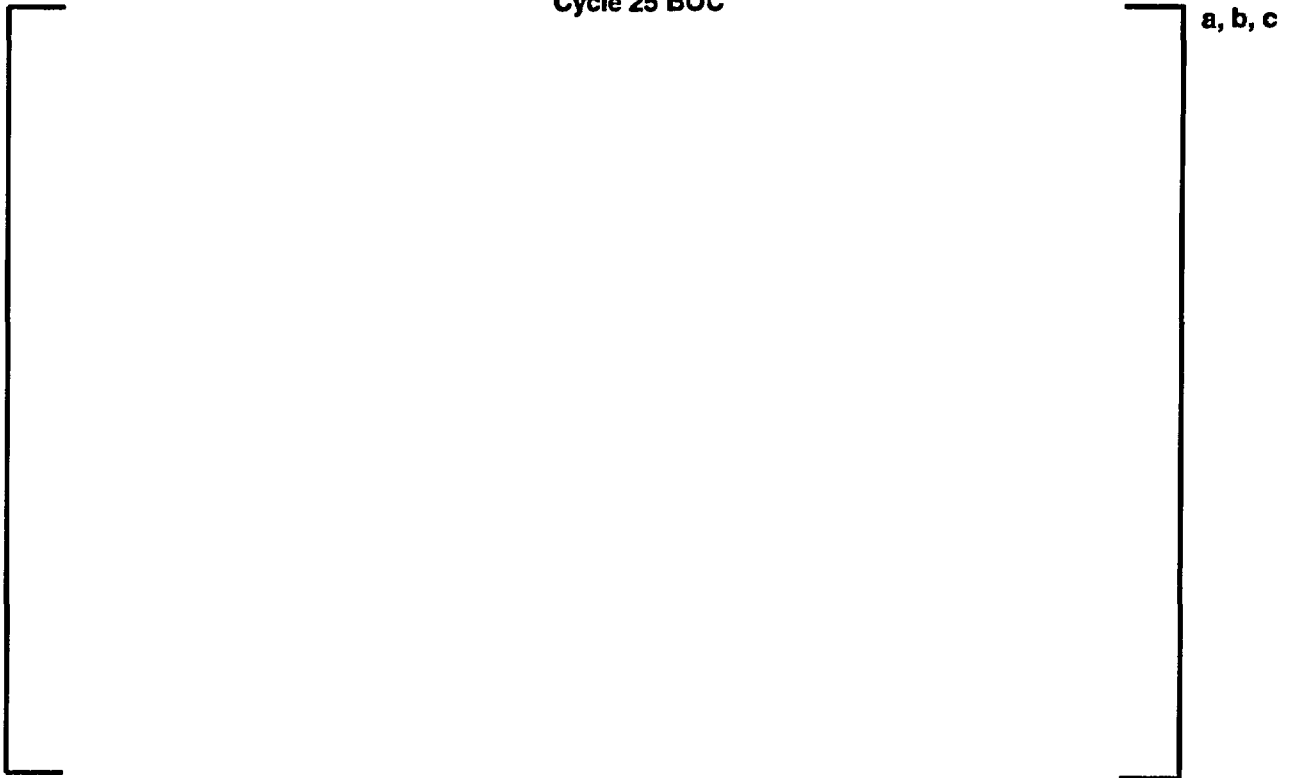


Figure 4-59: Assembly Average Power Distribution (PARAGON versus PHOENIX-P): Plant C, Cycle 25 EOC



Figure 4-60: Assembly Average Burnup Distribution (PARAGON versus PHOENIX-P): Plant C, Cycle 25 EOC



Figure 4-61: Assembly Average Power Distribution (PARAGON versus PHOENIX-P): Plant C, Cycle 26 BOC

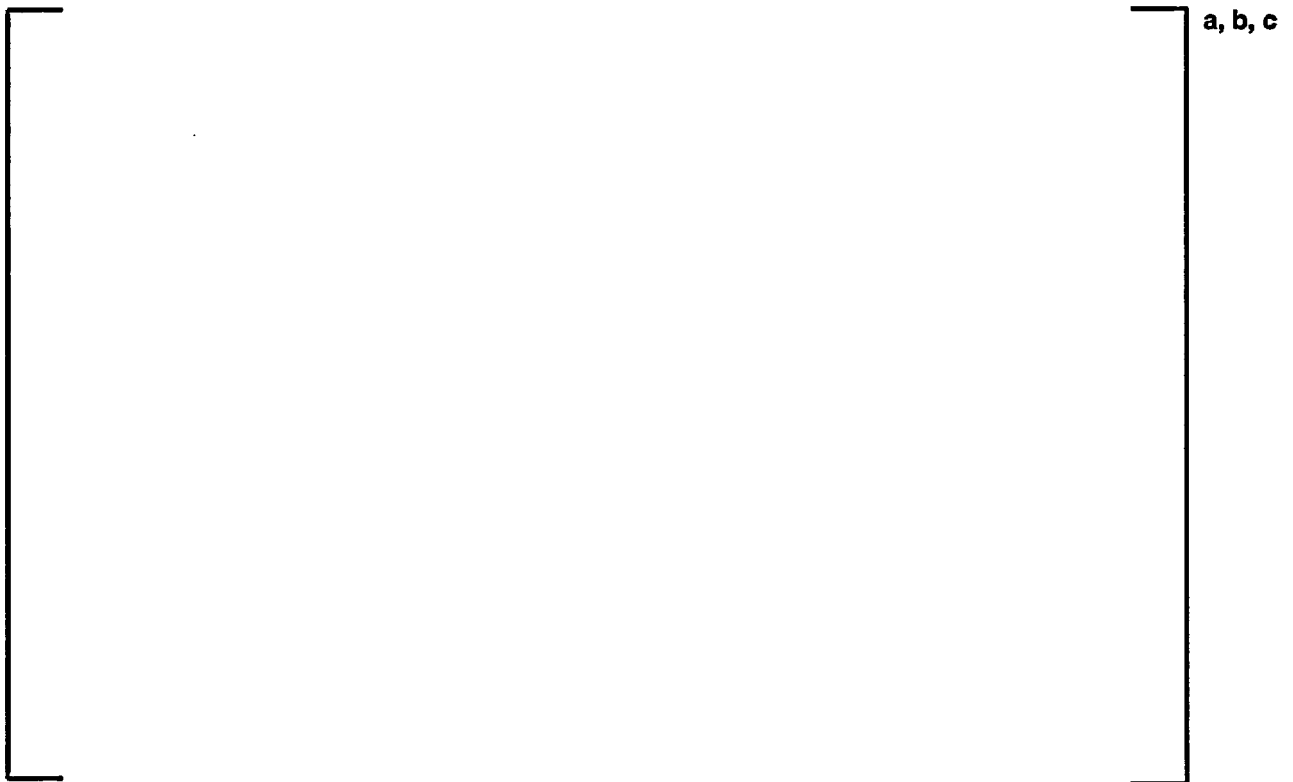


Figure 4-62: Assembly Average Power Distribution (PARAGON versus PHOENIX-P): Plant C, Cycle 26 EOC



Figure 4-63: Assembly Average Burnup Distribution (PARAGON versus PHOENIX-P): Plant C, Cycle 26 EOC



Figure 4-64: Assembly Average Power Distribution (PARAGON versus PHOENIX-P): Plant D, Cycle 10 BOC



Figure 4-65: Assembly Average Power Distribution (PARAGON versus PHOENIX-P): Plant D, Cycle 10 EOC



Figure 4-66: Assembly Average Burnup Distribution (PARAGON versus PHOENIX-P): Plant D, Cycle 10 EOC



Figure 4-67: Assembly Average Power Distribution (PARAGON versus PHOENIX-P): Plant D, Cycle 11 BOC



Figure 4-68: Assembly Average Power Distribution (PARAGON versus PHOENIX-P): Plant D, Cycle 11 EOC



Figure 4-69: Assembly Average Burnup Distribution (PARAGON versus PHOENIX-P): Plant D, Cycle 11 EOC



a, b, c

Figure 4-70: Assembly Average Power Distribution (PARAGON versus PHOENIX-P): Plant E, Cycle 25 BOC



Figure 4-71: Assembly Average Power Distribution (PARAGON versus PHOENIX-P): Plant E, Cycle 25 EOC



Figure 4-72: Assembly Average Burnup Distribution (PARAGON versus PHOENIX-P): Plant E, Cycle 25 EOC



Figure 4-73: Assembly Average Power Distribution (PARAGON versus PHOENIX-P): Plant F, Cycle 11 BOC

a, b, c

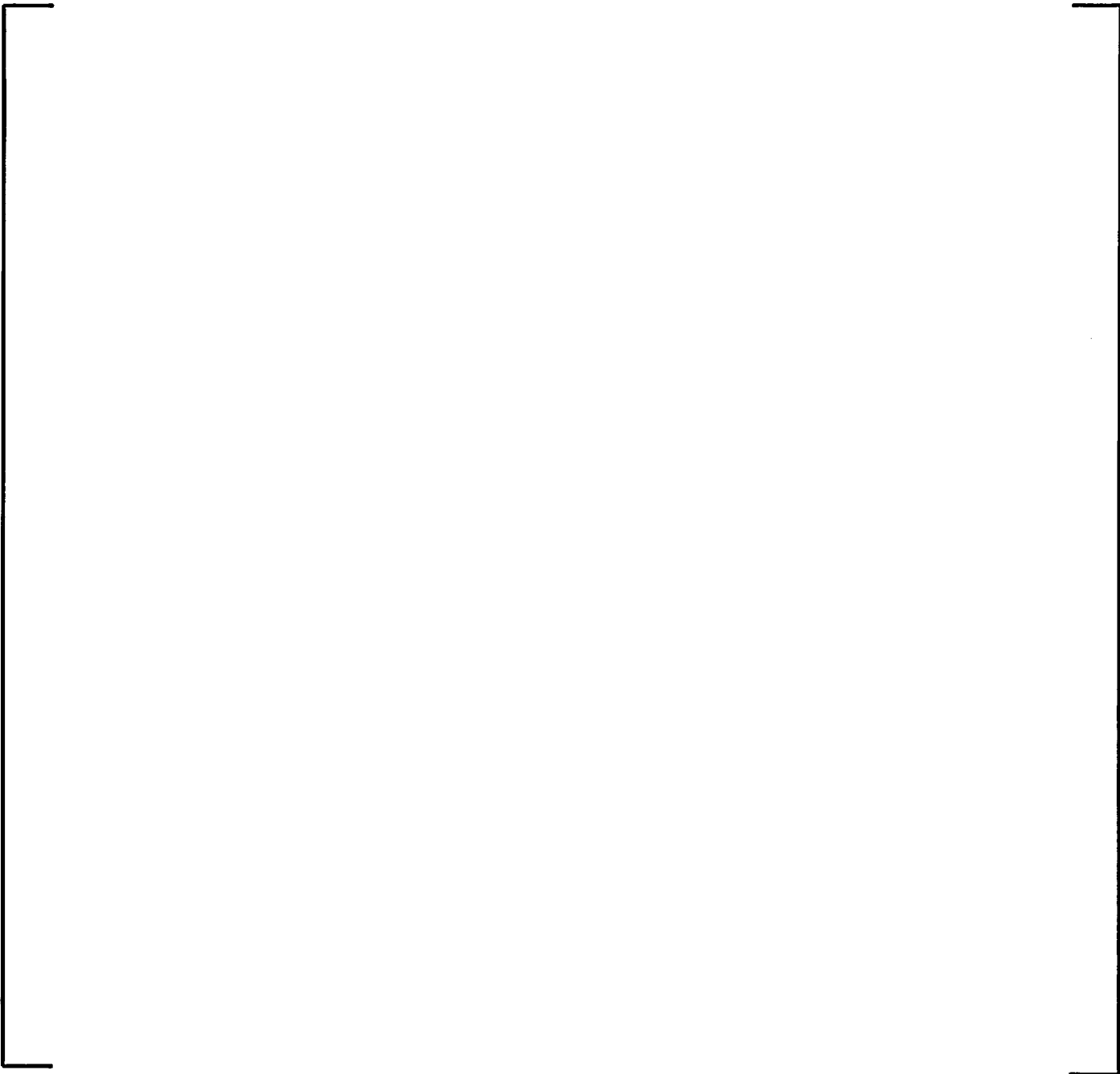


Figure 4-74: Assembly Average Power Distribution (PARAGON versus PHOENIX-P): Plant F, Cycle 11 EOC

a, b, c

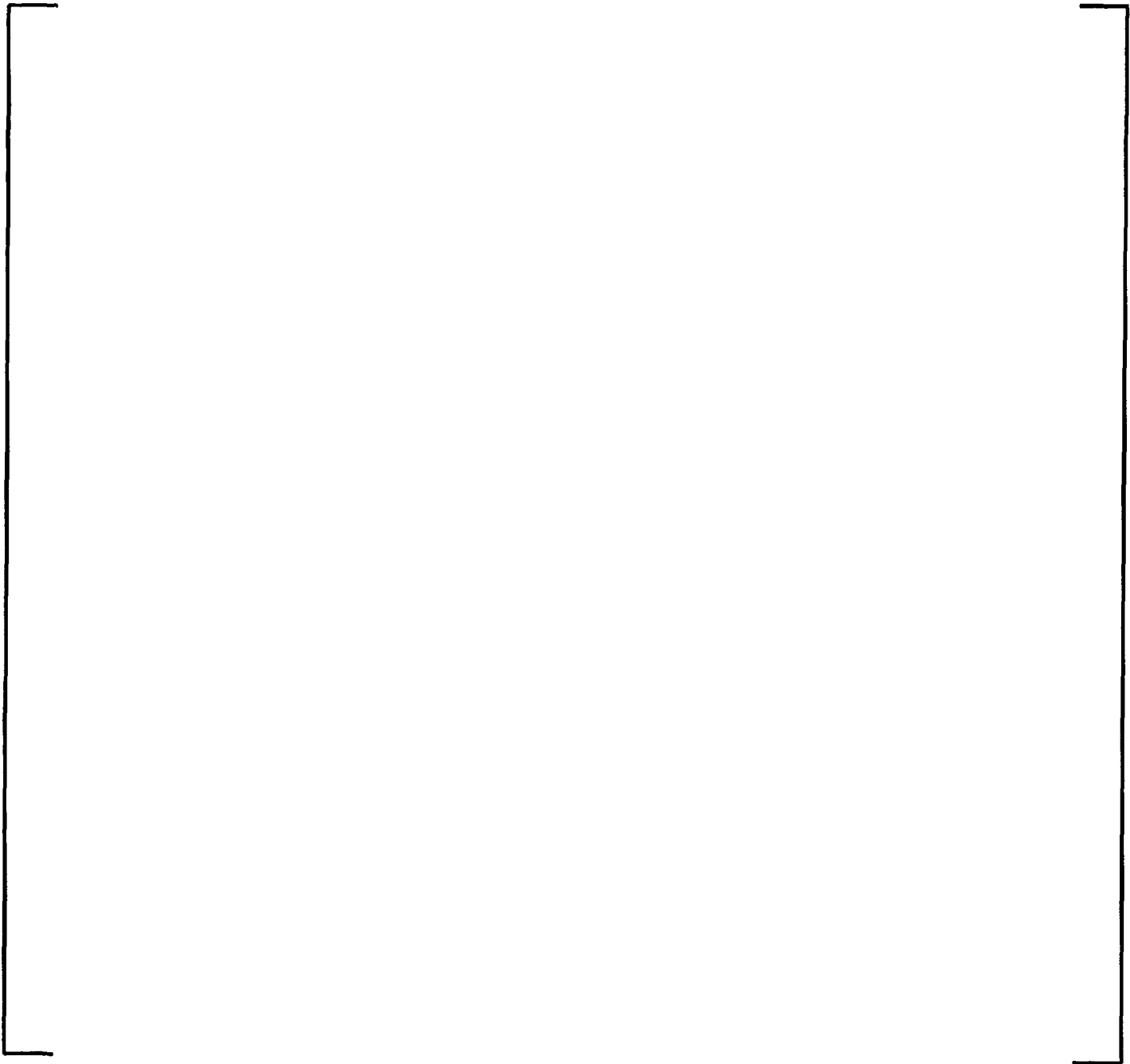


Figure 4-75: Assembly Average Burnup Distribution (PARAGON versus PHOENIX-P): Plant F, Cycle 11 EOC

a, b, c

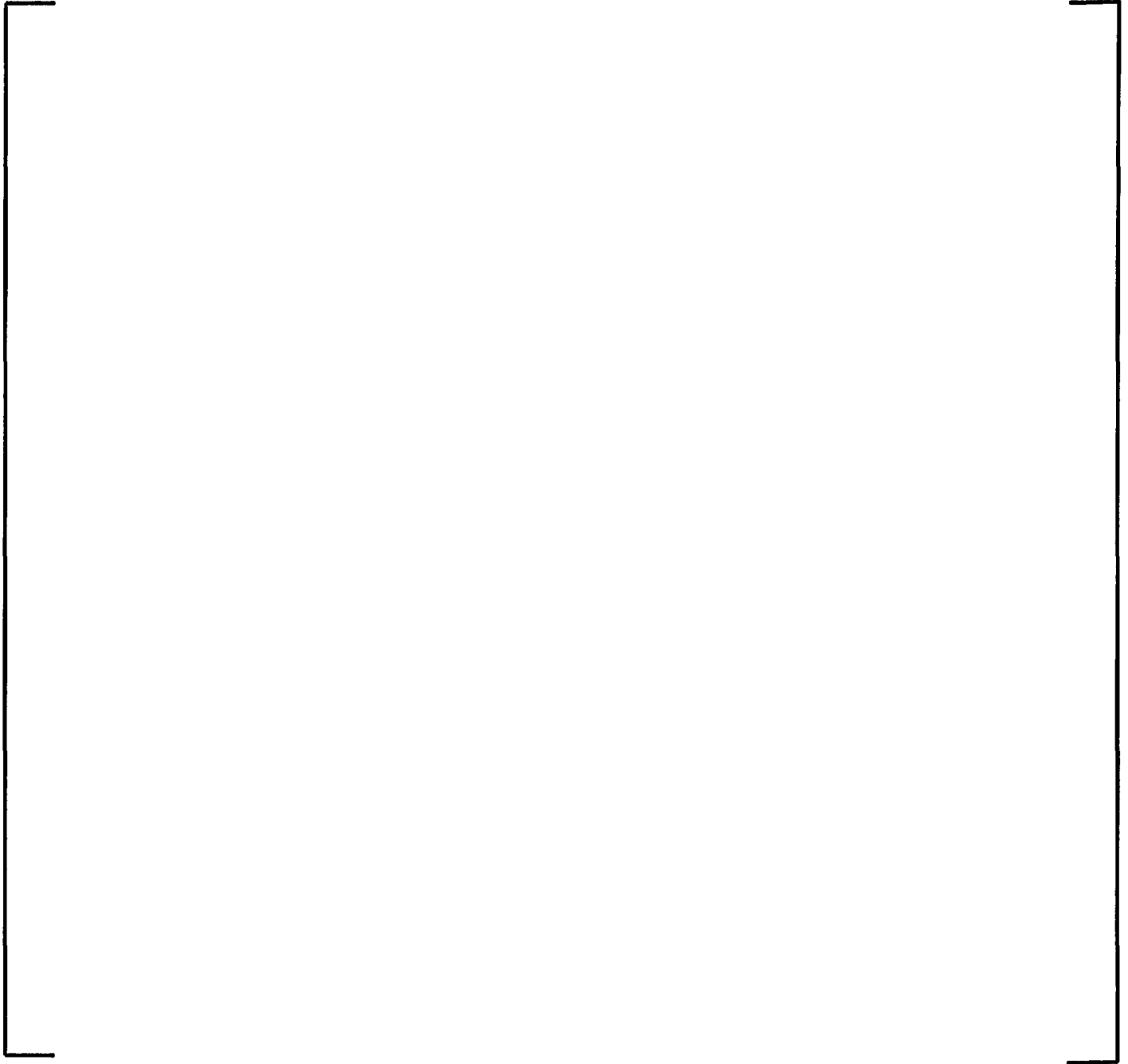


Figure 4-76: Assembly Average Power Distribution (PARAGON versus PHOENIX-P): Plant F, Cycle 12 BOC

a, b, c



**Figure 4-77: Assembly Average Power Distribution (PARAGON versus PHOENIX-P): Plant F,
Cycle 12 EOC**

a, b, c



Figure 4-78: Assembly Average Burnup Distribution (PARAGON versus PHOENIX-P): Plant F, Cycle 12 EOC

a, b, c

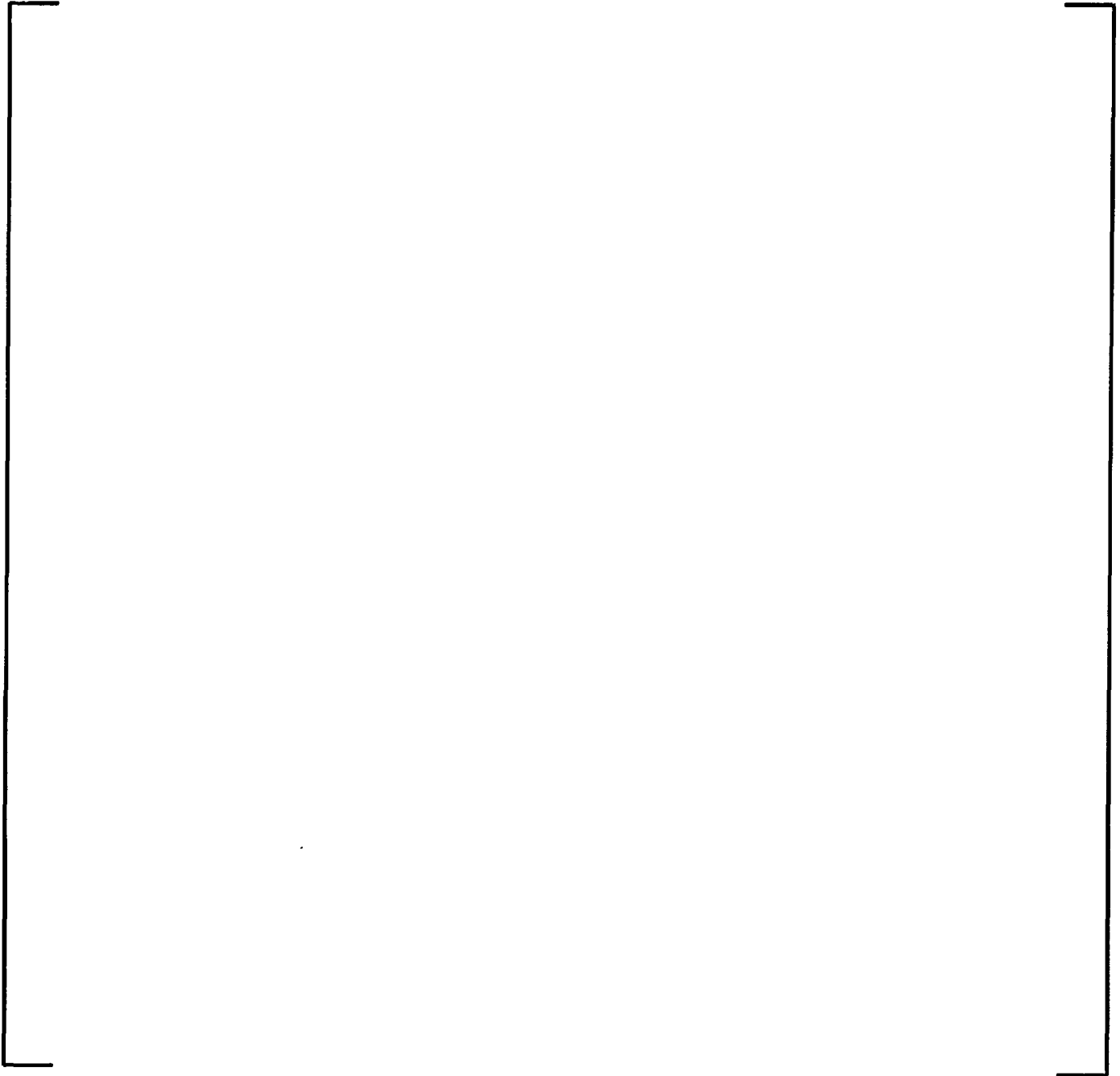


Figure 4-79: Core Average Axial Power Distribution (PARAGON versus PHOENIX-P): Plant A, Cycle 10, BOC

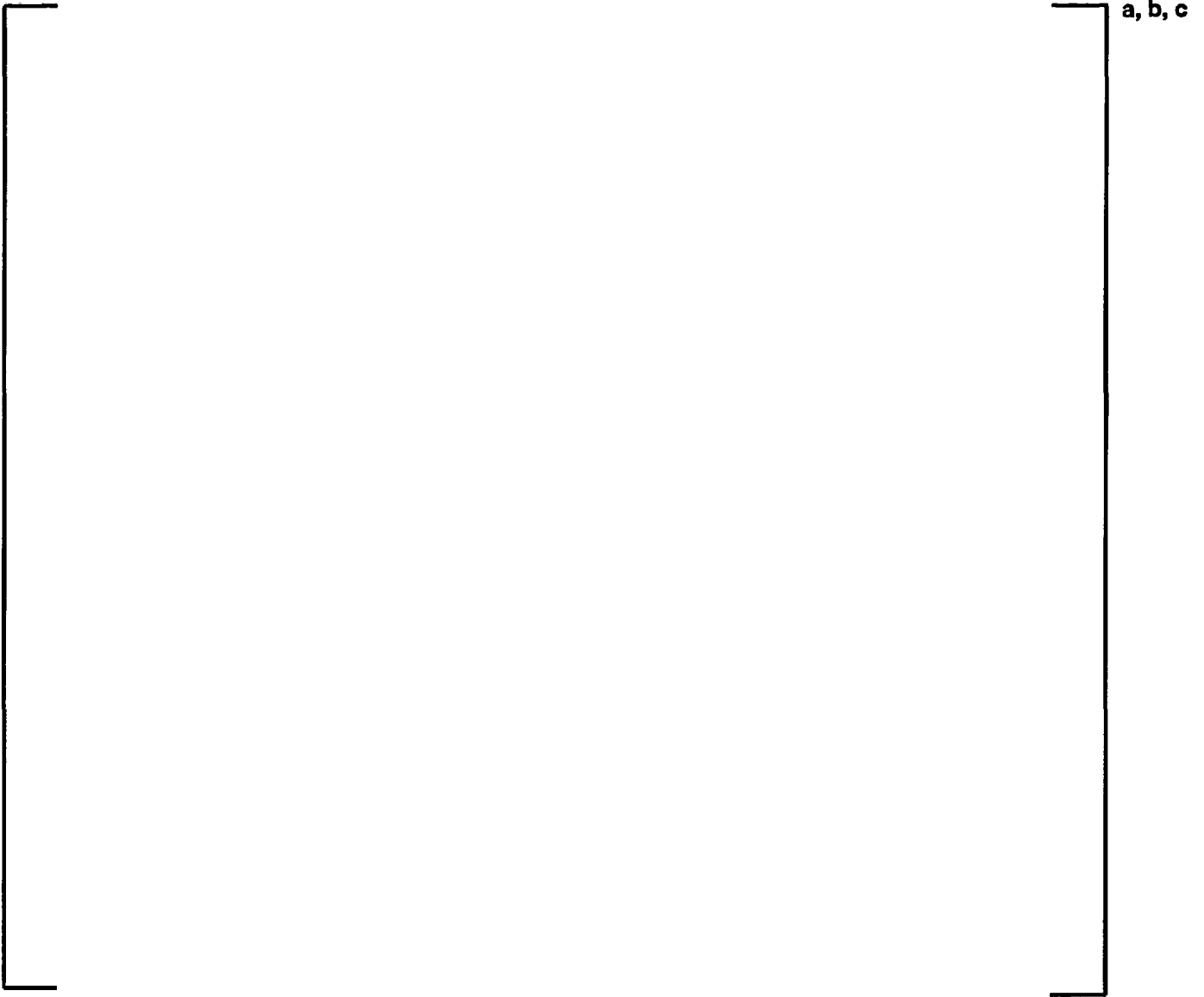


Figure 4-80: Core Average Axial Power Distribution (PARAGON versus PHOENIX-P): Plant A, Cycle 10, MOC



Figure 4-81: Core Average Axial Power Distribution (PARAGON versus PHOENIX-P): Plant A, Cycle 10, EOC



Figure 4-82: Core Average Axial Power Distribution (PARAGON versus PHOENIX-P): Plant A, Cycle 11, BOC

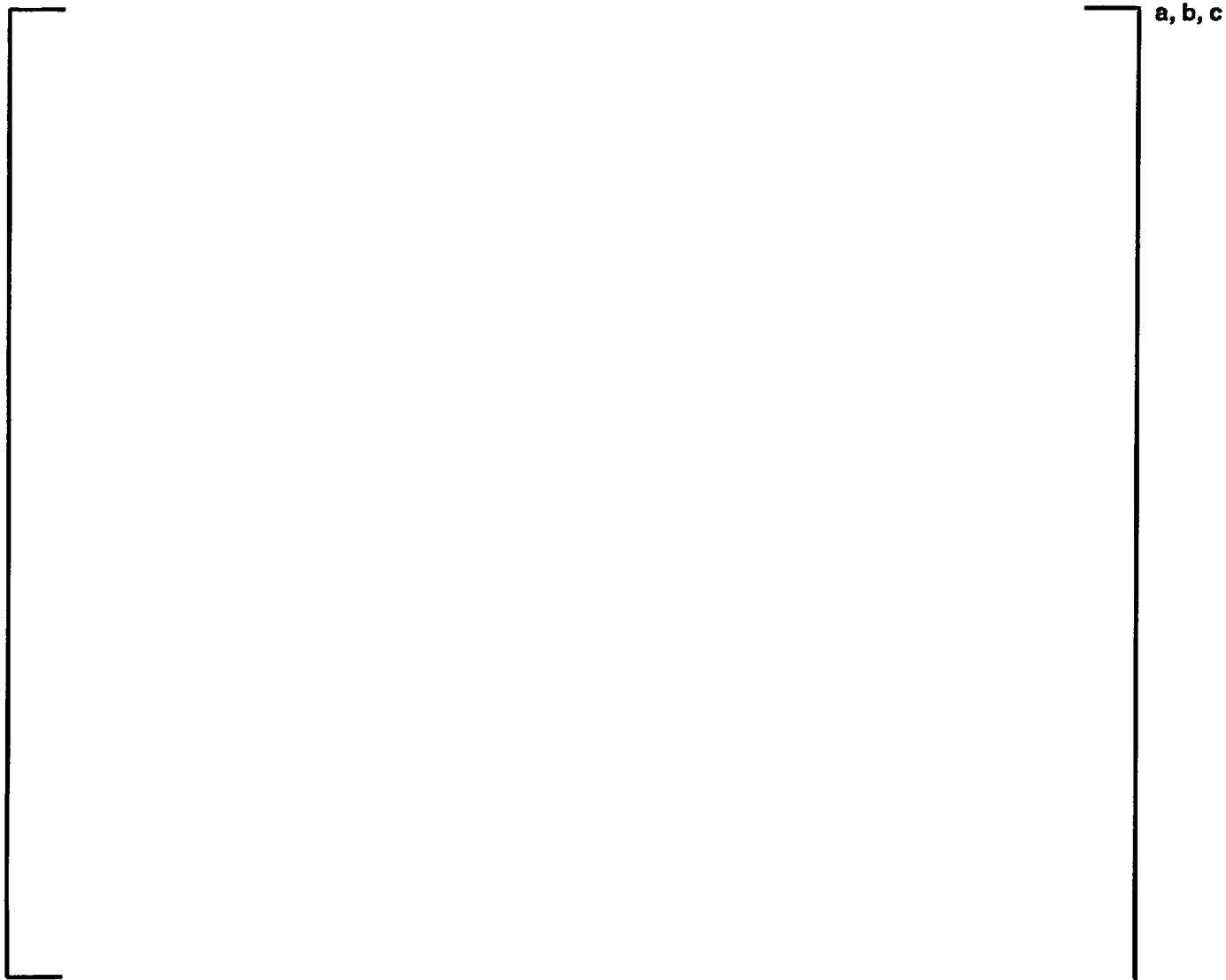


Figure 4-83: Core Average Axial Power Distribution (PARAGON versus PHOENIX-P): Plant A, Cycle 11, MOC



Figure 4-84: Core Average Axial Power Distribution (PARAGON versus PHOENIX-P): Plant A, Cycle 11, EOC



Figure 4-85: Core Average Axial Power Distribution (PARAGON versus PHOENIX-P): Plant C, Cycle 25, BOC

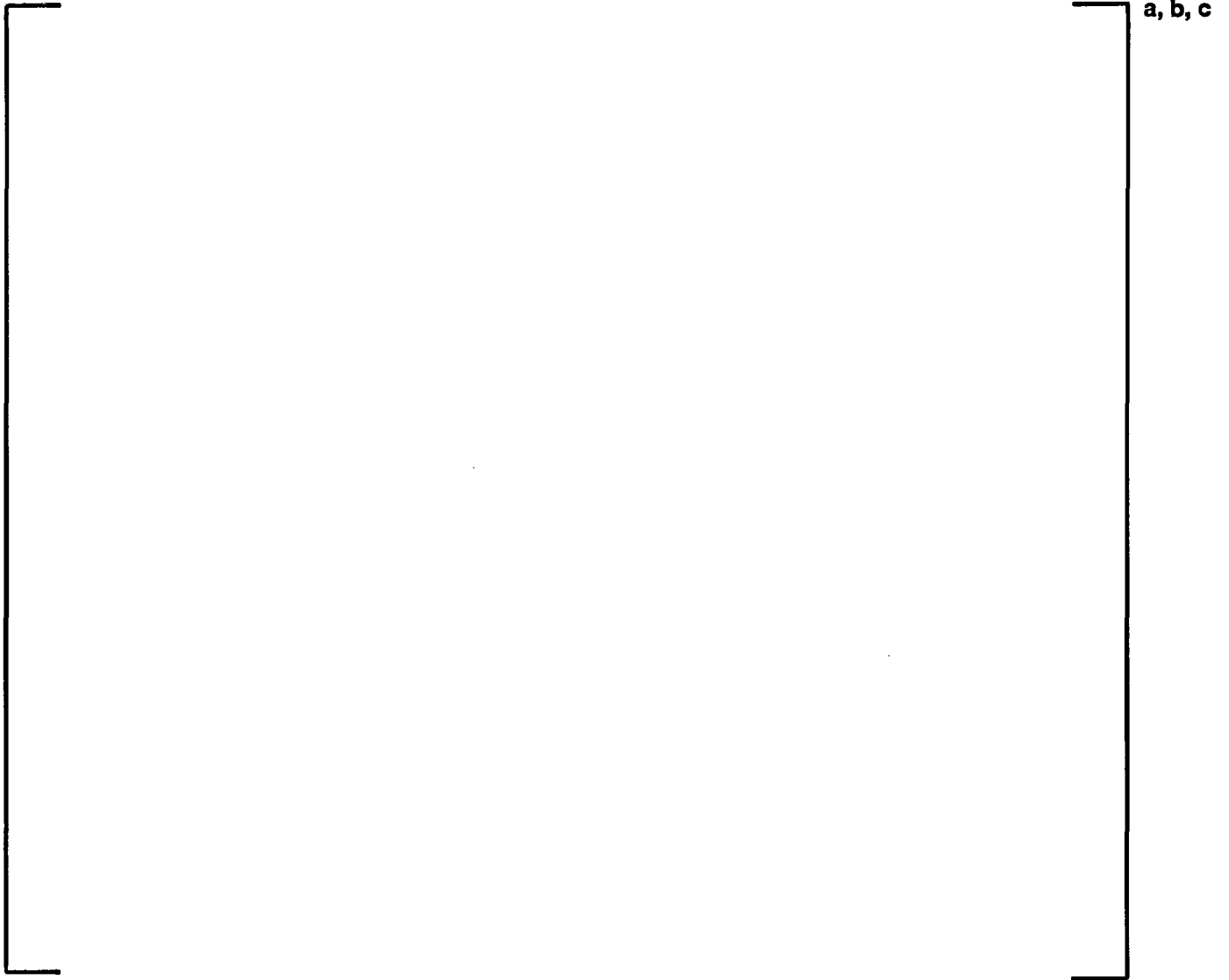


Figure 4-86: Core Average Axial Power Distribution (PARAGON versus PHOENIX-P): Plant C, Cycle 25, MOC



Figure 4-87: Core Average Axial Power Distribution (PARAGON versus PHOENIX-P): Plant C, Cycle 25, EOC

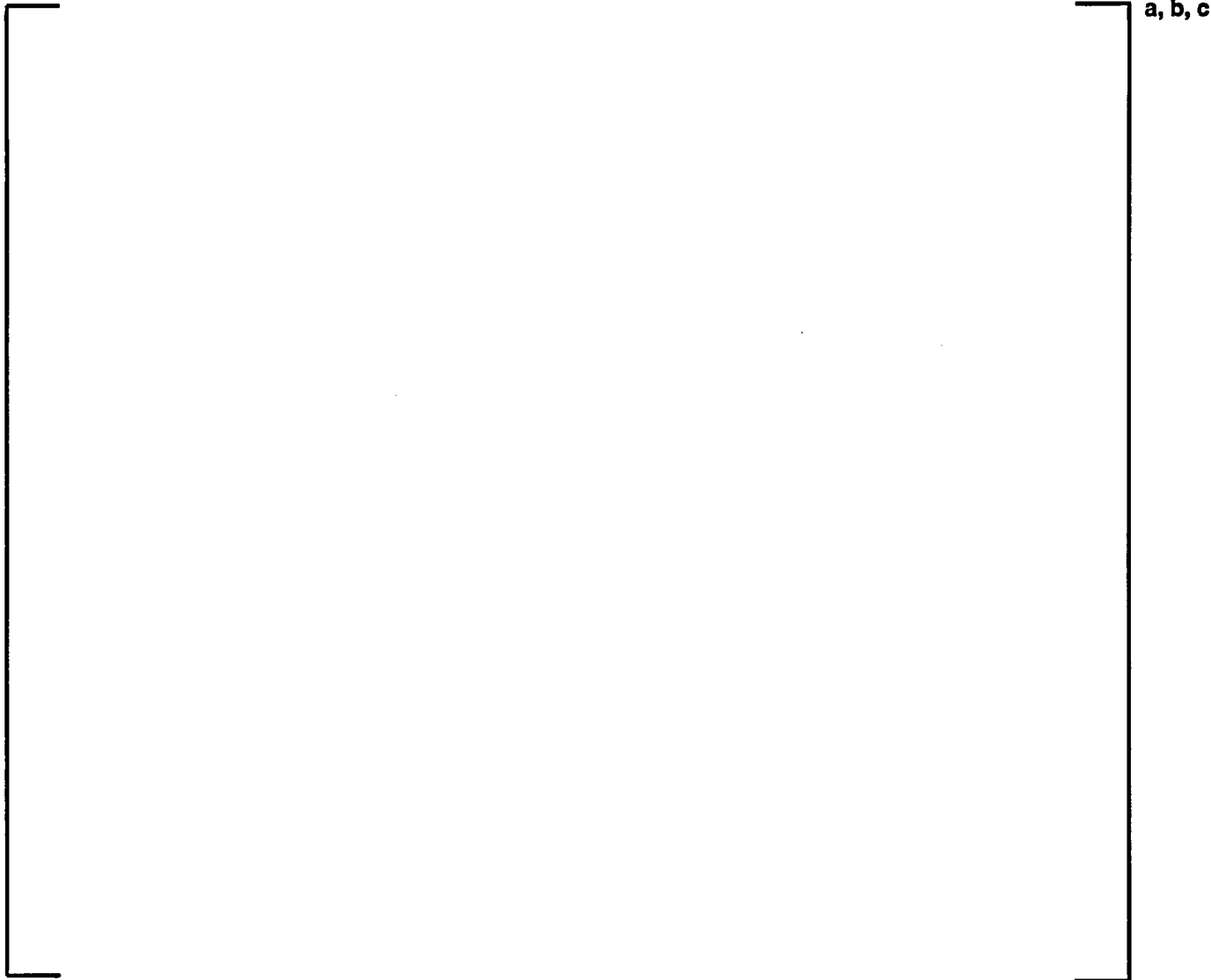


Figure 4-88: Core Average Axial Power Distribution (PARAGON versus PHOENIX-P): Plant C, Cycle 26, BOC



Figure 4-89: Core Average Axial Power Distribution (PARAGON versus PHOENIX-P): Plant C, Cycle 26, MOC

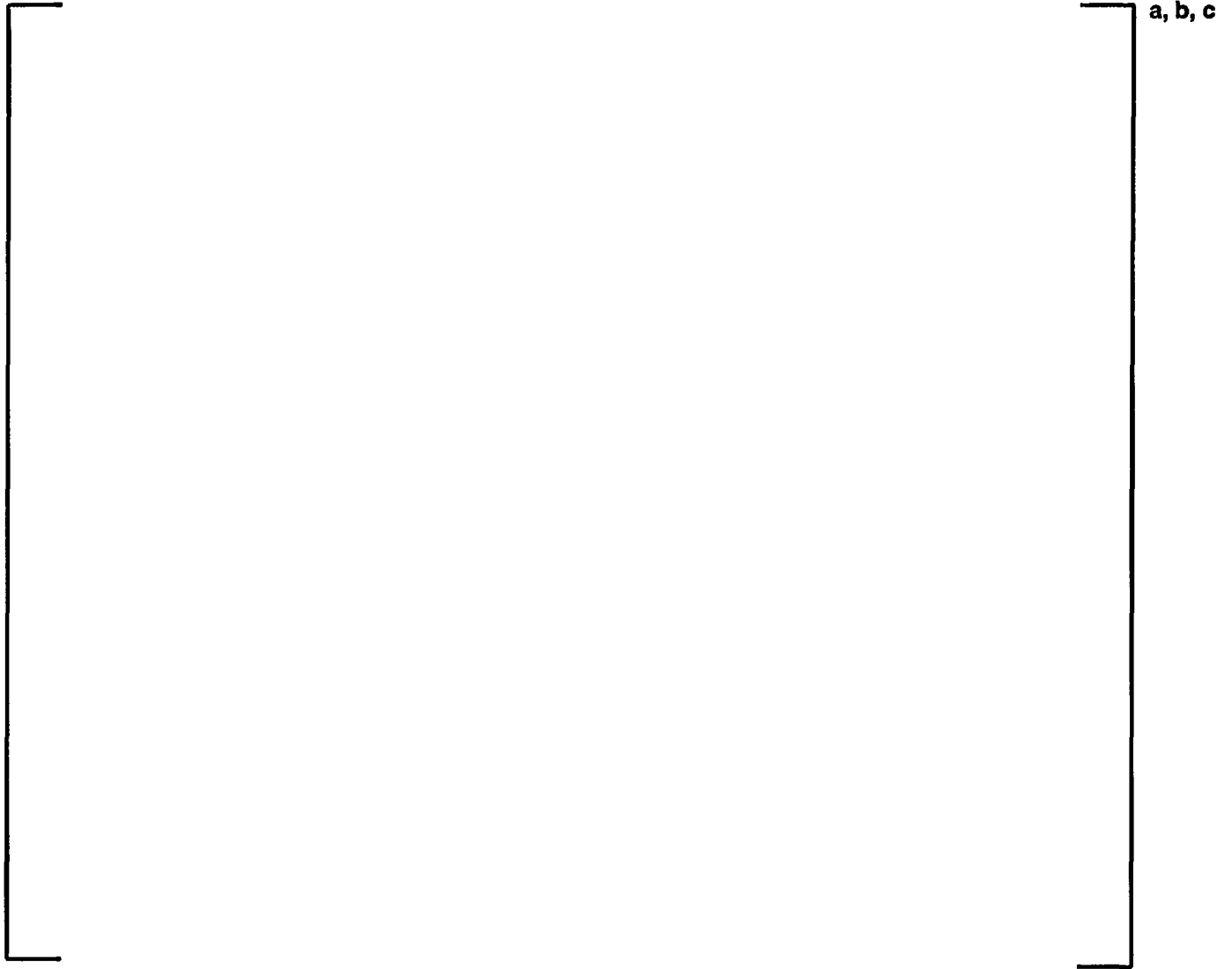


Figure 4-90: Core Average Axial Power Distribution (PARAGON versus PHOENIX-P): Plant C, Cycle 26, EOC



Figure 4-91: Core Average Axial Power Distribution (PARAGON versus PHOENIX-P): Plant F, Cycle 11, BOC

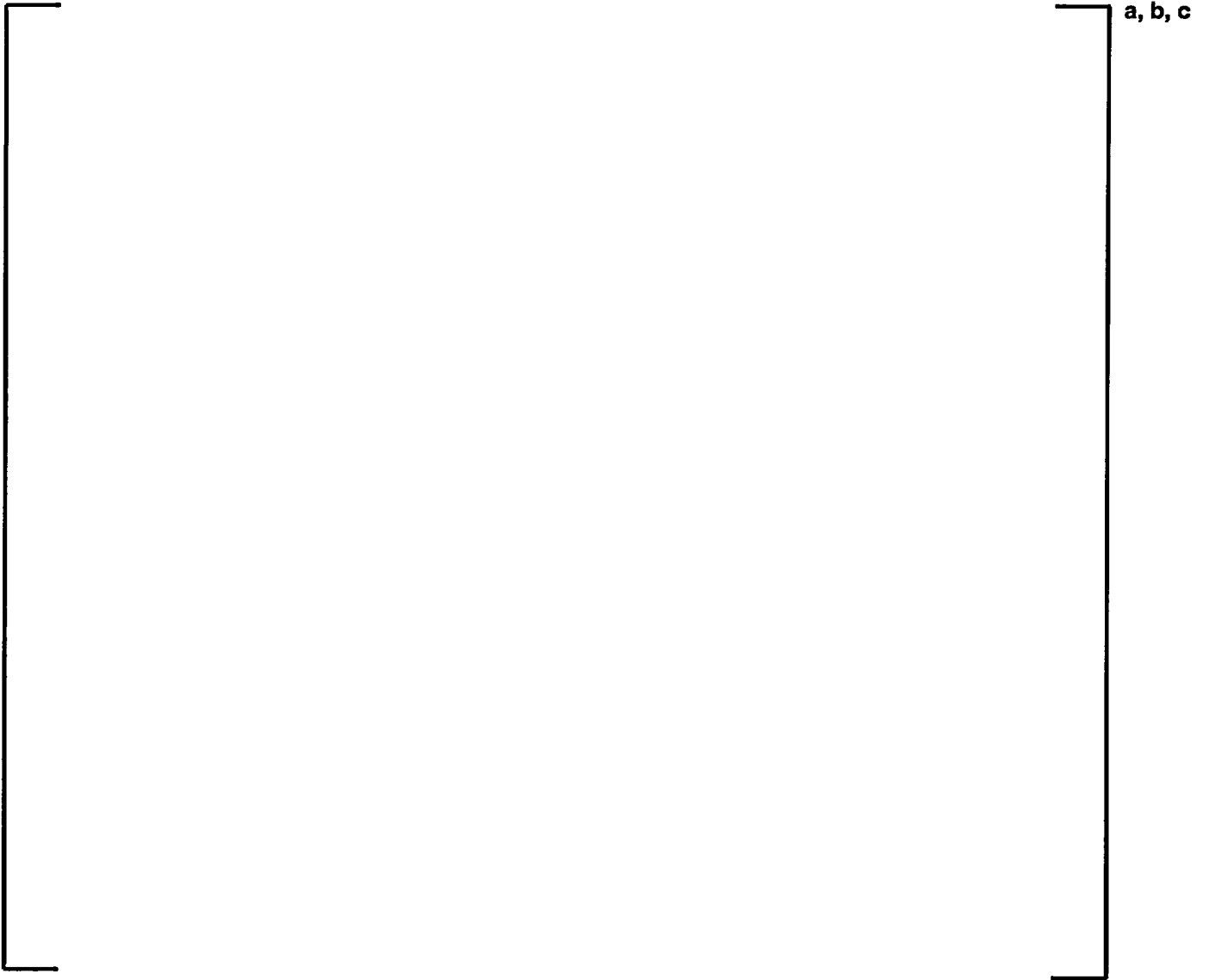


Figure 4-92: Core Average Axial Power Distribution (PARAGON versus PHOENIX-P): Plant F, Cycle 11, MOC

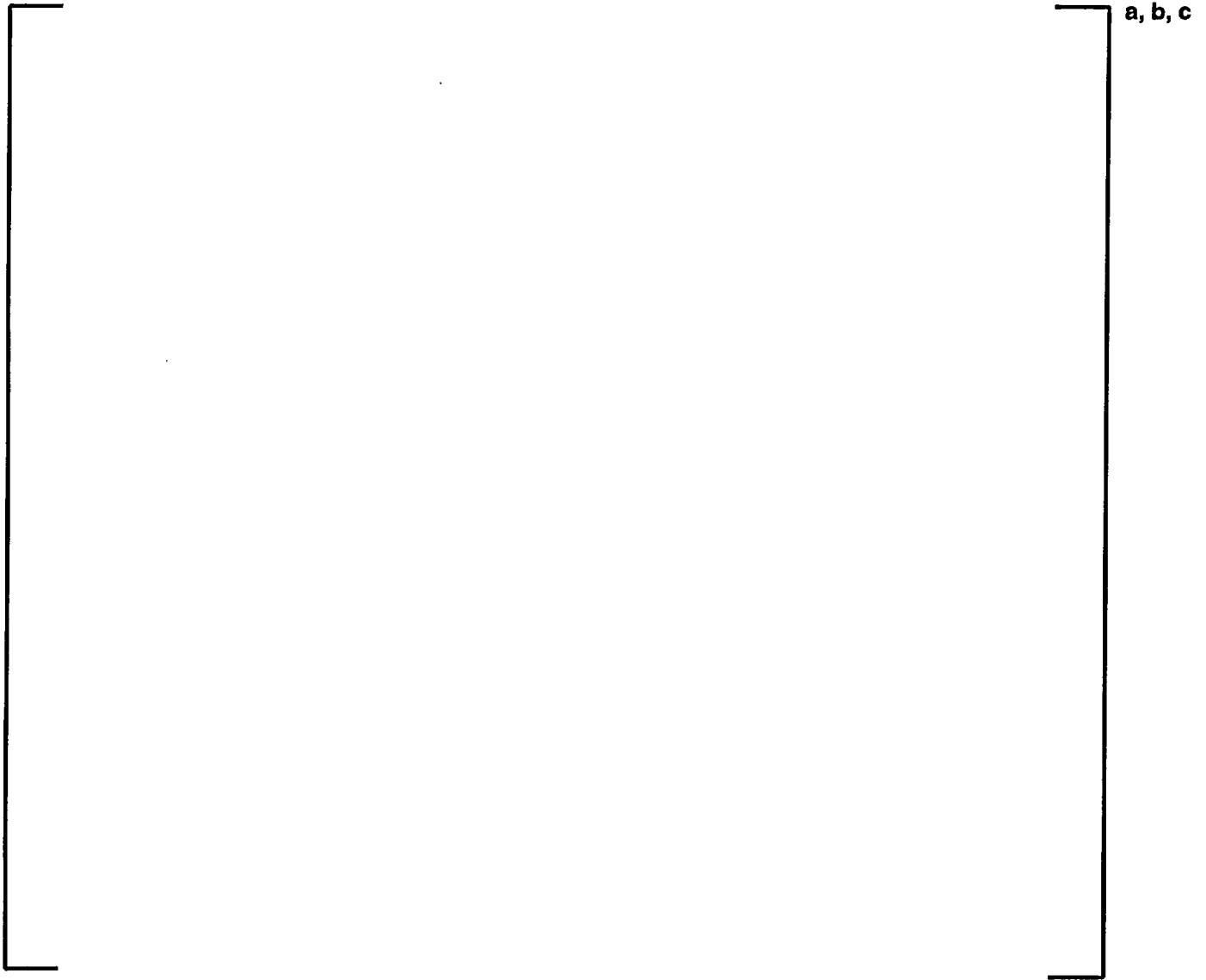


Figure 4-93: Core Average Axial Power Distribution (PARAGON versus PHOENIX-P): Plant F, Cycle 11, EOC



a, b, c

Figure 4-94: Core Average Axial Power Distribution (PARAGON versus PHOENIX-P): Plant F, Cycle 12, BOC

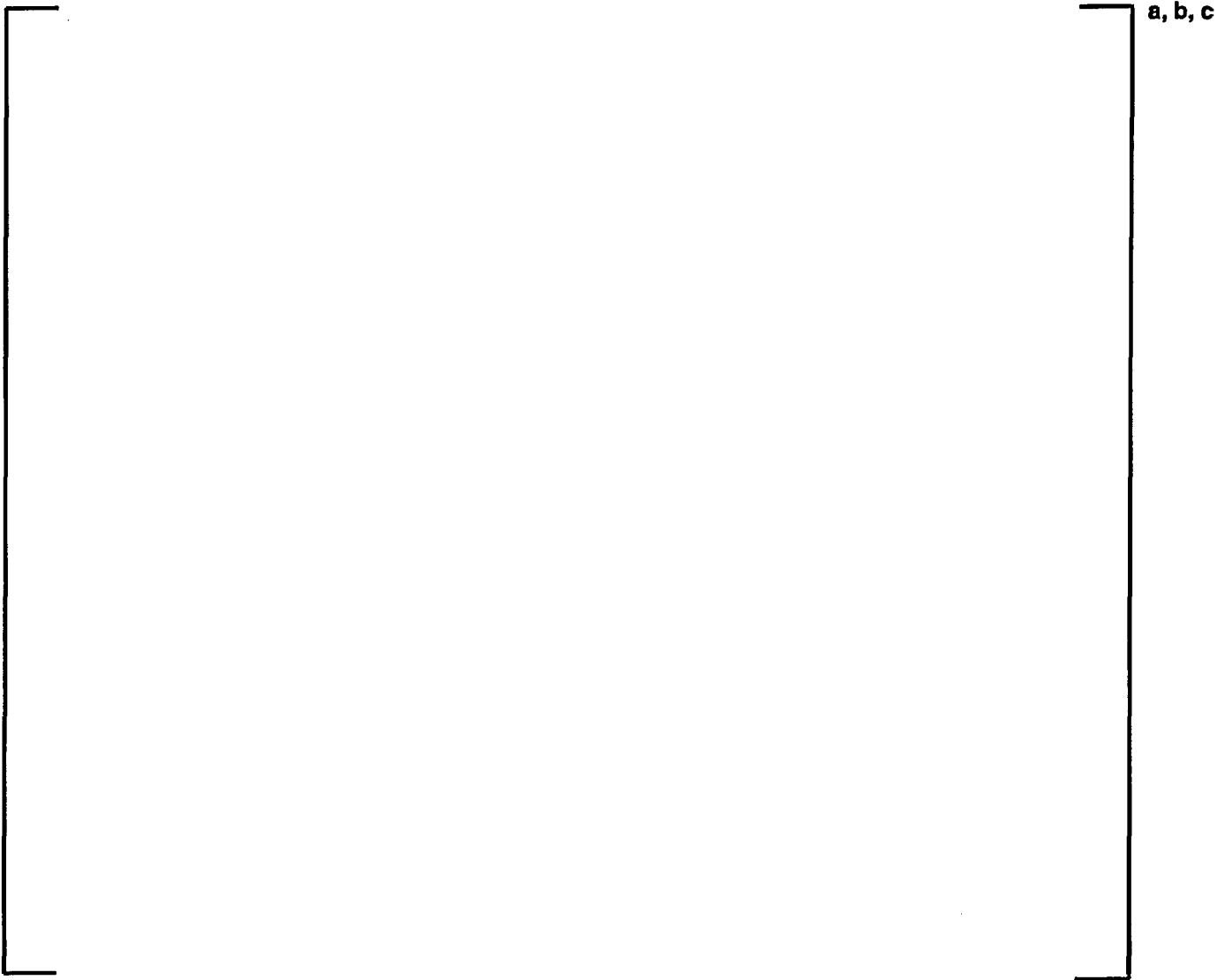


Figure 4-95: Core Average Axial Power Distribution (PARAGON versus PHOENIX-P): Plant F, Cycle 12, MOC

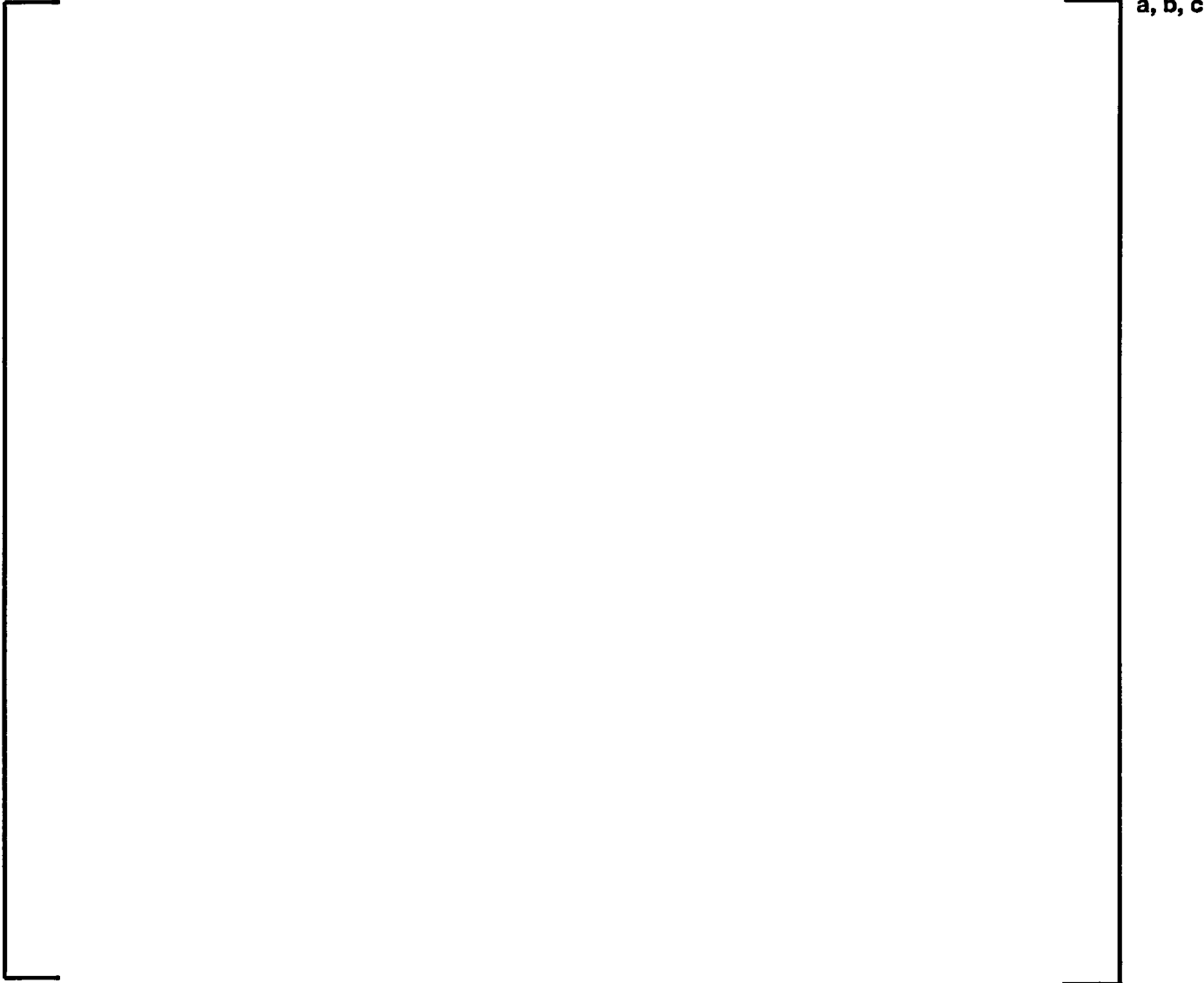


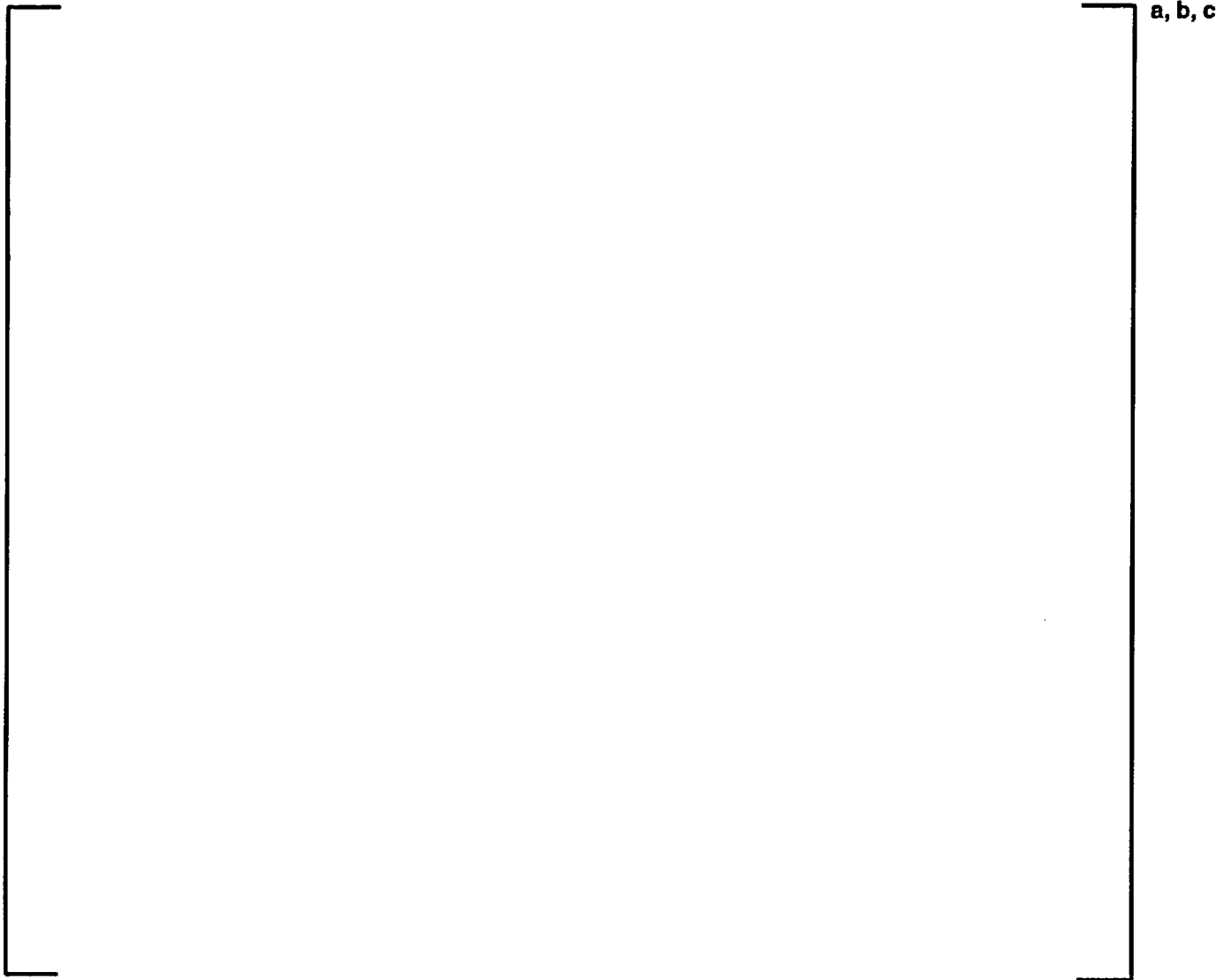
Figure 4-96: Core Average Axial Power Distribution (PARAGON versus PHOENIX-P): Plant F, Cycle 12, EOC



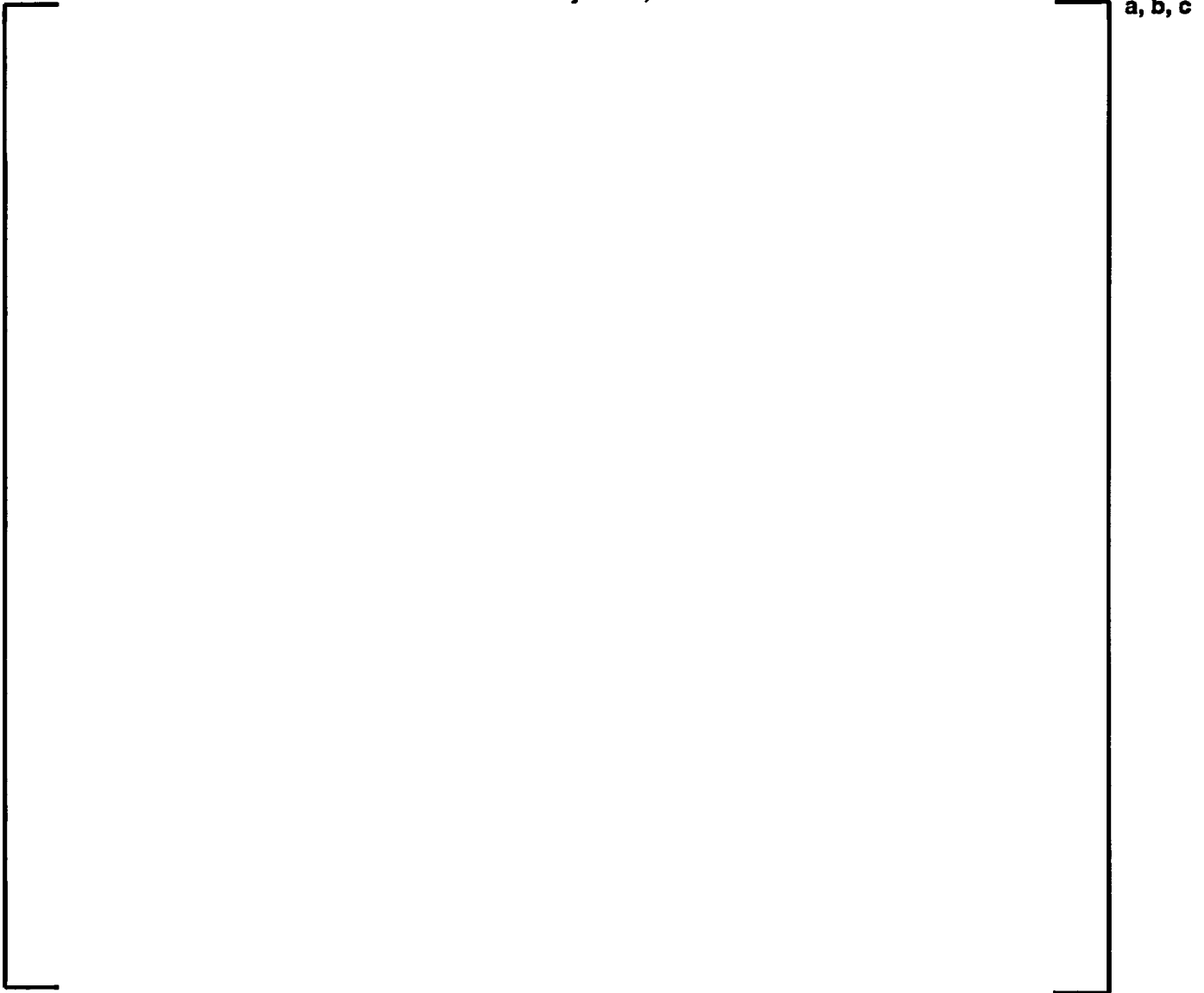
Figure 4-97: Core Average Axial Power Distribution (PARAGON versus PHOENIX-P): Plant G, Cycle 13, BOC



Figure 4-98: Core Average Axial Power Distribution (PARAGON versus PHOENIX-P): Plant G, Cycle 13, MOC



**Figure 4-99: Core Average Axial Power Distribution (PARAGON versus PHOENIX-P): Plant G,
Cycle 13, EOC**



**Figure 4-100: Core Average Axial Power Distribution (PARAGON versus PHOENIX-P): Plant G,
Cycle 14, BOC**



**Figure 4-101: Core Average Axial Power Distribution (PARAGON versus PHOENIX-P): Plant G,
Cycle 14, MOC**

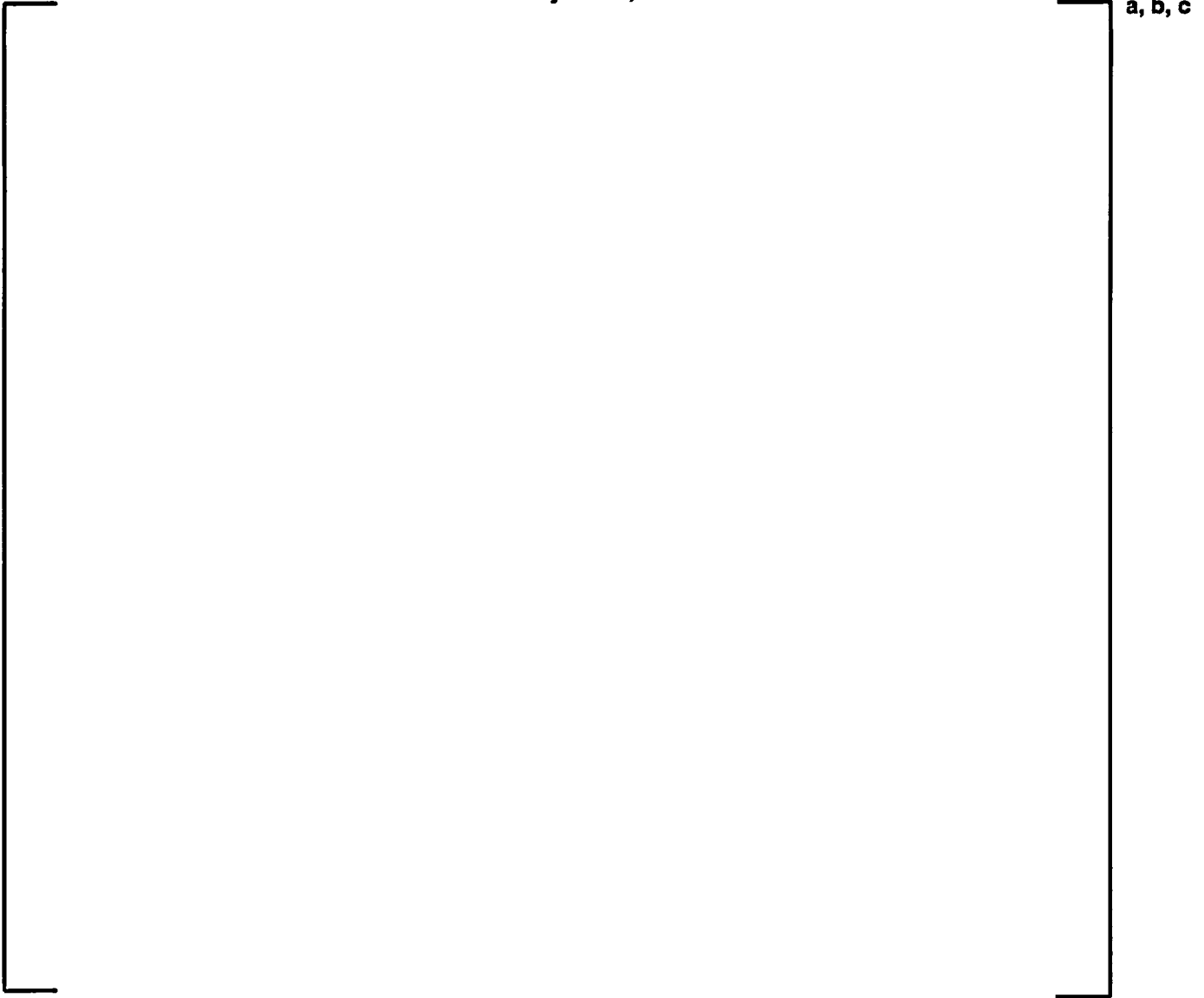
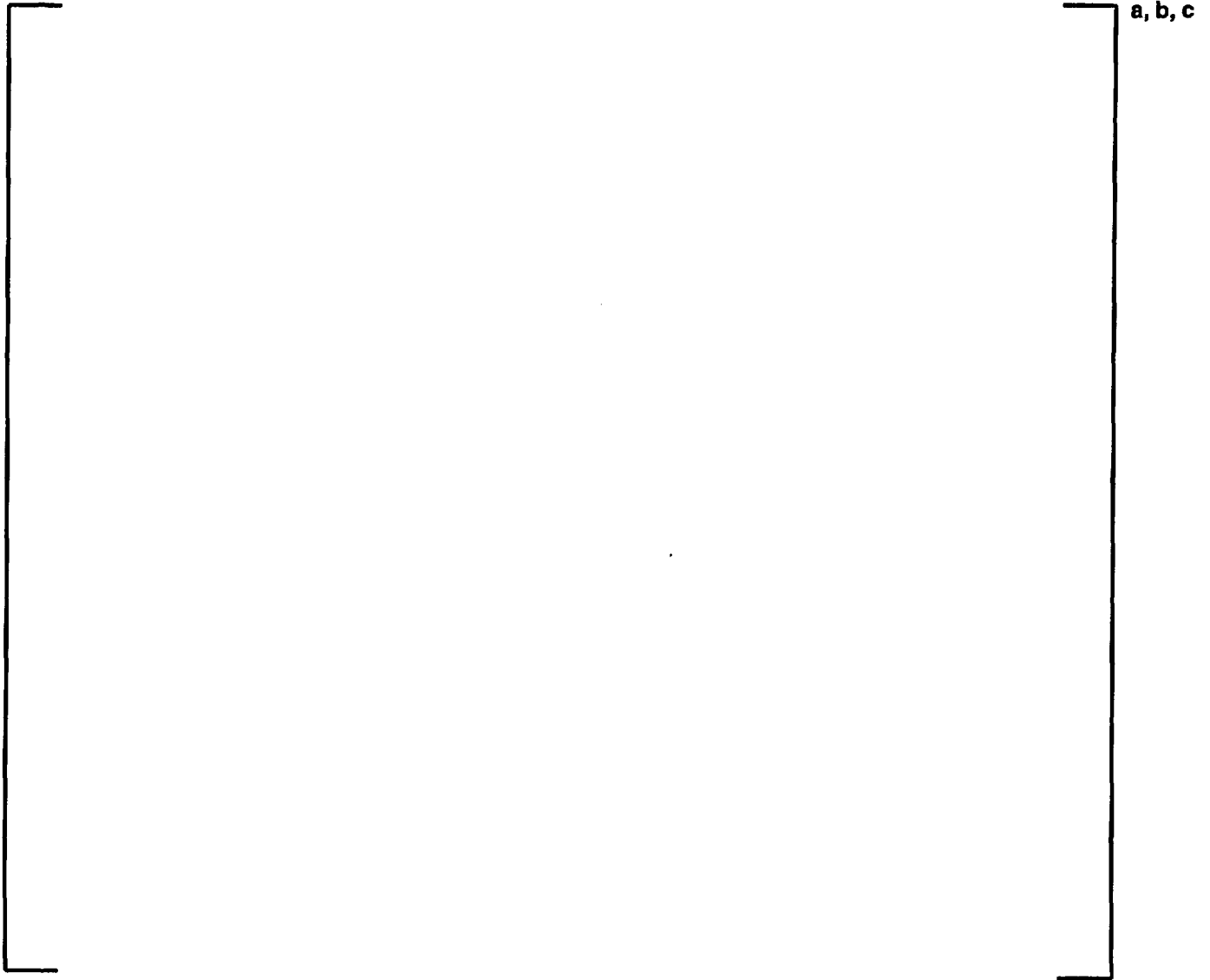


Figure 4-102: Core Average Axial Power Distribution (PARAGON versus PHOENIX-P): Plant G, Cycle 14, EOC



Page Intentionally Left Blank

Section 5.0: Conclusion

The objective of this report was to provide the information and data necessary to license PARAGON both as a standalone transport code and as a nuclear data source for a core simulator in a complete nuclear design code system for core design, safety and operational calculations. PARAGON is a new transport code developed by Westinghouse. PARAGON is based on collision probability methods and is written entirely in FORTRAN 90/95. PARAGON can provide nuclear data, both cross sections and pin power information, to a core simulator code such as ANC.

Section 2 presented an overview of the PARAGON code and theory.

The qualification presented in this report followed a systematic qualification process which has been used previously by Westinghouse to qualify nuclear design codes. This process starts with the qualification of the basic methodology used in the code and proceeds in logical steps to qualification of the code as applied to a complete nuclear design code system.

5.1 PARAGON Benchmarking

Consistent with the qualification process described above, Section 3 presented the results of PARAGON run as a standalone code for a series of critical experiments. These experiments included the Strawbridge-Barry 101 criticals, the KRITZ high temperature criticals, and a large number of spatial criticals from the B&W physics verification program. The B&W criticals provided both reactivity and power distribution measurements.

5.1.1 Strawbridge-Barry Critical Experiments

The Strawbridge-Barry 101 criticals cover a wide range of lattice parameters and therefore provide a severe test for the lattice code. Since these experiments are uniform lattices, the criticals were run as single pin cells in PARAGON. There are 40 UO₂ experiments among the 101 criticals. The mean K_{eff} for these experiments calculated by PARAGON is []^{a,c} with a standard deviation of []^{a,c}. The mean K_{eff} for all experiments was []^{a,c} with a standard deviation of []^{a,c}. The results of these criticals were graphed as a function of water to uranium ratio, enrichment, experimental buckling, pellet diameter, and soluble boron. No biases or trends were seen as a function of any of these parameters.

5.1.2 KRITZ high temperature critical experiments

The KRITZ high-temperature criticals provide critical benchmark data for uranium-fueled, water-moderated lattices at high temperatures. The criticals were run at temperatures as high as 245 °C. Twelve KRITZ experiments were modeled in PARAGON. The mean K_{eff} for the twelve experiments was []^{a,c} with a standard deviation of []^{a,c}. No significant trends across the large temperature range of these criticals were observed. The small standard deviation shows that PARAGON predicts very consistently across the large temperature range.

5.1.3 B&W spatial critical experiments

The B&W spatial criticals provided data on both reactivity and power distribution for a variety of uranium-oxide fueled lattices. A total of twenty nine configurations were analyzed: [

] ^{a,c}. K-infinity comparisons were made between PARAGON and the Monte Carlo code MCNP for all twenty-nine experiments. In addition, the measured axial bucklings were used with the PARAGON results to calculate K_{eff} . The reactivity results for all configurations were very good with the overall K_{eff} for the twenty-nine experiments being [] ^{a,c} with a standard deviation of [] ^{a,c}.

Rod power distribution comparisons of PARAGON results against measurements were provided for six of the experiments – two with no burnable absorbers, two with gadolinia burnable absorbers, and two with Pyrex burnable absorbers. The average difference between the measured and PARAGON power distribution for the six experiments was []^{a,c} per cent with an average standard deviation of []^{a,c} per cent.

5.1.4 Monte Carlo Assembly Benchmarks

Thirteen different assembly configurations were calculated in both PARAGON and the Monte Carlo code MCNP. These assembly configurations were chosen to cover a variety of lattice types and burnable absorbers over a large enrichment range. Eleven Westinghouse and two CE assemblies were included in these calculations. The PARAGON and MCNP calculations were compared for both reactivity and power distribution. The mean difference in reactivity between the MCNP and PARAGON calculations over the thirteen assemblies was []^{a,c} with a standard deviation of []^{a,c}. The comparison between the MCNP and PARAGON power distributions showed very good agreement. The average difference in rod powers for each assembly ranged from []^{a,c}. Standard deviations of the rod power differences for each assembly range from []^{a,c}.

5.1.5 Saxton and Yankee Isotopics Data

The spectrograph-measured isotopics data for Saxton Cores 2 and 3 with mixed oxide fuel, Yankee cores 1, 2, and 4 with stainless steel clad fuel, and Yankee Core 5 with zircaloy clad fuel have been compared to isotopic concentrations from PARAGON calculations simulating the power history corresponding to these cores. These isotopic comparisons show no significant trend for any isotope with burnup. These excellent results demonstrate the capability of PARAGON for predicting the depletion characteristics of both UO₂ and PuO₂ LWR fuel over a wide range of burnup conditions.

5.2 Plant comparisons

The primary use of PARAGON will be to generate nuclear data for use in Westinghouse core simulator codes. Thus the most important qualification for PARAGON is comparisons of results of core calculations using PARAGON supplied nuclear data against plant measured data. This report presented ANC results for PWR core calculations with nuclear data supplied by PARAGON which were compared to corresponding plant measurements where available and to PHOENIX-P/ANC results for the same calculations. These calculations demonstrated the accuracy of the PARAGON nuclear data when applied to a complete nuclear design system. The calculations also demonstrated that that PARAGON can replace all the previously licensed Westinghouse PWR lattice codes, such as PHOENIX-P, for use in all the previously licensed Westinghouse methodologies for PWR applications.

Cycles from eleven plants including both Westinghouse and Combustion Engineering type plants were used for measured to PARAGON/ANC predicted comparisons of startup data and at-power critical boron versus cycle burnup data. Measured radial power information was compared to PARAGON/ANC predicted values from 28 radial power maps from five different plants. BOC and EOC radial power and EOC burnup predictions from PHOENIX-P/ANC were compared to those calculated by PARAGON/ANC for nine cycles in five plants. PARAGON/ANC axial power predictions were compared to PHOENIX-P/ANC at BOC, MOC, and EOC for four plants. Finally, PARAGON/ANC results are compared to PHOENIX-P/ANC results for events for which measurements are generally not made or cannot be made. These are ARI-WSR (worst stuck rod) rodworth (four plants), dropped rod events (four plants) and rod ejection events (BOC and EOC for four plants).

5.2.1 Plants Cycles used for Comparison

The PARAGON qualification included 24 cycles in 11 plants. These plants included both Westinghouse (15 cycles) and Combustion Engineering (9 cycles) type cores. The plants were chosen to cover a wide variety of lattices, burnable absorbers, blanket types, and core sizes. The availability of reliable measured data was also a consideration.

5.2.2 Startup Test Results Comparisons

Comparisons were made for PARAGON/ANC predictions against measurements for BOC HZP ARO critical boron, BOC HZP ARO isothermal temperature (ITC), and BOC HZP rodworths. Results from twenty-two cycles from 11 plants were compared for the BOC HZP critical boron. The mean difference between measured and predicted was []^{a,c} for PARAGON/ANC and []^{a,c} for PHOENIX-P/ANC. The standard deviations were excellent for both code systems: []^{a,c} for PARAGON/ANC and []^{a,c} for PHOENIX-P/ANC.

Results from the BOC HZP ARO ITC were compared for the same twenty-two cycles. The statistics from the ITC comparison were quite similar between the two code systems. The mean predicted to measured difference in ITC was []^{a,c} pcm/°F for PARAGON/ANC and []^{a,c} for PHOENIX-P/ANC. The standard deviations were the same for both code systems at 0.8 pcm/°F.

Predicted versus measured rodworths were compared for nine cycles in seven plants. The cycles used three different methods for rodworth measurement: DRWM, rod swap, and boron dilution. All rodworth predictions met the measurement review criteria. The average measured to predicted difference for all the rods over all nine cycles was []^{a,c} for PARAGON/ANC with a standard deviation of []^{a,c}. The corresponding values for the PHOENIX-P/ANC code system were []^{a,c}.

5.2.3 Critical boron comparisons

At-power critical boron measurements were compared to results from PARAGON/ANC and PHOENIX-P/ANC core depletion calculations for twenty-two plant cycles. The results showed very good performance by PARAGON/ANC for EOC predictions. All plant cycles showed the effects of B¹⁰ depletion since the uncorrected measured and predicted critical boron values difference grew through the middle of the cycle. Accounting for B¹⁰ depletion reduces the difference between measured and predicted values through the middle of the cycle as was demonstrated in the report for one of the cycles.

5.2.4 Radial Power Distributions

Measured to PARAGON-predicted radial assembly power comparisons were made for five plants (28 total flux maps). These plants included both even (16x16 and 14x14) and odd (15x15 and 17x17) lattices. The range of cycle burnups for these maps was []^{a,c} MWD/MTU. When processing the flux maps, the measured values were folded into the lower right quadrant to remove any core tilts. The average value of the measured to predicted differences over the twenty-eight maps was []^{a,c} with an average standard deviation of []^{a,c}. These results show that the radial assembly powers are well predicted by PARAGON/ANC.

5.2.5 PARAGON/ANC to PHOENIX-P/ANC results

PARAGON/ANC and PHOENIX-P/ANC results were compared for radial assembly power distribution, axial power distribution, ARI-WSR rodworth, dropped rod, and rod ejection calculations. Radial assembly power (BOC and EOC) distributions were compared for nine cycles in five plants. EOC assembly burnup distributions were compared for the same cycles. Axial power distributions are shown at BOC, MOC, and EOC for eight cycles in four plants. The plant cycles for both radial and axial comparisons include Westinghouse and Combustion Engineering type cores. The results of both radial and axial power comparisons show very little difference between PARAGON/ANC and PHOENIX-P/ANC. Experience has shown that PHOENIX-P/ANC predicts radial and axial powers very well. The small difference between the PARAGON/ANC results and those from PHOENIX-P/ANC confirms that PARAGON/ANC also predicts these power distributions well.

ARI-WSR shutdown rodworths were calculated in PARAGON/ANC at BOC for four plants. The results were compared to PHOENIX-P/ANC for the same calculations. The largest difference for the worst stuck rodworth was []^{a,c}. The largest peaking factor difference was about []^{a,c}. Both differences are well within the uncertainties used with the ARI-WSR calculations.

Dropped rod calculations were also performed with PARAGON/ANC at BOC for four plants and the results were compared to corresponding PHOENIX-P/ANC results. The largest difference in the dropped rod worth was []^{a,c}. The largest difference in peaking factor was []^{a,c} in F_q .

The last set of comparisons between PARAGON/ANC and PHOENIX-P/ANC were for BOC and EOC rod ejection calculations for four plants. The rod ejection calculations were performed for both HZP and HFP conditions. Rod ejection calculations are similar to stuck rod calculations except the feedback is frozen from pre-ejection conditions leading to much larger peaking factors and rodworths. The largest difference in rodworth was []^{a,c} rod. The peaking factor differences were very small and well within the uncertainties used with this event.

5.3 Conclusion

The data presented in this report provide the basis for the qualification of PARAGON both as a standalone transport code and as the nuclear data source for core simulator codes. In chapter 3, standalone PARAGON was qualified against a wide variety of criticals and Monte Carlo calculations. In chapter 4, PARAGON was qualified as a supplier of core simulator code nuclear data through comparisons of the PARAGON results with ANC as the core simulator against measured data and against PHOENIX-P/ANC for a wide variety of plant designs and problems. The report demonstrates that PARAGON can replace all the previously licensed Westinghouse PWR lattice codes, such as PHOENIX-P, for use in all the previously licensed Westinghouse methodologies for PWR applications.

Section 6.0: References

Section 1.0

- 1-1. Liu, Y. S., et. al., "ANC: A Westinghouse Advanced Nodal Computer Code", WCAP-10965-P-A (Proprietary), and WCAP-10966-A (Nonproprietary), September, 1986
- 1-2. Nguyen, T. Q., et. al., "Qualification of the PHOENIX-P/ANC Nuclear Design System for Pressurized Water Reactor Cores", WCAP-11596-P-A (Proprietary), and WCAP-11597-A (Nonproprietary), June, 1988

Section 2.0

- 2-1 Nguyen, T. Q. et al., "Qualification of the PHOENIX-P/ANC Nuclear Design System for Pressurized Water Reactor Cores", WCAP-11596-P-A (Proprietary), and WCAP-11597-A (Nonproprietary), June, 1988.
- 2-2 Ouisloumen, M. et al., "The Two-Dimensional Collision Probability Calculation in Westinghouse Lattice Code: Methodology and Benchmarking", Proc. Int. Conf. On The Physics Of Reactors PHYSOR96, Vol. 1, A366, Mito, Japan, 1996.
- 2-3 MacFarlane R.E., "NJOY91.118: A code System For Producing Pointwise And Multigroup Neutron and Photon Cross Sections From ENDF/B Evaluated Nuclear Data", ORNL, RSIC, PSR-171(1994)
- 2-4 Stamm'ler R.J.J, Abbate M.J., "Methods Of Steady-State Reactor Physics in Nuclear Design", Academic Press, London (1983)
- 2-5 Villarino E.A., Nucl. Sci. Eng., 112, 16 (1992)
- 2-6 Thomsen K.L, Nucl. Sci. Eng., 119, 167 (1995)
- 2-7 Ouisloumen M. and Tahara Y., "PARAGON: The New Westinghouse Transport Code", Proc. Int. Conf. On The Physics of Nuclear Science and Technology, Vol. 1, 118, Long Island, New York, 1998.
- 2-8 Ouisloumen et al., "PARAGON: The New Westinghouse Lattice Code", Proc. ANS Int. Meeting on Mathematical Methods for Nuclear Applications, September 2001, Salt Lake City, Utah, USA
- 2-9 Hebert A, "Isotropic Streaming Effects in Thermal Lattices", Proc. ANS Int. Meeting on Mathematical Methods for Nuclear Applications, September 2001, Salt Lake City, Utah, USA

Section 3.0

- 3-1 Nguyen, T. Q., et. al., "Qualification of the PHOENIX-P/ANC Nuclear Design System for Pressurized Water Reactor Cores", WCAP-11596-P-A (Proprietary), and WCAP-11597-A (Nonproprietary), June, 1988.
- 3-2 Strawbridge, L. E., and Barry, R. F., "Criticality Calculations for Uniform Water-Moderated Lattices", Nucl. Sci. Eng. 23, pp 58-73 (1965).
- 3-3 Persson, R., Blomsjo, E., and Edenius, M., "High Temperature Critical Experiments with H2O Moderated Fuel Assemblies in KRITZ", Technical Meeting No. 2/11, NUCLEX 72, (1972).
- 3-4 Mosteller, R. D., "Critical Lattices of UO2 Fuel Rods and Perturbing Rods in Borated Water, LA-UR 95-1434, (1995)
- 3-5 Newman, L.W., "Urania-Gadolinia: Nuclear Model Development and Critical Experiment Benchmark, DOE/ET/34212-41 (April, 1984)
- 3-6 Nodvik, R. J., "Saxton Core II Fuel Performance Evaluation Part II: Evaluation of Mass Spectrometric and Radiochemical Analyses of Irradiated Saxton Plutonium Fuel," WCAP-3385-56 Part II (July, 1970).
- 3-7 Smalley, W. R., Saxton II – Fuel Performance Evaluation Part I: Materials", WCAP-3385-56 Part I (September, 1971).

- 3-8 Goodspeed, R. C., "Saxton Plutonium Project – Quarterly Progress Report for the Period Ending June 20, 1973", WCAP-3385-36 (July, 1973)
- 3-9 Crain, H. H., "Saxton Plutonium Project – Quarterly Progress Report for the Period Ending September 30, 1973", WCAP-3385-37 (December, 1973)
- 3-10 Melehan, J. B., "Yankee Core Evaluation Program Final Report", WCAP-3017-6094 (January, 1971).
- 3-11 Nodvik, R. J., "Supplementary Report on Evaluation of Mass Spectrometric and Radiochemical Analyses of Yankee Core I Spent Fuel, Including Isotopes of Elements Thorium through Curium", WCAP-6086 (August, 1969).
- 3-12 "MCNP4B - Monte Carlo N-Particle Transport Code System", CCC-660, RSICC Computer Code Collection, April, 1997.

Section 4.0

- 4-1 Liu, Y. S., et. al., "ANC: A Westinghouse Advanced Nodal Computer Code", WCAP-10965-P-A (Proprietary), and WCAP-10966-A (Nonproprietary), September, 1986
- 4-2 Nguyen, T. Q., et. al., "Qualification of the PHOENIX-P/ANC Nuclear Design System for Pressurized Water Reactor Cores", WCAP-11596-P-A (Proprietary), and WCAP-11597-A (Nonproprietary), June, 1988.

Section C

Page Intentionally Left Blank



Westinghouse Electric Company
Nuclear Services
P.O. Box 355
Pittsburgh, Pennsylvania 15230-0355
USA

U.S. Nuclear Regulatory Commission
Document Control Desk
Washington, DC 20555-0001

Direct tel: (412) 374-5282
Direct fax: (412) 374-4011
e-mail: sepp1ha@westinghouse.com

Our ref: LTR-NRC-03-55

Attn: J. S. Wermiel, Chief
Reactor Systems Branch
Division of Systems Safety and Analysis

September 9, 2003

- References:
1. Fax dated June 31, 2003 from Mr. B. Benney (NRC) to Mr. R. Sisk (Westinghouse); subject - "PARAGON formal RAI's, TAC #MB8040, WCAP-16045"
 2. WCAP-16045-P, "Qualification of the Two-Dimensional Transport Code PARAGON" (Proprietary)

Subject: Response to Request for Additional Information Regarding WCAP-16045-P "Qualification of the Two-Dimensional Transport Code PARAGON" (Proprietary)

Dear Mr. Wermiel:

Enclosed are copies of Westinghouse Electric Company LLC (Westinghouse) responses to the Nuclear Regulatory Commission (NRC) Request for Additional Information (RAI), Reference 1, regarding WCAP-16045-P "Qualification of the Two-Dimensional Transport Code PARAGON," Reference 2. This information is being submitted by Westinghouse Electric Company LLC to obtain Nuclear Regulatory Commission (NRC) generic approval of PARAGON, a new Westinghouse neutron transport code. Generic NRC approval is also requested for the use of PARAGON with Westinghouse's nuclear design code system or as a stand-alone code.

Also enclosed are:

1. One (1) copy of the Application for Withholding, AW-03-1700 with Proprietary Information Notice and Copyright Notice.
2. One (1) copy of Affidavit AW-03-1700.

This submittal contains proprietary information of Westinghouse Electric Company LLC. In conformance with the requirements of 10 CFR Section 2.790, as amended, of the Commission's regulations, we are enclosing with this submittal an Application for Withholding from Public Disclosure and an affidavit. The affidavit sets forth the basis on which the information identified as proprietary may be withheld from public disclosure by the Commission.

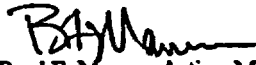
This material is for your internal use only and may be used solely for the purpose for which it is submitted. It should not be otherwise used, disclosed, duplicated, or disseminated, in whole or in part, to any other

Page 2 of 2
LTR-NRC-03-55
September 9, 2003

person or organization outside the Office of Nuclear Reactor Regulation without the expressed prior written approval of Westinghouse.

Correspondence with respect to this affidavit or Application for Withholding should reference AW-03-1700 and should be addressed to H. A. Sepp, Manager of Regulatory Compliance and Plant Licensing, Westinghouse Electric Company, P. O. Box 355, Pittsburgh, Pennsylvania 15230-0355.

Very truly yours,



Brad F. Maurer, Acting Manager
Regulatory Compliance and Plant Licensing

Enclosures

cc: F. Akstulewicz/NRR
B. Benney/NRR
U. Shoop/NRR
S. L. Wu/NRR
D. Holland/NRR
E. Peyton/NRR



Westinghouse Electric Company
Nuclear Services
P.O. Box 355
Pittsburgh, Pennsylvania 15230-0355
USA

U.S. Nuclear Regulatory Commission
Document Control Desk
Washington, DC 20555-0001

Direct tel: (412) 374-5282
Direct fax: (412) 374-4011
e-mail: scpp1ha@westinghouse.com

Our ref: AW-03-1700

September 9, 2003

**APPLICATION FOR WITHHOLDING PROPRIETARY
INFORMATION FROM PUBLIC DISCLOSURE**

Subject: Response to Request for Additional Information Regarding WCAP-16045-P, "Qualification of the Two-Dimensional Transport Code PARAGON" (Proprietary)

Reference: Letter from B. F. Maurer to J. S. Wermiel, LTR-NRC-03-55, dated September 9, 2003

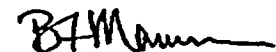
The Application for Withholding is submitted by Westinghouse Electric Company LLC (Westinghouse), pursuant to the provisions of Paragraph (b)(1) of Section 2.790 of the Commission's regulations. It contains commercial strategic information proprietary to Westinghouse and customarily held in confidence.

The proprietary material for which withholding is being requested is identified in the proprietary version of the enclosure to the referenced letter. In conformance with 10 CFR Section 2.790, Affidavit AW-03-1700 accompanies this Application for Withholding, setting forth the basis on which the identified proprietary information may be withheld from public disclosure.

Accordingly, it is respectfully requested that the subject information which is proprietary to Westinghouse be withheld from public disclosure in accordance with 10 CFR Section 2.790 of the Commission's regulations.

Correspondence with respect to this Application for Withholding or the accompanying affidavit should reference AW-03-1700 and should be addressed to H. A. Sepp, Manager of Regulatory Compliance and Plant Licensing, Westinghouse Electric Company, P. O. Box 355, Pittsburgh, Pennsylvania 15230-0355.

Very truly yours,


Brad F. Maurer, Acting Manager
Regulatory Compliance and Plant Licensing

Enclosures

AW-03-1700

AFFIDAVIT

COMMONWEALTH OF PENNSYLVANIA:

ss

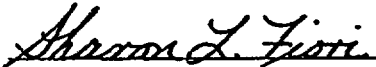
COUNTY OF ALLEGHENY:

Before me, the undersigned authority, personally appeared James W. Winters, who, being by me duly sworn according to law, deposes and says that he is authorized to execute this Affidavit on behalf of Westinghouse Electric Company LLC ("Westinghouse"), and that the averments of fact set forth in this Affidavit are true and correct to the best of his knowledge, information, and belief:

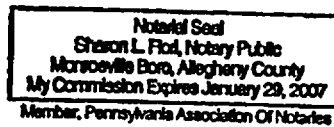


James W. Winters, Manager
Project Engineering and Integration

Sworn to and subscribed
before me this 9th day
of September, 2003



Notary Public



- (1) I am Manager, Project Engineering and Integration, in Nuclear Plant Programs, Westinghouse Electric Company LLC ("Westinghouse"), and as such, I have been specifically delegated the function of reviewing the proprietary information sought to be withheld from public disclosure in connection with nuclear power plant licensing and rule making proceedings, and am authorized to apply for its withholding on behalf of the Westinghouse Electric Company LLC.
- (2) I am making this Affidavit in conformance with the provisions of 10 CFR Section 2.790 of the Commission's regulations and in conjunction with the Westinghouse application for withholding accompanying this Affidavit.
- (3) I have personal knowledge of the criteria and procedures utilized by the Westinghouse Electric Company LLC in designating information as a trade secret, privileged or as confidential commercial or financial information.
- (4) Pursuant to the provisions of paragraph (b)(4) of Section 2.790 of the Commission's regulations, the following is furnished for consideration by the Commission in determining whether the information sought to be withheld from public disclosure should be withheld.
 - (i) The information sought to be withheld from public disclosure is owned and has been held in confidence by Westinghouse.
 - (ii) The information is of a type customarily held in confidence by Westinghouse and not customarily disclosed to the public. Westinghouse has a rational basis for determining the types of information customarily held in confidence by it and, in that connection, utilizes a system to determine when and whether to hold certain types of information in confidence. The application of that system and the substance of that system constitutes Westinghouse policy and provides the rational basis required.

Under that system, information is held in confidence if it falls in one or more of several types, the release of which might result in the loss of an existing or potential competitive advantage, as follows:

 - (a) The information reveals the distinguishing aspects of a process (or component, structure, tool, method, etc.) where prevention of its use by any of

Westinghouse's competitors without license from Westinghouse constitutes a competitive economic advantage over other companies.

- (b) It consists of supporting data, including test data, relative to a process (or component, structure, tool, method, etc.), the application of which data secures a competitive economic advantage, e.g., by optimization or improved marketability.
- (c) Its use by a competitor would reduce his expenditure of resources or improve his competitive position in the design, manufacture, shipment, installation, assurance of quality, or licensing a similar product.
- (d) It reveals cost or price information, production capacities, budget levels, or commercial strategies of Westinghouse, its customers or suppliers.
- (e) It reveals aspects of past, present, or future Westinghouse or customer funded development plans and programs of potential commercial value to Westinghouse.
- (f) It contains patentable ideas, for which patent protection may be desirable.

There are sound policy reasons behind the Westinghouse system which include the following:

- (a) The use of such information by Westinghouse gives Westinghouse a competitive advantage over its competitors. It is, therefore, withheld from disclosure to protect the Westinghouse competitive position.
- (b) It is information that is marketable in many ways. The extent to which such information is available to competitors diminishes the Westinghouse ability to sell products and services involving the use of the information.
- (c) Use by our competitor would put Westinghouse at a competitive disadvantage by reducing his expenditure of resources at our expense.

- (d) Each component of proprietary information pertinent to a particular competitive advantage is potentially as valuable as the total competitive advantage. If competitors acquire components of proprietary information, any one component may be the key to the entire puzzle, thereby depriving Westinghouse of a competitive advantage.
 - (e) Unrestricted disclosure would jeopardize the position of prominence of Westinghouse in the world market, and thereby give a market advantage to the competition of those countries.
 - (f) The Westinghouse capacity to invest corporate assets in research and development depends upon the success in obtaining and maintaining a competitive advantage.
- (iii) The information is being transmitted to the Commission in confidence and, under the provisions of 10 CFR Section 2.790, it is to be received in confidence by the Commission.
- (iv) The information sought to be protected is not available in public sources or available information has not been previously employed in the same original manner or method to the best of our knowledge and belief.
- (v) The proprietary information sought to be withheld in this submittal is that which is appropriately marked as "Responses to PARAGON RAIs," being transmitted by Westinghouse Electric Company letter (LTR-NRC-03-55) and Application for Withholding Proprietary Information from Public Disclosure, to the Document Control Desk, Attention Mr. J. S. Wermiel. The proprietary information as submitted by Westinghouse is that associated with Westinghouse's request for NRC approval of PARAGON.

This information is part of that which will enable Westinghouse to:

- (a) Obtain NRC approval of the Two-Dimensional Transport Code PARAGON.

- (b) Promote convergence between Westinghouse organizations.
- (c) Assist our customer in obtaining enhanced nuclear design input data for fuel reload analysis.

Further this information has substantial commercial value as follows:

- (a) Westinghouse plans to sell the use of this information to its customers for purposes of developing nuclear design input data into the Westinghouse nuclear design code system or as a stand-alone code.
- (b) Westinghouse can sell support for PARAGON.
- (c) The information requested to be withheld reveals the distinguishing aspects of a design developed by Westinghouse.

Public disclosure of this proprietary information is likely to cause substantial harm to the competitive position of Westinghouse because it would enhance the ability of competitors to provide similar manufacturing processes and licensing defense services for commercial power reactors without commensurate expenses. Also, public disclosure of the information would enable others to use the information to meet NRC requirements for licensing documentation without purchasing the right to use the information.

The development of the technology described in part by the information is the result of applying the results of many years of experience in an intensive Westinghouse effort and the expenditure of a considerable sum of money.

In order for competitors of Westinghouse to duplicate this information, similar technical programs would have to be performed and a significant manpower effort, having the requisite talent and experience, would have to be expended.

Further the deponent sayeth not.

PROPRIETARY INFORMATION NOTICE

Transmitted herewith are proprietary and/or non-proprietary versions of documents furnished to the NRC in connection with requests for generic and/or plant-specific review and approval.

In order to conform to the requirements of 10 CFR 2.790 of the Commission's regulations concerning the protection of proprietary information so submitted to the NRC, the information which is proprietary in the proprietary versions is contained within brackets, and where the proprietary information has been deleted in the non-proprietary versions, only the brackets remain (the information that was contained within the brackets in the proprietary versions having been deleted). The justification for claiming the information so designated as proprietary is indicated in both versions by means of lower case letters (a) through (f) located as a superscript immediately following the brackets enclosing each item of information being identified as proprietary or in the margin opposite such information. These lower case letters refer to the types of information Westinghouse customarily holds in confidence identified in Sections (4)(ii)(a) through (4)(ii)(f) of the affidavit accompanying this transmittal pursuant to 10 CFR 2.790(b)(1).

COPYRIGHT NOTICE

The reports transmitted herewith each bear a Westinghouse copyright notice. The NRC is permitted to make the number of copies of the information contained in these reports which are necessary for its internal use in connection with generic and plant-specific reviews and approvals as well as the issuance, denial, amendment, transfer, renewal, modification, suspension, revocation, or violation of a license, permit, order, or regulation subject to the requirements of 10 CFR 2.790 regarding restrictions on public disclosure to the extent such information has been identified as proprietary by Westinghouse, copyright protection notwithstanding. With respect to the non-proprietary versions of these reports, the NRC is permitted to make the number of copies beyond those necessary for its internal use which are necessary in order to have one copy available for public viewing in the appropriate docket files in the public document room in Washington, DC and in local public document rooms as may be required by NRC regulations if the number of copies submitted is insufficient for this purpose. Copies made by the NRC must include the copyright notice in all instances and the proprietary notice if the original was identified as proprietary.

Responses to PARAGON RAIs

- 1) On page 2-1, Sec. 2.3.1, 1st. paragraph, the 1st. sentence states that PARAGON can be "generalized" to handle multi-regions in cells..... Please provide clarification of what is meant by "generalized".

Response: PHOENIX-P uses the Dancoff method described in Reference 2-4 in the topical report for the resonance self-shielding calculation. PHOENIX-P assumes that only one single ring is used to model the fuel region of the pin. In PARAGON, the Dancoff method has been extended (generalized) to handle multi-regions (multi-rings) in the fuel, which is necessary to compute the radial power distribution within the pellet. The following reference (attached) provides more details on the method:

H. Matsumoto, et al., "Verification of PARAGON for LWR Applications" ,Proc. Int. Conf. On The New Frontiers of Nuclear Technology: Reactor Physics, Safety and High Performance Computing, PHYSOR2002, 14A-01, Seoul, Korea, 2002

PARAGON can also deplete the pellet in multi-regions. Fission product and actinide concentrations are tracked for each region in the pellet.

- 2) On page 2-5, Sec. 2.3.4, last paragraph, the 1st sentence states that the user has the option to hold any region depletable or non-depletable. What is the basis for the decision?

Response: The PHOENIX-P lattice code did not give the user the flexibility to control which regions were depletable. Instead, for a given cell type, the depletable region was defaulted. When setting up models, the user had to define the geometry of his model so that the regions which were to be depleted corresponded to these default regions. PARAGON allows the user to specify any region as depletable or non-depletable. This provides more flexibility for modeling and editing. The basis for this decision is the complexity of the geometry and the type of information desired.

This option is also convenient in other ways. For example, cross section generation methodologies often require a control rod or neutron detector be present in assembly calculations but that the control rod and/or neutron detector not be depleted with the assembly. This situation is easily modeled in PARAGON.

- 3) On page 2-5, Sec. 2.4.1, 11. paragraph, the 2nd sentence states that the user has the option to provide temperature tables. What assurance can be provided to the staff that the appropriate table is utilized at the appropriate time?

Response: In standard use, the temperature data will be internally calculated by PARAGON in the same manner as is currently done in PHOENIX-P. This was the procedure used for all plant calculations shown in the topical report. It is intended that no temperature tables be directly input by the user for design or safety calculations. The option to input temperature tables is maintained only for methods development purposes. If in some currently unforeseen

situation, a specific temperature table was required to be input for a particular design calculation, that would be an extraordinary situation and would be easily recognized by the verifier as such, and would require the temperature table input to be verified in the same manner as the rest of the code input.

- 4) **On page 2-5, Sec. 2.4.3, 1st. paragraph, the 2nd sentence states that the user has to provide a code with the coefficients and polynomial. What assurance can be provided to the staff that the appropriate coefficients and polynomials are used at the appropriate time?**

Response: In standard use, i.e., for design and safety calculations, this expansion data is defaulted and will not be input by the user. All the plant calculations performed in the topical report used the default expansion data.

- 5) **On page 3-1 and 3-2, reference is made to the Strawbridge-Barry and KRITZ high temperature critical experiments. Please provide additional as to why these experiments are still relevant since they are do not include the high enrichment and temperatures used in LWR today.**

Response: Strawbridge-Barry critical experiments cover a wide range of parameters of interest in light water reactor (LWR) designs such as moderator to fuel volume ratio, fuel enrichment, and soluble boron concentration. These are clean critical experiments which are used throughout the industry for the qualification of the basic methodology and the associated cross-sections library.

The KRITZ high temperature critical experiments were included to validate the predictions at higher than room temperatures. There are very few critical experiments available at these conditions.

Numerical benchmarking with comparisons to Monte Carlo and PHOENIX-P results was used to qualify PARAGON at higher enrichments (up to 5 w/o). In addition, the plant cycles used for the qualification included fuel up to 4.95 enrichment as shown in Table 4.1 of the topical report. These plant cycles included some of the highest temperature PWR plants currently operating.

- 6) **On page 3-3, Section 3.2, reference is made to UO2 and MOX in the Monte Carlo Assembly bench-marking. In the 2nd Paragraph it is pointed out that the largest difference is due to the MOX assembly (276 pcm). Please provide additional justification for this discrepancy.**

Response: Benchmarking of the MOX assemblies did show relatively higher discrepancy vis a vis Monte Carlo results. However, the observed deviations are deemed to be acceptable from a practical standpoint as has been shown in the qualification of the mixed oxide core shown in chapter 4.0 of the topical report.

- 7) **On page 3-5, Table 3-1, Please provide the expression for the mean in the second column of this table.**

Response: In Table 3-1, the mean is the arithmetic average of the predicted eigenvalues contained in a particular set. This is defined as :

$$\text{Mean} = \Sigma k_{\text{effective}_i} / (\text{Number of data points})$$

The summation in the numerator is over the number of data points.

- 8) **On page 4-2, Section 4.2, makes reference to start-up tests. Where there any mixed cores start-up tests modeled?**

Response: Cycles 24, 25 and 26 of Plant E (specifications in Table 4.1) had both uranium and MOX fuel. Cycle 25 had MOX fuel fed in previous cycles while Cycles 24 and 26 had a mix feed of both uranium and MOX assemblies. The startup test results for cycles 25 and 26 are provided in Tables 4-2 and 4-3. The rodworth measurement results for cycle 24 are provided in Table 4-8.

- 9) **On page 4-3, Section 4.3, makes reference to the availability of B10 isotopic concentration But, no reason was given as to why this information was no available. Please provide this information.**

Response: B¹⁰ isotopic information was not available to Westinghouse for all the plants modeled in Chapter 4. The availability of this data varies from plant to plant and even from cycle to cycle for the same plant. There are currently no standard requirements in the industry for collecting this data. Rather than mix data with B¹⁰ depletion with that without B¹⁰ depletion, Westinghouse decided not to use B¹⁰ depletion for any of the plants. An example of the effect of B¹⁰ depletion is given by Figure 4-23. B¹⁰ depletion does not have a significant effect on EOC boron and therefore on the prediction of cycle length. The use of B¹⁰ depletion data would not alter the conclusion that cycle depletion is well modeled by ANC using PARAGON nuclear data.

- 10) **Pages 4-3 and 4-4, Section 4,3, the 2nd and last paragraph, make reference to figures 4-10 and 4-20, predicting the boron concentration in the core. In Figure 4-10, both PARAGON and PHOENIX over-predict the concentration, while in Figure 4-20, both codes under-predict the concentration. Please explain the effect of these predictions with respect to be conservative or non-conservative in their predictions.**

Response: All the depletion calculations in Figures 4-1 through 4-23 are calculated at best estimate conditions. They are not intended to be conservative or non-conservative but are a reflection of the reactivity predictions of the Westinghouse codes with the best information available on plant conditions. If these calculations were performed during plant operation, the criteria which would be used to determine the acceptability of the measured to predicted differences would be the review criteria on reactivity in the Technical Specifications (usually 50 ppm or 500 pcm) and the acceptance criteria (1000 pcm).

11) On pages 4-4, Section 4.4, the 2nd. make reference to flux maps being folded into the right bottom core quadrant.

a) Please provide further clarification as to why this was carried out.

Response: Folding measured flux maps removes the effects of statistical variations from nominal values in fuel manufacture and operational parameters. Folding the core makes the actual core as consistent as possible to the core model. Comparison to the folded core thus gives the best estimate of the accuracy of PARAGON/ANC core model.

b) Also, it is stated in the same paragraph that flux maps were taken up to 20 GWD. Please provide technical justification as to why radial power comparisons were not made at higher burn-ups??

Response: The flux maps that were shown in the topical were primarily the result of the plant selection for the qualification. As seen in Table 4-1, a wide variety of plants were used for the qualification. These plants were chosen primarily to include most features present in current plant designs. Availability of the reliable plant measured data was another criteria for plant selection. For each of the plants included, available maps were chosen at cycle burnups close to beginning of cycle (BOC), middle of cycle (MOC), and end of cycle (EOC) conditions. There were four cycles included in the qualification with EOC burnup in the range from 19700 to 20800 MWD/MTU with assembly burnups exceeding 53,000 MWD/MTU. These represent long cycles of operation. Westinghouse believes that the EOC flux maps shown in the PARAGON topical demonstrate typical EOC performance.

12) On pages 4-4, Section 4.5, the subject of uncertainties is raised in the 1st paragraph. What uncertainties are being referred to and how are they determined??

Response: The uncertainties referred to are those used for with the current PHOENIX-P/ANC code system. Any uncertainty qualified for PHOENIX-P/ANC is applicable to PARAGON/ANC. An example of these uncertainties would be those currently used in reload analyses for Westinghouse type plants performed in accordance with the methodology presented in WCAP-9272-P-A.

13) On pages 4-5, Section 4.5, two of the tables listed on this page make reference to plant E regarding axial power profile and stuck rod analysis for MOX. Please explain?

Response: One of the plants used for qualifying PARAGON had mixed oxide (MOX) fuel (plant E). Core figures comparing radial average assembly powers and burnups for Plant E Cycle 25 were presented in Figures 4-70, 4-71, and 4-72. The axial maps presented in the topical report were selected to show representative performance. There was no specific reason that the MOX core was not included. Axial power shape comparisons between PARAGON/ANC and PHOENIX-P/ANC core models for plant E are shown in Figures 1-6 attached to this response. These axial power comparisons include BOC, MOC, and EOC for

both cycles 25 and 26 of plant E. These axial power shape comparisons show excellent agreement in axial power shape between the PARAGON and PHOENIX-P based models.

The topical report provided stuck rod worth comparisons for four plants in Table 4-13. The same comparison is provided for the MOX plant, plant E, in Table 1 attached to these responses. Comparison of the stuck rod worth difference between the PARAGON and PHOENIX-P models shows a small difference (i.e. 19 pcm). However, this difference is larger than those results for the other four cores shown in Table 4-13 of the topical. The difference in the MOX core results can be attributed to an improved treatment for Pu²⁴⁰ self-shielding in PARAGON. PARAGON employs space dependent temperature and composition-based shielding factors compared to one single value in PHOENIX-P.

The stuck rod peaking factor differences (Fq, FdH, and Fz) between the PARAGON and PHOENIX-P models for plant E are very small and actually considerably smaller than those seen for the uranium models in Table 4-13 of the topical report.

To complete the rodded comparisons for the MOX plant, Table 2 shows dropped rod comparisons for plant E for the PARAGON/ANC and PHOENIX-P/ANC models. This table presents the same data for plant E as was provided in Table 4-14 for four all uranium cores. Table 2 shows very good agreement between the PARAGON and PHOENIX-P based models both for dropped rod worth and for peaking factors.

- 14) On pages 4-18, Table 4-15, please explain the difference between the BOC HFP and the BOC HZP values for both the ejected rod and the peaking factors. Also, were similar calculations performed for the MOX core? If so, please provide that information.**

Response: Both HFP and HZP calculations are done in a similar way. Both cases start from a case with rods at their rod insertion limits (RILs) corresponding to the core power level. In both cases, a single control rod is fully withdrawn from the core with no change in feedback (i.e. both moderator and fuel temperature feedbacks are kept at their values at the start of the calculation). The control rod which causes the highest reactivity insertion and worst peaking factor is reported. The key difference between HFP and HZP calculations is in the control rod configuration at the start of the calculation. For HZP, the lead bank is full in and the next two banks are partially inserted. For HFP, the lead bank is inserted to its full power RIL condition which is about 25% of full insertion. This difference in rod insertion is the largest contributor to the large difference in the rod ejection results between HFP and HZP. The ejected rod starts from deeper insertion and therefore results in a larger worth for the HZP case. The greater numbers of rods inserted and the deep insertion at HZP also results in a worse peaking factor.

Rod ejection results for the MOX core (plant E, cycle 26) are shown in Table 3 attached to these responses. These results are comparable to the results shown in Table 4-15 for the all uranium cores and show that PARAGON and PHOENIX-P based models give essentially the same results for the rod ejection calculation at all conditions for both uranium and MOX cores.

- 15) On pages 4-19, Table 4-16, why were the calculation performed at 300 ppm rather than at zero ppm?**

Response: To comply with technical specifications, some PWR cores are still required to make a moderator temperature coefficient measurement at a cycle lifetime when HFP critical boron is near 300 ppm. The plants compare their results to calculations performed at the same conditions. This is the type of calculation that is shown in Table 4-16.

- 16) On pages 4-20 through 4-42, plots are provided showing boron concentration -vs- burnup. Some plots indicate under predictions by the codes, and some plots indicate over predictions by the codes. Please explain these predictions and state which of these predictions are conservative and are non-conservative.**

Response: Please see the response to question 10.

- 17) In the same plots stated in question 16, some of the plots demonstrate spurious peaks, especially figure 4-7 and 4-12. Please explain.**

Response: Where available, the raw boron follow data was used directly for the cycle depletion figures. This data includes part-power operation. Core reactivity is higher at part power requiring higher critical boron concentrations. The measured data shown in both plots in question were measured data which included part power operational data. On both these plots, many of the "spurious" points occur together at the same burnups indicating a startup situation with the boron values decreasing as the plant increases power.

- 18) Please explain why there is no assembly average power distribution for plant E, the MOX core? Nor are there any core average axial power distributions for comparisons between PARAGON and PHOENIX?**

Response: Incore maps for Plant E for cycles 25 and 26 are not easily obtained by Westinghouse since Westinghouse no longer supplies fuel to plant E. However, Westinghouse does have access to some maps from cycle 24 which also is a mixed core of MOX and uranium oxide fuel. A middle of cycle at-power map comparing the measured to PARAGON-predicted average powers for Plant E, cycle 24 is shown in Figure 7. The measured and predicted values for the MOX fuel are shown in bold italics in this figure. This map shows very good power predictions for both MOX and UO₂ fuel.

The core average axial power comparisons between PARAGON and PHOENIX-P based models for plant E, cycles 25 and 26 are presented in Figures 1-6 attached to these responses.

Table 1
ARI-WSR Control Rod Worth Comparison



Table 2
Dropped Rod Comparison



Table 3
Rod Ejection Comparison



Figure 1
Core Average Axial Power Distribution (PARAGON versus PHOENIX-P)
Plant E Cycle 25, BOC

a,b,c



Figure 2
Core Average Axial Power Distribution (PARAGON versus PHOENIX-P)
Plant E Cycle 25, MOC



Figure 3
Core Average Axial Power Distribution (PARAGON versus PHOENIX-P)
Plant E Cycle 25, EOC



Figure 4
Core Average Axial Power Distribution (PARAGON versus PHOENIX-P)
Plant E Cycle 26, BOC



Figure 5
Core Average Axial Power Distribution (PARAGON versus PHOENIX-P)
Plant E Cycle 26, MOC



Figure 6
Core Average Axial Power Distribution (PARAGON versus PHOENIX-P)
Plant E Cycle 26, EOC



Figure 7
Average Assembly Power Distribution: Plant E, Cycle 24, 5584 MWD/MTU

